

9

Physical Water and Wastewater Treatment Processes

- 9.1 [Screens](#)
Bar Screens • Coarse Screens • Comminutors and In-Line Grinders • Fine Screens • Microscreens • Orifice Walls
- 9.2 [Chemical Reactors](#)
Hydraulic Retention Time • Reaction Order • Effect of Tank Configuration on Removal Efficiency
- 9.3 [Mixers and Mixing](#)
Mixing Devices • Power Dissipation • Blending • Particle Suspension
- 9.4 [Rapid Mixing and Flocculation](#)
Rapid Mixing • Flocculation
- 9.5 [Sedimentation](#)
Kinds of Sedimentation • Kinds of Settling Tanks • Flocc Properties • Free Settling • Design of Rectangular Clarifiers • Design of Circular Tanks • Design of High-Rate, Tube, or Tray Clarifiers • Clarifier Inlets • Outlets • Sludge Zone • Freeboard • Hindered Settling • Thickener Design
- 9.6 [Filtration](#)
Granular Media Filters • Water Treatment • Wastewater Treatment
- 9.7 [Activated Carbon](#)
Preparation and Regeneration • Characteristics • Uses • Equilibria • Kinetics • Empirical Column Tests • Application
- 9.8 [Aeration and Gas Exchange](#)
Equilibria and Kinetics of Unreactive Gases • Oxygen Transfer • Absorption of Reactive Gases • Air Stripping of Volatile Organic Substances

Robert M. Sykes
The Ohio State University

Harold W. Walker
The Ohio State University

9.1 Screens

The important kinds of screening devices are bar screens, coarse screens, comminutors and in-line grinders, fine screens, and microscreens (Pankratz, 1988).

Bar Screens

Bar screens may be subdivided into (1) trash racks, (2) mechanically cleaned bar screens, and (3) manually cleaned bar screens.

Trash Racks

Trash racks are frequently installed in surface water treatment plant intakes to protect coarse screens from impacts by large debris and to prevent large debris from entering combined/storm water sewerage systems. Typical openings are 1 to 4 in. The bars are made of steel, and their shape and size depend on the expected structural loads, which are both static (due to the headloss through the rack) and dynamic (due to the impacts of moving debris). The racks are cleaned intermittently by mechanically driven rakes that are drawn across the outside of the bars. The raking mechanism should be able to lift and move that largest expected object.

Mechanically Cleaned Bar Screens

Mechanically cleaned bar screens are usually installed in the headworks of sewage treatment plants to intercept large debris. They may be followed by coarse screens and comminutors and in-line grinders. The clear openings between the bars are usually $\frac{1}{2}$ to $1\frac{3}{4}$ in. wide (Hardenbergh and Rodie, 1960; Pankratz, 1988; Wastewater Committee, 1990). In sewage treatment plants, the approach channel should be perpendicular to the plane of the bar screen and straight. Approach velocities should lie between 1.25 ft/sec (to avoid grit deposition) and 3 ft/sec (to avoid forcing material through the openings) (Wastewater Committee, 1990). Velocities through the openings should be limited to 2 to 4 ft/sec (Joint Task Force, 1992).

Several different designs are offered (Pankratz, 1988).

Inclined and Vertical Multirake Bar Screens

Multirake bar screens are used wherever intermittent or continuous heavy debris loads are expected. The spaces between the bars are kept clear by several rows of rakes mounted on continuous belts. The rake speed and spacing is adjusted so that any particular place on the screen is cleaned at intervals of less than 1 min. The bars may be either vertical or inclined, although the latter facilitates debris lifting.

The raking mechanism may be placed in front of the bars, behind them, or may loop around them. In the most common arrangement, the continuous belt and rakes are installed in front of the screen, and the ascending side of the belt is the cleaning side. At the top of the motion, a high-pressure water spray dislodges debris from the rake and deposits it into a collection device.

If the belt and rakes are installed so that the descending side is behind the screen (and the ascending side is either in front of or behind the screen), there will be some debris carryover.

Catenary, Multirake Bar Screens

Standard multirake bar screens support and drive the rake belt with chain guides, shafts, and sprockets at the top and the bottom of the screen. The catenary bar screen dispenses with the bottom chain guide, shaft, and sprocket. This avoids the problem of interference by deposited debris in front of the screen. The rakes are weighted so that they drag over debris deposits, and the bar screen is inclined so that the weighted rakes lie on it.

Reciprocating Rake Bar Screens

Reciprocating rake bar screens have a single rake that is intermittently drawn up the face of the screen. Because of their lower solids handling capacity, they are used only in low debris loading situations. The reciprocating mechanism also requires more head room than multirake designs. However, they are intrinsically simpler in construction, have fewer submerged moving parts, and are less likely to jam.

Arc, Single-Rake Bar Screens

In these devices, the bars are bent into circular arcs, and the cleaning rake describes a circular arc. The rake is normally cleaned at the top of the arc by a wiper. The flow is into the concave face of the screen, and the rakes are upstream of it.

Manually Cleaned Bar Screens

Manually cleaned bar screens are sometimes installed in temporary bypass channels for use when the mechanically cleaned bar screen is down for servicing. The bars should slope at 30 to 45° from the

TABLE 9.1 Kirschmer's Shape Factors for Bars

Bar Cross Section	Shape Factor (Dimensionless)
Sharp-edged, rectangular	2.42
Rectangular with semicircular upstream face	1.83
Circular	1.79
Rectangular with semicircular faces upstream and downstream	1.67
Teardrop with wide face upstream	0.76

Source: Fair, G.M. and Geyer, J.C. 1954. *Water Supply and Waste-Water Disposal*, John Wiley & Sons, Inc., New York.

horizontal, and the total length of bars from the invert to the top must be reachable by the rake. The opening between the bars should not be less than 1 in, and the velocity through it should be between 1 and 2 ft/sec. The screenings will usually be dragged up over the top of the bars and deposited into some sort of container. The floor supporting this container should be drained or grated.

Bar Screen Head Losses

The maximum headloss allowed for dirty bar racks is normally about 2.5 ft (Fair and Geyer, 1954). For clean bar racks, the minimum headloss can be calculated from Kirschmer's formula, Eq. (9.1) (Fair and Geyer, 1954):

$$h_L = \beta \left(\frac{w}{b} \right)^{4/3} h_v \sin \theta \quad (9.1)$$

- where
- b = the minimum opening between the bars (m)
 - h_L = the headloss through the bar rack (m)
 - h_v = the velocity head of the approaching flow (m)
 - w = the maximum width of the bars facing the flow (m)
 - β = a dimensionless shape factor for the bars
 - θ = the angle between the facial plane of the bar rack and the horizontal

Some typical values of the shape factor β are given in [Table 9.1](#).

The angle θ is an important design consideration, because a sloping bar rack increases the open area exposed to the flow and helps to keep the velocity through the openings to less than the desired maximum. Slopes as flat as 30° from the horizontal make manual cleaning of the racks easier, although nowadays, racks are always mechanically cleaned.

Coarse Screens

Coarse screens may be constructed as traveling screens, rotating drum screens, rotating disc screens, or fish screens (Pankratz, 1988).

Traveling Screens

Traveling screens are the most common type of coarse screen. They are used in water intakes to protect treatment plant equipment from debris and at wastewater treatment plants to remove debris from the raw sewage. They consist of flat panels of woven wire mesh supported on steel frames. The panels are hinged together to form continuous belt loops that are mounted on motor-driven shafts and sprockets. Traveling screens are used to remove debris smaller than 2 in., and the mesh openings are generally about 1/8 in. to 3/4 in., typically 1/4 to 3/8 in. Traveling screens are often preceded by bar racks to prevent damage by large objects. When used in water intakes in cold or temperate climates, the approach velocity to traveling screens is normally kept below 0.5 ft/sec in order to prevent the formation of frazil ice, to prevent resuspension of sediment near the intake, and to permit fish to swim away.

Traveling screens are cleaned intermittently by advancing the continuous belt so that dirty panels are lifted out of the water. The panels are cleaned by high-pressure water sprays, and the removed debris is deposited into a drainage channel for removal.

Traveling screens may be installed so that their face is either perpendicular to the flow or parallel to it, and either one or both sides of the continuous belt loop may be used for screening. The alternatives are as follows (Pankratz, 1988):

- Direct, through, or single flow — The screen is installed perpendicular to the flow, and only the outer face of the upstream side of the belt screens the flow. The chief advantage to this design is the simplicity of the inlet channel.
- Dual flow — The screen is installed so that both the ascending and descending sides of the belt screen the flow. This is accomplished either by arranging the inlet and outlet channels so that (1) the flow enters through the outside face of the loop and discharges along the center axis of the loop (dual entrance, single exit) or (2) the flow enters along the central axis of the loop and discharges through the inner face of the loop (single entrance, dual exit). The chief advantage to this design is that both sides of the belt loop screen the water, and the required screen area is half that of a direct flow design.

Rotating Drum Screens

In drum screens, the wire mesh is wrapped around a cylindrical framework, and the cylinder is partially submerged in the flow, typically to about two-thirds to three-fourths of the drum diameter. As the mesh becomes clogged, the drum is rotated, and high-pressure water sprays mounted above the drum remove the debris.

The flow may enter the drum along its central axis and exit through the inner face of the drum or enter the drum through the outer face of the mesh and exit along its central axis. The flow along the central axis may be one way, in which case one end of the drum is blocked, or two way.

Rotating Disc Screens

In disc screens, the wire mesh is supported on a circular disc framework, and the disc is partially submerged in the flow, typically to about two-thirds to three-fourths of the disc diameter. As the mesh becomes clogged, the disc is rotated, and the mesh is cleaned by a high-pressure water spray above it. The discs may be mounted so that the disc plane is either vertical or inclined.

For reasons of economy, disc screens are normally limited to flows less than 20,000 gpm (Pankratz, 1988).

Fish Screens

Surface water intakes must be designed to minimize injury to fish by the intake screens. This generally entails several design and operating features and may require consultation with fisheries biologists (Pankratz, 1988):

- Small mesh sizes — Mesh sizes should be small enough to prevent fish from becoming lodged in the openings.
- Low intake velocities — The clean screen should have an approach velocity of less than 0.5 fps to permit fish to swim away.
- Continuous operation — This minimizes the amount of debris on the screen and the local water velocities near the screen surface, which enables fish to swim away.
- Escape routes — The intake structure should be designed so that the screen is not at the downstream end of a channel. This generally means that the intake channel should direct flow parallel or at an angle to the screens with an outlet passage downstream of the screens.
- Barriers — The inlet end of the intake channel should have some kind of fish barrier, such as a curtain of air bubbles.

- Fish pans and two-stage cleaning — The screen panels should have a tray on their bottom edge that will hold fish in a few inches of water as the panels are lifted out of the flow. As the screen rotates over the top sprocket, the fish tray should dump its contents into a special discharge channel, and the screen and tray should be subjected to a low-pressure water spray to move the fish through the channel back to the water source. A second, high-pressure water spray is used to clean the screen once the fish are out of the way.

Wire Mesh Head Losses

Traveling screens are usually cleaned intermittently when the headloss reaches 3 to 6 in. The maximum design headloss for structural design is about 5 ft (Pankratz, 1988).

The headloss through a screen made of vertical, round, parallel wires or rods is (Blevins, 1984)

$$h_L = 0.52 \cdot \frac{1 - \epsilon^2}{\epsilon^2} \cdot \frac{U^2}{2g} \quad (9.2)$$

if

$$Re = \frac{\rho U d}{\epsilon \mu} > 500 \quad (9.3)$$

and

$$0.10 < \epsilon < 0.85 \quad (9.4)$$

where

- d = the diameter of the wires or rods in a screen (m)
- g = the acceleration due to gravity (9.806 65 m/s²)
- s = the distance between wire or rod centers in a screen (m)
- U = the approach velocity (m/sec or ft/sec)
- ϵ = the screen porosity, i.e., the ratio of the open area measured at the closest approach of the wires to the total area occupied by the screen (dimensionless)
- $= \frac{s-d}{s}$
- μ = the dynamic viscosity of water (N·sec/m²)
- ρ = the water density (kg/m³)

Blevins (1984) gives headloss data for a wide variety of other screen designs.

Comminutors and In-Line Grinders

Comminutors and in-line grinders are used to reduce the size of objects in raw wastewater. They are supposed to eliminate the need for coarse screens and screenings handling and disposal. They require upstream bar screens for protection from impacts from large debris.

Comminutors consist of a rotating, slotted drum that acts as a screen, and peripheral cutting teeth and shear bars that cut down objects too large to pass through the slots and that are trapped on the drum surface. The flow is from outside the drum to its inside. Typical slot openings are 1/4 to 3/8 in. Typical headlosses are 2 to 12 in.

In-line grinders consist of pairs of counterrotating, intermeshing cutters that shear objects in the wastewater. The product sizes also are typically 1/4 to 3/8 in., and the headlosses are typically 12 to 18 in.

Both in-line grinders and comminutors tend to produce “ropes” and “balls” from cloth, which can jam downstream equipment. If the wastewater contains large amounts of rags and solids, in-line grinders and comminutors may require protection by upstream coarse screens, which defeats their function. Comminutors and in-line grinders also chop up plastics and other nonbiodegradable materials, which

end up in wastewater sludges and may prevent disposal of the sludges on land because of aesthetics. Comminutors and in-line grinders are also subject to wear from grit and require relatively frequent replacement. Comminutors and, to a lesser extent, in-line grinders, are nowadays not recommended (Joint Task Force, 1992).

Fine Screens

Fine screens are sometimes used in place of clarifiers, in scum dewatering and in concentrate and sludge screening. In wastewater treatment, they are preceded by bar screens for protection from impact by large debris, but not by comminutors, because screen performance depends on the development of a “precoat” of solids. Fine screens generally remove fewer solids from raw sewage than do primary settling tanks, say 15 to 30% of suspended solids for openings of 1 to 6 mm (Joint Task Force, 1992). There are four kinds of fine screens (Hazen and Sawyer, Engineers, 1975; Metcalf & Eddy, Inc., 1991; Pankratz, 1988).

Continuous-Belt Fine Screens

Continuous-belt fine screens consist of stainless steel wedgewire elements mounted on horizontal supporting rods and forming a continuous belt loop. As the loop moves, the clogged region of the screen is lifted out of the water. The supporting rods or the upper head sprocket mount blades fit between the wires and dislodge accumulated debris as the wires are carried over the head sprocket. A supplementary brush or doctor blade may be used to remove sticky material.

The openings between the wires are generally between 3/16 to 1/2 in. The openings in continuous-belt fine screens are usually too coarse for use as primary sewage treatment devices, although they may be satisfactory for some industrial wastewaters containing fibrous or coarse solids.

Rotary Drum Fine Screens

In rotary drum fine screens, stainless steel wedgewire is wrapped around a horizontal cylindrical framework that is partially submerged. Generally, about 75% of the drum diameter and 66% of its mesh surface area are submerged. As the drum rotates, dirty wire is brought to the top, where it is cleaned by high-pressure water sprays and doctor blades.

The flow direction may be in along the drum axis and out through the inner surface of the wedgewire or in through the outer surface of the wedgewire and out along the axis.

Common openings are 0.01 to 0.06 in. (0.06 in. is preferred for raw wastewater), and the usual wire diameter is 0.06 in. Typical hydraulic loadings are 16 to 112 gpm/ft², and typical suspended solids removals for raw municipal sewage are 5 to 25%.

Inclined, Self-Cleaning Static Screens

Inclined, self-cleaning, static screens consist of inclined panes of stainless steel wedgewire. The wire runs horizontally. The flow is introduced at the top of the screen, and it travels downwards along the screen surface. Solids are retained on the surface, and screened water passes through it and is collected underneath the screen. As solids accumulate on the screen surface, they impede the water flow, which causes the water to move the solids downwards to the screen bottom.

Common openings are 0.01 to 0.06 in. (determined by *in situ* tests), and the usual wire diameter is 0.06 in. Typical hydraulic loadings are 4 to 16 gpm/in. of screen width, and typical suspended solids removals for raw municipal sewage are 5 to 25%.

Disc Fine Screens

Disc fine screens consist of flat discs of woven stainless steel wire supported on steel frameworks and partially submerged in the flow. As the disc rotates, the dirty area is lifted out of the flow and cleaned by high-pressure water sprays.

The mesh openings are generally about 1/32 in.

Disc fine screens are limited to small flows, generally less than 20,000 gpm for reasons of economy (Pankratz, 1988).

Microscreens

Microscreens are used as tertiary suspended solids removal devices following biological wastewater treatment and secondary clarification (Hazen and Sawyer, Engineers, 1975). Typical mesh openings are 20 to 25 μm and range from about 15 to 60 μm . The hydraulic loading is typically 5 to 10 gpm/ft^2 of submerged area. The suspended solids removal from secondary clarifier effluents is about 40 to 60%. Effluent suspended solids concentrations are typically 5 to 10 mg/L .

Most microscreens are rotary drums, but there are some disc microscreens. These are similar to rotary drum and disc fine screens, except for the mesh size and material, which is usually a woven polyester fiber.

Microscreen fabrics gradually become clogged despite the high-pressure water sprays, and the fabric must be removed from the drum or disc for special cleaning every few weeks.

Orifice Walls

Orifice walls are sometimes installed in the inlet zones of sedimentation tanks to improve the lateral and vertical distribution of the flow. Orifice walls will not disperse longitudinal jets, and if jet formation cannot be prevented, it may be desirable to install adjustable vertical vanes to redirect the flow over the inlet cross section.

The relationship between head across an orifice and the flow through it is (King and Brater, 1963):

$$Q = C_D A \sqrt{2gh_L} \quad (9.5)$$

Empirical discharge coefficients for sharp-edged orifices of any shape lie between about 0.59 and 0.66, as long as the orifice Reynolds number is larger than about 10^5 , which is usually the case (Lea, 1938; Smith and Walker, 1923). Most of the results are close to 0.60.

Orifice Reynolds number:

$$\left(Re = d \sqrt{gh_L} / \nu \right)$$

In Hudson's (1981) design examples, the individual orifices are typically 15 to 30 cm in diameter, and they are spaced 0.5 to 1.0 m apart. The jets from these orifices will merge about six orifice diameters downstream from the orifice wall — which would be about 1 to 2 m in Hudson's examples — and that imaginary plane should be taken as the boundary between the inlet zone and settling zone.

References

- Babbitt, H.E., Doland, J. J., and Cleasby, J.L. 1967. *Water Supply Engineering*, 6th ed. McGraw-Hill Book Co., Inc., New York.
- Blevins, R.D. 1984. *Applied Fluid Dynamics Handbook*. Van Nostrand Reinhold Co., Inc., New York.
- Hardenbergh, W.A. and Rodie, E.B. 1960. *Water Supply and Waste Disposal*. International Textbook Co., Scranton, PA.
- Hazen and Sawyer, Engineers. 1975. *Process Design Manual for Suspended Solids Removal*, EPA 625/1-75-003a. U.S. Environmental Protection Agency, Technology Transfer, Washington, DC.
- Hudson, H.E., Jr. 1981. *Water Clarification Processes: Practical Design and Evaluation*. Van Nostrand Reinhold Co., New York.
- Joint Task Force of the Water Environment Federation and the American Society of Civil Engineers. 1992. *Design of Municipal Wastewater Treatment Plants: Volume I — Chapters 1-12, WEF Manual of Practice No. 8, ASCE Manual and Report on Engineering Practice No. 76*. Water Environment Federation, Alexandria, VA; American Society of Civil Engineers, New York.
- King, H.W. and Brater, E.F. 1963. *Handbook of Hydraulics for the Solution of Hydrostatic and Fluid-Flow Problems*, 5th ed. McGraw-Hill, Inc., New York.

- Lea, F.C. 1938. *Hydraulics: For Engineers and Engineering Students*, 6th ed. Edward Arnold & Co., London.
- Metcalf & Eddy, Inc. 1991. *Wastewater Engineering: Treatment, Disposal and Reuse*, 3rd ed., revised by G. Tchobanoglous and F.L. Burton. McGraw-Hill, Inc., New York.
- Pankratz, T.M. 1988. *Screening Equipment Handbook: For Industrial and Municipal Water and Wastewater Treatment*. Technomic Publishing Co., Inc., Lancaster, PA.
- Smith, D. and Walker, W.J. 1923. "Orifice Flow," *Proceedings of the Institution of Mechanical Engineers*, 1(1): 23.

9.2 Chemical Reactors

Hydraulic Retention Time

Regardless of tank configuration, mixing condition, or the number or volume of recycle flows, the average residence for water molecules in a tank is as follows (Wen and Fan, 1975),

$$\tau = \frac{V}{Q} \quad (9.6)$$

- where τ = the hydraulic retention time (s)
 V = the active liquid volume in the tank (m³)
 Q = the volumetric flow rate through the tank not counting any recycle flows (m³/s)

Note that Q does not include any recycle flows. The *hydraulic retention time* is also called the *hydraulic detention time* and, by chemical engineers, the *space time*. It is often abbreviated HRT.

Reaction Order

The reaction order is the apparent number of reactant molecules participating in the reaction. Mathematically, it is the exponent on the reactant concentration in the rate expression:

$$r_{1,2} = kC_1^p C_2^q \quad (9.7)$$

- where C_1 = the concentration of substance 1 (mol/L)
 C_2 = the concentration of substance 2 (mol/L)
 k = the reaction rate coefficient (units vary)
 p = the reaction order of substance 1 (dimensionless)
 q = the reaction order of substance 2 (dimensionless)
 $r_{1,2}$ = the rate of reaction of components 1 and 2 (units vary)

In this case, the reaction rate is p th order with respect to substance 1 and q th order with respect to substance 2.

Many biological reactions are represented by the Monod equation (Monod, 1942):

$$r = \frac{r_{\max} \cdot C}{K_C + C} \quad (9.8)$$

- where r_{\max} = the maximum reaction rate (units vary, same as r)
 K_C = the affinity constant (same units as C)

The Monod function is an example of a "mixed" order rate expression, because the rate varies from first order to zero order as the concentration increases.

The units of the reaction rate vary depending on the mass balance involved. In general, one identifies a control volume (usually one compartment or differential volume element in a tank) and constructs a

mass balance on some substance of interest. The units of the reaction rate will then be the mass of the substance per unit volume per time. The units of the rate constant will be determined by the need for dimensional consistency.

It is important to note that masses in chemical reaction rates have identities, and they do not cancel. Consequently, the ratio kg COD/kg VSS·s does not reduce to 1/s. This becomes obvious if it is remembered that the mass of a particular organic substance can be reported in a variety of ways: kg, mol, BOD, COD, TOC, etc. The ratios of these various units are not unity, and the actual numerical value of a rate will depend on the method of expression of the mass.

Many reactions in environmental engineering are represented satisfactorily as first order. This is a consequence of the fact that the substances are contaminants, and the goal of the treatment process is to reduce their concentrations to very low levels. In this case, the Maclaurin series representation of the rate expression may be truncated to the first-order terms:

$$r(C_1) = \underbrace{r(0)}_{=0} + \underbrace{(C_1 - 0) \frac{\partial r}{\partial C_1} \Big|_{C_1=0}}_{\text{first order in } C_1} + \underbrace{\text{higher order terms}}_{\text{truncated}} \quad (9.9)$$

Many precipitation and oxidation reactions are first order in the reactants. Disinfection is frequently first order in the microbial concentration, but the order of the disinfectant may vary. Flocculation is second order. Substrate removal reactions in biological processes generally are first order at low concentration and zero order at high concentration.

Effect of Tank Configuration on Removal Efficiency

The general steady state removal efficiency is,

$$E = \frac{C_o - C}{C_o} \quad (9.10)$$

This is affected by the reaction kinetics and the hydraulic regime in the reactor.

Completely Mixed Reactors

The completely mixed reactor (CMR) is also known as the continuous flow, stirred tank reactor (CFSTR or, more commonly, CSTR). Because of mixing, the contents of the tank are homogeneous, and a mass balance yields:

$$\frac{dVC}{dt} = QC_o - QC - kC^nV \quad (9.11)$$

where C = the concentration in the homogeneous tank and its effluent flow (kg/m³ or slug/ft³)
 C_o = the concentration in the influent liquid (kg/m³ or slug/ft³)
 k = the reaction rate constant (here, m³ⁿ/kgⁿ·sec or ft³ⁿ/slugⁿ·sec)
 n = the reaction order (dimensionless)
 Q = the volumetric flow rate (m³/s or ft³/sec)
 V = the tank volume (m³ or ft³)
 t = elapsed time (s)

The steady state solution is,

$$\frac{C}{C_o} = \frac{1}{1 + kC^{n-1}\tau} \quad (9.12)$$

For first-order reactions, this becomes,

$$\frac{C}{C_o} = \frac{1}{1+k\tau} \quad (9.13)$$

In the case of zero-order reactions, the steady state solution is,

$$C_o - C = k\tau \quad (9.14)$$

If the mixing intensity is low, CSTRs may develop “dead zones” that do not exchange water with the inflow.

If the inlets and outlets are poorly arranged, some of the inflow may pass directly to the outlet without mixing with the tank contents. This latter phenomenon is called “short-circuiting.” In the older literature, short-circuiting and complete mixing were often confused. They are opposites. Short-circuiting cannot occur in a tank that is truly completely mixed.

Short-circuiting in clarifiers is discussed separately, below.

The analysis of short-circuiting and dead zones in mixed tanks is due to Cholette and Cloutier (1959) and Cholette et al. (1960). For a “completely mixed” reactor with both short-circuiting and dead volume, the mass balance of an inert tracer on the mixed volume is:

$$\underbrace{f_m V \frac{dC_m}{dt}}_{\text{accumulation in mixed volume}} = \underbrace{(1-f_s)QC_o}_{\text{fraction of influent entering mixed volume}} - \underbrace{(1-f_s)QC_m}_{\text{flow leaving mixed volume}} \quad (9.15)$$

where C_m = the concentration of tracer in the mixed zone (kg/m^3)

C_o = the concentration of tracer in the feed (kg/m^3)

f_m = the fraction of the reactor volume that is mixed (dimensionless)

f_s = the fraction of the influent that is short-circuited directly to the outlet (dimensionless)

The observed effluent is a mixture of the short-circuited flow and the flow leaving the mixed zone:

$$QC = f_s QC_o + (1-f_s)QC_m \quad (9.16)$$

Consequently, for a slug application of tracer (in which the influent momentarily contains some tracer and is thereafter free of it), the observed washout curve is,

$$\frac{C}{C_i} = (1-f_s) \exp \left\{ -\frac{(1-f_s)Qt}{f_m V} \right\} \quad (9.17)$$

where C_i = the apparent initial concentration (kg/m^3).

Equation (9.17) provides a convenient way to determine the mixing and flow conditions in “completely mixed” tanks. All that is required is a slug tracer study. The natural logarithms of the measured effluent concentrations are then plotted against time, and the slope and intercept yield the values of the fraction short-circuited and the fraction mixed.

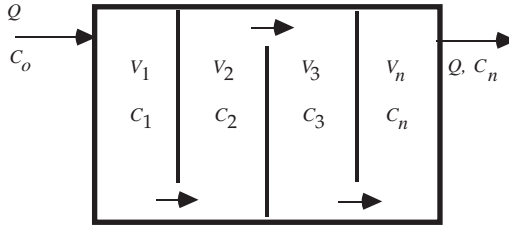


FIGURE 9.1 Mixed-cells-in-series flow pattern.

Mixed-Cells-in-Series

Consider the rapid mixing tank shown in Fig. 9.1. This particular configuration is called “mixed-cells-in-series” or “tanks-in-series,” because the liquid flows sequentially from one cell to the next. Each cell has a mixer, and each cell is completely mixed. Mixed-cells-in-series is the usual configuration for flocculation tanks and activated sludge aeration tanks.

The flow is assumed to be continuous and steady, and each compartment has the same volume, i.e., $V_1 = V_2 = V_3 = \dots = V_n$. The substance concentrations in the first through last compartments are $C_1, C_2, C_3, \dots, C_n$, respectively. The substance mass balance for each compartment has the same mathematical form as Eq. (9.11), above, and the steady state concentration in each compartment is given by Eq. (9.12) (Hazen, 1904; MacMullin and Weber, 1935; Kehr, 1936; Ham and Coe, 1918; Langelier, 1921).

Because of the mixing, the concentration in the last compartment is also the effluent concentration. Consequently, the ratio of effluent to influent concentrations is:

$$\frac{C_n}{C_o} = \frac{C_1}{C_o} \cdot \frac{C_2}{C_1} \cdot \frac{C_3}{C_2} \cdot \dots \cdot \frac{C_n}{C_{n-1}} \quad (9.18)$$

Because all compartments have the same volume and process the same flow, all their HRTs are equal. Therefore, for a first-order reaction, Eq. (9.18) becomes,

$$\frac{C_n}{C_o} = \left(\frac{1}{1 + k\tau_1} \right)^n \quad (9.19)$$

where τ_1 = the HRT of a single compartment (s)
 $= V/nQ$
 n = the number of mixed-cells-in-series

Equation (9.19) has significant implications for the design of all processing tanks used in natural and used water treatment. Suppose that all the internal partitions in Fig. 9.1 are removed, so that the whole tank is one completely mixed, homogenous compartment. Because there is only one compartment, its HRT is n times the HRT of a single compartment in the partitioned tank. Now, divide Eq. (9.12) by Eq. (9.19) and expand the bracketed term in Eq. (9.19) by the binomial theorem:

$$\frac{C(\text{one cell})}{C_n(\text{n cells})} = \frac{1 + nk\tau_1 + \frac{n(n-1)}{2!}(k\tau_1)^2 + \dots + (k\tau_1)^n}{1 + nk\tau_1} > 1 \quad (9.20)$$

Therefore, the effect of partitioning the tank is to reduce the concentration of reactants in its effluent, i.e., to increase the removal efficiency.

The effect of partitioning on second- and higher-order reactions is even more pronounced. Partitioning has no effect in the case of zero-order reactions (Levenspiel, 1972).

The efficiency increases with the number of cells. It also increases with the hydraulic retention time. This means that total tank volume can be traded against the number of cells. A tank can be made smaller — more economical — and still achieve the same degree of particle destabilization, if the number of compartments in it is raised.

Ideal Plug Flow

As n becomes very large, the compartments approach differential volume elements, and, if the partitions are eliminated, the concentration gradient along the tank becomes continuous. The result is an “ideal plug flow” tank. The only transport mechanism along the tank is advection: there is no dispersion. This means that water molecules that enter the tank together stay together and exit together. Consequently, ideal plug flow is hydraulically the same as batch processing. The distance traveled along the plug flow tank is simply proportional to the processing time in a batch reactor, and the coefficient of proportionality is the average longitudinal velocity.

Referring to Fig. 9.2, the mass balance on a differential volume element is:

$$\frac{\partial C}{\partial t} = -U \frac{\partial C}{\partial x} - kC^p \quad (9.21)$$

where U = the plug flow velocity (m/sec or ft/sec).

For steady state conditions, this becomes for reaction orders greater than one:

$$C^{1-p} = C_o^{1-p} - (1-p)k\tau \quad (9.22)$$

For first-order reactions, one gets,

$$C = C_o \exp\{-k\tau\} \quad (9.23)$$

The relative efficiencies of ideal plug flow tanks and tanks that are mixed-cells-in-series is easily established. In the case of first-order reactions, the power series expansion of the exponential is,

$$\exp\{-k\tau\} = 1 - k\tau + \frac{(k\tau)^2}{2!} - \frac{(k\tau)^3}{3!} + \dots < \lim_{n \rightarrow \infty} \left(\frac{1}{1 + k\tau_1} \right)^n \quad (9.24)$$

Consequently, ideal plug flow tanks are the most efficient; completely mixed tanks are the least efficient; and tanks consisting of mixed-cells-in-series are intermediate.

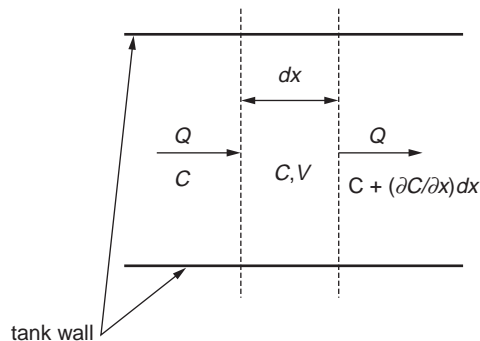


FIGURE 9.2 Control volume for ideal plug-flow mass balance.

Plug Flow with Axial Dispersion

Of course, no real plug flow tank is ideal. If it contains mixers, they will break down the concentration gradients and tend to produce a completely mixed tank. Furthermore, the cross-sectional velocity variations induced by the wall boundary layer will produce a longitudinal mixing called shear-flow dispersion. Shear-flow dispersion shows up in the mass balance equation as a “diffusion” term, so Eq. (9.21) should be revised as follows:

$$\frac{\partial C}{\partial t} = K \frac{\partial^2 C}{\partial x^2} - U \frac{\partial C}{\partial x} - kC^p \quad (9.25)$$

where K = the (axial) shear flow dispersion coefficient (m^2/s or ft^2/sec).

Langmuir’s (1908) boundary conditions for a tank are:

Inlet:

$$x = 0; \quad QC_o = QC - KA \frac{dC}{dx} \quad (9.26)$$

Outlet:

$$x = L; \quad \frac{dC}{dx} = 0 \quad (9.27)$$

where A = the cross-sectional area of the reactor (m^2 or ft^2)

L = the length of the reactor (m or ft).

The first condition is a mass balance around the tank inlet. The rate of mass flow (kg/sec) approaching the tank inlet in the influent pipe must equal the mass flow leaving the inlet in the tank itself. Transport within the tank is due to advection and dispersion, but dispersion in the pipe is assumed to be negligible, because the pipe velocity is high. The outlet condition assumes that the reaction is nearly complete — which is, of course, the goal of tank design — so the concentration gradient is nearly zero, and there is no dispersive flux. The Langmuir boundary conditions produce a formula that reduces the limit to ideal plug flow as K approaches zero and to ideal complete mixing as K approaches infinity. A correct formula must do this. No other set of boundary conditions produces this result (Wehner and Wilhelm, 1956; Pearson, 1959; Bishoff, 1961; Fan and Ahn, 1963). The general solution is (Danckwerts, 1953):

$$\frac{C}{C_o} = \frac{4a \cdot \exp\left\{\frac{1}{2}(1+a)Pe\right\}}{(1+a)^2 \cdot \exp\{aPe\} - (1-a)^2} \quad (9.28)$$

where a = part of the solution to the characteristic equation of the differential equation ($1/\text{m}$ or $1/\text{ft}$)

$$= \sqrt{1 + \frac{4kK}{U^2}}$$

Pe = the turbulent Peclet number (dimensionless)

$$= UL/K$$

A tank with axial dispersion has an efficiency somewhere between ideal plug flow and ideal complete mixing. Consequently, a real plug flow tank with axial dispersion behaves as if it were compartmentalized. The equivalence of the number of compartments and the shear flow diffusivity can be represented by (Levenspiel and Bischoff, 1963):

$$\frac{1}{n} = 2 \cdot Pe^{-1} - 2 \cdot Pe^{-2} \cdot \left[1 - \exp\{-Pe^{-1}\}\right] \quad (9.29)$$

The axial dispersion — and, consequently, the Peclet number — in pipes and ducts has been extensively studied, and the experimental results can be summarized as follows (Wen and Fan, 1975):

Reynolds numbers less than 2000:

$$\frac{1}{Pe} = \frac{1}{Pe \cdot Sc} + \frac{Re \cdot Sc}{192} \quad (9.30)$$

Reynolds numbers greater than 2000:

$$\frac{1}{Pe} = \frac{30 \cdot 10^6}{Re^{2.1}} + \frac{1.35}{Re^{1/8}} \quad (9.31)$$

where D = the molecular diffusivity of the substance (m²/s or ft²/sec)
 d = the pipe or duct diameter (m or ft)
 Pe = the duct Peclet number (dimensionless)
 $= Ud/K$
 Re = the duct Reynolds number (dimensionless)
 $= Ud/\nu$
 ν = the kinematic viscosity (m²/s or ft²/sec)
 Sc = the Schmidt number (dimensionless)
 $= \nu/D$

These formulae assume that the dispersion is generated entirely by the shear flow of the fluid in the pipe or duct. When mixers are installed in tanks, Eqs. (9.30) and (9.31) no longer apply, and the axial dispersion coefficient must be determined experimentally.

More importantly, the use of mixers generally results in very small Peclet numbers, and the reactors tend to approach completely mixed behavior, which is undesirable, because the efficiency is reduced. Thus, there is an inherent contradiction between high turbulence and ideal plug flow, both of which are wanted in order to maximize tank efficiency. The usual solution to this problem is to construct the reactor as a series of completely mixed cells. This allows the use of any desired mixing power and preserves the reactor efficiency.

References

- Bishoff, K.B. 1961. "A Note on Boundary Conditions for Flow Reactors," *Chemical Engineering Science*, 16(1/2): 131.
- Cholette, A. and Cloutier, L. 1959. "Mixing Efficiency Determinations for Continuous Flow Systems," *Canadian Journal of Chemical Engineering*, 37(6): 105.
- Cholette, A., Blanchet, J., and Cloutier, L. 1960. "Performance of Flow Reactors at Various Levels of Mixing," *Canadian Journal of Chemical Engineering*, 38(2): 1.
- Dankwerts, P.V. 1953. "Continuous Flow Systems — Distribution of Residence Times," *Chemical Engineering Science*, 2(1): 1.
- Fan, L.-T. and Ahn, Y.-K. 1963. "Frequency Response of Tubular Flow Systems," *Process Systems Engineering, Chemical Engineering Progress Symposium* No. 46, vol. 59(46): 91.
- Ham, A. and Coe, H.S. 1918. "Calculation of Extraction in Continuous Agitation," *Chemical and Metallurgical Engineering*, 19(9): 663.
- Hazen, A. 1904. "On Sedimentation," *Transactions of the American Society of Civil Engineers*, 53: 45.
- Kehr, R.W. 1936. "Detention of Liquids Being Mixed in Continuous Flow Tanks," *Sewage Works Journal*, 8(6): 915.
- Langelier, W.F. 1921. "Coagulation of Water with Alum by Prolonged Agitation," *Engineering News-Record*, 86(22): 924.

- Langmuir, I. 1908. "The Velocity of Reactions in Gases Moving Through Heated Vessels and the Effect of Convection and Diffusion," *Journal of the American Chemical Society*, 30(11): 1742.
- Levenspiel, O. 1972. *Chemical Reaction Engineering*, 2nd ed., John Wiley & Sons, Inc., New York.
- Levenspiel, O. and Bischoff, K.B. 1963. "Patterns of Flow in Chemical Process Vessels," *Advances in Chemical Engineering*, 4: 95.
- MacMullin, R.B. and Weber, M. 1935. "The Theory of Short-Circuiting in Continuous-Flow Mixing Vessels in Series and the Kinetics of Chemical Reactions in Such Systems," *Transactions of the American Institute of Chemical Engineers*, 31(2): 409.
- Monod, J. 1942. "Recherches sur la croissance des cultures bacteriennes," *Actualités Scientifiques et Industrielles*, No. 911, Hermann & Cⁱ.e., Paris.
- Pearson, J.R.A. 1959. "A Note on the 'Danckwerts' Boundary Conditions for Continuous Flow Reactors," *Chemical Engineering Science*, 10(4): 281.
- Wehner, J.F. and Wilhelm, R.H. 1956. "Boundary Conditions of Flow Reactor," *Chemical Engineering Science*, 6(2): 89.
- Wen, C.Y. and Fan, L.T. 1975. *Models for Flow Systems and Chemical Reactors*, Marcel Dekker, Inc., New York.

9.3 Mixers And Mixing

The principal objects of mixing are (1) blending different liquid streams, (2) suspending particles, and (3) mass transfer. The main mass transfer operations are treated in separate sections below. This section focuses on blending and particle suspension.

Mixing Devices

Mixing devices are specialized to either laminar or turbulent flow conditions.

Laminar/High Viscosity

Low-speed mixing in high-viscosity liquids is done in the laminar region with impeller Reynolds numbers below about 10. (See below.) The mechanical mixers most commonly used are:

- Gated anchors and horseshoes (large U-shaped mixers that fit against or near the tank wall and bottom, usually with cross members running between the upright limbs of the U called gates)
- Helical ribbons
- Helical screws
- Paddles
- Perforated plates (usually in stacks of several separated plates having an oscillatory motion, with the flat portion of the plate normal to the direction of movement)

Turbulent/Low to Medium Viscosity

High-speed mixing in low- to moderate-viscosity fluids is done in the turbulent region with impeller Reynolds numbers above 10,000. The commonly used agitators are:

- Anchors and horseshoes
- Disk (either with or without serrated or sawtooth edge for high shear)
- Jets
- Propellers
- Static in-line mixers (tubing with internal vanes fixed to the inner tubing wall that are set at an angle to the flow to induce cross currents in the flow)
- Radial flow turbines [blades are mounted either to a hub on the drive shaft or to a flat disc (Rushton turbines) attached to the drive shaft; blades are oriented radially and may be flat with the flat side

oriented perpendicular to the direction of rotation or curved with the convex side oriented perpendicular to the direction of rotation]

- Axial flow turbines [blades are mounted either to a hub on the drive shaft or to a flat disc (Rushton turbines) attached to the drive shaft; blades flat and pitched with the flat side oriented at an angle (usually 45°) to the direction of rotation]
- Smith turbines (turbines specialized for gas transfer with straight blades having a C-shaped cross section and oriented with the open part of the C facing the direction of rotation)
- Fluidfoil (having hub-mounted blades with wing-like cross sections to induce axial flow)

Power Dissipation

Fluid Deformation Power

Energy is dissipated in turbulent flow by the internal work due to volume element compression, stretching, and twisting (Lamb, 1932):

$$\frac{\Phi}{\mu} = 2\left(\frac{\partial u}{\partial x}\right)^2 + 2\left(\frac{\partial v}{\partial y}\right)^2 + 2\left(\frac{\partial w}{\partial z}\right)^2 + \left(\frac{\partial u}{\partial y} + \frac{\partial v}{\partial x}\right)^2 + \left(\frac{\partial u}{\partial z} + \frac{\partial w}{\partial x}\right)^2 + \left(\frac{\partial v}{\partial z} + \frac{\partial w}{\partial y}\right)^2 \quad (9.32)$$

where u, v, w = the local velocities in the x, y, z directions, respectively (m/s or ft/sec)

Φ = Stokes' (1845) energy dissipation function (W/m³ or ft lbf/ft³·sec)

μ = the absolute or dynamic viscosity (N s/m² or lbf sec/ft²)

The first three terms on the right-hand-side of Eq. (9.32) are compression and stretching terms, and the last three are twisting terms. The left-hand-side of Eq. (9.32) can also be written as:

$$\frac{\Phi}{\mu} = \frac{\varepsilon}{\nu} = \Gamma^2 \quad (9.33)$$

where ε = the local power dissipation per unit mass (watts/kg or ft·lbf/sec·slug)

ν = the kinematic viscosity (m²/s or ft²/sec)

Γ = the characteristic strain rate (per sec)

Equation (9.33) applies only at a point. If the total energy dissipated in a mixed tank is needed, it must be averaged over the tank volume. If the temperature and composition are uniform everywhere in the tank, the kinematic viscosity is a constant, and one gets,

$$\bar{\Gamma}^2 = \frac{1}{V} \iiint \varepsilon \cdot dx dy dz \quad (9.34)$$

where V = the tank volume (m³ or ft³)

$\bar{\Gamma}$ = the spatially averaged (root-mean-square) characteristic strain rate (per sec).

With this definition, the total power dissipated by mixing is,

$$P = \Phi V = \mu \bar{\Gamma}^2 V \quad (9.35)$$

where P = the mixing power (W or ft·lbf/sec).

Camp–Stein Theory

Camp and Stein (1943) assumed that the axial compression/stretching terms can always be eliminated by a suitable rotation of axes so that a differential volume element is in pure shear. This may not be true

for all three-dimensional flow fields, but there is numerical evidence that it is true for some (Clark, 1985). Consequently, the power expenditure per unit volume is,

$$\frac{dP}{dV} = \Phi = \mu \left[\left(\frac{\partial u}{\partial y} + \frac{\partial v}{\partial x} \right)^2 + \left(\frac{\partial u}{\partial z} + \frac{\partial w}{\partial x} \right)^2 + \left(\frac{\partial v}{\partial z} + \frac{\partial w}{\partial y} \right)^2 \right] = \mu G^2 \quad (9.36)$$

where dP = the total power dissipated deforming the differential volume element (N·m/sec, ft·lbf/sec)
 dV = the volume of the element (m³ or ft³)
 G = the absolute velocity gradient (per sec)
 Φ = Stoke's (1845) dissipation function (watts/m³ or lbf/ft²·sec)

If the velocity gradient is volume-averaged over the whole tank, one gets,

$$P = \mu \bar{G}^2 V \quad (9.37)$$

where \bar{G} = the root-mean-square (r.m.s.) velocity gradient (per sec).

The Camp–Stein r.m.s. velocity gradient is numerically identical to the r.m.s. characteristic strain rate, but (because of the unproved assumption of pure shear embedded in \bar{G}) $\bar{\Gamma}$ is the preferred concept. Camp and Stein used the assumption of pure shear to derive a formula for the flow around a particle and the resulting particle collision rate, thereby connecting the flocculation rate to \bar{G} and P . However, it is also possible to derive collision rate based on $\bar{\Gamma}$ (Saffman and Turner, 1956), which yields a better physical representation of the flocculation process and is nowadays preferred.

Energy Spectrum and Eddy Size

Mixing devices are pumps, and they create macroscopic, directed currents. As the currents flow away from the mixer, they rub against and collide with the rest of the water in the tank. These collisions and rubbings break off large eddies from the current. The large eddies repeat the process of collision/shear, producing smaller eddies, and these do the same until there is a spectrum of eddy sizes. The largest eddies in the spectrum are of the same order of size as the mixer. The large eddies move quickly, they contain most of the kinetic energy of the turbulence, and their motion is controlled by inertia rather than viscosity. The small eddies move slowly, and they are affected by viscosity.

The size of the smallest eddies is called the “Kolmogorov length scale” (Landahl and Mollo-Christensen, 1986):

$$\eta = \left(\frac{\nu^3}{\varepsilon} \right)^{1/4} \quad (9.38)$$

where ε = the power input per unit mass (watts/kg or ft·lbf/sec·slug)
 η = the Kolmogorov length (m or ft).

The Kolmogorov wave number is defined by custom as (Landahl and Mollo-Christensen, 1986):

$$k_K = \frac{1}{\eta} \quad (9.39)$$

where k_K = the Kolmogorov wave number (per m or per ft).

The general formula for the wave number is,

$$k = \frac{2\pi}{L} \quad (9.40)$$

where L = the wave length (m or ft).

The kinetic energy contained by an eddy is one-half the square of its velocity times its mass. It is easier to calculate the energy per unit mass, because this is merely one-half the square of the velocity. The mean water velocity in mixed tanks is small, so nearly all the kinetic energy of the turbulence is in the velocity fluctuations, and the kinetic energy density function can be defined in terms of these fluctuations:

$$E(k)dk = \frac{1}{2}(u_k^2 + v_k^2 + w_k^2)n(k)dk \quad (9.41)$$

where $E(k)dk$ = the total kinetic energy contained in the eddies between wave numbers k and $k + dk$
 m^2/s^2 or ft^2/sec^2

$n(k)dk$ = the number of eddies between the wave numbers k and $k + dk$ (dimensionless)

u_k, v_k, w_k = the components of the velocity fluctuation in the $x, y,$ and z directions for eddies in the wave length interval k to $k + dk$ (m/s or ft/sec)

A plot of $E(k)dk$ vs. k is called the energy spectrum. An energy spectrum plot can have a wide variety of shapes, depending on the power input and the system geometry (Brodkey, 1967). However, if the power input is large enough, all spectra contain a range of small-sized eddies that are a few orders of magnitude larger than the Kolmogorov length scale η . The turbulence in this range of eddy sizes is isotropic and independent of the geometry of the mixing device, although it depends on the power input. Consequently, it is called the “universal equilibrium range.” At very high power inputs, the universal equilibrium range subdivides into a class of larger eddies that are influenced only by inertial forces and a class of smaller eddies that are influenced by molecular viscous forces. These subranges are called the “inertial convective subrange” and the “viscous dissipation subrange,” respectively.

When the energy density, $E(k)$, is measured, the inertial convection subrange is found to occur at wave numbers less than about one-tenth the Kolmogorov wave length, and the viscous dissipation subrange lies entirely between about $0.1 k_K$ and k_K (Grant, Stewart, and Moillet, 1962; Stewart and Grant, 1962). Similar results have been obtained theoretically (Matsuo and Unno, 1981). Therefore, η is the diameter of the smallest eddy in the viscous dissipative subrange, and the largest eddy in the viscous dissipation subrange has a diameter of about $20\pi\eta$.

The relative sizes of floc particles and eddies is important in understanding how they interact. If the eddies are larger than the floc particles, they entrain the flocs and transport them. If the eddies are smaller than the flocs, the only interaction is shearing of the floc by the eddies. It is also important whether the flocs interact with the inertial convective subrange eddies or the viscous dissipative subrange eddies, because the formulae connecting eddy diameter and velocity with mixing power are different for the two subranges. In particular, a collision rate formula based on \bar{V} would be correct only in the viscous dissipative subrange (Cleasby, 1984).

Typical recommended \bar{V} values are on the order of 900/sec for rapid mixing tanks and 75/sec for flocculation tanks (Joint Committee, 1969). At 20°C, the implied power inputs per unit volume are about $0.81 \text{ m}^2/\text{sec}^3$ for rapid mixing and $0.0056 \text{ m}^2/\text{sec}^3$ for flocculation. The diameter of the smallest eddy in the viscous dissipative subrange in rapid mixing tanks is 0.030 mm, and the diameter of the largest eddy is 1.9 mm. The sizes of flocculated particles generally range from a few hundredths of a millimeter to a few millimeters, and the sizes tend to decline as the mixing power input rises (Boadway, 1978; Lagvankar and Gemmill, 1968; Parker, Kaufman, and Jenkins, 1972; Tambo and Watanabe, 1979; Tambo and Hozumi, 1979). Therefore, they are usually contained within the viscous dissipative subrange, or they are smaller than any possible eddy and lie outside the universal equilibrium range. In water treatment, only the viscous dissipative subrange processes need to be considered.

Turbines

An example of a typical rapid mixing tank is shown in Fig. 9.3. Such tanks approximate cubes or right cylinders; the liquid depth approximates the tank diameter. The impeller is usually a flat disc with several short blades mounted near the disc’s circumference. The blades may be flat and perpendicular to the

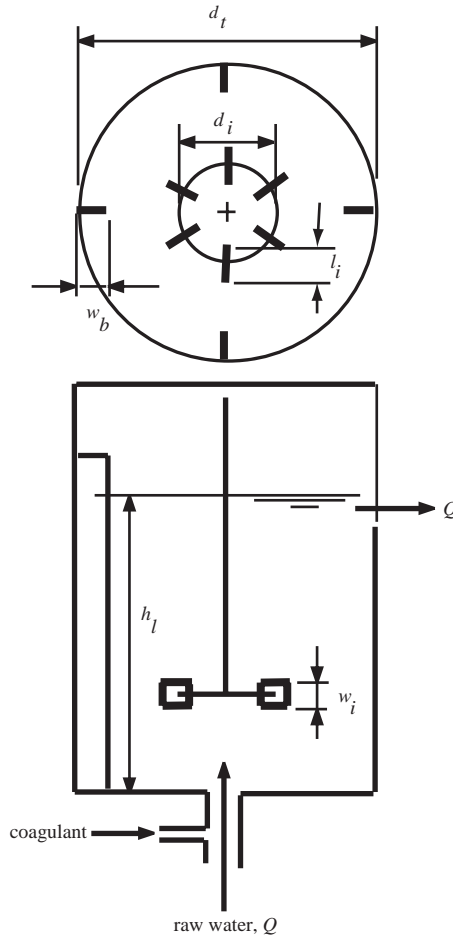


FIGURE 9.3 Turbine definition sketch.

disc, as shown, or they may be curved or pitched at an angle to the disc. The number of blades varies, but a common choice is six. Almost always, there are several baffles mounted along the tank wall to prevent vortexing of the liquid. The number of baffles and their width are design choices, but most commonly, there are four baffles.

The power dissipated by the turbulence in a tank is related to the geometry of the tank and mixer and the rotational speed of the mixer. Dimensional analysis suggests an equation of the following form (Rushton, Costich, and Everett, 1950):

$$Ru = f(\mathbf{Re}, \mathbf{Fr}, d_i, d_t, h_i, h_l, l_i, N_b, N_i, n_b, n_i, P_i, w_b, w_i) \quad (9.42)$$

- where
- d_i = the impeller diameter (m or ft)
 - d_t = the tank diameter (m or ft)
 - \mathbf{Fr} = the Froude number of the impeller (dimensionless)
 - $= \omega^2 d_i / g$
 - g = the acceleration due to gravity (m/s^2 or ft/sec^2)
 - h_l = the depth of liquid in the tank (m or ft)
 - h_i = the height of the impeller above the tank bottom (m or ft)
 - l_i = the impeller blade length (m or ft)

N_b = the baffle reference number, i.e., the number of baffles in some arbitrarily chosen “standard” tank (dimensionless)
 n_b = the number of baffles in the tank (dimensionless)
 N_i = the impeller reference number, i.e., the number of impeller blades on some arbitrarily chosen “standard” impeller (dimensionless)
 n_i = the number of impeller blades (dimensionless)
 P = the power dissipated by the turbulence (watts or ft·lbf/sec)
 p_i = the impeller blade pitch (m or ft)
 Re = the impeller Reynolds number (dimensionless)
 $= \omega d_i^2 / \nu$
 Ru = the Rushton power number (dimensionless)
 $= P / \rho \omega^3 d_i^5$
 w_b = the width of the baffles (m or ft)
 w_i = the impeller blade width (m or ft)
 ν = the kinematic viscosity of the liquid (m²/sec or ft²/sec)
 ρ = the mass density of the liquid (kg/m³ or slugs/ft³)
 ω = the rotational speed of the impeller (Hz, revolutions per sec)

The geometry of turbine/tank systems has been more or less standardized against the tank diameter (Holland and Chapman, 1966; Tatterson, 1994):

$$\frac{h_t}{d_t} = 1 \quad (9.43)$$

$$\frac{1}{6} \leq \frac{h_i}{d_t} \leq \frac{1}{2}; \text{ usually } d_i \quad (9.44)$$

$$\frac{1}{4} \leq \frac{d_i}{d_t} \leq \frac{1}{2}; \text{ usually } 1/3 \quad (9.45)$$

$$\frac{1}{6} \leq \frac{w_i}{d_t} \leq \frac{1}{4}; \text{ usually } 1/5 \quad (9.46)$$

$$\frac{l_i}{d_t} = \frac{1}{4}; \text{ for hub-mounted blades} \quad (9.47)$$

$$\frac{l_i}{d_t} = \frac{1}{8}; \text{ for disk-mounted blades} \quad (9.48)$$

$$\frac{1}{12} \leq \frac{w_b}{d_t} \leq \frac{1}{10}; \text{ usually } 1/10 \quad (9.49)$$

Turbines usually have six blades, and tanks usually have four baffles extending from the tank bottom to somewhat above the highest liquid operating level.

For any given tank, all the geometric ratios are constants, so the power number is a function of only the Reynolds number and the Froude number. Numerous examples of such relationships are given by Holland and Chapman (1966).

For impeller Reynolds numbers below 10, the hydraulic regime is laminar, and Eq. (9.42) is found experimentally to be,

$$Re \cdot Ru = \text{a constant} \quad (9.50)$$

The value of the constant is typically about 300, but it varies between 20 and 4000 (Tatterson, 1994). Equation (9.50) indicates that the power dissipation is proportional to the viscosity, the square of the impeller rotational speed and the cube of the impeller diameter:

$$P \propto \mu \omega^2 d_i^3 \quad (9.51)$$

For impeller Reynolds numbers above 10,000, the hydraulic regime is turbulent, and the experimental relationship for baffled tanks is,

$$Ru = \text{a constant} \quad (9.52)$$

Typical values of the constant are (Tatterson, 1994):

- Hub-mounted flat blades, 4
- Disk-mounted flat blades, 5
- Pitched blades, 1.27
- Propellers, 0.6

The power number for any class of impeller varies significantly with the details of the design. Impeller design and performance are discussed by Oldshue and Trussell (1991).

Equation (9.52) indicates that the power dissipation is proportional to the liquid density, the cube of the impeller rotational speed, and the fifth power of the impeller diameter:

$$P \propto \rho \omega^3 d_i^5 \quad (9.53)$$

The typical turbine installation operates in the turbulent region. Operation in the transition region between the laminar and turbulent zones is not recommended, because mass transfer rates in the transition region tend to be lower and less predictable than in the other regions (Tatterson, 1994).

Paddle Wheel Flocculators

A typical flocculation tank compartment is depicted in Fig. 9.4. Paddle flocculators similar to this design, but without the stators and baffles and with the axles transverse to the flow, were first introduced by Smith (1932). A set of flocculation paddles is mounted on a drive axle, which runs along the length of the compartment parallel to the flow. The axle may be continuous throughout the whole tank, or it may serve only one or two compartments. Alternatively, the axle may be mounted vertically in the compartment or horizontally but transverse to the flow. In these cases, each compartment has its own axle. The paddles are mounted parallel to the drive axle. The number of paddles may be the same in each compartment or may vary. The compartments in the flocculator are separated from each other by cross walls called “baffles.” The baffles are not continuous across the tank; there are openings between the baffles and tank walls so that water can flow from one compartment to the next. In Fig. 9.4, an opening is shown at one end of each baffle, and the openings alternate from one side of the tank to the other, so they do not line up. This arrangement minimizes short-circuiting. The spaces are sometimes put at the top or bottom of the baffles so as to force an over-and-under flow pattern. The compartments also contain stators. These are boards fixed to the baffle walls. They are intended to prevent the setup of a vortex in the compartment.

Although flocculator performance is usually correlated with tank-average parameters like \bar{V} and HRT, it should be remembered that the actual flocculation process occurs in the immediate vicinity of the paddles and their structural supports. The flow around the paddles and supports is sensitive to their exact geometry and their rotational speed. This means that precise prediction of flocculator performance

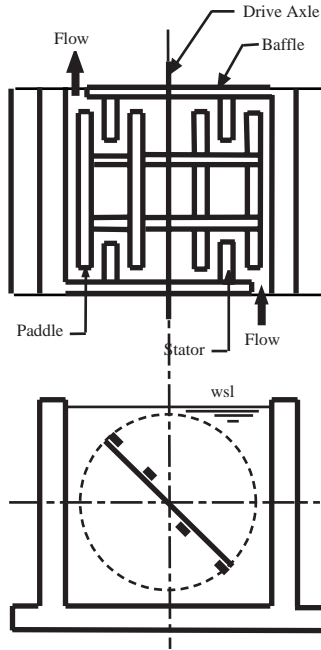


FIGURE 9.4 Flocculation tank plan and cross section.

requires the testing of full-scale units. Facilities may require redesign and reconstruction of the paddle system in the light of operating experience. Some engineers will prefer to specify commercially available paddle systems, which have demonstrated satisfactory performance on similar waters. Contracts with vendors should include performance specifications and guarantees.

Paddle geometry can be connected to power input by Camp's (1955) method. The drag force on the paddle is given by:

$$F_D = \frac{1}{2} C_D \rho A (v_p - v)^2 \quad (9.54)$$

- where
- F_D = the drag force on the paddle (N or lbf)
 - C_D = the drag coefficient (dimensionless)
 - A = the area of the paddle normal to the direction of movement (m^2 or ft^2)
 - v_p = the velocity of the paddle relative to the tank (m/s or ft/sec)
 - v = the velocity of the water relative to the tank (m/s or ft/sec)
 - ρ = the density of the water (kg/m^3 or slug/ft^3)

The power dissipated by the paddle is simply the drag force multiplied by the velocity of the paddle relative to the tank (not relative to the water, as is often incorrectly stated):

$$P_p = \frac{1}{2} C_D \rho A v_p (v_p - v)^2 \quad (9.55)$$

where P_p = the power dissipated by the paddle (W or ft·lb/sec).

Once steady state mixing is established, the water velocity will be some constant fraction of the paddle velocity, i.e., $v = kv_p$. The paddle speed is taken to be the speed of its centroid around the axle, which is related to its radial distance from the axle. Making these substitutions yields:

$$P_p = 4\pi^3 C_D \rho (1-k)^2 A r^3 \omega^3 \quad (9.56)$$

where k = the ratio of the water velocity to the paddle velocity (dimensionless)
 r = the radial distance of the centroid of the paddle to the axle (m or ft)
 ω = the rotational velocity of the paddle (revolutions/sec)

If the paddle is wide, the area should be weighted by the cube of its distance from the axle (Fair, Geyer, and Okun, 1968).

$$r^3 A = \int_{r_o}^{r_1} r^3 L dB = \frac{1}{4} (r_1 - r_o)^4 L \quad (9.57)$$

where B = the width of the paddle (m or ft)
 L = the length of the paddle (m or ft)
 r_1 = the distance of the outer edge of the paddle from the axle (m or ft)
 r_o = the distance of the inner edge of the paddle from the axle (m or ft)

This refinement changes Eq. (9.56) to:

$$P_p = \pi^3 C_D \rho (1-k)^2 (r_1 - r_o)^4 L \omega^3 \quad (9.58)$$

Equation (9.56) or Eq. (9.58) should be applied to each paddle and support in the tank, and the results should be summed to obtain the total power dissipation:

$$P = 4\pi^3 C_D \rho (1-k)^2 \omega^3 \sum_{i=1}^n A_i r_i^3 \quad (9.59)$$

$$P = \pi^3 C_D \rho (1-k)^2 \omega^3 \sum_{i=1}^n (r_{1,i} - r_{o,i})^4 L_i \quad (9.60)$$

Equations (9.59) and (9.60) provide the needed connection to the volume-averaged characteristic strain rate:

$$\bar{\Gamma}^2 = \frac{\epsilon}{\nu} = \frac{P}{\mu V} \quad (9.61)$$

It is generally recommended that the strain rate be tapering downwards from the inlet chamber to the outlet chamber, say from 100/sec to 50/sec. The tapering of $\bar{\Gamma}$ that is required can be achieved by reducing, from inlet to outlet, either the rotational speed of the paddle assemblies or the paddle area.

Another criterion sometimes encountered is the “Bean Number” (Bean, 1953). This is defined as the volume swept out by the elements of the paddle assembly per unit time — called the “displacement” — divided by the flow through the flocculation tank:

$$Be = \frac{2\pi\omega \sum_{i=1}^n r_i A_i}{Q} \quad (9.62)$$

where Be = the Bean number (dimensionless).

Bean’s recommendation, based on a survey of actual plants, is that Be should be kept between 30 and 40, if it is calculated using all the paddle assemblies in the flocculation tank (Bean, 1953). For a given facility, the Bean number is proportional to the spatially averaged characteristic strain rate and the total water power. However, the ratio varies as the square of the rotational speed.

The mixing conditions inside a tank compartment are usually turbulent, so the drag coefficient is a constant.

Camp reports that the value of k for paddle flocculators *with stators* varies between 0.32 and 0.24 as the rotational speed increases (Camp, 1955).

The peripheral speed of the paddle assembly is usually kept below 2 ft/sec, and speeds of less than 1 ft/sec are recommended for the final compartment (Bean, 1953; Hopkins and Bean, 1966). In older plants, peripheral speeds were generally below 1.8 ft/sec (Bean, 1953). This practice appears to have been based on laboratory data that was developed using 1 gal jars without stators. The laboratory data indicated impaired flocculation at peripheral speeds above 1.8 ft/sec, but the results may have been caused by vortexing, which would actually reduce the velocity gradients in the liquid (Leipold, 1934).

Paddles are usually between 4 and 8 in. wide, and the spacing between paddles should be greater than this (Bean, 1953). The total paddle area should be less than 25% of the plan area of the compartment.

Jets

The power expended by a jet is simply the kinetic energy of the mass of liquid injected into the tank:

$$P = \frac{1}{2} \dot{m} v^2 \quad (9.63)$$

where \dot{m} is the mass flow rate in the jet at its inlet (kg/s or slug/sec). The mass flow rate is determined by the mixing requirements.

Static In-Line Mixers

The energy dissipated by static mixers is determined by the pressure drop through the unit:

$$P = Q \cdot \Delta p \quad (9.64)$$

where Δp = the pressure drop (N/m² or lbf/ft²)
 Q = the volumetric flow rate (m³/s or ft³/sec).

The pressure drop depends on the details of the mixer design.

Gas Sparging

The power dissipated by gas bubbles is,

$$P = \rho g Q H \quad (9.65)$$

where g = the acceleration due to gravity (9.80665 m/s² or 32.174 ft/sec²)
 H = the depth of bubble injection (m or ft)
 Q = the gas flow rate (m³/s or ft³/sec)
 ρ = the liquid density (kg/m³ or slug/ft³)

Blending

The principal purpose of all mixing is blending two or more different liquid streams.

Batch Mixing Times

The time required to blend two or more liquids to some acceptable level of macroscopic homogeneity is determined by batch blending tests. The test results are usually reported in terms of a homogenization number that is defined to be the number of impeller revolutions required to achieve homogenization (Tatterson, 1994):

$$Ho = \omega \tau_m \quad (9.66)$$

where \mathbf{Ho} = the homogenization number (dimensionless)
 τ_m = the blending time (sec)
 ω = the rotational speed of the impeller (Hz, revolutions per sec)

The degree of mixing is often determined from tracer data by calculating the “fractional unmixedness,” which is defined in terms of measured concentration fluctuations (Godfrey and Amirtharajah, 1991; Tatterson, 1994):

$$X_t = \left| \frac{C_t - C_\infty}{C_\infty - C_o} \right| \quad (9.67)$$

where C_o = the initial tracer concentration the tank, if any, prior to tracer addition and mixing (kg/m³ or lb/ft³)
 C_t = the maximum tracer concentration at any point in the tank at time t (kg/m³ or lb/ft³)
 C_∞ = the calculated tracer concentration for perfect mixing (kg/m³ or lb/ft³)
 X_t = the fractional unmixedness (dimensionless)

Blending is considered to be complete when X_t falls to 0.05, meaning that the observed concentration fluctuations are within 5% of the perfectly mixed condition.

Turbines

The Prochazka-Landau correlation (Tatterson, 1994) for a turbine with six flat, disk-mounted blades in a baffled tank is,

$$\omega\tau_m = 0.905 \left(\frac{d_t}{d_i} \right)^{2.57} \log \left(\frac{X_o}{X_f} \right) \quad (9.68)$$

For a turbine with four pitched blades, their correlation is,

$$\omega\tau_m = 2.02 \left(\frac{d_t}{d_i} \right)^{2.20} \log \left(\frac{X_o}{X_f} \right) \quad (9.69)$$

And for a three-bladed marine propeller, it is,

$$\omega\tau_m = 3.48 \left(\frac{d_t}{d_i} \right)^{2.05} \log \left(\frac{X_o}{X_f} \right) \quad (9.70)$$

where d_t = the impeller diameter (m or ft)
 d_i = the tank diameter (m or ft)
 X_o = the initial fractional unmixedness, typically between 2 and 3 in the cited report (dimensionless)
 X_f = the final fractional unmixedness, typically 0.05
 τ_m = the required batch mixing time (sec)
 ω = the impeller rotational speed (Hz, revolutions per sec)

Note that impeller diameter is more important than impeller speed, because the mixing time is inversely proportional to the impeller diameter raised to a power greater than 2, whereas it is inversely proportional to the speed to the first power.

Equations (9.68) through (9.70) demonstrate that for any particular design, the homogenization number is a constant. The equations are best used to convert data from one impeller size to another.

The homogenization number is also a constant in the laminar region, but the constant is independent of impeller size. Turbines are seldom used in laminar conditions, but propellers mounted in draft tubes are. Reported homogenization numbers for propeller/tube mixers range from 16 to 130 (Tatterson, 1994).

Static In-Line Mixers

A wide variety of proprietary static in-line mixers is available. Some designs are specialized to laminar or turbulent flow conditions, and other designs are general purpose mixers. Static mixers are liable to clog with large suspended solids and require filtered or screened feed streams.

The usual specification is that the coefficient of variation of concentration measurements in the mixer outlet be equal to less than 0.05 (Godfrey and Amirtharajah, 1991; Tatterson, 1994). Mixer unit lengths are typically 5 to 50 times the pipe diameter, depending on the design.

The standard deviation of concentration measurements over any mixer cross section declines exponentially with mixer length and may be correlated by (Godfrey and Amirtharajah, 1991),

$$\frac{s}{s_0} = 2 \exp\left(-\frac{1.54 f^{0.5} L}{D}\right) \quad (9.71)$$

where D = the mixer's diameter

f = the mixer's Darcy-Weisbach friction factor (dimensionless)

L = the mixer's length (m or ft)

s = the standard deviation of the concentration measurements over the outlet cross section (kg/m³ or lb/ft³)

s_0 = the standard deviation of the concentration measurements over the inlet cross section (kg/m³ or lb/ft³)

Jets

Jet mixers have relatively high power requirements, but they are low-maintenance devices. They are restricted to turbulent, medium- to low-viscosity liquid mixing, and the jet Reynolds number at the inlet should be above 2100 (Tatterson, 1994). The required pump may be inside or outside the tank, depending on equipment design.

Jets may enter the tank axially on the tank bottom or radially along the tank side. Axial entry can be used for deep tanks in which the liquid depth to tank diameter ratio is between 0.75 and 3, and radial entry can be used for shallow tanks in which the depth–diameter ratio is between 0.25 and 1.25 (Godfrey and Amirtharajah, 1991). If the depth–diameter ratio exceeds 3, multiple jets are required at different levels. Radial inlets are frequently angled upwards.

Mixing of the jet and surrounding fluid does not begin until the jet has traveled at least 10 inlet diameters, and effective mixing occurs out to about 100 inlet diameters. Oldshue and Trussell (1991) recommend that the tank diameter to jet inlet diameter ratio be between 50 and 500.

If the initial jet Reynolds number is 5000 or more, the batch mixing time is given by (Godfrey and Amirtharajah, 1991),

$$\frac{\tau_m v_j}{d_j} = 6 \left(\frac{d_t}{d_j}\right)^{3/2} \left(\frac{d_t}{d_j}\right)^{1/2} \quad (9.72)$$

For initial jet Reynold's numbers below 5000, the mixing time is given by,

$$\frac{\tau_m v_j}{d_j} = \frac{30\,000}{Re} \left(\frac{d_t}{d_j}\right)^{3/2} \left(\frac{d_t}{d_j}\right)^{1/2} \quad (9.73)$$

where d_j = the jet's inlet diameter (m or ft)
 d_l = the liquid depth (m or ft)
 d_t = the tank diameter (m or ft)
 Re = the jet's inlet Reynold's number (dimensionless)
 $= v_j d_j / \nu$
 v_j = the jet's inlet velocity (m/s or ft/sec)
 τ_m = the required mixing time (sec)

Other correlations are given by Tatterson (1994).

Continuous Flow

In order to account for their exponential residence time distributions, the required hydraulic retention time in continuous flow tanks ranges from 50 to 200 times the batch mixing time, and is typically about 100 times τ_m (Tatterson, 1994):

$$\tau_h \approx 100\tau_m \quad (9.74)$$

Particle Suspension

Settleable Solids

Settleable solids are usually put into suspension using downwards-directed axial flow turbines, sometimes with draft tubes. Tank bottoms should be dished, and the turbine should be placed relatively close to the bottom, say between 1/6 and 1/4 of the tank diameter (Godfrey and Amirtharajah, 1991). Antivortex baffles are required. Sloping side walls, bottom baffles, flat bottoms, radial flow turbines, and large tank diameter to impeller diameter ratios should be avoided, as they permit solids accumulation on the tank floor (Godfrey and Amirtharajah, 1991; Tatterson, 1994).

The impeller speed required for the suspension of settleable solids is given by the Zweitering (1958) correlation:

$$\omega_{js} = \frac{Sv^{0.1}d_p^{0.2} \left[\frac{g(\rho_p - \rho)}{\rho} \right]^{0.45} X_p^{0.13}}{d_i^{0.85}} \quad (9.75)$$

where d_p = the particle diameter (m or ft)
 d_i = the turbine diameter (m or ft)
 g = the acceleration due to gravity (9.80665 m/s² or 32.174 ft/sec²)
 S = the impeller/tank geometry factor (dimensionless)
 X_p = the weight fraction of solids in the suspension (dimensionless)
 ω_{js} = the impeller rotational speed required to just suspend the particles (Hz, revolutions per sec)
 ρ = the liquid density (kg/m³ or slug/ft³)
 ρ_p = the particle density (kg/m³ or slug/ft³)

Equation (9.75) is the "just suspended" criterion. Lower impeller speeds will allow solids to deposit on the tank floor. The impeller/tank geometry factor varies significantly. Typical values for many different configurations are given by Zweitering (1958).

The Zweitering correlation leads to a prediction for power scale-up that may not be correct. In the standard geometry, the liquid depth, tank diameter, and impeller diameter are proportional. Combining this geometry with the power correlation for the turbulent regime [Eq. (9.57)], one gets,

$$\frac{P}{V} \propto \frac{\omega^3 d_i^5}{d_l d_t^2} \propto \frac{d_i^{-2.55} d_l^5}{d_l d_t^2} \propto d_i^{-0.55} \quad (9.76)$$

Some manufactures prefer to scale power per unit volume as $d_t^{-0.28}$ and others prefer to keep the power per unit volume constant.

If solids are to be distributed throughout the whole depth of the liquid, then the modified Froude number must be greater than 20 (Tatterson, 1994):

$$Fr = \frac{\rho \omega^2 d_i^2}{g(\rho_p - \rho) d_p} \left(\frac{d_p}{d_i} \right)^{0.45} > 20 \quad (9.77)$$

The concentration profile can be estimated from (Tatterson, 1994):

$$\frac{X_p(z)}{\bar{X}_p} = \frac{Pe \cdot \exp\left(-\frac{Pe \cdot z}{d_i}\right)}{1 - \exp(-Pe)} \quad (9.78)$$

$$Pe = 330 \left(\frac{\omega d_i}{v_p} \right)^{-1.17} \left(\frac{\varepsilon d_p^4}{v^3} \right)^{-0.095} \quad (9.79)$$

- where
- d_i = the impeller's diameter (m or ft)
 - d_l = the total liquid depth (m or ft)
 - d_p = the particle's diameter (m or ft)
 - Pe** = the solid's Peclet number (dimensionless)
 - = $v_{ps} d_i / d_p$
 - v_p = the particle's free settling velocity in still liquid (m/s or ft/sec)
 - v_{ps} = the particle's free settling velocity in stirred liquid (m/s or ft/sec)
 - \bar{X}_p = the mean particle mass fraction in the tank (dimensionless)
 - $X_p(z)$ = the particle mass fraction at elevation z above the tank bottom (dimensionless)
 - z = the elevation above the tank bottom (m or ft)
 - ε = the power per unit mass (W/kg or ft·lbf/slug·sec)
 - ρ = the density of the liquid (kg/m³ or slug/ft³)
 - ρ_p = the density of the particle (kg/m³ or slug/ft³)
 - v = the kinematic viscosity (m²/s or ft²/sec)
 - ω = the rotational speed of the impeller (Hz, revolutions per sec)

Floatable Solids

The submergence of low-density, floating solids requires the development of a vortex, so only one antivortex baffle or narrow baffles ($w_b = d_i/50$) should be installed (Godfrey and Amirtharajah, 1991). The axial flow turbine should be installed close to the tank bottom and perhaps off-center. The tank bottom should be dished. The minimum Froude number for uniform mixing is given by,

$$Fr_{\min} = 0.036 \left(\frac{d_i}{d_t} \right)^{-3.65} \left(\frac{\rho_p - \rho}{\rho} \right)^{0.42} \quad (9.80)$$

- where **Fr**_{min} = the required minimum value of the Froude number (dimensionless)
- Fr** = the impeller Froude number (dimensionless)
 - = $\omega^2 d_i / g$

References

- Bean, E.L. 1953. "Study of Physical Factors Affecting Flocculation," *Water Works Engineering*, 106(1): 33 and 65.
- Boadway, J.D. 1978. "Dynamics of Growth and Breakage of Alum Flocc in Presence of Fluid Shear," *Journal of the Environmental Engineering Division, Proceedings of the American Society of Civil Engineers*, 104(EE5): 901.
- Brodkey, R.S. 1967. *The Phenomena of Fluid Motions*, 2nd printing with revisions. Private Printing, Columbus, OH. [First Printing: Addison-Wesley Publishing Co., Inc., Reading, MA.]
- Camp, T.R. 1955. "Flocculation and Flocculation Basins," *Transactions of the American Society of Civil Engineers*, 120: 1.
- Camp, T.R. and Stein, P.C. 1943. "Velocity Gradients and Internal Work in Fluid Motion," *Journal of the Boston Society of Civil Engineers*, 30(4): 219.
- Clark, M.M. 1985. "Critique of Camp and Stein's Velocity Gradient," *Journal of Environmental Engineering*, 111(6): 741.
- Cleasby, J.L. 1984. "Is Velocity Gradient a Valid Turbulent Flocculation Parameter?," *Journal of Environmental Engineering*, 110(5): 875.
- Fair, G.M., Geyer, J.C., and Okun, D.A. 1968. *Water and Wastewater Engineering: Vol. 2, Water Purification and Wastewater Treatment and Disposal*. John Wiley & Sons, Inc., New York.
- Godfrey, J.C. and Amirtharajah, A. 1991. "Mixing in Liquids," p. 35 in *Mixing in Coagulation and Flocculation*, A. Amirtharajah, M.M. Clark, and R.R. Trussell, eds. American Water Works Association, Denver, CO.
- Grant, H.L., Stewart, R.W., and Moillet, A. 1962. "Turbulence Spectra from a Tidal Channel," *Journal of Fluid Mechanics*, 12(part 2): 241.
- Holland, F.A. and Chapman, F.S. 1966. *Liquid Mixing and Processing in Stirred Tanks*. Reinhold Publishing Corp., New York.
- Hopkins, E.S. and Bean, E.L. 1966. *Water Purification Control*, 4th ed. The Williams & Wilkins Co., Inc., Baltimore, MD.
- Joint Committee of the American Society of Civil Engineers, the American Water Works Association and the Conference of State Sanitary Engineers. 1969. *Water Treatment Plant Design*. American Water Works Association, Inc., New York.
- King, H.W. and Brater, E.F. 1963. *Handbook of Hydraulics for the Solution of Hydrostatic and Fluid-Flow Problems*, 5th ed. McGraw-Hill Book Co., Inc., New York.
- Lagvankar, A.L. and Gemmell, R.S. 1968. "A Size-Density Relationship for Floccs," *Journal of the American Water Works Association*, 60(9): 1040. See errata: *Journal of the American Water Works Association*, 60(12): 1335.
- Lamb, H. 1932. *Hydrodynamics*, 6th ed. Cambridge University Press, Cambridge, MA.
- Landahl, M.T. and Mollo-Christensen, E. 1986. *Turbulence and Random Processes in Fluid Mechanics*. Cambridge University Press, Cambridge, MA.
- Leipold, C. 1934. "Mechanical Agitation and Alum Flocc Formation," *Journal of the American Water Works Association*, 26(8): 1070.
- Matsuo, T. and Unno, H. 1981. "Forces Acting on Flocc and Strength of Flocc," *Journal of the Environmental Engineering Division, Proceedings of the American Society of Civil Engineers*, 107(EE3): 527.
- Oldshue, J.Y. and Trussell, R.R. 1991. "Design of Impellers for Mixing," p. 309 in *Mixing in Coagulation and Flocculation*, A. Amirtharajah, M.M. Clark, and R.R. Trussell, eds. American Water Works Association, Denver, CO.
- Parker, D.S., Kaufman, W.J., and Jenkins, D. 1972. "Flocc Breakup in Turbulent Flocculation Processes," *Journal of the Sanitary Engineering Division, Proceedings of the American Society of Civil Engineers*, 98(SA1): 79.

- Rushton, J.H., Costich, E.W., and Everett, H.J. 1950. "Power Characteristics of Mixing Impellers, Part I," *Chemical Engineering Progress*, 46(8): 395.
- Saffman, P.G. and Turner, J.S. 1956. "On the Collision of Drops in Turbulent Clouds," *Journal of Fluid Mechanics*, 1(part 1): 16.
- Smith, M.C. 1932. "Improved Mechanical Treatment of Water for Filtration," *Water Works and Sewerage*, 79(4): 103.
- Stewart, R.W. and Grant, H.L. 1962. "Determination of the Rate of Dissipation of Turbulent Energy near the Sea Surface in the Presence of Waves," *Journal of Geophysical Research*, 67(8): 3177.
- Stokes, G.G. 1845. "On the Theories of Internal Friction of Fluids in Motion, etc.," *Transactions of the Cambridge Philosophical Society*, 8: 287.
- Streeter, V.L. 1948. *Fluid Dynamics*. McGraw-Hill, Inc., New York.
- Tambo, N. and Hozumi, H. 1979. "Physical Characteristics of Floccs — II. Strength of Flocc," *Water Research*, 13(5): 421.
- Tambo, N. and Watanabe, Y. 1979. "Physical Characteristics of Floccs — I. The Flocc Density Function and Aluminum Flocc," *Water Research*, 13(5): 409.
- Tatterson, G.B. 1994. *Scaleup and Design of Industrial Mixing Processes*. McGraw-Hill, Inc., New York.
- Zweirter, T.N. 1958. "Suspending Solid Particles in Liquids by Agitation," *Chemical Engineering Science*, 8(3/4): 244.

9.4 Rapid Mixing and Flocculation

Rapid Mixing

Rapid or flash mixers are required to blend treatment chemicals with the water being processed. Chemical reactions also occur in the rapid mixer, and the process of colloid destabilization and flocculation begins there.

Particle Collision Rate

Within the viscous dissipation subrange, the relative velocity between two points along the line connecting them is (Saffman and Turner, 1956; Spielman, 1978):

$$\overline{|u|} = \sqrt{\frac{2\varepsilon}{15\pi\nu}} \cdot r \quad (9.81)$$

- where
- r = the radial distance between the two points (m or ft)
 - $\overline{|u|}$ = the average of the absolute value of the relative velocity of two points in the liquid along the line connecting them (m/s or ft/sec)
 - ε = the power input per unit mass (W/kg or ft·lbf/slug·sec)
 - ν = the kinematic viscosity (m²/s or ft²/sec)

One selects a target particle of radius r_1 and number concentration C_1 and a moving particle of radius r_2 and number concentration C_2 . The moving particle is carried by the local eddies, which may move toward or away from the target particle at velocities given by Eq. (9.81). A collision will occur whenever the center of a moving particle crosses a sphere of radius $r_1 + r_2$ centered on the target particle. The volume of liquid crossing this sphere is:

$$Q = \frac{1}{2} \overline{|u|} 4\pi(r_1 + r_2)^2 = \sqrt{\frac{8\pi}{15}} \sqrt{\frac{\varepsilon}{\nu}} (r_1 + r_2)^3 \quad (9.82)$$

where Q = the volumetric rate of flow of liquid into the collision sphere (m³/sec or ft³/sec).

The Saffman–Turner collision rate is, therefore:

$$R_{1,2} = \sqrt{\frac{8\pi}{15}} \sqrt{\frac{\varepsilon}{\nu}} C_1 C_2 (r_1 + r_2)^3 \quad (9.83)$$

A similar formula has been derived by Delichatsios and Probstein (1975).

Particle Destabilization

The destabilization process may be visualized as the collision of colloidal particles with eddies containing the coagulants. If the diameter of the eddies is estimated to be η , then Eq. (9.83) can be written as,

$$\sqrt{\frac{\pi}{120}} \sqrt{\frac{\varepsilon}{\nu}} C_1 C_\eta (d_1 + \eta)^3 \quad (9.84)$$

where C_η = the “concentration” of eddies containing the coagulant (dimensionless)

d_1 = the diameter of the colloidal particles (m or ft)

$R_{1,\eta}$ = the rate of particle destabilization (no./m³·s or no./ft³·sec)

η = the diameter of the eddies containing the coagulant (m or ft)

Equation (9.84) is the Amirtharajah–Trusler (1986) destabilization rate formula. The “concentration” C_η may be regarded as an unknown constant that is proportional to the coagulant dosage.

The effect of a collision between a stable particle and an eddy containing coagulant is a reduction in the net surface charge of the particle. The particle’s surface charge is proportional to its zeta potential, which in turn, is proportional to its electrophoretic mobility. Consequently, $R_{1,\eta}$ is the rate of reduction of the average electrophoretic mobility of the suspension.

Equation (9.84) has unexpected implications. First, the specific mixing power may be eliminated from Eq. (9.84) by means of the definition of the Kolmogorov length scale, yielding (Amirtharajah and Trusler, 1986):

$$R_{1,\eta} = \sqrt{\frac{\pi}{120}} C_\eta \frac{(d_1 + \eta)^3}{\eta^2} C_1 \quad (9.85)$$

The predicted rate has a minimum value when the Kolmogorov length scale is twice the particle diameter, i.e., $\eta = 2d_1$ and the mixing power per unit mass required to produce this ratio is:

$$\varepsilon = \frac{\nu^3}{16d_1} \quad (9.86)$$

In strongly mixed tanks, the power dissipation rate varies greatly from one part of the tank to another. It is highest near the mixer, and ε should be interpreted as the power dissipation at the mixer.

The predicted minimum is supported by experiment, and it occurs at about $\eta = 2d_1$, if η is calculated for the conditions next to the mixer (Amirtharajah and Trusler, 1986). For a given tank and mixer geometry, the energy dissipation rate near the mixer is related to the average dissipation rate for the whole tank. In the case of completely mixed tanks stirred by turbines, the minimum destabilization rate will occur at values of $\bar{\Gamma}$ between about 1500 and 3500 per sec, which is substantially above the usual practice. (See below.)

Second, the destabilization rate is directly proportional to the stable particle concentration:

$$R_{1,\eta} = kC_1 \quad (9.87)$$

where k = the first-order destabilization rate coefficient (per sec).

The rate coefficient, k , applies to the conditions near the mixer. However, what is needed for design is the rate $R_1\eta$ volume averaged over the whole tank. If the tank is completely mixed, C_1 is the same everywhere and can be factored out of the volume average. Thus, the volume average of the rate, $R_1\eta$ becomes a volume average of the rate coefficient, k . Throughout most of the volume, the power dissipation rate is much smaller than the rate near the mixer, and in general, $\eta \gg d_1$. Therefore, the particle diameter can be neglected, and to a first-order approximation one has:

$$\bar{k} = \sqrt{\frac{\pi}{120}} \sqrt{\frac{v^3}{\bar{\Gamma}}} C_\eta \quad (9.88)$$

Equation (9.88) is limited to power dissipation rates less than 1500 per sec.

Inspection of Eq. (9.88) shows that the rate of destabilization should *decrease* if the temperature or the mixing power *increases*. This is counterintuitive. Experience with simple chemical reactions and flocculation indicates that reaction rates always rise whenever the temperature or mixing power is increased. However, in chemical reactions and particle flocculation, the driving forces are the velocity of the particles and their concentrations. In destabilization, the driving forces are these plus the size of the eddies, and eddy size dominates.

The prediction that the destabilization rate decreases as the mixing power increases has indirect experimental support, although it may be true only for completely mixed tanks (Amirtharajah and Trusler, 1986; Camp, 1968; Vrale and Jorden, 1971). The prediction regarding temperature has not been tested.

Optimum Rapid Mixing Time

It is known that there is a well-defined optimum rapid mixing time (Letterman, Quon, and Gemmell, 1973; Camp, 1968). This optimum is not predicted by the Amirtharajah–Trusler formula. If rapid mixing is continued beyond this optimum, the flocculation of the destabilized particles and their settling will be impaired, or at least there will be no further improvement. For the flocculation of activated carbon with filter alum, the relationship between the r.m.s. strain rate, batch processing time, and alum dose is (Letterman, Quon, and Gemmell, 1973):

$$\bar{\Gamma} t C^{1.46} = 5.9 \times 10^6 \left(\text{mg/L} \right)^{1.46} \quad (9.89)$$

where C = the dosage of filter alum, $\text{Al}_2(\text{SO}_4)_3(\text{H}_2\text{O})_{18}$ (mg/L)
 t = the duration of the batch mixing period (sec).

Equation (9.89) does not apply to alum dosages above 50 mg/L, because optimum rapid mixing times were not always observed at higher alum dosages. The experiments considered powdered activated carbon concentrations between 50 and 1000 mg/L, alum dosages between 10 and 50 mg/L, and values of $\bar{\Gamma}$ between 100 and 1000 per sec. At the highest mixing intensities, the optimum value of t ranged from 14 sec to 2.5 min. These results have not been tested for other coagulants or particles. Consequently, it is not certain that they are generally applicable. Also, the underlying cause of the optimum is not known.

It is also clear that very high mixing powers in the rapid mixing tank impair subsequent flocculation in the flocculation tank. For example, Camp (1968) reports that rapid mixing for 2 min at a $\bar{\Gamma}$ of 12,500/sec prevents flocculation for at least 45 min. If $\bar{\Gamma}$ is reduced to 10,800/sec, flocculation is prevented for 30 min. The period of inhibition was reduced to 10 min when $\bar{\Gamma}$ was reduced to 4400/sec. Strangely enough, if the particles were first destabilized at a $\bar{\Gamma}$ of 1000/sec, subsequent exposure to 12,500/sec had no effect. Again, the cause of the phenomenon is not known.

Design Criteria for Rapid Mixers

Typical engineering practice calls for a r.m.s. characteristic strain rate in the rapid mixing tank of about 600 to 1000/sec (Joint Task Force, 1990). Recommendations for hydraulic retention time vary from 1 to 3 sec for particle destabilization (Joint Task Force, 1990) to 20 to >40 sec for precipitate enmeshment (AWWA, 1969). Impeller tip speeds should be limited to less than 5 m/s to avoid polymer shear.

Flocs begin to form within 2 sec, and conduits downstream of the rapid mixing chamber should be designed to minimize turbulence. Typical conduit velocities are 1.5 to 3 ft/sec.

Flocculation

Quiescent and Laminar Flow Conditions

In quiescent water, the Brownian motion of the destabilized colloids will cause them to collide and agglomerate. Eventually, particles large enough to settle will form, and the water will be clarified. The rate of agglomeration is increased substantially by mixing. This is due to the fact that mixing creates velocity differences between neighboring colloidal particles, which increases their collision frequency.

Perikinetic Flocculation

Coagulation due to the Brownian motion is called “perikinetic” flocculation. The rate of perikinetic coagulation was first derived by v. Smoluchowski in 1916/17 as follows (Levich, 1962). Consider a reference particle having a radius r_1 . A collision will occur with another particle having a radius r_2 whenever the distance between the centers of the two particles is reduced to $r_1 + r_2$. (Actually, because of the van der Waals attraction, the collision will occur even if the particles are somewhat farther apart.) The collision rate will be the rate at which particles with radius r_2 diffuse across a sphere of radius $r_1 + r_2$ centered on the reference particle. For a spherically symmetrical case like this, the mass conservation equation becomes (Crank, 1975):

$$\frac{\partial C_2(r,t)}{\partial t} = \frac{D_{1,2}}{r^2} \frac{\partial}{\partial r} \left[r^2 \frac{\partial C_2(r,t)}{\partial r} \right] \quad (9.90)$$

where $C_2(r,t)$ = the number concentration of the particle with radius r_2 at a point a distance r from the reference particle at time t (no./m³ or no./ft³)

$D_{1,2}$ = the mutual diffusion coefficient of the two particles (m²/sec or ft²/sec)

= $D_1 + D_2$

D_1 = the diffusion coefficient of the reference particle (m²/s or ft²/sec)

D_2 = the diffusion coefficient of the particle with radius r_2 (m²/sec or ft²/sec)

r = the radial distance from the center of the reference particle (m or ft)

t = elapsed time (sec)

Only the steady state solution is needed, so the left-hand-side of Eq. (9.90) is zero. The boundary conditions are:

$$r \rightarrow \infty; \quad C_2(r) = C_2 \quad (9.91)$$

$$r = r_1 + r_2; \quad C_2(r) = 0 \quad (9.92)$$

Therefore, the particular solution is:

$$C_2(r) = C_2 \left(1 - \frac{r_1 + r_2}{r} \right) \quad (9.93)$$

The rate at which particles with radius r_2 diffuse across the spherical surface is:

$$4\pi(r_1 + r_2)^2 D_{1,2} \left. \frac{dC_2(r)}{dr} \right|_{r=r_1+r_2} = 4\pi D_{1,2} C_2 (r_1 + r_2) \quad (9.94)$$

If the concentration of reference particles is C_1 , the collision rate will be:

$$R_{1,2} = 4\pi D_{1,2} C_1 C_2 (r_1 + r_2) \quad (9.95)$$

where $R_{1,2}$ = the rate of collisions between particles of radius r_1 and radius r_2 due to Brownian motion (collisions/m³·sec or collisions/ft³·sec).

Orthokinetic Flocculation

If the suspension is gently stirred, so as to produce a laminar flow field, the collision rate is greatly increased. The mixing is supposed to produce a velocity gradient near the reference particle, $G = du/dy$. The velocity, u , is perpendicular to the axis of the derivative y . The collisions now are due to the velocity gradient, and the process is called “gradient” or “orthokinetic” flocculation. As before, a collision is possible if the distance between the centers of two particles is less than the sum of their radii, $r_1 + r_2$. v. Smoluchowski selects a reference particle with a radius of r_1 , and, using the local velocity gradient, one calculates the total fluid flow through a circle centered on the reference particle with radius $r_1 + r_2$ (Freundlich, 1922):

$$Q = 4 \int_0^{r_1+r_2} G y (r^2 - y^2)^{1/2} dy = \frac{4}{3} G (r_1 + r_2)^3 \quad (9.96)$$

where G = the velocity gradient (per sec)

Q = the total flow through the collision circle (m³/s or ft³/sec)

v = the distance from the center of the reference particle normal to the local velocity field (m or ft)

The total collision rate between the two particle classes will be:

$$R_{1,2} = \frac{4}{3} G C_1 C_2 (r_1 + r_2)^3 \quad (9.97)$$

The ratio of the orthokinetic to perikinetic collision rates for equal size particles is:

$$\frac{R_{1,2}(\text{ortho})}{R_{1,2}(\text{peri})} = \frac{4\mu G N_A r^3}{RT} \quad (9.98)$$

where N_A = Avogadro’s constant (6.022 137∞10²³ particles per mol)

R = the gas constant (8.3243 J/mol·K or 1.987 Btu/lb·°R)

T = the absolute temperature (K or °R)

Einstein’s (1956) formula for the diffusivity of colloidal particles has been used to eliminate the joint diffusion constant. Note that the effect of mixing is very sensitive to the particle size, varying as the cube of the radius. In fact, until the particles have grown by diffusion to some minimal size, mixing appears to have little or no effect. Once the minimal size is reached, however, flocculation is very rapid (Freundlich, 1922).

Corrections to v. Smoluchowski’s analysis to account for van der Waals forces and hydrodynamic effects are reviewed by Spielman (1978).

Turbulent Flocculation and Deflocculation

The purposes of the flocculation tank are to complete the particle destabilization begun in the rapid mixing tank and to agglomerate the destabilized particles. Flocculation tanks are operated at relatively low power dissipation rates, and destabilization proceeds quite rapidly; it is probably completed less than 1 min after the water enters the tank. Floc agglomeration is a much slower process, and its kinetics are

different. Furthermore, the kinds of mixing devices used in flocculation are different from those used in rapid mixing. The effects of tank partitioning upon the degree of agglomeration achieved are quite striking, and flocculation tanks are always partitioned into at least four mixed-cells-in-series.

Flocculation Rate

First, consider the kinetics of flocculation. Floc particles form when smaller particles collide and stick together. The basic collision rate is given by the Saffman–Turner equation (Harris, Kaufman, and Krone, 1966; Argaman and Kaufman, 1970; Parker, Kaufman, and Jenkins, 1972):

$$R_{1,2} = \sqrt{\frac{8\pi}{15}} \sqrt{\frac{\epsilon}{\nu}} C_1 C_2 (r_1 + r_2)^3 \quad (9.99)$$

This needs to be adapted to the situation in which there is a wide variety of particle sizes, not just two. This may be done as follows (Harris, Kaufman, and Krone, 1966). It is first supposed that the destabilized colloids, also called the “primary particles,” may be represented as spheres, each having the same radius r . The volume of such a sphere is:

$$V_1 = \frac{4}{3} \pi r^3 \quad (9.100)$$

Floc particles are aggregations of these primary particles, and the volume of the aggregate is equal to the sum of the volumes of the primary particle it contains. An aggregate consisting of i primary particles is called an “ i -fold” particle and has a volume equal to:

$$V_i = \frac{4}{3} \pi i r^3 \quad (9.101)$$

From this, it is seen that the i -fold particle has an effective radius given by:

$$r_i = \sqrt[3]{i r^3} \quad (9.102)$$

The total floc volume concentration is:

$$\Phi = \frac{4}{3} \pi r^3 \sum_{i=1}^p i C_i \quad (9.103)$$

where C_i = the number concentration of aggregates containing i primary particles (no./m³ or no./ft³)
 p = the number of primary particles in the largest floc in the suspension (dimensionless)
 Φ = the floc volume concentration (m³ floc/m³ water or ft³ floc/ft³ water)

A k -fold particle can arise in several ways. All that is required is that the colliding flocs contain a total of k particles, so the colliding pairs may be:

- A floc having $k - 1$ primary particles and a floc having one primary particle
- A floc having $k - 2$ primary particles and a floc having two primary particles
- A floc having $k - 3$ primary particles and a floc having three primary particles, etc.

The k -fold particle will disappear, and form a larger particle, if it collides with anything except a p -fold particle. Collisions with p -fold particles cannot result in adhesion, because the p -fold particle is supposed to be the largest possible. In both kinds of collisions, it is assumed that the effective radius of a particle is somewhat larger than its actual radius because of the attraction of van der Waals forces. Each kind of collision can be represented by a summation of terms, like Eq. (9.99), and the net rate of formation of k -fold particles is the difference between the summations (Harris, Kaufman, and Krone, 1966):

$$R_k = \bar{\Gamma} \sqrt{\frac{8\pi}{15}} \cdot \left[\frac{1}{2} \sum_{\substack{i=1, \\ j=k-1}}^k (ar_i + ar_j)^3 C_i C_j - \sum_{i=1}^{p-1} (ar_k + ar_i)^3 C_k C_i \right] \quad (9.104)$$

where R_k = the net rate of formation of k -fold particles (no./sec·m³ or no./sec·ft³)
 a = the ratio of the effective particle radius to its actual radius (dimensionless).

Note that the factor 1/2 in the first summation is required to avoid double counting of collisions.
 If there is no formation process for primary particles, Eq. (9.104) reduces to:

$$R_1 = -\bar{\Gamma} \sqrt{\frac{8\pi}{15}} \cdot \left[\sum_{i=1}^{p-1} (ar + ar_i)^3 C_i \right] \cdot C_1 \quad (9.105)$$

where R_1 = the rate of loss of primary particles due to flocculation (no./sec·m³ or no./sec·ft³).

The summation may be rearranged by factoring out r , which requires use of Eq. (9.102) to eliminate r_i , and by using Eq. (9.103) to replace the resulting r^3 :

$$R_1 = -\sqrt{\frac{3}{10\pi}} \bar{\Gamma} a^3 \Phi \sigma C_1 \quad (9.106)$$

where σ = the particle size distribution factor (dimensionless)

$$\sigma = \frac{\sum_{i=1}^{p-1} C_i (1+i^{1/3})^3}{\sum_{i=1}^{p-1} i C_i}$$

Except for a factor reflecting particle attachment efficiency (which is not included above) and substitution of the Saffman–Turner collision rate for the Camp–Stein collision rate, Eq. (9.106) is the Harris–Kaufman–Krone flocculation rate formula for primary particles.

In any given situation, the resulting rate expression involves only two variables: the number concentration of primary particles, C_p , and the particle size distribution factor, σ . The power dissipation rate, kinematic viscosity, and floc volume concentration will be constants. Initially, all the particles are primary, and the size distribution factor has a value of 8. As flocculation progresses, primary particles are incorporated into ever larger aggregates, and σ declines in value, approaching a lower limit of 1.

If the flocculation tank consists of mixed-cells-in-series, σ will approach a constant but different value in each compartment. If the mixing power in each compartment is the same, the average particle size distribution factor will be (Harris, Kaufman, and Krone, 1966):

$$\bar{\sigma} = \frac{\left(\frac{C_{1,o}}{C_{1,e}} \right)^{1/n} - 1}{\sqrt{\frac{3}{10\pi}} \bar{\Gamma} a^3 \Phi} \quad (9.107)$$

where $\bar{\sigma}$ = the average particle size distribution factor for a flocculation tank consisting of n mixed-cells-in-series (dimensionless)

$C_{1,o}$ = the number concentration of primary particles in the raw water (no./m³ or no./ft³)

$C_{1,e}$ = the number concentration of primary particles in the flocculated water (no./m³ or no./ft³)

An equation of the same form as Eq. (9.105) has been derived by Argaman and Kaufman (1970) by substituting a formula for a turbulent eddy diffusivity into Smoluchowski's quiescent rate formula [Eq. (9.95)]. They make two simplifications. First, they observe that the radius of a typical floc is much larger than that of a primary particle, so r can be eliminated from Eq. (9.95). Second, ignoring the primary particles and the largest flocs, the total floc volume concentration, which is a constant everywhere in the flocculation tank, would be:

$$\Phi \approx \frac{4}{3} \sum_{i=2}^{p-1} C_i r_i^3 \quad (9.108)$$

Therefore:

$$R_1 \approx -\sqrt{\frac{3}{10\pi}} \bar{\Gamma} \Phi a^3 C_1 \quad (9.109)$$

These two substitutions eliminate any explicit use of the particle size distribution function. However, early in the flocculation process, the primary particles comprise most of the particle volume, so Eq. (9.109) is at some points of the process grossly in error.

Equations (9.106) and (9.109) are devices for understanding the flocculation process. The essential prediction of the models is that flocculation of primary particles can be represented as a first-order reaction with an apparent rate coefficient that depends only on the total floc volume concentration, the mixing power, and the water viscosity.

Experiments in which a kaolin/alum mixture was flocculated in a tank configured as one to four mixed-cells-in-series were well described by the model, as long as the value of $\bar{\Gamma}$ as kept below about 60/sec (Harris, Kaufman, and Krone, 1966). The average particle size distribution factor, $\bar{\sigma}$, was observed to vary between about 1 and 4, and it appeared to decrease as the mixing power increased.

Deflocculation Rate

If the mixing power is high enough, the collisions between the flocs and the surrounding liquid eddies will scour off some of the floc's primary particles, and this scouring will limit the maximum floc size that can be attained.

The maximum size can be estimated from the Basset-Tchen equation for the sedimentation of a sphere in a turbulent liquid (Basset, 1888; Hinze, 1959):

$$\begin{aligned} \rho_p V \frac{du_p}{dt} = \rho_p Vg - \rho Vg - 3\pi\rho v d_p (u - u_p) + \rho V \frac{du}{dt} - \frac{1}{2} \rho v \frac{d(u - u_p)}{dt} \\ - \frac{9\rho V \sqrt{v/\pi}}{d_p} \int_0^t \frac{d[u(t-\tau) - u_p(t-\tau)]}{\sqrt{t-\tau}} \end{aligned} \quad (9.110)$$

where d_p = the floc diameter (m or ft)
 g = the acceleration due to gravity (9.80665 m/s² or 32.174 ft/sec²)
 t = the elapsed time from the beginning of the floc's motion(s)
 u = the velocity of the liquid near the floc (m/sec or ft/sec)
 u_p = the velocity of the floc (m/s or ft/s)
 V = the floc volume (m³ or ft³)
 v = the kinematic viscosity (m²/sec or ft²/sec)
 ρ = the density of the liquid (kg/m³ or slug/ft³)
 ρ_p = the density of the floc (kg/m³ or slug/ft³)
 τ = the variable of integration(s)

The terms in this equation may be explained as follows. The term on the left-hand-side is merely the rate of change of the floc's downward momentum. According to Newton's second law, this is equal to the resultant force on the floc, which is given by the terms on the right-hand-side. The first term is the floc's weight. The second term is the buoyant force due to the displaced water. The density of the floc is assumed to be nearly equal to the density of the liquid, so the gravitational and buoyant forces nearly cancel. The third term is Stoke's drag force, which is written in terms of the difference in velocity between the floc and the liquid. Stoke's drag force would be the only drag force experienced by the particle, if the particle were moving at a constant velocity with a Reynold's number much less than one and the liquid was stationary. However, the moving floc displaces liquid, and when the floc is accelerated, some liquid must be accelerated also, and this gives rise to the remaining terms. The fourth term is an acceleration due to the local pressure gradients set up by the acceleration of the liquid. The fifth and sixth terms represent the additional drag forces resulting from the acceleration of the displaced liquid. The fifth term is the "virtual inertia" of the floc. It represents the additional drag due to the acceleration of displaced liquid in the absence of viscosity. The sixth term is the so-called "Basset term." It is a further correction to the virtual inertia for the viscosity of the liquid.

Parker, Kaufman, and Jenkins (1972) used the Basset-Tchen equation to estimate the largest possible floc diameter in a turbulent flow. They first absorb the last term into the Stoke's drag force. Then, they subtract from both sides the following quantity:

$$\rho_p V \frac{du}{dt} + \frac{1}{2} \rho V \frac{du}{dt}$$

getting

$$(\rho_p + \frac{1}{2} \rho) V \frac{d(u - u_p)}{dt} = (\rho_p - \rho) V \frac{du}{dt} - 3b\pi\rho v d_p (u - u_p) \quad (9.111)$$

where b = a coefficient greater than one that reflects the contribution of the Basset term to the drag force (dimensionless).

They argue that the relative acceleration of the liquid and floc, which is the term on the left-hand-side, is small relative to the acceleration of the liquid:

$$3b\pi\rho v d_p (u - u_p) \approx (\rho_p - \rho) V \frac{du}{dt} \quad (9.112)$$

The time required by an eddy to move a distance equal to its own diameter is approximately:

$$t \approx \frac{d}{u} \quad (9.113)$$

This is also approximately the time required to accelerate the eddy from zero to u , so the derivative in the right-hand-side of Eq. (9.112) is:

$$\frac{du}{dt} \approx \frac{u^2}{d} \quad (9.114)$$

Therefore:

$$3b\pi\rho v d_p (u - u_p) \approx (\rho_p - \rho) V \frac{u^2}{d} \quad (9.115)$$

Finally, it is assumed that the effective eddy is the same size as the floc; this also means the distance between them is the floc diameter. The eddy velocity is estimated as its fluctuation, which is given by the Saffman-Turner formula, yielding:

$$3b\pi v d_p (u - u_p) \approx (\rho_p - \rho) V \frac{2\epsilon d_p^2}{15\pi v d_p} \quad (9.116)$$

Now, the left-hand-side is the total drag force acting on the floc. Ignoring the contribution of the liquid pressure, an upper bound on the shearing stress on the floc surface can be calculated as:

$$\tau_s 4\pi d_p^2 \approx 3b\pi \rho v d_p (u - u_p) = (\rho_p - \rho) \frac{\pi d_p^3}{6} \frac{2\epsilon d_p^2}{15\pi v d_p} \quad (9.117)$$

Note that the shearing stress τ_s increases as the square of the floc diameter. If τ_s is set equal to the maximum shearing strength that the floc surface can sustain, without loss of primary particles, then the largest possible floc diameter is (Parker, Kaufman, and Jenkins, 1972):

$$d_{p \max} \approx \left[\frac{180\pi \tau_{s \max}}{(\rho_p - \rho) \left(\frac{\epsilon}{v} \right)} \right]^{1/2} \quad (9.118)$$

The rate at which primary particles are eroded from flocs by shear may now be estimated; it is assumed that only the largest flocs are eroded. The largest flocs are supposed to comprise a constant fraction of the total floc volume:

$$\frac{4}{3} \pi r_p^3 C_p = f \frac{4}{3} \pi r^3 \sum_{i=1}^p i C_i \quad (9.119)$$

$$C_p = \frac{f}{p} \sum_{i=1}^p i C_i \quad (9.120)$$

where f = the fraction of the total floc volume contained in the largest flocs (dimensionless)
 r_p = the effective radius of the largest floc (m or ft)
 $= p^{1/3} r$

Each erosion event is supposed to remove a volume ΔV_p from the largest flocs:

$$\Delta V_p = f_e 4\pi r_p^2 \cdot \Delta r_p \quad (9.121)$$

where ΔV_p = the volume eroded from the largest floc surface in one erosion event (m³ or ft³)
 f_e = the fraction of the surface that is eroded per erosion event (dimensionless).

If the surface layer is only one primary particle thick, Δr_p is equal to the diameter of a primary particle, i.e., $2r$. The number of primary particles contained in the eroded layer is equal to the fraction of its volume that is occupied by primary particles divided by the volume of one primary particle (Parker, Kaufman, and Jenkins, 1972):

$$n = \frac{f_p f_e 4\pi r_p^2 2r}{\frac{4}{3} \pi r^3} \quad (9.122)$$

$$n = 6 f_p f_e p^{2/3} \quad (9.123)$$

where n = the number of primary particles eroded per erosion event (no. primary particles/floc·erosion)
 f_p = the fraction of the eroded layer occupied by primary particles (dimensionless)
 p = the number of primary particles in the largest floc (dimensionless)

The frequency of erosion events is approximated by dividing the velocity of the effective eddy by its diameter. This represents the reciprocal of the time required for an eddy to travel its own diameter and the reciprocal of the time interval between successive arrivals. If it is assumed that the effective eddy is about the same size as the largest floc, then the Saffman–Turner formula gives:

$$f = \left(\frac{2\varepsilon}{15\pi\nu} \right)^{1/2} \quad (9.124)$$

Combining these results, one obtains the primary particle erosion rate (Parker, Kaufman, and Jenkins, 1972):

$$R_{1e} = \bar{\Gamma} \sqrt{\frac{24}{5\pi}} \cdot \left(\frac{f \cdot f_p \cdot f_e}{p^{1/3}} \right) \cdot \sum_{i=1}^p i C_i \quad (9.125)$$

The radius of the largest floc may be eliminated from Eq. (9.125) by using Eq. (9.118), producing:

$$R_{1e} = \bar{\Gamma}^2 \sqrt{\frac{3}{200}} \cdot \frac{f \cdot f_p \cdot f_e \Phi \sqrt{\rho_p - \rho}}{\pi \sqrt{\tau_s} r} \quad (9.126)$$

$$R_{1e} = k_e \Phi \bar{\Gamma}^2 \quad (9.127)$$

where k_e = the erosion rate coefficient (no. primary particles·sec/m³ floc).

The rate of primary particle removal by flocculation, given by Eq. (9.106), can be written as follows:

$$R_{1f} = k_f \Phi \bar{\Gamma} C_1 \quad (9.128)$$

where k_f = the flocculation rate coefficient (m³ water/m³ floc).

The derivation makes it obvious that k_f depends on the floc size distribution. It should be remembered, however, that the coefficient k_e contains f , which is the fraction of the floc volume contained in the largest flocs. Consequently, k_e is also a function of the floc size distribution. Also, note that the rate of primary particle loss due to flocculation varies as the square root of the mixing power, while the rate of primary particle production due to erosion varies directly as the mixing power. This implies that there is a maximum permissible mixing power.

If the products $k_e \Phi$ and $k_f \Phi$ are constants, then a steady state particle balance on a flocculator consisting of equivolume mixed-cells-in-series yields (Argaman and Kaufman, 1970):

$$\frac{C_{1,e}}{C_{1,o}} = \frac{1 + \frac{k_e \Phi \bar{\Gamma}^2 V_1}{C_{1,o} Q} \sum_{i=1}^{n-1} \left(1 + \frac{k_f \Phi \bar{\Gamma} V_1}{Q} \right)^i}{\left(1 + \frac{k_f \Phi \bar{\Gamma} V_1}{Q} \right)^n} \quad (9.129)$$

where n = the number of mixed-cells-in-series (dimensionless)
 V_1 = the volume of one cell (m³ or ft³).

Equation (9.129) was tested in laboratory flocculators consisting of four mixed-cells-in-series with turbines or paddle mixers (Argaman and Kaufman, 1970). The raw water fed to the flocculators contained 25 mg/L kaolin that had been destabilized with 25 mg/L of filter alum. The total hydraulic retention times varied from 8 to 24 min, and the r.m.s. characteristic strain rate varied from 15 to 240/sec. The concentration of primary particles was estimated by allowing the flocculated water to settle quiescently for 30 min and measuring the residual turbidity. The experimental data for single compartment flocculators was represented accurately by the model. With both kinds of mixers, the optimum value of $\bar{\Gamma}$ varied from about 100/sec down to about 60/sec as the hydraulic retention time was increased from 8 to 24 min. The observed minimum in the primary particle concentration is about 10 to 15% lower than the prediction, regardless of the number of compartments in the flocculator.

Flocculation Design Criteria

The degree of flocculation is determined by the dimensionless number $\bar{\sigma}\Phi\bar{\Gamma}\tau_h$. The floc volume concentration is fixed by the amount and character of the suspended solids in the raw water, and the particle size distribution factor is determined by the mixing power, flocculator configuration, and raw water suspended solids. For a given plant, then, the dimensionless number can be reduced to $\bar{\Gamma}\tau_h$, which is sometimes called the “Camp Number” in honor of Thomas R. Camp, who promoted its use in flocculator design.

The Camp number is proportional to the total number of collisions that occur in the suspension as it passes through a compartment. Because flocculation is a result of particle collisions, the Camp number is a performance indicator and a basic design consideration. In fact, specification of the Camp number and either the spatially averaged characteristic strain rate or hydraulic detention time suffices to determine the total tankage and mixing power required. It is commonly recommended that flocculator design be based on the product $\bar{\Gamma}\tau_h$ and some upper limit on $\bar{\Gamma}$ to avoid floc breakup (Camp, 1955; James M. Montgomery, Inc., 1985; Joint Task Force, 1990). Many regulatory authorities require a minimum HRT in the flocculation tank of at least 30 min (Water Supply Committee, 1987). In this case, the design problem is reduced to selection of $\bar{\Gamma}$.

Another recommendation is that flocculator design requires only the specification of the product $\bar{\Gamma}\Phi\tau_h$; sometimes Φ is replaced by something related to it, like raw water turbidity or coagulant dosage (O’Melia, 1972; Ives, 1968; Culp/Wesner/Culp, Inc., 1986). This recommendation really applies to upflow contact clarifiers in which the floc volume concentration can be manipulated.

The average absolute velocity gradient employed in the flocculation tanks studied by Camp ranged from 20 to 74/sec, and the median value was about 40/sec; hydraulic retention times ranged from 10 to 100 min, and the median value was 25 min (Camp, 1955). Both the $\bar{\Gamma}$ values and HRTs are somewhat smaller than current practice. Following the practice of Langelier (1921), who introduced mechanical flocculators, most existing flocculators are designed with tapered power inputs. This practice is supposed to increase the settling velocity of the flocs produced. In a study of the coagulation of colloidal silica with alum, TeKippe and Ham (1971) showed that tapered flocculation produced the fastest settling floc. Their best results were obtained with a flocculator divided into four equal compartments, each having a hydraulic retention time of 5 min, and $\bar{\Gamma}$ values of 140, 90, 70 and 50/sec respectively. The $\bar{\Gamma}\tau_h$ product was 105,000. A commonly recommended design for flocculators that precede settlers calls for a Camp number between 30,000 to 60,000, an HRT of at least 1000 to 1500 sec (at 20°C and maximum plant flow), and a tapered r.m.s. characteristic strain rate ranging from about 60/sec in the first compartment to 10/sec in the last compartment (Joint Task Force, 1990). For direct filtration, smaller flocs are desired, and the Camp number is increased from 40,000 to 75,000, the detention time is between 900 and 1500 sec, and the r.m.s. characteristic strain rate is tapered from 75 to 20/sec.

None of these recommendations is fully in accord with the kinetic model or the empirical data. They ignore the effect of the size distribution factor, which causes the flocculation rate for primary particles to vary by a factor of at least four, and which is itself affected by mixing power and configuration. The consequence of this omission is that different flocculators designed for the same $\bar{\Gamma}\tau_h$ or $\bar{\Gamma}\Phi\tau_h$ will produce different results if the mixing power distributions or tank configurations are different. Also, pilot

data obtained at one set of mixing powers or tank configurations cannot be extrapolated to others. The recommendations quoted above merely indicate in a general way the things that require attention. In every case, flocculator design requires a special pilot plant study to determine the best combination of coagulant dosage, tank configuration, and power distribution.

Finally, the data of Argaman and Kaufman suggest that at any given average characteristic strain rate, there is an optimum flocculator hydraulic retention time, and the converse is also true. The existence of an optimum HRT has also been reported by Hudson (1973) and by Griffith and Williams (1972). This optimum HRT is not predicted by the Argaman–Kaufman model; Eq. (9.129) predicts the degree of flocculation will increase uniformly as τ_h increases. Using an alum/kaolin suspension and a completely mixed flocculator, Andreu-Villegas and Letterman (1976) showed that the conditions for optimum flocculation were approximately:

$$\bar{\Gamma}^{2.8} C \tau_h = 44 \times 10^5 \text{ (mg min/L s}^{2.8}\text{)} \quad (9.130)$$

The Andreu-Villegas–Letterman equation gives optimum $\bar{\Gamma}$ and HRT values that are low compared to most other reports. In one study, when the $\bar{\Gamma}$ values were tapered from 182 to 16/sec in flocculators with both paddles and stators, the optimum mixing times were 30 to 40 min (Wagner, 1974).

References

- AWWA. 1969. *Water Treatment Plant Design*, American Water Works Association, Denver, CO.
- Amirtharajah, A. and Trusler, S.L. 1986. "Destabilization of Particles by Turbulent Rapid Mixing," *Journal of Environmental Engineering*, 112(6): 1085.
- Andreu-Villegas, R. and Letterman, R.D. 1976. "Optimizing Flocculator Power Input," *Journal of the Environmental Engineering Division, Proceedings of the American Society of Civil Engineers*, 102(EE2): 251.
- Argaman, Y. and Kaufman, W.J. 1970. "Turbulence and Flocculation," *Journal of the Sanitary Engineering Division, Proceedings of the American Society of Civil Engineers*, 96(SA2): 223.
- Basset, A.B. 1888. *A Treatise on Hydrodynamics: With Numerous Examples*. Deighton, Bell and Co., Cambridge, UK.
- Camp, T.R. 1955. "Flocculation and Flocculation Basins," *Transactions of the American Society of Civil Engineers*, 120: 1.
- Camp, T.R. 1968. "Floc Volume Concentration," *Journal of the American Water Works Association*, 60(6): 656.
- Crank, J. 1975. *The Mathematics of Diffusion*, 2nd ed. Oxford University Press, Clarendon Press, Oxford.
- Culp/Wesner/Culp, Inc. 1986. *Handbook of Public Water Systems*. R.B. Williams and G.L. Culp, eds. Van Nostrand Reinhold Co., Inc., New York.
- Delichatsios, M.A. and Probstein, R.F. 1975. "Scaling Laws for Coagulation and Sedimentation," *Journal of the Water Pollution Control Federation*, 47(5): 941.
- Einstein, A. 1956. *Investigations on the Theory of the Brownian Movement*, R. Furth, ed., trans. A.D. Cowper. Dover Publications, Inc., New York.
- Freundlich, H. 1922. *Colloid & Capillary Chemistry*, trans. H.S. Hatfield. E.P. Dutton and Co., New York.
- Griffith, J.D. and Williams, R.G. 1972. "Application of Jar-Test Analysis at Phoenix, Ariz.," *Journal of the American Water Works Association*, 64(12): 825.
- Harris, H.S., Kaufman, W.J., and Krone, R.B. 1966. "Orthokinetic Flocculation in Water Purification," *Journal of the Sanitary Engineering Division, Proceedings of the American Society of Civil Engineers*, 92(SA6): 95.
- Hinze, J.O. 1959. *Turbulence: An Introduction to Its Mechanism and Theory*. McGraw-Hill, New York.
- Hudson, H.E., Jr. 1973. "Evaluation of Plant Operating and Jar-Test Data," *Journal of the American Water Works Association*, 65(5): 368.

- Ives, K.J. 1968. "Theory of Operation of Sludge Blanket Clarifiers," *Proceedings of the Institution of Civil Engineers*, 39(2): 243.
- James M. Montgomery, Inc. 1985. *Water Treatment Principles and Design*. John Wiley & Sons, Inc., New York.
- Joint Committee of the American Society of Civil Engineers, the American Water Works Association and the Conference of State Sanitary Engineers. 1969. *Water Treatment Plant Design*. American Water Works Association, Inc., New York.
- Joint Task Force. 1990. *Water Treatment Plant Design*, 2nd ed. McGraw-Hill, Inc., New York.
- Langelier, W.F. 1921. "Coagulation of Water with Alum by Prolonged Agitation," *Engineering News-Record*, 86(22): 924.
- Letterman, R.D., Quon, J.E., and Gemmell, R.S. 1973. "Influence of Rapid-Mix Parameters on Flocculation," *Journal of the American Water Works Association*, 65(11): 716.
- Levich, V.G. 1962. *Physicochemical Hydrodynamics*, trans. Scripta Technica, Inc. Prentice-Hall, Inc., Englewood Cliffs, NJ.
- O'Melia, C.R. 1972. "Coagulation and Flocculation," p. 61 in *Physicochemical Processes for Water Quality Control*, W.J. Weber, Jr., ed. John Wiley & Sons, Inc., Wiley-Interscience, New York.
- Parker, D.S., Kaufman, W.J., and Jenkins, D. 1972. "Floc Breakup in Turbulent Flocculation Processes," *Journal of the Sanitary Engineering Division, Proceedings of the American Society of Civil Engineers*, 98(SA1): 79.
- Saffman, P.G. and Turner, J.S. 1956. "On the Collision of Drops in Turbulent Clouds," *Journal of Fluid Mechanics*, 1(part 1): 16.
- Spielman, L.A. 1978. "Hydrodynamic Aspects of Flocculation," p. 63 in *The Scientific Basis of Flocculation*, K.J. Ives, ed. Sijthoff & Noordhoff International Publishers B.V., Alphen aan den Rijn, the Netherlands.
- TeKippe, J. and Ham, R.K. 1971. "Velocity-Gradient Paths in Coagulation," *Journal of the American Water Works Association*, 63(7): 439.
- Vrale, L. and Jorden, R.M. 1971. "Rapid Mixing in Water Treatment," *Journal of the American Water Works Association*, 63(1): 52.
- Wagner, E.G. 1974. "Upgrading Existing Water Treatment Plants: Rapid Mixing and Flocculation," p. IV-56 in *Proceedings AWWA Seminar on Upgrading Existing Water-Treatment Plants*. American Water Works Association, Denver, CO.
- Water Supply Committee, Great Lakes-Upper Mississippi River Board of State Public Health and Environmental Managers. 1987. *Recommended Standards for Water Works, 1987 Edition*. Health Research Inc., Albany, NY.

9.5 Sedimentation

Kinds of Sedimentation

Four distinct kinds of sedimentation processes are recognized:

- Free settling — When discrete particles settle independently of each other and the tank walls, the process is called "free," "unhindered," "discrete," "Type I," or "Class I" settling. This is a limiting case for dilute suspensions of noninteracting particles. It is unlikely that free settling ever occurs in purification plants, but its theory is simple and serves as a starting point for more realistic analyses.
- Flocculent settling — In "flocculent," "Class II," or "Type II" settling, the particle agglomeration process continues in the clarifier. Because the velocity gradients in clarifiers are small, the particle collisions are due primarily to the differences in the particle settling velocities. Aside from the collisions, and the resulting flocculation, there are no interactions between particles or between particles and the tank wall. This is probably the most common settling process in treatment plants designed for turbidity removal.

- **Hindered settling** — “Hindered” settling — also known as “Type III,” “Class III,” and “Zone” settling — occurs whenever the particle concentration is high enough that particles are influenced either by the hydrodynamic wakes of their neighbors or by the counterflow of the displaced water. When observed, the process looks like a slowly shrinking lattice, with the particles representing the lattice points. The rate of sedimentation is dependent on the local particle concentration. Hindered settling is the usual phenomenon in lime/soda softening plants, upflow contact clarifiers, secondary clarifiers in sewage treatment plants, and sludge thickeners.
- **Compressive settling** — “Compressive settling” is the final stage of sludge thickening. It occurs in sludge storage lagoons. It also occurs in batch thickeners, if the sludge is left in them long enough. In this process, the bottom particles are in contact with the tank or lagoon floor, and the others are supported by mutual contact. A slow compaction process takes place as water is exuded from between and within the particles, and the particle lattice collapses.

Kinds of Settling Tanks

There are several kinds of settlement tanks in use:

- **Conventional** — The most common are the “conventional rectangular” and “conventional circular” tanks. “Rectangular” and “circular” refer to the tank’s shape in plan sections. In each of the designs, the water flow is horizontal, and the particles settle vertically relative to the water flow (but at an angle relative to the horizontal). The settling process is either free settling or flocculent settling.
- **Tube, tray, or high-rate** — Sometimes, sedimentation tanks are built with an internal system of baffles, which are intended to regulate the hydraulic regime and impose ideal flow conditions on the tank. Such tanks are called “tube,” “tray,” or “high-rate” settling tanks. The water flow is parallel to the plane of the baffles, and the particle paths form some angle with the flow. The settling process is either free settling or flocculent settling.
- **Upflow** — In “upflow contact clarifiers,” the water flow is upwards, and the particles settle downwards. The rise velocity of the water is adjusted so that it is equal to the settling velocity of the particles, and a “sludge blanket” is trapped within the clarifier. The settling process in an upflow clarifier is hindered settling, and the design methodology is more akin to that of thickeners.
- **Thickeners** — “Thickeners” are tanks designed to further concentrate the sludges collected from settling tanks. They are employed when sludges require some moderate degree of dewatering prior to final disposal, transport, or further treatment. They look like conventional rectangular or circular settling tanks, except they contain mixing devices. An example is shown in [Fig. 9.8](#). The settling process is hindered settling.
- **Flotation** — Finally, there are “flotation tanks.” In these tanks, the particles rise upwards through the water, and they may be thought of as upside down settling tanks. Obviously, the particle density must be less than the density of water, so the particles can float. Oils and greases are good candidates for flotation. However, it is possible to attach air bubbles to almost any particle, so almost any particle can be removed in a flotation tank. The process of attaching air bubbles to particles is called “dissolved air flotation.” Flotation tanks can be designed for mere particle removal or for sludge thickening

Floc Properties

The most important property of the floc is its settling velocity. Actually, coagulation/flocculation produces flocs with a wide range of settling velocities, and plant performance is best judged by the velocity distribution curve. It is the slowest flocs that control settling tank design. In good plants, one can expect the slowest 5% by wt of the flocs to have settling velocities less than about 2 to 10 cm/min. The higher velocity is found in plants with high raw water turbidities, because the degree of flocculation increases

with floc volume concentration. The slowest 2% by wt. will have velocities less than roughly 0.5 to 3 cm/min. Poor plants will produce flocs that are much slower.

Alum/clay floc sizes range from a few hundredths of a mm to a few mm (Boadway, 1978; Dick, 1970; Lagvankar and Gemmell, 1968; Parker, Kaufman, and Jenkins, 1972; Tambo and Hozumi, 1979; Tambo and Watanabe, 1979). A typical median floc diameter for alum coagulation might be a few tenths of a mm; the largest diameter might be 10 times as large. Ferric iron/clay flocs are generally larger than alum flocs (Ham and Christman, 1969; Parker, Kaufman, and Jenkins, 1972). Floc size is correlated with the mixing power and the suspended solids concentration. Relationships of the following form have been reported (Boadway, 1978; François, 1987):

$$d_p \propto \frac{X^b}{\bar{\Gamma}^a} \quad (9.131)$$

where a = a constant ranging from 0.2 to 1.5 (dimensionless)
 b = a constant (dimensionless)
 d_p = the minimum, median, mean, or maximum floc size (m or ft)
 X = the suspended solids concentration (kg/m³ or lb/ft³)
 $\bar{\Gamma}$ = the r.m.s. characteristic strain rate (per sec)

Equation (9.131) applies to all parts of the floc size distribution curve, including the largest observed floc diameter, the median floc diameter, etc. The floc size distribution is controlled by the forces in the immediate vicinity of the mixer, and these forces are dependent on the geometry of the mixing device (François, 1987). This makes the reported values of the coefficients highly variable, and, although good correlations may be developed for a particular facility or laboratory apparatus, the correlations cannot be transferred to other plants or devices unless the conditions are identical.

When flocs grown at one root mean square velocity gradient are transferred to a higher one, they become smaller. The breakdown process takes less than a minute (Boadway, 1978). If the gradient is subsequently reduced to its former values, the flocs will regrow, but the regrown flocs are weaker and smaller than the originals (François, 1987).

Flocs consist of a combination of silt/clay particles, the crystalline products of the coagulant, and entrained water. The specific gravities of aluminum hydroxide and ferric hydroxide crystals are about 2.4 and 3.4, respectively, and the specific gravities of most silts and clays are about 2.65 (Hudson, 1972). However, the lattice of solid particles is loose, and nearly all of the floc mass is due to entrained water. Consequently, the mass density of alum/clay flocs ranges from 1.002 to 1.010 g/cm³, and the density of iron/clay flocs ranges from 1.004 to 1.040 g/cm³ (Lagvankar and Gemmell, 1968; Tambo and Watanabe, 1979). With both coagulants, density decreases with floc diameter and mixing power. Typically,

$$\rho_p - \rho \propto \frac{1}{d_p^a} \quad (9.132)$$

Free Settling

Free settling includes nonflocculent and flocculent settling.

Calculation of the Free, Nonflocculent Settling Velocity

Under quiescent conditions in settling tanks, particles quickly reach a constant, so-called “terminal” settling velocity, Basset’s (1888) equation for the force balance on a particle becomes:

$$\underbrace{0}_{\text{change in momentum}} = \underbrace{\rho_p V_p g}_{\text{particle weight}} - \underbrace{\rho V_p g}_{\text{buoyant force}} - \underbrace{C_D \rho A_p \frac{v_s^2}{2g}}_{\text{drag force}} \quad (9.133)$$

$$v_s = \sqrt{\frac{2gV_p(\rho_p - \rho)}{C_D \rho A_p}} \quad (9.134)$$

where A_p = the cross-sectional area of the particle normal to the direction of fall (m^2 or ft^2)
 C_D = the drag coefficient (dimensionless)
 g = the acceleration due to gravity (9.80665 m/s^2 or 32.174 ft/sec^2)
 V_p = the volume of the particle (m^3 or ft^3)
 v_s = the terminal settling velocity of the particle (m/s or ft/sec)
 ρ = the density of the liquid (kg/m^3 or $slug/ft^3$)
 ρ_p = the density of the particle (kg/m^3 or $slug/ft^3$)

For a sphere, Eq. (9.134) becomes:

$$v_s = \sqrt{\frac{4gd_p(\rho_p - \rho)}{3C_D \rho}} \quad (9.135)$$

where d_p = the particle's diameter (m or ft).

Newton assumed that the drag coefficient was a constant, and indeed, if the particle is moving very quickly it is a constant, with a value of about 0.44 for spheres. However, in general, the drag coefficient depends upon the size, shape, and velocity of the particle. It is usually expressed as a function of the particle Reynolds number. For spheres, the definition is as follows:

$$Re = \frac{\rho v_s d_p}{\mu} \quad (9.136)$$

The empirical correlations for C_D and Re for spheres are shown in Fig. 9.5 (Rouse, 1937). Different portions of the empirical curve may be represented by the following theoretical and empirical formulae:

Theoretical Formulas

Stokes (1856) (for $Re < 0.1$)

$$C_D = \frac{24}{Re} \quad (9.137)$$

For spheres, the Stokes terminal settling velocity is

$$v_s = \frac{g(\rho_p - \rho)d_p^2}{18\mu} \quad (9.138)$$

Oseen (1913)–Burgess (1916) (for $Re < 1$)

$$C_D = \frac{24}{Re} \cdot \left(1 + \frac{3Re}{16}\right) \quad (9.139)$$

Goldstein (1929) (for $Re < 2$)

$$C_D = \frac{24}{Re} \cdot \left[1 + \frac{3Re}{16} - \frac{19Re^2}{1,280} + \frac{71Re^3}{20,480} - \frac{30,179Re^4}{34,406,400} + \frac{122,519Re^5}{560,742,400} - \dots\right] \quad (9.140)$$

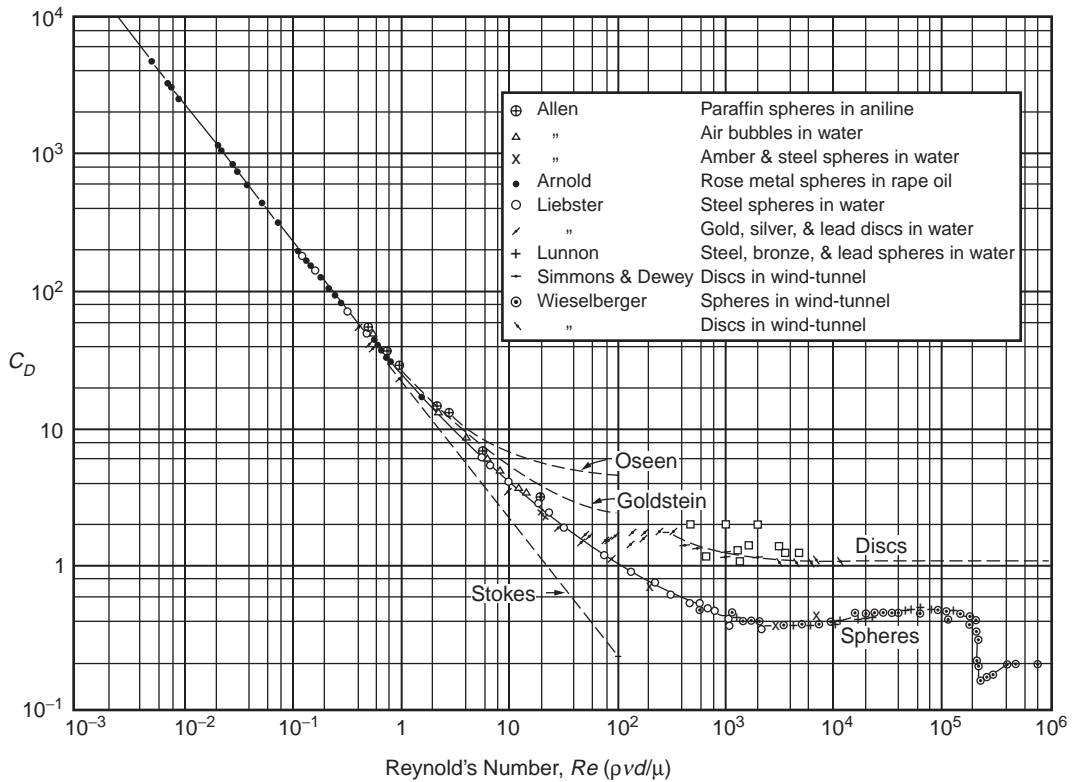


FIGURE 9.5 Drag coefficients for sedimentation (Rouse, H. 1937. Nomogram for the Settling Velocity of Spheres. *Report of the Committee on Sedimentation*, p. 57, P.D. Trask, chm., National Research Council, Div. Geol. and Geog.)

Empirical Formulas

Allen (1900) (for $10 < Re_{eff} < 200$)

$$C_D = \frac{10.7}{\sqrt{Re_{eff}}} \quad (9.141)$$

The Reynolds number in Eq. (9.141) is based on an “effective” particle diameter:

$$Re_{eff} = \frac{\rho v_s d_{eff}}{\mu} \quad (9.142)$$

where d_p = the actual particle diameter (m or ft)
 d_2 = the diameter of a sphere that settles at a Reynolds number of 2 (m or ft)
 d_{eff} = the effective particle diameter (m or ft)
 $= d_p - 0.40 d_2$

The effective diameter was introduced by Allen to improve the curve fit. The definition of d_2 was arbitrary: Stokes’ Law does not apply at a Reynolds number of 2. For spheres, the Allen terminal settling velocity is,

$$v_s = 0.25 d_{eff} \left[\frac{g(\rho_p - \rho)}{\sqrt{\rho \mu}} \right]^{2/3} \quad (9.143)$$

Shepherd (Anderson, 1941) (for $1.9 < Re < 500$)

$$C_D = \frac{18.5}{Re^{0.60}} \quad (9.144)$$

For spheres, the Shepherd terminal settling velocity is (McGaughey, 1956),

$$v_s = 0.153d_p^{1.143} \left[\frac{g(\rho_p - \rho)}{\rho^{0.40} \mu^{0.60}} \right]^{0.714} \quad (9.145)$$

Examination of Fig. 9.5 shows that the slope of the curve varies from -1 to 0 as the Reynolds number increases from about 0.5 to about 4000 . This is the transition region between the laminar Stokes' Law and the fully turbulent Newton's Law. For this region, the drag coefficient may be generalized as follows:

$$C_D = kRe^{n-2} \quad (9.146)$$

$$v_s^n = \frac{4g}{3k} d_p^{3-n} \left(\frac{\rho_p - \rho}{\rho^{n-1} \cdot \mu^{2-n}} \right) \quad (9.147)$$

where k = a dimensionless curve-fitting constant ranging in value from 24 to 0.44
 n = a dimensionless curve-fitting constant ranging in value from 1 to 2 .

Equation (9.146) represents the transition region as a series of straight line segments. Each segment will be accurate for only a limited range of Reynolds numbers.

Fair–Geyer (1954) (for $Re < 10^4$)

$$C_D = \frac{24}{Re} + \frac{3}{\sqrt{Re}} + 0.34 \quad (9.148)$$

Newton (Anderson, 1941) (for $500 < Re < 200,000$)

$$C_D = 0.44 \quad (9.149)$$

For spheres, the Newton terminal settling velocity is

$$v_s = 1.74 \sqrt{\frac{gd_p(\rho_p - \rho)}{\rho}} \quad (9.150)$$

Referring to Fig. 9.5, it can be seen that there is a sharp discontinuity in the drag coefficient for spheres at a Reynolds number of about $200,000$. The discontinuity is caused by the surface roughness of the particles and turbulence in the surrounding liquid. It is not important, because Reynolds' numbers this large are never encountered in water treatment.

A sphere with the properties of a median alum floc ($d_p = 0.50$ mm and $S_p = 1.005$) would have a settling velocity of about 0.5 mm/sec and a Reynolds number of about 0.2 (at 10°C). Most floc particles are smaller than 0.5 mm, so they will be slower and have smaller Reynolds numbers. This means that Stokes' Law is an acceptable approximation in most cases of alum/clay floc sedimentation.

For sand grains, the Reynolds number is well into the transition region, and the Fair–Geyer formula is preferred. If reduced accuracy is acceptable, one of the Allen/Shepherd formulae may be used.

Except for the Stokes, Newton, Allen, and Shepherd laws, the calculation of the terminal settling velocity is iterative, because the drag coefficient is a polynomial function of the velocity. Graphical solutions are presented by Camp (1936a), Fair, Geyer, and Morris (1954), and Anderson (1941).

Nonspherical particles can be characterized by the ratios of their diameters measured along their principal axes of rotation. Spherical and nonspherical particles are said to be “equivalent,” if they have the same volume and weight. If Re is less than 100 and the ratios are 1:1:1 (as in a cube), the nonspherical particles settle at 90 to 100% of the velocity of the equivalent sphere (Task Committee, 1975). For ratios of 4:1:1, 4:2:1, or 4:4:1, the velocity of the nonspherical particle is about two-thirds the velocity of the equivalent sphere. If the ratios are increased to 8:1:1, 8:2:1, or 8:4:1, the settling velocity of the nonspherical particles falls to a little more than half that of the equivalent sphere. The shape problem is lessened by the fact that floc particles are formed by the drag force into roughly spherical or teardrop shapes.

In practice, Eqs. (9.138) through (9.150) are almost never used to calculate settling velocities. The reason for this is the onerous experimental and computational work load their use requires. Floc particles come in a wide range of sizes, and the determination of the size distribution would require an extensive experimental program. Moreover, the specific gravity of each size class would be needed. In the face of this projected effort, it is easier to measure settling velocities directly using a method like Seddon’s, which is described below.

The settling velocity equations are useful when experimental data obtained under one set of conditions must be extrapolated to another. For example, terminal settling velocities depend on water temperature, because temperature strongly affects viscosity. The ratio of water viscosities for 0 to 30°C, which is the typical range of raw water temperatures in the temperature zone, is about 2.24. This means that a settling tank designed for winter conditions will be between 1.50 and 2.24 times as big as a tank designed for summer conditions, depending on the Reynolds number.

The terminal velocity also varies with particle diameter and specific gravity. Because particle size and density are inversely correlated, increases in diameter tend to be offset by decreases in specific gravity, and some intermediate particle size will have the fastest settling velocity. This is the reason for the traditional advice that “pinhead” flocs are best.

Settling Velocity Measurement

The distribution of particle settling velocities can be determined by the method first described by Seddon (1889) and further developed by Camp (1945). Tests for the measurement of settling velocities must be continued for at least as long as the intended settling zone detention time. Furthermore, samples must be collected at several time intervals in order to determine whether the concentration trajectories are linear or concave downwards.

A vertical tube is filled from the bottom with a representative sample of the water leaving the flocculation tank, or any other suspension of interest. The depth of water in the tube should be at least equal to the expected depth of the settling zone, and there should be several sampling ports at different depths. The tube and the sample in it should be kept at a constant, uniform temperature to avoid the development of convection currents. A tube diameter at least 100 times the diameter of the largest particle is needed to avoid measurable “wall effects” (Dryden, Murnaghan, and Bateman, 1956). The effect of smaller tube/particle diameter ratios can be estimated using McNown’s (Task Committee, 1975) formula:

$$\frac{v_s}{v_t} = 1 + \frac{9d_p}{4d_t} + \left(\frac{9d_p}{4d_t} \right)^2 \quad (9.151)$$

where d_p = the particle’s diameter (m or ft)
 d_t = the tube’s diameter (m or ft)
 v_s = the particle’s free terminal settling velocity (m/s or ft/sec)
 v_t = the particle’s settling velocity in the tube (m/s or ft/sec)

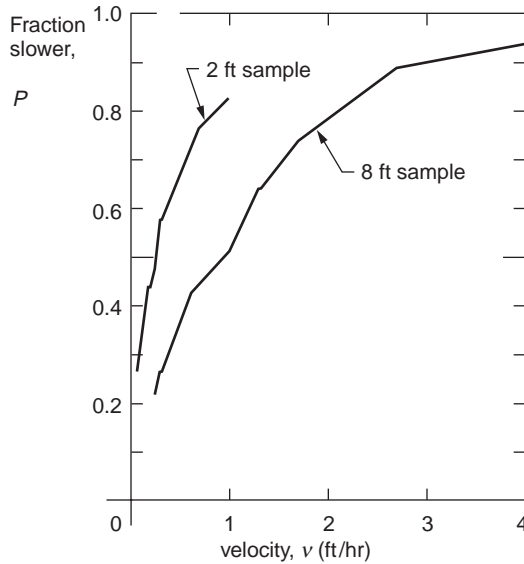


FIGURE 9.6 Settling velocity distributions for Mississippi River sediments. [Seddon, J.A. 1889. Clearing Water by Settlement, *J. Assoc. Eng'g Soc.*, 8(10): 477.]

The largest expected flocs are on the order of a few mm in diameter, so the minimum tube diameter will be tens of cm.

Initially, all the various particle velocity classes are distributed uniformly throughout the depth of the tube. Therefore, at any particular sampling time after the settling begins, say t_i the particles sampled at a distance h below the water surface must be settling at a velocity less than,

$$v_i = \frac{h_i}{t_i} \quad (9.152)$$

where h_i = the depth below the water's surface of the sampling port for the i -th sample (m or ft)
 t_i = the i -th sampling time (sec)
 v_i = the limiting velocity for the particles sampled at t_i (m/s or ft/sec)

The weight fraction of particles that are slower than this is simply the concentration of particles in the sample divided by the initial particle concentration:

$$P_i = \frac{X_i}{X_0} \quad (9.153)$$

where P_i = the weight fraction of the suspended solids that settle more slowly than v_i (dimensionless)
 X_i = the suspended solids concentration in the sample collected at t_i (kg/m^3 or lb/ft^3)
 X_0 = the initial, homogeneous suspended solids concentration in the tube (kg/m^3 or lb/ft^3)

The results of a settling column test would look something like the data in Fig. 9.6, which are taken from Seddon's paper. The data represent the velocities of river muds, which are slower than alum or iron flocs.

Flocculent versus Nonflocculent Settling

In nonflocculent settling, the sizes and velocities of the particles do not change. Consequently, if the trajectory of a particular concentration is plotted on depth-time axes, a straight line is obtained. In flocculent settling, the particles grow and accelerate as the settling test progresses, and the concentration

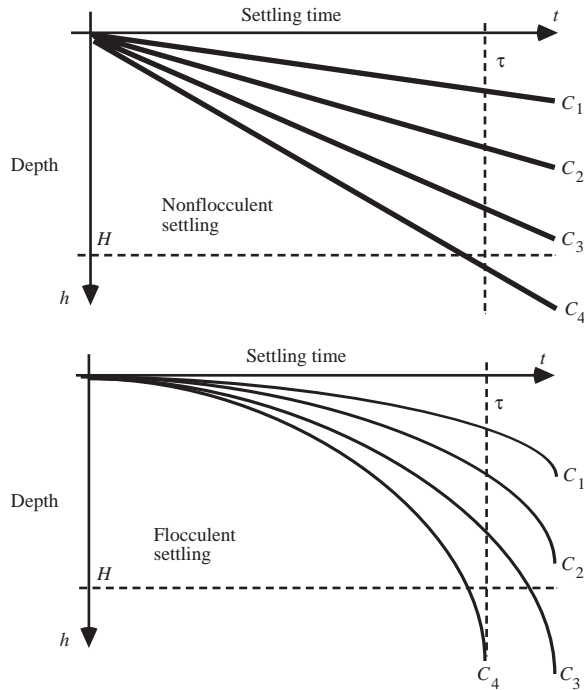


FIGURE 9.7 Particle depth-time trajectories for nonflocculent and flocculent settling.

trajectories are concave downwards. These two possibilities are shown in Fig. 9.7. The same effect is seen in Fig. 9.6, where the samples from 8 ft, which represent longer sampling times, yield higher settling velocities than the 2 ft samples.

Design of Rectangular Clarifiers

What follows is the Hazen (1904)–Camp (1936a, 1936b) theory of free settling in rectangular tanks. Refer to Fig. 9.8. The liquid volume of the tank is divided into four zones: (1) an inlet or dispersion zone, (2) a settling zone, (3) a sludge zone, and (4) an outlet or collection zone (Camp, 1936b).

The inlet zone is supposed to be constructed so that each velocity class of the incoming suspended particles is uniformly distributed over the tank's transverse vertical cross section. A homogeneous distribution is achieved in many water treatment plants as a consequence of the way flocculation tanks and rectangular settling tanks must be connected. It is not achieved in circular tanks or in rectangular tanks in sewage treatment plants, unless special designs are adopted.

The sludge zone contains accumulated sludge and sludge removal equipment. Particles that enter the sludge zone are assumed to remain there until removed by the sludge removal equipment. Scour of the sludge must be prevented. Sludge thickening and compression also occur in the sludge zone, but this is not normally considered in clarifier design.

The water flow through the settling zone is supposed to be laminar and horizontal, and the water velocity is supposed to be the same at each depth. Laminar flow is readily achievable by baffling, but the resulting water velocities are not uniform, and often they are not horizontal. The corrections needed for these conditions are discussed below.

The outlet zone contains the mechanisms for removing the clarified water from the tank. Almost always, water is removed from near the water surface, so the water velocity in the outlet zone has a net upwards component. This upwards component may exceed the settling velocities of the slowest particles, so it is assumed that any particle that enters the outlet zone escapes in the tank effluent.

where C = the suspended solids' concentration at depth h (kg/m³ or lb/ft³)
 \bar{C}_H = the depth-averaged suspended solids' concentration over the settling zone outlet's outlet plane (kg/m³ or lb/ft³)
 H = the settling zone's depth (m or ft)
 L = the settling zone's length (m or ft)
 Q = the flow through the settling zone (m³/s or ft³/sec)
 U = the horizontal water velocity through the settling zone (m/s or ft/sec)
 W = the settling zone's width (m or ft)

The settling zone particle removal efficiency is (San, 1989),

$$E = \frac{C_i - \bar{C}_H}{C_i} = \frac{1}{H} \int_0^H f \cdot dh \quad (9.155)$$

where C_i = the suspended solids' concentration in the influent flow to the settling zone (kg/m³ or lb/ft³)
 E = the removal efficiency (dimensionless)
 f = the fraction removed at each depth at the outlet plane of the settling zone (dimensionless)

The removal efficiency can also be calculated from the settling velocity distribution, such as in Fig. 9.6 (Sykes, 1993):

$$E = 1 - P_o + \frac{1}{v_o} \int_0^{P_o} v \cdot dP \quad (9.156)$$

where P = the weight fraction of the suspended solids that settles more slowly than v (dimensionless)
 P_o = the weight fraction of the suspended solids that settles more slowly than v_o (dimensionless)
 v = any settling velocity between zero and v_o (m/s or ft/sec)
 v_o = the tank overflow rate (m/s or ft/sec) (See below.)

Note that the integration is performed along the vertical axis, and the integral represents the area between the velocity distribution curve and the vertical axis. The limiting velocities are calculated using Eq. (9.152) by holding the sampling time t_i constant at τ and using concentration data from different depths. Equation (9.156) reduces to the formulas used by Zanoni and Blomquist (1975) to calculate removal efficiencies for flocculating suspensions.

Nonfloculent Settling

Certain simplifications occur if the settling process is nonfloculent. However, nonfloculent settling is probably limited to grit chambers (Camp, 1953). Referring to Fig. 9.8, the critical particle trajectory goes from the top of the settling zone on the inlet end to the bottom of the settling zone on the outlet end. The settling velocity that produces this trajectory is v_o . Any particle that settles at v_o or faster is removed from the flow. A particle that settles more slowly than v_o , say v_1 , is removed only if it begins its trajectory within h_1 of the settling zone's bottom. Similar triangles show that this critical settling velocity is also the tank overflow rate, and to the ratio of the settling zone depth to hydraulic retention time:

$$v_o = \frac{Q}{WL} = \frac{H}{\tau} \quad (9.157)$$

where v_o = the critical particles' settling velocity (m/s or ft/sec).

In nonfloculent free settling, the settling velocity distribution does not change with settling time, and the efficiency predicted by Eq. (9.156) depends only on overflow rate, regardless of the combination of depth and detention time that produces it. Increasing the overflow rate always reduces the efficiency, and reducing the overflow rate always increases it.

Flocculent Settling

This is not the case in flocculent settling. Consider a point on one of the curvilinear contours shown in Fig. 9.7. Equation (9.152) now represents the average velocity of the selected concentration up to the selected instant. In the case of the contour that exits the settling zone at its bottom, the slope of the chord is v_0 . The average velocity of any given contour increases as the sampling time increases. This has several consequences:

- Fixing v_0 and increasing both H and τ increases the efficiency.
- Fixing v_0 and reducing both H and τ reduces the efficiency.
- Increasing v_0 by increasing both H and τ may increase, decrease, or not change the efficiency depending on the trajectories of the contours; if the curvature of the contours is large, efficiency increases will occur for new overflow rates that are close to the original v_0 .
- Reducing v_0 by reducing both H and τ may increase, decrease, or not change the efficiency, depending on the trajectories of the contours; if the curvature of the contours is large, efficiency reductions will occur for new overflow rates that are close to the original v_0 .

Any other method of increasing or decreasing v_0 yields the same results as those obtained in nonflocculent settling.

Scour

Settling zone depth is important. The meaning of Eq. (9.157) is that if a particle's settling velocity is equal to the overflow rate, it will reach the top of the sludge zone. However, once there, it still may be scoured from the sludge zone and resuspended in the flow. Repeated depositions and scourings would gradually transport the particle through the tank and into the effluent flow, resulting in clarifier failure. Whether or not this happens depends on the depth-to-length ratio of the settling zone.

Camp (1942) assumes that the important variable is the average shearing stress in the settling zone/sludge zone interface. In the case of steady, uniform flow, the accelerating force due to the weight of the water is balanced by retarding forces due to the shearing stresses on the channel walls and floor (Yalin, 1977):

$$\tau_o = \gamma HS \quad (9.158)$$

The shearing stress depends on the water velocity and the settling zone depth. The critical shearing stress is that which initiates mass movement in the settled particles. Dimensional analysis suggests a correlation of the following form (Task Committee, 1975):

$$\frac{\tau_c}{(\gamma_p - \gamma)d_p} = f(\text{Re}_*) \quad (9.159)$$

where d_p = the particle's diameter (m or ft)

Re_* = the boundary Reynolds number (dimensionless)

$$= v_* d_p / \nu$$

v_* = the shear velocity (m/s or ft/sec)

$$= \sqrt{\frac{\tau_c}{\rho}}$$

γ = the specific weight of the liquid (N/m³ or lbf/ft³)

γ_p = the specific weight of the particle (N/m³ or lbf/ft³)

ν = the kinematic viscosity of the liquid (m²/s or ft²/sec)

ρ = the density of the liquid (kg/m³ or slug/ft³)

τ_c = the critical shearing stress that initiates particle movement (N/m² or lbf/ft²)

Equation (9.159) applies to granular, noncohesive materials like sand. Alum and iron flocs are cohesive. The cohesion is especially well-developed on aging, and individual floc particles tend to merge together. However, a conservative assumption is that the top layer of the deposited floc, which is fresh, coheres weakly.

For the conditions in clarifiers, Eq. (9.159) becomes (Mantz, 1977),

$$\frac{\tau_c}{(\gamma_p - \gamma)d_p} = \frac{0.1}{Re_*^{0.30}} \quad (9.160)$$

This leads to relationships among the settling zone's depth and length. For example, the horizontal velocity is related to the critical shearing stress by the following (Chow, 1959):

$$U_c = \sqrt{8/f} \sqrt{\tau_c/\rho} \quad (9.161)$$

where f = the Darcy-Weisbach friction factor (dimensionless)

U_c = the critical horizontal velocity that initiates particle movement (m/s or ft/sec).

Consequently,

$$\frac{H}{L} \geq \frac{v_o}{\sqrt{8/f} \sqrt{\tau_c/\rho}} = \text{a constant} \quad (9.162)$$

Equation (9.162) is a lower limit on the depth-to-length ratio.

Ingersoll, McKee, and Brooks (1956) assume that the turbulent fluctuations in the water velocity at the interface cause scour. They hypothesize that the deposited flocs will be resuspended if the vertical fluctuations in the water velocity at the sludge interface are larger than the particle settling velocity. Using the data of Laufer (1950), they concluded that the vertical component of the root-mean-square velocity fluctuation of these eddies is approximately equal to the shear velocity, and they suggested that scour and resuspension will be prevented if,

$$\frac{v_o}{\sqrt{\tau_o/\rho}} > 1.2 \text{ to } 2.0 \quad (9.163)$$

This leads to the following:

$$\frac{H}{L} > (1.2 \text{ to } 2.0) \sqrt{f/8} \quad (9.164)$$

The Darcy–Weisbach friction factor for a clarifier is about 0.02, so the right-hand-side of Eq. (9.164) is between 0.06 and 0.1, which means that the length must be *less than* 10 to 16 times the depth. Camp's criterion would permit a horizontal velocity that is 2 to 4 times as large as the velocity permitted by the Ingersoll–McKee–Brooks analysis.

Short-Circuiting

A tank is said to “short-circuit” if a large portion of the influent flow traverses a small portion of the tank's volume. In extreme cases, some of the tank's volume is a “dead zone” that neither receives nor discharges liquid. Two kinds of short-circuiting occur: “density currents” and “streaming.”

Density Currents

Density currents develop when the density of the influent liquid is significantly different from the density of the tank's contents. The result is that the influent flow either floats over the surface of the tank or

sinks to its bottom. The two common causes of density differences are differences in (1) temperature and (2) suspended solids concentrations.

Temperature differences arise because the histories of the water bodies differ. For example, the influent flow may have been drawn from the lower portions of a reservoir, while the water in the tank may have been exposed to surface weather conditions for several hours. Small temperature differences can be significant.

Suspended solids have a similar effect. The specific gravity of a suspension can be calculated as follows (Fair, Geyer, and Morris, 1954):

$$S_s = \frac{S_p S_w}{f_w S_p + (1 - f_w) S_w} \quad (9.165)$$

where f_w = the weight fraction of water in the suspension (dimensionless)
 S_p = the specific gravity of the particles (dimensionless)
 S_s = the specific gravity of the suspension (dimensionless)
 S_w = the specific gravity of the water (dimensionless)

By convention, all specific gravities are referenced to the density of pure water at 3.98°C, where it attains its maximum value. Equation (9.165) can be written in terms of the usual concentration units of mass/volume as follows:

$$S_s = S_w + \frac{X}{\rho} \cdot \left(1 - \frac{S_w}{S_p} \right) \quad (9.166)$$

where X = the concentration of suspended solids (kg/m³ or slug/ft³)
 ρ = the density of water (kg/m³ or slug/ft³)

Whether or not the density current has important effects depends on its location and its speed (Eliassen, 1946; Fitch, 1957). If the influent liquid is lighter than the tank contents and spreads over the tank surface, any particle that settles out of the influent flow enters the stagnant water lying beneath the flow and settles vertically all the way to the tank bottom. During their transit of the stagnant zone, the particles are protected from scour, so once they leave the flow, they are permanently removed from it. If the influent liquid spreads across the entire width of the settling zone, then the density current may be regarded as an ideal clarifier. In this case, the depth of the settling zone is irrelevant. Clearly, this kind of short-circuiting is desirable.

If the influent liquid is heavier than the tank contents, it will settle to the bottom of the tank. As long as the flow uniformly covers the entire bottom of the tank, the density current may be treated as an ideal clarifier. Now, however, the short-circuiting flow may scour sludge from the tank bottom. The likelihood of scour depends on the velocity of the density current. According to von Karman (1940), the density current velocity is:

$$U_{dc} = \left[\frac{2gQ(\rho_{dc} - \rho)}{\rho W} \right]^{1/3} \quad (9.167)$$

where g = the acceleration due to gravity (9.80665 m/s² or 32.174 ft/sec²)
 Q = the flow rate of the density current (m³/s or ft³/sec)
 U_{dc} = the velocity of the density current (m/s or ft/sec)
 W = the width of the clarifier (m or ft)
 ρ = the density of the liquid in the clarifier (kg/m³ or slug/ft³)
 ρ_{dc} = the density of the density current (kg/m³ or slug/ft³)

Streaming

Density currents divide the tank into horizontal layers stacked one above the other. An alternative arrangement would be for the tank to be divided into vertical sections placed side-by-side. The sections would be oriented to run the length of the tank from inlet to outlet. Fitch (1956) calls this flow arrangement “streaming.”

Suppose that the flow consists of two parallel streams, each occupying one-half of the tank width. A fraction f of the flow traverses the left section, and a fraction $1 - f$ traverses the right section. Within each section, the flow is distributed uniformly over the depth. The effective overflow rate for the left-hand section is v_1 , and a weight fraction P_1 settles slower than this. For the right-hand section, the overflow rate is v_2 , and the slower fraction is P_2 . The flow-weighted average removal efficiency would be:

$$\bar{E} = f \cdot \left(1 - P_1 + \frac{1}{v_1} \int_0^{P_1} v \cdot dP \right) + (1 - f) \cdot \left(1 - P_2 + \frac{1}{v_2} \int_0^{P_2} v \cdot dP \right) \quad (9.168)$$

This can also be written as:

$$\begin{aligned} \bar{E} = & 1 - P_o + \frac{1}{v_o} \int_0^{P_o} v \cdot dP \\ & + f(P_o - P_1) - \frac{1}{2v_o} \int_{P_1}^{P_o} v \cdot dP \\ & - (1 - f)(P_2 - P_o) + \frac{1}{2v_o} \int_{P_o}^{P_2} v \cdot dP \end{aligned} \quad (9.169)$$

The first line on the right-hand side is the removal efficiency without streaming. The second and third lines represent corrections to the ideal removal efficiency due to streaming. Fitch shows that both corrections are always negative, and the effect of streaming is to reduce tank efficiency. The degree of reduction depends on the shape of the velocity distribution curve and the design surface loading rate.

The fact that tanks have walls means that some streaming is inevitable: the drag exerted by the walls causes a lateral velocity distribution. However, more importantly, inlet and outlet conditions must be designed to achieve and maintain uniform lateral distribution of the flow. One design criterion used to achieve uniform lateral distribution is a length-to-width ratio. The traditional recommendation was that the length-to-width ratio should lie between 3:1 and 5:1 (Joint Task Force, 1969). However, length-to-width ratio restrictions are no longer recommended (Joint Committee, 1990). It is more important to prevent the formation of longitudinal jets. This can be done by properly designing inlet details.

The specification of a surface loading rate, a length-to-depth ratio, and a length-to-width ratio uniquely determine the dimensions of a rectangular clarifier and account for the chief hydraulic problems encountered in clarification.

Traditional Rules of Thumb

Some regulatory authorities specify a minimum hydraulic retention time, a maximum horizontal velocity, or both: e.g., for water treatment (Water Supply Committee, 1987),

$$\tau = \frac{WHL}{Q} \geq 4 \text{ hr} \quad (9.170)$$

$$U = \frac{Q}{WH} \leq 0.5 \text{ fpm} \quad (9.171)$$

Hydraulic detention times for primary clarifiers in wastewater treatment tend to be 2 h at peak flow (Joint Task Force, 1992).

Some current recommendations for the overflow rate for rectangular and circular clarifiers for water treatment are (Joint Committee, 1990):

Lime/soda softening —

low magnesium, $v_o = 1700$ gpd/ft²

high magnesium, $v_o = 1400$ gpd/ft²

Alum or iron coagulation —

turbidity removal, $v_o = 1000$ gpd/ft²

color removal, $v_o = 700$ gpd/ft²

algae removal, $v_o = 500$ gpd/ft²

The recommendations for wastewater treatment are (Wastewater Committee, 1990):

Primary clarifiers —

average flow, $v_o = 1000$ gpd/ft²

peak hourly flow, $v_o = 1500$ to 3000 gpd/ft²

Activated sludge clarifiers, at peak hourly flow, not counting recycles —

conventional, $v_o = 1200$ gpd/ft²

extended aeration, $v_o = 1000$ gpd/ft²

second stage nitrification, $v_o = 800$ gpd/ft²

Trickling filter humus tanks, at peak hourly flow —

$v_o = 1200$ gpd/ft²

The traditional rule-of-thumb overflow rates for conventional rectangular clarifiers in alum coagulation plants are 0.25 gal/min·ft² (360 gpd/ft²) in regions with cold winters and 0.38 gal/min·ft² (550 gpd/ft²) in regions with mild winters. The Joint Task Force (1992) summarizes an extensive survey of the criteria used by numerous engineering companies for the design of wastewater clarifiers. The typical practice appears to be about 800 gpd/ft² at average flow for primary clarifiers and 600 gpd/ft² for secondary clarifiers. The latter rate is doubled for peak flow conditions.

Typical side water depths for all clarifiers is 10 to 16 ft. Secondary wastewater clarifiers should be designed at the high end of the range.

Hudson (1981) reported that in manually cleaned, conventional clarifiers, the sludge deposits often reach to within 30 cm of the water surface near the tank inlets, and scour velocities range from 3.5 to 40 cm/sec. The sludge deposits in manually cleaned tanks are often quite old, at least beneath the surface layer, and the particles in the deposits are highly flocculated and “sticky.” Also, the deposits are well-compacted, because there is no mechanical collection device to stir them up. Consequently, Hudson’s data represent the upper limits of scour resistance.

The limit on horizontal velocity, Camp’s shearing stress criterion, and the Ingersoll–McKee–Brook’s velocity fluctuation criterion are different ways of representing the same phenomenon. In principle, all three criteria should be consistent and produce the same length-to-depth ratio limit. However, different workers have access to different data sets and draw somewhat different conclusions. Because scour is a major problem, a conservative criterion should be adopted. This means a relatively short length-to-depth ratio, which means a relatively deep tank.

The limits on tank overflow rate, horizontal velocity, length-to-depth ratio, and hydraulic retention time overdetermine the design; only three of them are needed to specify the dimensions of the settling zone. They may also be incompatible.

Design of Circular Tanks

In most designs, the suspension enters the tank at the center and flows radially to the circumference. Other designs reverse the flow direction, and in one proprietary design, the flow enters along the circumference and follows a spiral path to the center.

The collection mechanisms in circular tanks have no bearings under water and are less subject to corrosion, reducing maintenance. However, center-feed tanks tend to exhibit streaming, especially in tank diameters larger than about 125 ft. Streaming is reduced in peripheral feed tanks and in center feed tanks with baffles (Joint Committee, 1990).

The design principles used for rectangular tanks also apply, with a few exceptions, to circular tanks.

Free, Nonflocculent Settling

The analysis of particle trajectories for circular tanks is given by Fair, Geyer, and Morris (1954) for center-feed, circular clarifiers. The trajectory of a freely settling, nonflocculent particle curves downwards, because as the distance from the center-feed increases, the horizontal water velocity decreases. At any point along the trajectory, the slope of the trajectory is given by the ratio of the settling velocity to the water velocity:

$$\frac{dz}{dr} = -\frac{v_s}{U_r} = -\frac{2\pi H v_s}{Q} \quad (9.172)$$

- where
- H = the water depth in the settling zone (m or ft)
 - Q = the flow through the settling zone (m³/s or ft³/sec)
 - r = the distance from the center of the tank (m or feet)
 - U_r = the horizontal water velocity at r (m/s or ft/sec)
 - v_s = the particle's settling velocity (m/s or ft/sec)
 - z = the elevation of the particle about the tank's bottom (m or ft)

The minus sign on the right-hand-side is needed, because the depth variable is positive upwards, and the particle is moving down.

Equation (9.172) can be solved for the critical case of a particle that enters the settling zone at the water surface and reaches the bottom of the settling zone at its outlet cylinder:

$$v_o = \frac{Q}{\pi(r_o^2 - r_i^2)} \quad (9.173)$$

- where
- r_i = the radius of the inlet baffle (m or ft)
 - r_o = the radius of the outlet weir (m or ft).

The denominator in Eq. (9.173) is the plan area of the settling zone. Consequently, the critical settling velocity is equal to the settling zone overflow rate.

The analysis leading to Eq. (9.173) also applies to tanks with peripheral feed and central takeoff. The only change required is the deletion of the minus sign in the right-hand side of Eq. (9.172), because the direction of the flow is reversed, and the slope of the trajectory is positive in the given coordinate system. Furthermore, the analysis applies to spiral flow tanks, if the integration is performed along the spiral stream lines. Consequently, all horizontal flow tanks are governed by the same principle.

Free, Flocculent Settling

The trajectories of nonflocculating particles in a circular clarifier are curved in space. However, if the horizontal coordinate were the time-of-travel along the settling zone, the trajectories would be linear. This can be shown by a simple change of variable:

$$\frac{dz}{dt} = \frac{dz}{dr} \cdot \frac{dr}{dt} = -\frac{v_s}{U_r} \cdot U_r = -v_s \quad (9.174)$$

This means that Fig. 9.7 also applies to circular tanks, if the horizontal coordinate is the time-of-travel. Furthermore, it applies to flocculent and nonflocculent settling in circular tanks.

Equation (9.156) applies to circular tanks with uniform feed over the inlet depth, whether they are center-feed, peripheral-feed, or spiral-flow tanks.

Unfortunately, the inlet designs of most circular clarifiers do not produce a vertically uniform feeding pattern. Usually, all of the flow is injected over a small portion of the settling zone depth. As long as the flow is injected at the top of the settling zone, this does not change matters, but other arrangements may.

One case where Camp's formula for clarifier efficiency does not apply is the upflow clarifier. However, this is also a case of hindered settling, and it will be discussed later.

The plan area of the circular settling zone is determined by the overflow rate, and this rate will be equal to the one used for a rectangular tank having the same efficiency. The design is completed by choosing a settling zone depth or a detention time. No general analysis for the selection of these parameters has been published, and designers are usually guided by traditional rules of thumb. The traditional rule of thumb in the United States is a detention time of 2 to 4 hr (Joint Task Force, 1969). Many regulatory agencies insist on a 4 hr detention time (Water Supply Committee, 1987).

Design of High-Rate, Tube, or Tray Clarifiers

"High-rate" settlers, also known as "tray" or "tube" settlers, are laminar flow devices. They eliminate turbulence, density currents, and streaming, and the problems associated with them. Their behavior is nearly ideal and predictable. Consequently, allowances for nonideal and uncertain behavior can be eliminated, and high-rate settlers can be made much smaller than conventional rectangular and circular clarifiers; hence, their name.

Hayden (1914) published the first experimental study of the efficiency of high-rate clarifiers. His unit consisted of a more-or-less conventional rectangular settler containing a system of corrugated steel sheets. This is a form of Camp's tray clarifier. The sheets were installed 45° from the horizontal, so that particles that deposited on them would slide down the sheets into the collection hoppers below. The sheets were corrugated for structural stiffness. The high-rate clarifier had removal efficiencies that were between 40 and 100% higher than simple rectangular clarifiers having the same geometry and dimensions and treating the same flow.

Nowadays, Hayden's corrugated sheets and the Hazen–Camp trays are replaced by modules made out of arrays of plastic tubes. The usual tube cross section is an area-filling polygon, such as the isosceles triangle, the hexagon, the square, and the chevron. Triangles, squares, and chevrons are preferred, because alternate rows of tubes can be sloped in different directions, which stiffens the module and makes it self-supporting. When area-filling hexagons are used, the alternate rows interdigitate and must be strictly parallel. Alternate rows of hexagons can be sloped at different angles, if the space-filling property is sacrificed.

Sedimentation

Consider a particle being transported along a tube that is inclined at an angle θ from the horizontal. Yao (1970, 1973) analyzes the situation as follows. Refer to Fig. 9.9. The coordinate axes are parallel and perpendicular to the tube axis. The trajectory of the particle along the tube will be resultant of the particle's settling velocity and the velocity of the water in the tube:

$$\frac{dx}{dt} = v_x = u - v_s \sin \theta \quad (9.175)$$

$$\frac{dy}{dt} = v_y = -v_s \cos \theta \quad (9.176)$$

where t = time (sec)

u = the water velocity at a point in the tube (m/s or ft/sec)

v_s = the particle's settling velocity (m/s or ft/sec)

v_x = the particle's resultant velocity in the x direction (m/s or ft/sec)

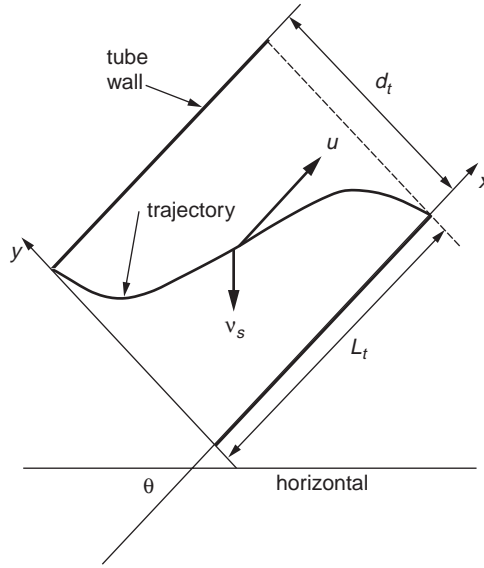


FIGURE 9.9 Trajectory of the critical particle in a tube. [Yao, K.M. 1970. Theoretical Study of High-Rate Sedimentation, *J. Water Pollut. Control Fed.*, 42 (no. 2, part 1): 218.]

v_y = the particle's resultant velocity in the y direction (m/s or ft/sec)
 θ = the angle of the tube with the horizontal (rad)

Equations (9.175) and (9.176) may be combined to yield the differential equation of the trajectory of a particle transitting the tube:

$$\frac{dy}{dx} = -\frac{v_s \cos \theta}{u - v_s \sin \theta} \quad (9.177)$$

The water velocity u varies from point to point across the tube cross section. For fully developed laminar flow in a circular tube, the distribution is a parabola (Rouse, 1978):

$$\frac{u}{U_t} = 8 \left(\frac{y}{d_t} - \frac{y^2}{d_t^2} \right) \quad (9.178)$$

where d_t = the tube diameter (m or ft)
 U_t = the mean water velocity in the tube (m/s or ft/sec)
 y = the distance from the tube invert (m or ft)

The critical trajectory begins at the crown of the tube and ends at its invert. Substituting for u and integrating between these two points yields the following relationship between the settling velocity of a particle that is just captured and the mean water velocity in a circular tube (Yao, 1970):

Laminar flow in circular tubes:

$$\frac{v_s}{U_t} = \frac{4/3}{\sin \theta + \frac{L_t}{d_t} \cdot \cos \theta} \quad (9.179)$$

where L_t = the effective length of the tube (m or ft).

Yao (1970) has performed the same analysis for other cross-sectional shapes, and the equations differ only in the numerical value of the numerator on the right-hand side.

Laminar flow in square tubes:

$$\frac{v_s}{U_t} = \frac{11/8}{\sin\theta + \frac{L_t}{a_t} \cdot \cos\theta} \quad (9.180)$$

where a = the length of one side of the square cross section (m or ft).

Laminar flow between parallel plates, or for laminar flow over a plane, or for an idealized flow that has a uniform velocity everywhere:

$$\frac{v_s}{U_t} = \frac{1}{\sin\theta + \frac{L_t}{h_p} \cdot \cos\theta} \quad (9.181)$$

where h_p = the thickness of the flow (m or ft).

This critical velocity may be related to the tube overflow rate. The definition of the overflow rate for a square tube is:

$$\begin{aligned} \text{tube overflow rate} &= \frac{\text{flow through tube}}{\text{horizontally projected area}} \\ v_{or} &= \frac{U_t a_t^2}{L_t a_t \cos\theta} = \frac{U_t}{\frac{L_t}{a_t} \cos\theta} \end{aligned} \quad (9.182)$$

where v_{or} = the tube overflow rate (m/s or ft/sec).

Therefore,

$$v_s = \frac{11/8 v_{or}}{1 + \frac{L_t}{a_t} \cdot \tan\theta} \quad (9.183)$$

In the ideal Hazen–Camp clarifier, the critical settling velocity is equal to the tank overflow rate. This is not true for tubes. Tubes are always installed as arrays, and the critical velocity for the array is much less than the tank overflow rate. The number of tubes in such an array can be calculated as follows. First, the fraction of the settling zone surface occupied by the tube ends is less than the plan area of the zone, because the inclination of the tubes prevents full coverage. The area occupied by open tube ends that can accept flow is:

$$A_0 = W(L - L_t \cdot \cos\theta) \quad (9.184)$$

- where
- A_0 = the area of the settling zone occupied by tube ends (m² or ft²)
 - L = the length of the settling zone (m or ft)
 - L_t = the length of the tubes (m or ft)
 - W = the width of the settling zone (m or ft)
 - θ = the angle of the tubes with the horizontal plane (rad)

The number of square tubes in this area is:

$$n_t = \frac{W(L - L_t \cos \theta)}{a_t^2 / \sin \theta} \quad (9.185)$$

The effective plan area of the array of square tubes is simply the number of tubes times the plan area of a single tube:

$$A_{eff} = n_t L_t a_t \cos \theta = W(L - L_t \cos \theta) \frac{L_t}{a_t} \sin \theta \cos \theta \quad (9.186)$$

The overflow rate of the array of square tubes is:

$$v_o = \frac{Q}{W(L - L_t \cos \theta) \cdot \frac{L_t}{a_t} \cdot \sin \theta \cdot \cos \theta} \quad (9.187)$$

This is also the overflow rate of each tube in the array, if the flow is divided equally among them.

Assuming equal distribution of flow, the critical settling velocity may be related to the overflow rate of the array of square tubes by substituting Eq. (9.187) into (9.183):

$$v_s = \frac{\frac{11}{8}Q}{\left(1 + \frac{L_t}{a_t} \tan \theta\right) W(L - L_t \cos \theta) \frac{L_t}{a_t} \sin \theta \cos \theta} \quad (9.188)$$

For parallel plates, the equivalent formula is:

$$v_s = \frac{Q}{\left(1 + \frac{L_t}{h_p} \tan \theta\right) W(L - L_t \cos \theta) \frac{L_t}{h_p} \sin \theta \cos \theta} \quad (9.189)$$

Tube Inlets

Near the tube inlet, the velocity distribution is uniform, not parabolic:

$$u = U_t \quad (9.190)$$

The relationships just derived do not apply in the inlet region, and the effective length of the tubes should be diminished by the inlet length.

The distance required for the transition from a uniform to a parabolic distribution in a circular tube is given by the Schiller–Goldstein equation (Goldstein, 1965):

$$L_{en} = 0.0575 r_t \mathbf{Re}_t \quad (9.191)$$

where L_{en} = the length of the inlet region (m or ft)
 \mathbf{Re}_t = the tube's Reynolds number (dimensionless)
 $= U_t d_t / \nu$
 r_t = the tube's radius (m or ft)

Tube diameters are typically 2 in., and tube lengths are typically 2 ft (Culp/Wesner/Culp, 1986). The transition zone length near the inlet of a circular tube will be about 0.15 to 0.75 ft. Tubes are normally 2 ft long, depending on water temperature and velocity.

If the velocity remained uniform everywhere for the whole length of the tube, the formula for the critical velocity in a circular tube would be,

$$\frac{v_s}{U_t} = \frac{1}{\sin\theta + \frac{L_t}{d_t} \cdot \cos\theta} \quad (9.192)$$

Comparison with Eq. (9.179) shows that this is actually one-fourth less than the critical velocity for a fully developed parabolic velocity profile, so the effect of a nonuniform velocity field is to reduce the efficiency of the tube.

Performance Data

Long, narrow tubes with low water velocities perform best (Hansen and Culp, 1967). However, water velocity is more important than tube diameter, and tube diameter is more important than tube length. For tubes that were 2 in. in diameter and 2 ft long, turbidity removal was seriously degraded when the water velocity exceeded 0.0045 ft/sec.

Recommended tank overflow rates for tube settlers range from 2.5 to 4.0 gpm/ft² (Culp/Wesner/Culp, Inc., 1986). It is assumed that the tubes are 2 in. in diameter, 2 ft long, and inclined at 60°. For conventional rapid sand filters, a settled water turbidity of less than 3 TU is preferred, and the overflow rate should not exceed 2.5 gpm/ft² at temperatures above 50°F. A settled water turbidity of up to 5 TU is acceptable to dual media filters, and the overflow rate should not exceed 2.5 gpm/ft² at temperatures below 40°F and 3.0 gpm/ft² at temperatures above 50°F.

Clarifier Inlets

Conventional Clarifiers

The inlet zone should distribute the influent flow uniformly over the depth and the width of the settling zone. If both goals cannot be met, then uniform distribution across the width has priority, because streaming degrades tank performance more than do density currents. Several design principles should be followed:

- In order to prevent floc breakage, the r.m.s. characteristic strain rates in the influent channel, piping, and appurtenances must not exceed the velocity gradient in the final compartment of the flocculation tank. Alum/clay flocs and sludges should not be pumped or allowed to free-fall over weirs at any stage of their handling. This rule does not apply to the transfer of settled water to the filters (Hudson and Wolfner, 1967; Hudson, 1981).
- The influent flow should approach the inlet zone parallel to the longitudinal axis of the clarifier. Avoid side-overflow weirs. The flow in channels feeding such weirs is normal to the axis of the clarifier, and its momentum across the tank will cause a nonuniform lateral distribution. At low flows, most of the water will enter the clarifier from the upstream end of the influent channel, and at high flows, most of it will enter the clarifier from the downstream end of the channel. These maldistributions occur even if baffles and orifice walls are installed in the inlet zone (Yee and Babb, 1985).
- A simple inlet pipe is unsatisfactory, even if it is centered on the tank axis and even if there is an orifice wall downstream of it, because the orifice wall will not dissipate the inlet jet. The inlet pipe must end in a tee that discharges horizontally, and an orifice wall should be installed downstream of the tee (Kleinschmidt, 1961). A wall consisting of adjustable vertical vanes may be preferable to an orifice wall.

The orifice wall should have about 30 to 40% open area (Hudson, 1981). The orifice diameters should be between 1/64 and 1/32 of the smallest dimension of the wall, and the distance between the wall and

the inlet tee should be approximately equal to the water depth. The headloss through the orifice wall should be about four times the approaching velocity head.

High-Rate Clarifiers

In a high-rate clarifier, the settling zone is the tube modules. The inlet zone consists of the following regions and appurtenances:

- A region near the tank inlet that contains the inlet pipe and tee, a solid baffle wall extending from above the water surface to below the tube modules, and, perhaps, an orifice wall below the solid baffle
- The water layer under the settling modules and above the sludge zone

The inlet pipe and tee are required for uniform lateral distribution of the flow. The solid baffle wall must deflect the flow under the tube modules. Horizontally, it extends completely across the tank. Vertically, it extends from a few inches above maximum water level to the bottom of the tube modules. If the raw water contains significant amounts of floatables, the baffle wall should extend sufficiently above the maximum water surface to accommodate some sort of skimming device. The orifice wall extends across the tank and from the bottom of the baffle wall to the tank floor. The extension of the orifice wall to the tank bottom requires that special consideration be given to the sludge removal mechanism.

Most tube modules are installed in existing conventional clarifiers to increase their hydraulic capacity. The usual depth of submergence of tube modules in retrofitted tanks is 2 to 4 ft, in order to provide room for the outlet launders, and the modules are generally about 2 to 3 ft thick.

The water layer under the tube modules needs to be thick enough to prevent scour of the sludge deposited on the tank floor. Conley and Hansen (1978) recommend a minimum depth under the modules of 4 ft.

Outlets

Outlet structures regulate the depth of flow in the settling tank and help to maintain a uniform lateral flow distribution. In high-rate clarifiers, they also control the flow distribution among the tubes, which must be uniform.

Launders

The device that collects the clarified water usually is called a “launder.” There are three arrangements:

- Troughs with side-overflow weirs (the most common design)
- Troughs with submerged perforations along the sides
- Submerged pipes with side perforations

Launders may be constructed of any convenient, stable material; concrete and steel are the common choices. A supporting structure is needed to hold them up when the tank is empty and down when the tank is full. Launders are usually provided with invert drains and crown vents to minimize the loads on the supports induced by tank filling and draining. The complete outlet structure consists of the launder plus any ancillary baffles and the supporting beams and columns.

Clarified water flows into the launders either by passing over weirs set along the upper edges of troughs or by passing through perforations in the sides of troughs or pipes. The launders merge downstream until only a single channel pierces the tank’s end wall.

The outlet structures in some old plants consist of simple overflow weirs set in the top of the downstream end wall. This design is unacceptable.

If troughs-with-weirs are built, the weir settings will control the water surface elevation in the tank. “V-notch” weirs are preferred over horizontal sharp-crested weirs, because they are more easily adjusted. V-notch weirs tend to break up large, fragile alum flocs. This may not be important.

Perforated launders are built with the perforations set 1 to 2 ft below the operating water surface (Hudson, 1981; Culp/Wesner/Culp, Inc., 1986). This design is preferred when the settled water contains significant amounts of scum or floating debris, when surface freezing is likely, and when floc breakage must be minimized (Hudson, 1981; Culp/Wesner/Culp, Inc., 1986). Perforated launders permit significant variations in the water surface elevation, which may help to break up surface ice.

“Finger launders” (James M. Montgomery, Consulting Engineers, Inc., 1985) consist of long troughs or pipes run the length of the settling zone and discharged into a common channel or manifold at the downstream end of the tank. Finger launders are preferred for all rectangular clarifiers, with or without settling tube modules, because they maximize floc removal efficiency. There are several reasons for the superiority of finger launders (James M. Montgomery, Consulting Engineers, Inc., 1985):

- By drawing off water continuously along the tank, they reduce tank turbulence, especially near the outlet end.
- They dampen wind-induced waves. This is especially true of troughs with weirs, because the weirs protrude above the water surface.
- If a diving density current raises sludge from the tank bottom, the sludge plume is concentrated at the downstream end of the tank. Therefore, most of the launder continues to draw off clear water near the center and upstream end of the tank.
- Finger launders impose a nearly uniform vertical velocity component everywhere in the settling zone, which produces a predictable, uniform velocity field. This uniform velocity field eliminates many of the causes of settler inefficiency, including bottom scour, streaming, and gradients in the horizontal velocity field.
- Finger launders eliminate the need for a separate outlet zone. Settled water is collected from the top of the settling zone, so the outlet and settling zones are effectively merged.

The last two advantages are consequences of Fisherström’s (1955) analysis of the velocity field under finger launders. The presence or absence of settling tube modules does not affect the analysis, or change the conclusions. The modules merely permit the capture of particles that would otherwise escape.

The outlet design should include so-called “hanging” or “cross” baffles between the launders. Hanging baffles run across the width of the clarifier, and they extend from a few inches above the maximum water surface elevation to a few feet below it. If settling tube modules are installed in the clarifier, the hanging baffle should extend all the way to the top of the modules. In this case, it is better called a cross baffle. The baffles are pierced by the launders. The purpose of the baffles is to promote a uniform vertical velocity component everywhere in the settling/outlet zone. They do this by suppressing the longitudinal surface currents in the settling/outlet zone that are induced by diving density currents and wind.

The number of finger launders is determined by the need to achieve a uniform vertical velocity field everywhere in the tank. There is no firm rule for this. Hudson (1981) recommends that the center-to-center distance between launders be 1 to 2 tank depths. The number of hanging baffles is likewise indeterminate. Slechta and Conley (1971) successfully suppressed surface currents by placing the baffles at the quarter points of the settling/outlet zone. However, this spacing may be too long. The clarifier in question also had tube modules, which helped to regulate the velocity field below the launders.

Other launder layouts have serious defects and should be avoided. The worst choice for the outlet of a conventional rectangular clarifier consists of a weir running across the top of the downstream end wall, which was a common design 50 years ago. The flow over the weir will induce an upward component in the water velocity near the end wall. This causes strong vertical currents, which carry all but the fastest particles over the outlet weir.

Regulatory authorities often attempt to control the upward velocity components in the outlet zone by limiting the so-called “weir loading” or “weir overflow rate.” This number is defined to be the ratio of the volumetric flow rate of settled water to the total length of weir crest or perforated wall. If water enters both sides of the launder, the lengths of both sides may be counted in calculating the rate.

A commonly used upper limit on the weir rate is the “Ten States” specification of 20,000 gal/ft·day for peak hourly flows ≤ 1 mgd and 30,000 gal/ft·day for peak hourly flows > 1 mgd (Wastewater Committee, 1990). Babbitt, Dolan, and Cleasby (1967) recommend an upper limit of 5000 gal/ft·day. Walker Process Equipment, Inc., recommends the following limits, which are based on coagulant type:

- Low raw water turbidity/alum — 8 to 10 gpm/ft (11,520 to 14,400 gal/day ft)
- High raw water turbidity/alum — 10 to 15 gpm/ft (14,400 to 21,600 gal/day ft)
- Lime/soda softening — 15 to 18 gpm/ft (21,600 to 25,920 gal/ft day)

The “Ten States” weir loading yields relatively short launders and high upward velocity components. Launders designed according to the “Ten States” regulation require a separate outlet zone, which would be defined to be all the water under the horizontal projection of the launders. A commonly followed recommendation (Joint Task Force, 1969) is to make the outlet zone one-third of the total tank length and to cover the entire outlet zone with a network of launders. More recently, it is recommended that the weirs cover enough of the settling zone surface so that the average rise rate under them not exceed 1 to 1.5 gpm/ft² (Joint Committee, 1990).

Weir/Trough Design

The usual effluent launder weir consists of a series of “v-notch” or “triangular” weirs. The angle of the notch is normally 90°, because this is the easiest angle to fabricate, it is less likely to collect trash than narrower angles, and the flow through it is more predictable than wider angles. Individual weir plates are typically 10 cm wide, and the depth of the notch is generally around 5 cm. The spacing between notches is about 15 cm, measured bottom point to bottom point. The flat surface between notches is for worker safety. If the sides of the notches merged in a point, the point would be hazardous to people working around the launders. The sides of the “V” are beveled at 45° to produce a sharp edge, the edge being located on the weir inlet side. The stock from which the weirs are cut is usually hot-dipped galvanized steel or aluminum sheet 5 to 13 mm thick. Fiberglass also has been used. Note the bolt slots, which permit vertical adjustment of the weir plates.

The usual head-flow correlation for 90° v-notch weirs is King’s (1963) equation:

$$Q = 2.52H^{2.47} \quad (9.193)$$

where Q = the flow over the weir in ft³/sec
 H = the head over the weir notch in ft

Adjacent weirs behave nearly independently of one another as long as the distance between the notches is at least 3.5 times the head (Barr, 1910a, 1910b; Rowell, 1913). Weir discharge is independent of temperature between 39 and 165°F (Switzer, 1915).

Because finger launders are supposed to produce a uniform vertical velocity field in the settling zone, each weir must have the same discharge. This means that the depth of flow over each notch must be the same. The hydraulic gradient along the tank is also small, and the water surface may be regarded as flat, at least for design purposes. Wind setup may influence the water surface more than clarifier wall friction.

The water profile in the effluent trough may be derived by writing a momentum balance for a differential cross-sectional volume element. The result is the so-called Hinds (1926)–Favre (1933) equation (Camp, 1940; Chow, 1959):

$$\frac{dy}{dx} = \frac{S_o - S_f - \frac{2nq_w Q_x}{gA_x^2}}{1 - \frac{Q_x^2}{gA_x^2 H_x}} \quad (9.194)$$

where A_x = the cross-sectional area of the flow at x (m^2 or ft^2)
 B_x = the top-width of the flow at x (m or ft)
 g = the acceleration due to gravity ($9.80665 m/s^2$ or $32.174 ft/sec^2$)
 H_x = the mean depth of flow at x (m or ft)
 $= A_x/B_x$
 n = the number of weir plates attached to the trough (dimensionless)
 $= 1$, if flow enters over one edge only
 $= 2$, if flow enters over both edges
 Q_x = the flow at x (m^3/s or ft^3/sec)
 q_w = the weir loading rate ($m^3/m \cdot s$ or $ft^3/ft \cdot sec$)
 S_f = the energy gradient (dimensionless)
 S_0 = the invert slope (dimensionless)
 x = the distance along the channel (m or ft)
 y = the depth above the channel invert at x (m or ft)

For a rectangular cross section, which is the usual trough shape, the mean depth is equal to the depth. If it is assumed that the energy gradient is caused only by wall friction, then it may be replaced by the Darcy–Weisbach formula (or any other wall friction formula):

$$S_f = \frac{fU^2}{8gR} \quad (9.195)$$

where f = the Darcy–Weisbach friction factor (dimensionless)
 R = the hydraulic radius (m or ft)
 U = the mean velocity (m/s or ft/sec)

An approximate solution to Eq. (9.194) may be had by substituting the average values of the depth and the hydraulic radius into the integral. The information desired is the depth of water at the upstream end of the trough, because this will be the point of highest water surface elevation (even if not the greatest depth in the trough). Camp's (1940) solution for the upstream depth is as follows:

$$H_o = \sqrt{H_x^2 + \frac{2Q_x^2}{gb^2H_x} - 2x\bar{H}(S_o - \bar{S}_f)} \quad (9.196)$$

where \bar{H} = the mean depth along the channel (m or ft)
 H_o = the depth of flow at the upstream end of the channel (m or ft)
 \bar{S}_f = the average energy gradient along the channel (dimensionless)

H_o can be calculated if the depth of flow is known at any point along the trough. The most obvious and convenient choice is the depth at the free overflow end of the channel, where the flow is critical. The critical depth for a rectangular channel is given by (King and Brater, 1963):

$$H_c = \sqrt[3]{\frac{Q_c^2}{gb^2}} \quad (9.197)$$

In smooth channels, the critical depth section is located at a distance of about $4H_c$ from the end of the channel (Rouse, 1936; O'Brien, 1932). In a long channel, the total discharge can be used with little error.

The actual location of the critical depth section is not important, because the overflow depth is simply proportional to the critical depth (Rouse, 1936, 1943; Moore, 1943):

$$H_e = 0.715H_c \quad (9.198)$$

Estimation of the mean values of the depth, hydraulic radius, and energy gradient for use in Eq. (9.196) requires knowledge of H_o , so an iterative calculation is required. An initial estimate for H_o can be obtained by assuming that the trough is flat and frictionless and that the critical depth occurs at the overflow. This yields:

$$H_o \cong \sqrt[3]{3 \cdot \frac{Q^2}{gb^2}} \quad (9.199)$$

A first estimate for the average value of the depth of flow may now be calculated. Because the water surface in the trough is nearly parabolic, the best estimators for the averages are as follows (Camp, 1940):

$$\bar{H} = \frac{2H_o + H_e}{3} \quad (9.200)$$

$$\bar{R} = \frac{b\bar{H}}{b + 2\bar{H}} \quad (9.201)$$

The average energy gradient can be approximated using any of the standard friction formulae, e.g., the Manning equation. The side inflow has the effect of slowing the velocity in the trough, because the inflow must be accelerated, and a somewhat higher than normal friction factor is needed.

Combining-Flow Manifold Design

A perforated trough may be treated as a trough with weirs, if the orifices discharge freely to the air. In this case, all the orifices have the same diameter, and the orifice equation may be used to calculate the required diameters. If the orifices are submerged, then the launder is a combining flow manifold, and a different design procedure is required.

Consider a conduit with several perpendicular laterals. The hydraulic analysis of each junction involves eight variables (McNown, 1945, 1954):

- The velocity in the conduit upstream of the junction
- Velocity in the lateral
- Velocity of the combined flow in the conduit downstream of the junction
- Pressure difference in the conduit upstream and downstream of the junction
- Pressure difference between the lateral exit and the conduit downstream of the junction
- Conduit diameter (assumed to be the same upstream and downstream of the junction)
- Lateral diameter
- Density of the fluid

There are three equations connecting these variables, namely:

- Continuity
- Headloss for the lateral flow
- Headloss for the conduit flow

Besides these equations, there is the requirement that all laterals deliver the same flow. The conduit diameter is usually kept constant.

The continuity equation for the junction is simply:

$$Q_d = Q_u + Q_l \quad (9.202)$$

where Q_d = the flow downstream from the lateral (m³/s or ft³/sec)
 Q_l = the flow entering from the lateral (m³/s or ft³/sec)
 Q_u = the flow upstream from the lateral (m³/s or ft³/sec)

If the conduit has the same diameter above and below the junction with the lateral, the headloss for the conduit flow may be represented as a sudden contraction (McNown, 1945; Naiz, 1954):

$$h_{Lc} = K_c \left(\frac{U_d^2}{2g} - \frac{U_u^2}{2g} \right) \quad (9.203)$$

where h_{Lc} = the headloss in the conduit at the lateral (m or ft)
 K_c = the headloss coefficient (dimensionless)
 U_d = the velocity downstream of the lateral (m/s or ft/sec)
 U_u = the velocity upstream of the lateral (m/s or ft/sec)

The headloss coefficient, K_c , depends upon the ratio of the lateral and conduit diameters (Soucek and Zelnick, 1945; McNown, 1954; Naiz, 1954; Powell, 1954). Niaz's (1954) analysis of McNown's data yields the following approximate relationships:

$$\begin{aligned} \frac{d_l}{d_c} = \frac{1}{4} &\rightarrow K_c = 1.4 \\ \frac{d_l}{d_c} = \frac{1}{2} &\rightarrow K_c = 1.0 \\ \frac{d_l}{d_c} = 1 &\rightarrow K_c = 0.5 \end{aligned} \quad (9.204)$$

where d_c = the diameter of the conduit (m or ft)
 d_l = the diameter of the lateral (m or ft).

The situation with respect to the lateral headloss is more complicated. The headloss may be expressed in terms of the lateral velocity or in terms of the downstream conduit velocity (McNown, 1954):

$$h_{Ll} = K_{ll} \cdot \frac{U_l^2}{2g} \quad (9.205)$$

$$h_{Ll} = K_{lc} \cdot \frac{U_d^2}{2g} \quad (9.206)$$

where h_{Ll} = the headloss in the lateral (m or ft)
 K_{lc} = the lateral's headloss coefficient based on the conduit's velocity (dimensionless)
 K_{ll} = the lateral's headloss coefficient based on the lateral's velocity (dimensionless)
 U_d = the conduit's velocity downstream of the lateral (m/s or ft/sec)
 U_l = the lateral's velocity (m/s or ft/sec)

The headloss coefficients depend upon the ratio of the lateral and conduit diameters and the ratio of the lateral and conduit flows (or velocities). If the lateral velocity is much larger than the conduit velocity, all of the lateral velocity head is lost, and K_{ll} is equal to 1. The situation here is similar to that of a jet entering a reservoir. If the lateral velocity is much smaller than the conduit velocity, the lateral flow loses no energy. In fact, the headloss calculated from the Bernoulli equation will be negative, and its magnitude will approach the velocity head in the conduit downstream of the junction. For this case, K_{lc} will approach -1. The negative headloss is an artifact caused by the use of cross-sectional average velocities in the Bernoulli equation. If the lateral discharge is small relative to the conduit flow, it enters the conduit boundary layer, which has a small velocity. Some empirical data on the variation of the headloss coefficients are given by McNown (1954) and Powell (1954).

The energy equation is written for an arbitrary element of water along its path from the clarifier to the outlet of the launder. To simplify matters, it is assumed that the launder discharges freely to the atmosphere. The water element enters the launder through the “jth” lateral, counting from the downstream end of the launder:

$$\frac{U_o^2}{2g} + \frac{p_o}{\gamma} + z_o = \frac{U_e^2}{2g} + \frac{p_e}{\gamma} + z_e + h_{Li}(j) + h_{Li}(j) + \sum_{i=1}^{j-1} h_{Lc}(i) \quad (9.207)$$

where p_e = the pressure at the conduit’s exit (N/m² or lbf/ft²)
 p_o = the pressure in the clarifier (N/m² or lbf/ft²)
 U_e = the velocity at the conduit’s exit (m/s or ft/sec)
 U_o = the velocity in the clarifier (m/s or ft/sec)
 z_e = the elevation at the conduit’s exit (m or ft)
 z_o = the elevation in the clarifier (m or ft)

Wall friction losses in the launder and its laterals are ignored, because they are usually small compared to the other terms. The velocity of the water element at the beginning of its path in the clarifier will be small and can be deleted. The sum of the pressure and elevation terms at the beginning is simply the water surface elevation. The pressure of a free discharge is zero (gauge pressure). Consequently, Eq. (9.207) becomes:

$$h_{Li}(j) + h_{Li}(j) + \sum_{i=1}^{j-1} h_{Lc}(i) = z_{cws} - z_{ews} - \frac{U_e^2}{2g} \quad (9.208)$$

where z_{cws} = the clarifier’s water surface (m or ft)
 z_{ews} = the conduit exit’s water surface (m or ft).

Equation (9.208) assumes that the laterals do not interact. This will be true as long as the lateral spacing is at least six lateral diameters (Soucek and Zelnick, 1945).

The right-hand side of Eq. (9.208) is a constant and is the same for each lateral. All the water elements begin with the same total energy, and they all end up with the same total energy, so the total energy loss for each element must be the same.

The flows into laterals far from the outlet of the launder experience more junction losses than those close to the outlet. This means that the head available for lateral entrance and exit is reduced for the distant laterals. Consequently, if all the lateral diameters are equal, the lateral discharge will decrease from the launder outlet to its beginning (Soucek and Zelnick, 1945). The result will be a nonuniform vertical velocity distribution in the settling zone of the clarifier. This can be overcome by increasing the lateral diameters from the launder outlet to its beginning.

Most perforated launders are built without lateral tubes. The headloss data quoted above do not apply to this situation, because the velocity vectors for simple orifice inlets are different from the velocity vectors for lateral tube inlets. Despite this difference, some engineers use the lateral headloss data for orifice design (Hudson, 1981).

Data are also lacking for launders with laterals or orifices on each side. These data deficiencies make perforated launder design uncertain. It is usually recommended that the design be confirmed by full-scale tests.

The usual reason given for perforated launders is their relative immunity to clogging by surface ice. However, the need for a uniform velocity everywhere in the settling zone controls the design. If freezing is likely, it would be better to cover the clarifiers. The launders could then be designed for v-notch weirs or freely discharging orifices, which are well understood.

Sludge Zone

Sludge Collection

The sludge collection zone lies under the settling zone. It provides space for the sludge removal equipment and, if necessary, for temporary sludge storage.

The most common design consists of a bottom scraper and a single hopper. Periodically, the solids deposited on the clarifier floor are scraped to the hopper set into the tank floor. The solids are collected as a sludge that is so dilute it behaves hydraulically, like pure water. Periodically, the solids are removed from the hopper via a discharge line connected to the hopper bottom.

An alternative scheme is sometimes found in the chemical and mining industries and in dust collection facilities. In these cases, the entire tank floor is covered with hoppers. No scraper mechanisms are required. However, the piping system needed to drain the hoppers is more complex.

A third system consists of perforated pipes suspended near the tank floor and lying parallel to it. A slight suction head is put on the pipes, and they are drawn over the entire tank floor, sucking up the deposited solids. This system eliminates the need for hoppers, but it produces a very dilute sludge.

Sludge Composition

The composition of the sludges produced by the coagulation and sedimentation of natural waters is summarized in [Table 9.2](#), and by wastewater treatment, in [Table 9.3](#). Alum coagulation is applied to surface waters containing significant amounts of clays and organic particles, so the sludges produced also contain significant amounts of these materials. Lime softening is often applied to groundwaters, which are generally clear. Consequently, lime sludges consist mostly of calcium and magnesium precipitates.

TABLE 9.2 Range of Composition of Water Treatment Sludges

Sludge Component	Alum Sludges	Iron Sludges	Lime Sludges
Total Suspended Solids: (% by wt)	0.2–4.0	0.25–3.5	2.0–15.0
Aluminum: (% by wt of TSS, as Al)	4.0–11.0	—	—
(mg/L, as Al)	295–3750	—	—
Iron: (% by wt of TSS, as Fe)	—	4.6–20.6	—
(mg/L, as Fe, for 2% TSS)	—	930–4120	—
Calcium: (% by wt of TSS, as Ca)	—	—	30–40
Silica/Ash: (% by wt of TSS)	35–70	—	3–12
Volatile Suspended Solids: (% by wt of TSS)	15–25	5.1–14.1	7 (as carbon)
BOD ₅ (mg/L)	30–300	—	Little or none
COD (mg/L)	30–5000	—	Little or none
pH (standard units)	6–8	7.4–8.5	9–11
Color (sensory)	Gray-brown	Red-brown	White
Odor (sensory)	None	—	None to musty
Absolute viscosity: (g/cm·sec)	0.03 (non-Newtonian)	—	—
Dewaterability	Concentrates to 10% solids in 2 days on sand beds, producing a spongy semisolid	—	Compacts to 50% solids in lagoons, producing a sticky semisolid; dewatering impaired if Ca/Mg ratio is 2 or less
Settleability	50% in 8 hr	—	50% in 1 week
Specific resistance: (sec ² /g)	1.0×10^9 – 5.4×10^{11}	4.1×10^8 – 2×10^{12}	0.20×10^7 – 26×10^7
Filterability	Poor	—	Poor

Compiled from Culp/Wesner/Culp, Inc. (1986); James M. Montgomery, Inc. (1985); and J.T. O'Connor (1971).

TABLE 9.3 Range of Composition of Wastewater Sludges

Sludge Component	Primary Sludge	Waste-Activated Sludge	Trickling Filter Humus
pH	5–8	6.5–8	—
Higher heating value (Btu/lb TSS)	6800–10,000	6500	—
Specific gravity of particles	1.4	1.08	1.3–1.5
Specific gravity of sludge	1.02–1.07	$1 + 7 \times 10^{-8} X$	1.02
Color	Black	Brown	Grayish brown to black
COD/VSS	1.2–1.6	1.4	—
C/N	—	3.5–14.6	—
C (% by wt of TSS)	—	17–44	—
N (% by wt of TSS)	1.5–4	2.4–6.7	1.5–5.0
P as P ₂ O ₅ (% by wt of TSS)	0.8–2.8	2.8–11	1.2–2.8
K as K ₂ O (% by wt of TSS)	0.4	0.5–0.7	—
VSS (% by wt of TSS)	60–93	61–88	64–86
Grease and fat (% by wt of TSS)	7–35	5–12	—
Cellulose (% by wt of TSS)	4–15	7	—
Protein (% by wt of TSS)	20–30	32–41	—

Source: Anonymous. 1979. *Process Design Manual for Sludge Treatment and Disposal*, EPA 625/1–79–011. U.S. Environmental Protection Agency, Municipal Environmental Research Laboratory, Technology Transfer, Cincinnati, OH.

Sludge Collectors/Conveyors

There are a variety of patented sludge collection systems offered for sale by several manufacturers. The two general kinds of sludge removal devices are “flights” or “squeegees” and “suction manifolds.”

The first consists of a series of boards, called “flights” or “squeegees,” that extend across the width of the tank. The boards may be constructed of water-resistant woods, corrosion-resistant metals, or engineering plastics. In traditional designs, the flights are attached to continuous chain loops, which are mounted on sprockets and moved by a drive mechanism. The flights, chains, and sprockets are submerged. The drive mechanism is placed at ground level and connected to the sprocket/chain system by some sort of transmission. In addition to the primary flight system, which moves sludge to one end of the tank, there may be a secondary flight system, which moves the sludge collected at the tank end to one or more hoppers.

In some newer designs, the flights are suspended from a traveling bridge, which moves along tracks set at ground level along either side of the clarifier. Bridge-driven flights cannot be used with high-rate settlers, because the flight suspension system interferes with the tube modules. Bridge systems also require careful design to assure compatibility with effluent launders. If finger launders extending the whole length of the settling zone are used, bridge systems may not be feasible.

In either system, the bottom of the tank is normally finished with a smooth layer of grout, and two or more longitudinal rails are placed along the length of the tank to provide a relatively smooth bearing surface for the flights. The tops of the rails are set slightly above the smooth grout layer. The grout surface is normally pitched toward the sludge hopper to permit tank drainage for maintenance. The recommended minimum pitch is 1/16 in./ft (0.5%) (Joint Task Force, 1969).

The flights are periodically dragged along the bottom of the tank to scrape the deposited sludge into the sludge hoppers. The scraping may be continuous or intermittent depending on the rate of sludge deposition. Flight speeds are generally limited to less than 1 ft/min to avoid solids resuspension (Joint Task Force, 1969).

In some traveling bridge designs, the flights are replaced by perforated pipes, which are subjected to a slight suction head. The pipes suck deposited solids off the tank floor and transfer them directly to the sludge processing and disposal systems. Suction manifolds dispense with the need for sludge hoppers, which simplifies and economizes tank construction, but they tend to produce dilute sludges, and they may not be able to collect large, dense flocs.

The sludge zone should be deep enough to contain whatever collection device is used and to provide storage for sludge solids accumulated between removal operations. Generally, 12 to 18 in. of additional tank depth is provided.

Sludge Hoppers

Sludge hoppers serve several purposes. First, they store the sludge until it is removed for processing and storage. For this reason, the hoppers should have sufficient volume to contain all the solids deposited on the tank floor between sludge removals. Second, they channel the flow of the sludge to the inlet of the drainpipe. To facilitate this, the bottom of the hoppers should be square and only somewhat larger than the inlet pipe bell. Third, the hoppers provide sufficient depth of sludge over the pipe inlet to prevent short-circuiting of clear water. There is no general rule regarding the minimum hopper depth. Fourth, hoppers prevent resuspension of solids by diving density currents near the inlet and by the upflow at the outlet end of the tank. Fourth, hoppers provide some sludge thickening.

The number of hoppers and their dimensions are determined by the width of the tank and the need, if any, for cross collectors. For example, the length of a hopper side at the top of the hopper will be the minimum width of the cross collector. At the bottom of the hopper, the minimum side length will be somewhat larger than the diameter of the pipe inlet bell. The minimum side wall slopes are generally set at 45° to prevent sludge adhesion.

Freeboard

The tops of the sedimentation tank walls must be higher than the maximum water level that can occur in the tank. Under steady flow, the water level in the tank is set by the backwater from the effluent launder. In the case of effluent troughs with v-notch weirs, the maximum steady flow water level is the depth over the notch for the maximum expected flow, which is the design flow. From time to time, waves caused by hydraulic surges and the wind will raise the water above the expected backwater. In order to provide for these transients, some “freeboard” is provided. The freeboard is defined to be the distance between the top of the tank walls and the predicted water surface level for the (steady) design flow. The actual amount of freeboard is somewhat arbitrary, but a common choice in the U.S. is 18 in. (Joint Task Force, 1969).

The freeboard may also be set by safety considerations. In order to minimize pumping, the operating water level in most tanks is usually near the local ground surface elevation. Consequently, the tops of the tank walls will be near the ground level. In this situation, the tanks require some sort of guardrail and curb in order to prevent pedestrians, vehicles, and debris from falling in. The top of the curb becomes the effective top of the tank wall. Curbs are usually at least 6 in. above the local ground level.

Hindered Settling

In hindered settling, particles are close enough to be affected by the hydrodynamic wakes of their neighbors, and the settling velocity becomes a property of the suspension. The particles move as a group, maintaining their relative positions like a slowly collapsing lattice: large particles do not pass small particles. The process is similar to low Reynolds number bed expansion during filter backwashing, and the Richardson–Zaki (1954) correlation would apply, if the particles were of uniform size and density and their settling velocity were known. Instead, the velocity must be measured.

Hindered settling is characteristic of activated sludge clarifiers, many lime-soda sludge clarifiers, and gravity sludge thickeners.

Settling Column Tests

If the particle concentration is large enough, a well-defined interface forms between the clear supernatant and the slowly settling particles. Formation of the interface is characteristic of hindered settling; if a sharp interface does not form, the settling is free.

Hindered settling velocities are frequently determined in laboratory-scale settling columns. Vesilind (1974) identifies several deficiencies in laboratory-scale units, which do not occur in field units:

- The initial settling velocity depends on the liquid depth (Dick and Ewing, 1967).
- “Channeling” takes place in narrow diameter cylinders, where the water tends to flow along the cylinder wall, which is the path of least resistance, and the measured settling velocity is increased.
- “Volcanoing” takes place in the latter part of the settling process, during compression, when small columns of clear liquid erupt at various places across the sludge/water interface, which increases the measured interface velocity. (This is a form of channeling that occurs in wide, unmixed columns.)
- At high solids concentrations, narrow cylinders also permit sludge solids bridging across the cylinder, which inhibits settling.
- Narrow cylinders dampen liquid turbulence, which prevents flocculation and reduces measured settling velocities.

Vesilind (1974) recommends the following procedure for laboratory settling column tests:

- The minimum column diameter should be 8 in., but larger diameters are preferred.
- The depth should be that of the proposed thickener, but at least 3 ft.
- The column should be filled from the bottom from an aerated, mixed tank.
- The columns less than about 12 in. in diameter should be gently stirred at about 0.5 rpm.

In any settling test, the object is to produce a plot of the batch flux (the rate of solids transport to settling across a unit area) versus the solids concentration. There are two procedures in general use.

Kynch’s Method

Kynch’s (1952) batch settling analysis is frequently employed. The movement of the interface is monitored and plotted as in Fig. 9.10. The settling velocity of the interface is obviously the velocity of the particles in it, and it can be calculated as the slope of the interface height-time plot:

$$v_x = \frac{z' - z}{t} \quad (9.209)$$

where t = the sampling time (sec)

v_x = the settling velocity of the particles (which are at concentration X) in the interface (m/s or ft/sec)

z = the height of the interface at time t (m or ft)

z' = the height of the vertical intercept of the tangent line to the interface height-time plot (m or ft)

Initially the slope is linear, and the calculated velocity is the velocity of the suspension’s initial concentration. As settling proceeds, the interface particle concentration increases, and its settling velocity decreases, which is indicated by the gradual flattening of the interface/time plot. The interface concentration at any time can be calculated from Kynch’s (1952) formula:

$$X = \frac{X_0 z_0}{z'} \quad (9.210)$$

where X = the interface suspended solids concentration (kg/m³ or lb/ft³)

X_0 = the initial, homogeneous suspended solids’ concentration (kg/m³ or lb/ft³)

z_0 = the initial interface height and the liquid depth (m or ft)

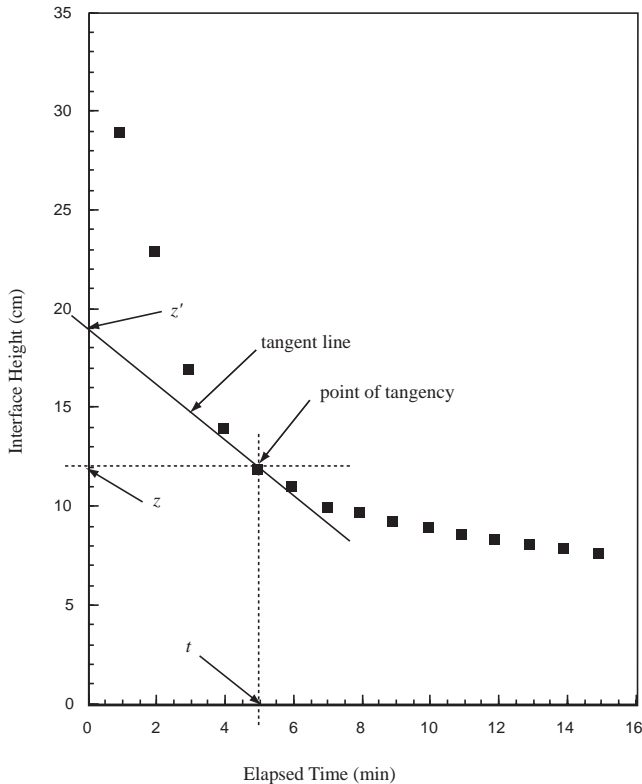


FIGURE 9.10 Typical interface height-time plot for hindered settling.

Note that the elevation in the denominator is the intercept of the extrapolated tangent to the interface height/time curve; it is not the elevation of the interface.

The batch flux for any specified solids concentration is as follows:

$$F = v_x X \quad (9.211)$$

where F = the flux of solids settling through a horizontal plane in a batch container ($\text{kg}/\text{m}^2 \cdot \text{s}$ or $\text{lb}/\text{ft}^2 \cdot \text{sec}$).

In the derivation of Eq. (9.210), Kynch shows that if the water is stationary, a concentration layer that appears on the bottom of the settling column travels at a constant velocity upwards until it intersects the interface. The concentration exists momentarily at the interface and then is replaced by another higher concentration. Dick and Ewing (1967) reviewed earlier studies and concluded that there were several deficiencies with the Kynch analysis, namely:

- Concentration layers do not travel at constant velocities, at least in clay suspensions.
- Stirring the bottom of a suspension increases the rate of subsidence of the interface.
- The Talmadge–Fitch (1955) procedure, which is an application of Kynch’s method for estimating interface concentrations, underestimates the settling velocities at high sludge concentrations (Fitch, 1962; Alderton, 1963).

Vesilind (1974) recommends that this method not be used for designing thickeners for wastewater sludges or for other highly compressible sludges.

Initial Settling Velocity Method

Most engineers prefer to prepare a series of dilutions of the sludge to be tested and to determine only the initial settling velocity that occurs during the linear portion of the interface height/time curve. The

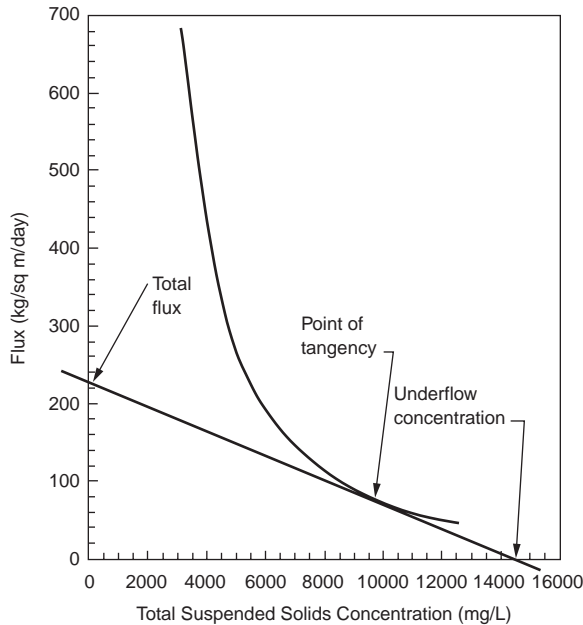


FIGURE 9.11 Yoshioka construction for the total flux.

resulting correlation between the initial settling velocities and the initial solids concentration can usually be represented by the simple decaying exponential proposed by Duncan and Kawata (1968):

$$v_{X_0} = aX_0^{-b} \quad (9.212)$$

where a = a positive constant (units vary)

b = a positive constant (dimensionless)

X_0 = the initial suspended solids concentration in the column (kg/m^3 lb/ft^3)

v_{X_0} = the settling velocity for a suspended solids' concentration of X_0 (m/s or ft/sec)

The batch flux for each initial concentration is calculated using Eq. (9.211), and it is plotted versus the suspended solids concentration. An example is shown in Fig. 9.11. This method assumes that the concentration in the interface is not changing as long as the height–time plot is linear, and by doing so, it necessarily entails Kynch's theory.

Thickener Design

Thickeners can conceptually be divided into three layers. On the top is a clear water zone in which free, flocculent settling occurs. Below this is a sludge blanket. The upper portion of the sludge blanket is a zone of hindered settling. The lower portion is a zone of compression. Many engineers believe that the particles in the compression zone form a self-supporting lattice, which must be broken down by gentle mixing. The compression zone may not exist in continuous flow thickeners.

Hindered Settling Zone

In free settling, the critical loading parameter is the hydraulic flow per unit plan area (e.g., $\text{m}^3/\text{m}^2 \cdot \text{s}$ or $\text{ft}^3/\text{ft}^2 \cdot \text{sec}$). In hindered settling, the critical loading parameter is the total solids flux, which is the solids mass loading rate per unit area (e.g., $\text{kg}/\text{m}^2 \cdot \text{s}$ or $\text{lbm}/\text{ft}^2 \cdot \text{sec}$). The result of a hindered settling analysis is the required thickener cross-sectional area. The depth must be determined from a consideration of the clarification and compression functions of the thickener.

The total solids flux can be expressed three ways for an efficient thickener, each of which yields the same numerical value. First, it is the total solids loading in the influent flow divided by the plan area of the clarifier. For an activated sludge plant or a lime-soda plant with solids recycling, this would be calculated as

$$F_t = \frac{(Q + Q_r)X_i}{A} \quad (9.213)$$

where A = the thickener plan area (m^2 or ft^2)
 F_t = the total solids flux ($\text{kg}/\text{m}^2 \cdot \text{s}$ or $\text{lb}/\text{ft}^2 \cdot \text{sec}$)
 Q = the design water or wastewater flow rate (m^3/s or ft^3/sec)
 Q_r = the recycle flow rate (m^3/s or ft^3/sec)
 X_i = the suspended solids' concentration in the flow entering the thickener (kg/m^3 or lb/ft^3)

Second, it can be calculated as the flux through the sludge blanket inside the thickener divided by the plan area. In a continuous flow thickener, this consists of the flux due to the water movement through the tank plus the flux due to the settling of particles through the moving water. If sludge is wasted from the thickener underflow, the total water flow through the sludge blanket and in the underflow is $Q_r + Q_w$:

$$F_t = \frac{(Q_r + Q_w)X_c + v_{X_c}X_c}{A} \quad (9.214)$$

where Q_w = the waste sludge flow rate (m^3/s or ft^3/sec)
 v_{X_c} = the settling velocity at a suspended solids' concentration X_c (m/s or ft/sec)
 X_c = the suspended solids' concentration in the sludge blanket in the thickener (kg/m^3 or lb/ft^3)

Third, it is equal to the solids in the underflow divided by the tank area:

$$F_t = \frac{(Q_r + Q_w)X_u}{A} \quad (9.215)$$

where X_u = the suspended solids' concentration in the clarifier underflow (kg/m^3 or lb/ft^3).

Two design methods for continuous flow thickeners that are in common use are the Coe–Clevenger (1916) procedure and the Yoshioka et al. (1957) graphical method. These procedures are mathematically equivalent, but the Yoshioka method is easier to use.

The Yoshioka construction is shown in Fig. 9.11. First, the calculated batch fluxes are plotted against their respective suspended solids concentrations. Then, the desired underflow concentration is chosen, and a straight line is plotted (1) from the underflow concentration on the abscissa, (2) through a point of tangency on the batch flux curve, and (3) to an intercept on the ordinate. The intercept on the ordinate is the total flux that can be imposed on the thickener, F_t . Equation (9.213), (9.214), or (9.215) is then used to calculate the required plan area. Parker (1983) recommends that the peak hydraulic load rather than the average hydraulic load be used in the calculation.

If the right-hand side of Eq. (9.214) is plotted for all possible values of X_c , it will be found that F_t is the minimum of the function (Dick, 1970). Consequently, Eq. (9.212) may be used to eliminate v_{X_c} from Eq. (9.214), and the minimum of the total flux formula may be found by differentiating with respect to X_c (Dick and Young, no date):

$$F_t = [a(b-1)]^{1/b} \left(\frac{b}{b-1} \right) \left(\frac{Q_r + Q_w}{A} \right)^{(b-1)/b} \quad (9.216)$$

Clarification Zone

Clarification is impaired if the sludge blanket comes too close to the water surface and if the overflow rate is too high. If effluent suspended solids concentrations must be consistently below about 20 mg/L, then a clarifier side water depth must be at least 16 ft, and the overflow rate must be less than 600 gpd/ft² (Parker, 1983).

Compression Zone

If high sludge solids concentrations are required, a compression zone may form. Its depth can be estimated from the Roberts–Behn formula in terms of the suspension dilution, D , which is defined to be the mass of water in the sludge divided by the mass of particles (Roberts, 1949; Behn, 1957),

$$D_t - D_\infty = (D_o - D_\infty)e^{-Kt} \quad (9.217)$$

where D_o = the initial dilution (kg water/kg solids or lb water/lb solids)
 D_t = the dilution at time t (kg water/kg solids or lb water/lb solids)
 D_∞ = the ultimate dilution (kg water/kg solids or lb water/lb solids)
 K = the rate constant (per sec)
 t = the elapsed compression time (sec)

or, alternatively, in terms of the interface height, H , (Behn and Liebman, 1963),

$$H_t - H_\infty = (H_o - H_\infty)e^{-Kt} \quad (9.218)$$

where H_o = the initial interface height (m or ft)
 H_t = the interface height at time t (m or ft)
 H_∞ = the ultimate interface height (m or ft)

These are connected by

$$D_t = \frac{\rho H_t}{X_o H_o} - \frac{\rho}{\rho_p} \quad (9.219)$$

where ρ = the water density (kg/m³ or lb/ft³)
 ρ_p = the density of the particles (kg/m³ or lb/ft³)

The unknown is the time required to achieve the desired compressive thickening. The compression parameters are D_o (or H_o), D_∞ (or H_∞) and K , and these are determined from a batch settling test. The computational procedure is iterative. One selects a trial value for D_∞ (or H_∞) and plots the differences on semi-log paper. If the data come from the compression region, a value of the ultimate dilution factor or depth can be found that will produce a straight line.

The volume of the compression zone that produces the required underflow dilution factor, D_u , is given by (Behn and Liebman, 1963),

$$V_{cz} = (Q + Q_r) X_i \left(\frac{t_u}{\rho_p} + \frac{D_o - D_u}{\rho K} + \frac{D_\infty t_u}{\rho} \right) \quad (9.220)$$

where t_u = the compression time required to produce a dilution ratio of D_u (sec)
 V_{cz} = the volume of the compression zone (m³ or ft³)
 X_i = the suspended solids concentration in the influent flow (kg/m³ or lb/ft³)

The compression time to reach the underflow dilution factor, t_u , is calculated from Eq. (9.220) once D_u is selected. The depth of the compression zone is calculated by dividing the compression zone volume by the plan area determined from the hindered settling analysis.

In Behn's (1957) soil consolidation theory of compression, the parameter K depends on the depth at which compression begins, H_o :

$$K = \frac{k(\rho_p - \rho)g}{\gamma H_o} \quad (9.221)$$

where k = Darcy's permeability coefficient (m/s or ft/sec).

This relationship arises because the force that expels water from the sludge is the net weight of the solids. Consequently, one can expect the parameter K to vary with the depth of the compression zone in the thickener. An iterative solution is required. The value of K determined from the batch settling test is used to get a first estimate of the compression zone volume and depth. The calculated depth is then compared with the value of H_o that occurred in the test, and K is adjusted accordingly until the calculated depth matches H_o .

Rules of Thumb

Commonly used limits on total solids fluxes on activated sludge secondary clarifiers for the maximum daily flow and maximum return rate are (Wastewater Committee, 1990):

- Conventional — $F_t = 50 \text{ lb/ft}^2 \cdot \text{day}$
- Extended aeration — $F_t = 35 \text{ lb/ft}^2 \cdot \text{day}$
- Second-stage nitrification — $F_t = 35 \text{ lb/ft}^2 \cdot \text{day}$

Current practice for average flow conditions is around 20 to 30 $\text{lb/ft}^2 \cdot \text{day}$ (Joint Task Force, 1992).

References

- Alderton, J.L. 1963. "Discussion of: 'Analysis of Thickener Operation,' by V.C. Behn and J.C. Liebman," *Journal of the Sanitary Engineering Division, Proceedings of the American Society of Civil Engineers*, 89(SA6): 57.
- Allen, H.S. 1900. "The Motion of a Sphere in a Viscous Fluid," *The London, Edinburgh, and Dublin Philosophical Magazine and Journal of Science*, 50, 5th Series, no. 304, p. 323, and no. 306, p. 519.
- Anderson, E. 1941. "Separation of Dusts and Mists," p. 1850 in *Chemical Engineers Handbook*, 2nd ed., 9th imp., J. H. Perry, ed., McGraw-Hill Book Co., Inc., New York. The source of Shepherd's formula is cited as a personal communication.
- Anonymous. 1979. *Process Design Manual for Sludge Treatment and Disposal*, EPA 625/1-79-011. U.S. Environmental Protection Agency, Municipal Environmental Research Laboratory, Technology Transfer, Cincinnati, OH.
- Babbitt, H.E., Dolan, J.J., and Cleasby, J.L. 1967. *Water Supply Engineering*, 6th ed., McGraw-Hill Book Co., Inc., New York.
- Barr, J. 1910a. "Experiments on the Flow of Water over Triangular Notches," *Engineering*, 89(8 April): 435.
- Barr, J. 1910b. "Experiments on the Flow of Water over Triangular Notches," *Engineering*, 89(15 April): 470.
- Basset, A.B. 1888. *A Treatise on Hydrodynamics: With Numerous Examples*, Deighton, Bell and Co., Cambridge, UK.
- Behn, V.C. 1957. "Settling Behavior of Waste Suspensions," *Journal of the Sanitary Engineering Division, Proceedings of the American Society of Civil Engineers*, 83(SA5): Paper No. 1423.
- Behn, V.C. and Liebman, J.C. 1963. "Analysis of Thickener Operation," *Journal of the Sanitary Engineering Division, Proceedings of the American Society of Civil Engineers*, 89(SA3): 1.

- Boadway, J.D. 1978. "Dynamics of Growth and Breakage of Alum Flocc in Presence of Fluid Shear," *Journal of the Environmental Engineering Division, Proceedings of the American Society of Civil Engineers*, 104(EE5): 901.
- Burgess, R.W. 1916. "The Uniform Motion of a Sphere Through a Viscous Liquid," *American Journal of Mathematics*, 38: 81.
- Camp, T.R. 1936a. "A Study of the Rational Design of Settling Tanks," *Sewage Works Journal*, 8(5): 742.
- Camp, T.R. 1936b. "Discussion: 'Sedimentation in Quiescent and Turbulent Basins,' by J.J. Slade, Jr., Esq.," *Proceedings of the American Society of Civil Engineers*, 62(2): 281.
- Camp, T.R. 1940. "Lateral Spillway Design," *Transactions of the American Society of Civil Engineers*, 105: 606.
- Camp, T.R. 1942. "Grit Chamber Design," *Sewage Works Journal*, 14(2): 368.
- Camp, T.R. 1945. "Sedimentation and the Design of Settling Tanks," *Proceedings of the American Society of Civil Engineers*, 71(4, part 1): 445.
- Camp, T.R. 1953. "Studies of Sedimentation Basin Design," *Sewage and Industrial Wastes*, 25(1): 1.
- Chow, V.T. 1959. *Open-Channel Hydraulics*. McGraw-Hill Book Co., Inc., New York.
- Coe, H.S. and Clevenger, G.H. 1916. "Methods for Determining the Capacities of Slime Settling Tanks," *Transactions of the American Institute of Mining Engineers*, 55: 356.
- Conley, W.P. and Hansen, S.P. 1978. "Advanced Techniques for Suspended Solids Removal," p. 299 in *Water Treatment Plant Design for the Practicing Engineer*, R.L. Sanks, ed., Ann Arbor Science Publishers, Inc., Ann Arbor, MI.
- Culp/Wesner/Culp, Inc. 1986. *Handbook of Public Water Systems*, R.B. Williams and G.L. Culp., eds. Van Nostrand Reinhold Co., Inc., New York.
- Dick, R.I. 1970a. "Role of Activated Sludge Final Settling Tanks," *Journal of the Sanitary Engineering Division, Proceedings of the American Society of Civil Engineers*, 96(SA2): 423.
- Dick, R.I. 1970b. "Discussion: 'Agglomerate Size Changes in Coagulation,'" *Journal of the Sanitary Engineering Division, Proceedings of the American Society of Civil Engineers*, 96(SA2): 624.
- Dick, R.I. and Ewing, B.B. 1967. "Evaluation of Activated Sludge Thickening Theories," *Journal of the Sanitary Engineering Division, Proceedings of the American Society of Civil Engineers*, 93(SA4): 9.
- Dick, R.I. and Young, K.W. no date. "Analysis of Thickening Performance of Final Settling Tanks," p. 33 in *Proceedings of the 27th Industrial Waste Conference, May 2, 3 and 4, 1972*, Engineering Extension Series No. 141, J.M. Bell, ed. Purdue University, Lafayette, IN.
- Dryden, H.L., Murnaghan, F.D. and Bateman, H. 1956. *Hydrodynamics*, Dover Press, Inc., New York.
- Duncan, J.W.K. and Kawata, K. 1968. "Discussion of: 'Evaluation of Activated Sludge Thickening Theories,' by R.I. Dick and B.B. Ewing," *Journal of the Sanitary Engineering Division, Proceedings of the American Society of Civil Engineers*, 94(SA2): 431.
- Eliassen, R. 1946. "Discussion: 'Sedimentation and the Design of Settling Tanks by T.R. Camp,'" *Proceedings of the American Society of Civil Engineers*, 42(3): 413.
- Fair, G.M., Geyer, J.C. and Morris, J.C. 1954. *Water Supply and Waste-Water Disposal*, John Wiley & Sons, Inc., New York.
- Favre, H. 1933. *Contribution à l'Étude des Courants Liquides*, Dunod, Paris, France.
- Fisherström, C.N.H. 1955. "Sedimentation in Rectangular Basins," *Proceedings of the American Society of Civil Engineers*, 81(Separate No. 687): 1.
- Fitch, E.B. 1956. "Flow Path Effect on Sedimentation," *Sewage and Industrial Wastes*, 28(1): 1.
- Fitch, E.B. 1957. "The Significance of Detention in Sedimentation," *Sewage and Industrial Wastes*, 29(10): 1123.
- Fitch, E.B. 1962. "Sedimentation Process Fundamentals," *Transactions of the American Institute of Mining Engineers*, 223: 129.
- François, R.J. 1987. "Strength of Aluminum Hydroxide Floccs," *Water Research*, 21(9): 1023.
- Goldstein, S. 1929. "The Steady Flow of Viscous Fluid Past a Fixed Spherical Obstacle at Small Reynolds Numbers," *Proceedings of the Royal Society of London, Ser. A*, 123: 225.

- Goldstein, S., ed. 1965. *Modern Developments in Fluid Dynamics: An Account of Theory and Experiment Relating to Turbulent Boundary Layers, Turbulent Motion and Wakes*, composed by the Fluid Motion Panel of the Aeronautical Research Committee and others, in two volumes, Vol. I. Dover Publications, Inc., New York.
- Ham, R.K. and Christman, R.F. 1969. "Agglomerate Size Changes in Coagulation," *Journal of the Sanitary Engineering Division, Proceedings of the American Society of Civil Engineers*, 95(SA3): 481.
- Hansen, S.P. and Culp, G.L. 1967. "Applying Shallow Depth Sedimentation Theory," *Journal of the American Water Works Association*, 59(9): 1134.
- Hayden, R. 1914. "Concentration of Slimes at Anaconda, Mont.," *Transactions of the American Institute of Mining Engineers*, 46: 239.
- Hazen, A. 1904. "On Sedimentation," *Transactions of the American Society of Civil Engineers*, 53: 45.
- Hinds, J. 1926. "Side Channel Spillways: Hydraulic Theory, Economic Factors, and Experimental Determination of Losses," *Transactions of the American Society of Civil Engineers*, 89: 881.
- Hudson, H.E., Jr. 1972. "Density Considerations in Sedimentation," *Journal of the American Water Works Association*, 64(6): 382.
- Hudson, H.E., Jr. 1981. *Water Clarification Processes: Practical Design and Evaluation*, Van Nostrand Reinhold Co., New York.
- Hudson, H.E., Jr., and Wolfner, J.P. 1967. "Design of Mixing and Flocculating Basins," *Journal of the American Water Works Association*, 59(10): 1257.
- Ingersoll, A.C., McKee, J.E., and Brooks, N.H. 1956. "Fundamental Concepts of Rectangular Settling Tanks," *Transactions of the American Society of Civil Engineers*, 121: 1179.
- James M. Montgomery, Consulting Engineers, Inc. 1985. *Water Treatment Principles and Design*, John Wiley & Sons, Inc., New York.
- Joint Committee of the American Society of Civil Engineers, the American Water Works Association and the Conference of State Sanitary Engineers. 1990. *Water Treatment Plant Design*, 2nd ed. McGraw-Hill Publishing Co., Inc., New York.
- Joint Task Force of the American Society of Civil Engineers, the American Water Works Association and the Conference of State Sanitary Engineers. 1969. *Water Treatment Plant Design*, American Water Works Association, Inc., New York.
- Joint Task Force of the Water Environment Federation and the American Society of Civil Engineers. 1992. *Design of Municipal Wastewater Treatment Plants: Volume I. Chapters 1–12*, WEF Manual of Practice No. 8, ASCE Manual and Report on Engineering Practice No. 76. Water Environment Federation, Alexandria, VA; American Society of Civil Engineers, New York.
- King, H.W. and Brater, E.F. 1963. *Handbook of Hydraulics for the Solution of Hydrostatic and Fluid-Flow Problems*, 5th ed., McGraw-Hill Book Co., Inc., New York.
- Kleinschmidt, R.S. 1961. "Hydraulic Design of Detention Tanks," *Journal of the Boston Society of Civil Engineers*, 48(4, sect. 1): 247.
- Kynch, G.J. 1952. "A Theory of Sedimentation," *Transactions of the Faraday Society*, 48: 166.
- Lagvankar, A.L. and Gemmell, R.S. 1968. "A Size-Density Relationship for Floccs," *Journal of the American Water Works Association*, 60(9): 1040. See errata *Journal of the American Water Works Association*, 60(12): 1335 (1968).
- Laufer, J. 1950. "Some Recent Measurements in a Two-Dimensional Turbulent Channel," *Journal of the Aeronautical Sciences*, 17(5): 277.
- Mantz, P.A. 1977. "Incipient Transport of Fine Grains and Flakes by Fluids — Extended Shields Diagram," *Journal of the Hydraulics Division, Proceedings of the American Society of Civil Engineers*, 103(HY6): 601.
- McGaughey, P.M. 1956. "Theory of Sedimentation." *Journal of the American Water Works Association*, 48(4): 437.
- McNown, J.S. 1945. "Discussion of: 'Lock Manifold Experiments,' by E. Soucek and E.W. Zelnick," *Transactions of the American Society of Civil Engineers*, 110: 1378.

- McNown, J.S. 1954. "Mechanics of Manifold Flow," *Transactions of the American Society of Civil Engineers*, 119: 1103.
- Moore, W.L. 1943. "Energy Loss at the Base of a Free Overflow," *Transactions of the American Society of Civil Engineers*, 108: 1343.
- Naiz, S.M. 1954. "Discussion of: 'Mechanics of Manifold Flow,' by J.S. McNown," *Transactions of the American Society of Civil Engineers*, 119: 1132.
- O'Brien, M.P. 1932. "Analyzing Hydraulic Models for the Effects of Distortion," *Engineering News-Record*, 109(11): 313.
- O'Connor, J.T. 1971. "Management of Water-Treatment Plant Residues," p. 625 in *Water Quality and Treatment: A Handbook of Public Water Supplies*, 3rd ed., P.D. Haney et al., eds. McGraw-Hill Book Co., Inc., New York.
- Oseen, C.W. 1913. "Über den Gültigkeitsbereich der Stokesschen Widerstandformel," *Arkiv för Matematik, Astonomi och Fysik*, 9(16): 1.
- Parker, D.S. 1983. "Assessment of Secondary Clarification Design Concepts," *Journal of the Water Pollution Control Federation*, 55(4): 349.
- Parker, D.S., Kaufman, W.J., and Jenkins, D. 1972. "Floc Breakup in Turbulent Flocculation Processes," *Journal of the Sanitary Engineering Division, Proceedings of the American Society of Civil Engineers*, 98(SA1): 79.
- Powell, R.W. 1954. "Discussion of: 'Mechanics of Manifold Flow,' by J.S. McNown," *Transactions of the American Society of Civil Engineers*, 119: 1136.
- Richardson, J.F. and Zaki, W.N. 1954. "Sedimentation and Fluidization," *Transactions of the Institute of Chemical Engineers: Part I*, 32: 35.
- Roberts, E.J. 1949. "Thickening — Art or Science?," *Mining Engineering*, 101: 763.
- Rouse, H. 1936. "Discharge Characteristics of the Free Overfall," *Civil Engineering*, 6(4): 257.
- Rouse, H. 1937. "Nomogram for the Settling Velocity of Spheres," p. 57 in *Report of the Committee on Sedimentation*, P.D. Trask, chm., National Research Council, Division of Geology and Geography, Washington, DC.
- Rouse, H. 1943. "Discussion of: 'Energy Loss at the Base of a Free Overflow,' by W.L. Moore," *Transactions of the American Society of Civil Engineers*, 108: 1343.
- Rouse, H. 1978. *Elementary Mechanics of Fluids*, Dover Publications, Inc., New York.
- Rowell, H.S. 1913. "Note on James Thomson's V-Notches," *Engineering*, 95(2 May): 589.
- San, H.A. 1989. "Analytical Approach for Evaluation of Settling Column Data," *Journal of Environmental Engineering*, 115(2): 455.
- Seddon, J.A. 1889. "Clearing Water by Settlement," *Journal of the Association of Engineering Societies*, 8(10): 477.
- Slechta, A.F. and Conley, W.R. 1971. "Recent Experiences in Plant-Scale Application of the Settling Tube Concept," *Journal of the Water Pollution Control Federation*, 43(8): 1724.
- Soucek, E. and Zelnick, E.W. 1945. "Lock Manifold Experiments," *Transactions of the American Society of Civil Engineers*, 110: 1357.
- Stokes, G.G. 1856. "On the Effect of the Internal Friction of Fluids on the Motion of Pendulums," *Transactions of the Cambridge Philosophical Society*, 9(II) 8.
- Switzer, F.G. 1915. "Tests on the Effect of Temperature on Weir Coefficients," *Engineering News*, 73(13): 636.
- Sykes, R.M. 1993. "Flocculent and Nonflocculent Settling," *Journal of Environmental Science and Health, Part A, Environmental Science and Engineering*, A28(1): 143.
- Talmadge, W.P. and Fitch, E.B. 1955. "Determining Thickener Unit Areas," *Industrial and Engineering Chemistry*, 47: 38.
- Tambo, N. and Hozumi, H. 1979. "Physical Characteristics of Flocs — II. Strength of Floc," *Water Research*, 13(5): 421.
- Tambo, N. and Watanabe, Y. 1979. "Physical Characteristics of Flocs — I. The Floc Density Function and Aluminum Floc," *Water Research*, 13(5): 409.

- Task Committee for the Preparation of the Manual on Sedimentation. 1975. *Sedimentation Engineering*, ASCE Manuals and Reports on Engineering Practice No. 54, V.A. Vanoni, ed. American Society of Civil Engineers, New York.
- Vesilind, P.A. 1974. *Treatment and Disposal of Wastewater Sludges*, Ann Arbor Science Publishers, Inc., Ann Arbor, MI.
- von Karman, T. 1940. "The Engineer Grapples with Nonlinear Problems," *Bulletin of the American Mathematical Society*, 46(8): 615.
- Water Supply Committee of the Great Lakes-Upper Mississippi River Board of State Sanitary Engineers. 1987. *Recommended Standards for Water Works*, 1987 ed., Health Research, Inc., Albany, NY.
- Yalin, M.S. 1977. *Mechanics of Sediment Transport*, 2nd ed., Pergamon Press, Ltd., Oxford.
- Yao, K.M. 1970. "Theoretical Study of High-Rate Sedimentation," *Journal of the Water Pollution Control Federation*, 42(2, part 1): 218.
- Yao, K.M. 1973. "Design of High-Rate Settlers," *Journal of the Environmental Engineering Division, Proceedings of the American Society of Civil Engineers*, 99(EE5): 621.
- Yee, L.Y. and Babb, A.F. 1985. "Inlet Design for Rectangular Settling Tanks by Physical Modeling," *Journal of the American Water Works Association*, 57(12): 1168.
- Yoshioka, N., Hotta, Y., Tanaka, S., Naito, S., and Tsugami, S. 1957. "Continuous Thickening of Homogeneous Flocculated Slurries," *Chemical Engineering*, 21(2): 66.
- Zanoni, A.E. and Blomquist, M.W. 1975. "Column Settling Tests for Flocculant Suspensions," *Journal of the Environmental Engineering Division, Proceedings of the American Society of Civil Engineers*, 101(EE3): 309.

9.6 Filtration

Granular Media Filters

Particle Removal Mechanisms

The possible removal mechanisms are as follows (Ives, 1975; Tien, 1989):

- Mechanical straining — Straining occurs when the particles are larger than the local pore. It is important only if the ratio of particle diameter to pore size is larger than about 0.2 (Herzig, Leclerc, and Le Goff, 1970). Straining is undesirable, because it concentrates removed particles at the filter surface and reduces filter runs.
- Sedimentation — The effective horizontal surface in sand filters is roughly 3% of the surface area of the sand grains, and this amounts to nearly 400 times the plan area of the bed for each meter of sand depth (Fair and Geyer, 1954). Consequently, filters act in part like large sedimentation basins (Hazen, 1904).
- Inertial impact — Particles tend to persist in moving in a straight line, and if they are large enough, their momentum may overcome the liquid drag forces and lead to a collision with the media.
- Hydrodynamic diffusion — Because of the liquid velocity variation across the particle diameter, there is a net hydrodynamic force on the particle normal to the direction of flow. If the particles are spherical and the velocity gradient is linear (laminar flow), this force moves the particle toward high velocities and away from any media surface. However, if particle shape is irregular and the flow field is nonuniform and unsteady (turbulent flow), the particle drift appears to be random. In the first case, removals are reduced. In the second case, random movements produce a turbulent diffusion, with transport from high concentration to low concentration areas. Particle adsorption produces a low concentration region near the media surface, so the hydrodynamic diffusion transports particles to the media.
- Interception — If the liquid stream lines bring a particle center to within one particle radius of the media surface, the particle will strike the surface and may adhere.

- Brownian diffusion — Brownian diffusion will cause particles to move from high concentration zones to low concentration zones. Adsorption to the media surface creates a low concentration zone near the media, so Brownian diffusion will transport particles from the bulk flow toward the media.
- Electrostatic and London–Van der Waals attraction — Electrical fields due to electrostatic charges or to induced London–Van der Waals fields, may attract or repel particles and media.
- Adhesion — Once the particles collide with the media surface, they must adhere. Adhesion occurs with the clean media surface and with particles already collected on the surface. Consequently, particles that are to be removed must be colloiddally unstable (Gregory, 1975).

Performance

In general, granular media filters remove particles that are much smaller than the pore opening. Also, transport to the media surface depends on the local particle concentration in the flow. The result is that particle removal is more or less exponential with depth. This is usually expressed as Iwasaki's (1937) Law:

$$\frac{X}{X_o} = e^{-\lambda H} \quad (9.222)$$

where H = the depth of filter media (m or ft)
 X = the suspended solids concentration leaving the filter (kg/m³ or lb/ft³)
 X_o = the suspended solids concentration entering the filter (kg/m³ or lb/ft³)
 λ = the filter coefficient (per m or per ft)

Ives and Sholji (1965) and Tien (1989) summarized empirical data for the dependence of the Iwasaki filter coefficient upon diameter of the particle to be removed, d_p , the diameter of the filter media, d_m , the filtration rate, U_f , and the water viscosity, μ . The dependencies have the following form:

$$\lambda \propto \frac{d_p^\alpha}{U_f^\beta d_m^\gamma \mu^\delta} \quad (9.223)$$

The exponents on the variables are highly uncertain and system specific, but α appears to be on the order of 1 to 1.5; β appears to be on the order of 0.5 to 2; γ appears to be on the order of 0.5 to 2; and δ appears to be on the order of 1. A worst-case scenario may be estimated by adopting the most unfavorable exponent for a suggested process change.

For practical design purposes, γ is sometimes taken to be 1, and filter depth and media size are traded off according to (James M. Montgomery, Consulting Engineers, Inc., 1985),

$$\frac{H_1}{d_{m1}} = \frac{H_2}{d_{m2}} \quad (9.224)$$

The Committee of the Sanitary Engineering Division on Filtering Materials (1936) reported that the depth of penetration of suspended solids (silts and flocs) into filter media was more or less proportional to the square of the media particle diameter. In the Committee's studies, the coefficient of proportionality ranged from about 10 to 25 in./mm², and it appeared to be a characteristic of the specific sand source. They recommended Allan's procedure for formulating sand specifications, which reduces to

$$H_{\min} = \sum_{i=1}^n H_i \propto \frac{1}{\sum_{i=1}^n \frac{f_i}{d_{mi}^2}} \quad (9.225)$$

where d_{mi} = the grain diameter of media size class i (m or ft)
 f_i = the fraction by weight of media size d_{mi} (dimensionless)
 H_i = the depth of filter media size d_{mi} (m or ft)
 H_{\min} = the minimum depth of media (m or ft)

Equation (9.225) was derived by assuming that the penetration of suspended particles into the sand mixture should be equal to the penetration into any single grade.

Because the removal rate is exponential, there is no combination of filtration rate or media depth that will remove all particles. A minimum filtered water turbidity of 0.1 to 0.2 seems to be the best that can be expected; this minimum will be proportional to the influent turbidity.

For many years, the standard filtration rate in the U.S. was 2 gpm/ft², which is usually attributed to Fuller's (1898) studies at Louisville. Cleasby and Baumann (1962) have shown that increasing the filtration rate to 6 gpm/ft² triples the effluent turbidity, but that turbidities less than 1 TU were still achievable at the higher rate. Their filters held 30 in. of sand, either with an effective size of 0.5 mm and a uniformity coefficient of 1.89 or sieved to lie between 0.59 and 0.84 mm. The suspended particles were ferric hydroxide flocs. Reviewing a number of filtration studies, Cleasby (1990) concluded that filtration rates up to 4 gpm/ft² were acceptable as long as coagulation of the raw water is nearly complete and no sudden increases in filtration rate occur. Higher filtration rates required filter aids, but effluent turbidities of less than 0.5 NTU are achievable.

Fair and Geyer (1954) summarized whole-plant coliform removal data reported by the U.S. Public Health Service as Eq 322:

$$C_f = aC_o^b \quad (9.226)$$

where a, b = empirical coefficients
 C_o = the concentration of total coliform bacteria in the raw, untreated water in no./100 mL
 C_f = the finished water concentration of total coliform bacteria in no./100 mL

Values of the coefficients for different plant designs are shown in Table 9.4. Also shown is the concentration of bacteria in the filter influent, C_{pi} , that will permit achievement of a finished water concentration of 1/100 mL. The filtration rates, bed depths, and grain sizes were not specified.

Hazen's (1896) empirical rule for the proportion of bacteria passing through filters is

$$P_{pass} = \frac{1}{2} \frac{U_f^2 d_{es}}{\sqrt{H}} \quad (9.227)$$

where d_{es} = the effective size on the filter media in mm
 H = the media depth (in.)
 P_{pass} = the percentage of the bacteria passing through the filter
 U_f = the filtration rate in mgd

TABLE 9.4 Coliform Removal Efficiencies For Different Water Treatment Plant Configurations

Treatment Process	Turbid River Water			Clear Lake Water		
	a	b	C_{pi}	a	b	C_{pi}
Chlorination only	0.015	0.96	80	0.050	0.76	50
Flocculation, settling, filtration	0.070	0.60	80	0.087	0.60	60
Flocculation, settling, filtration, postchlorination	0.011	0.52	6000	0.040	0.38	4500

Source: Fair, G.M. and Geyer, J.C. 1954. *Water Supply and Waste-Water Disposal*, John Wiley & Sons, Inc., New York.

Hazen's formula appears to approximate the median of a log-normal distribution. Approximately 40% of the cases will lie between one-half and twice the predicted value. In somewhat less than one-fourth of the cases, the percentage passing will be greater than twice the predicted value. One-sixth of the cases will exceed four times the predicted value. The proportion of cases exceeding 10 times the predicted value is less than 1%.

Immediately after backwashing, the water in the filter pores is turbid, and the initial product following the startup of filtration must be discarded. Approximately 10 bed volumes must be discarded to obtain stable effluent suspended solids concentrations (Cleasby and Baumann, 1962).

Water Balance and Number of Filter Boxes

The water balance (in units of volume) for a rapid sand filter for a design period T is,

$$\underbrace{U_f A t_f}_{\text{gross product}} = \underbrace{U_b A t_b}_{\text{wash water}} + \underbrace{F_p P Q_{pc} T}_{\text{community demand}} \quad (9.228)$$

where A = the plan area of the filter media (m^2 or ft^2)
 F_p = the peaking factor for the design period (dimensionless)
 P = the projected service population (capita)
 Q_{pc} = the per caput water demand ($\text{m}^3/\text{s} \cdot \text{cap}$ or $\text{ft}^3/\text{sec} \cdot \text{cap}$)
 T = the design period (sec)
 T_b = the time spent backwashing during the design period (sec)
 T_f = the time spent filtering during the design period (sec)
 U_b = the backwash rate (m/s or ft/sec)
 U_f = the filtration rate (m/s or ft/sec)

The design period T is determined by balancing costs of storage vs. filtration capacity. It is typically on the order of one to two weeks. The peaking factor F_p corresponds to the design period. Typical values are given in Tables 8.11 and 8.12. The service population P is the projected population, usually 20 years hence.

A commonly used filtration rate is 4 gpm/ ft^2 . The duration of the filter run is determined by the required effluent quality. A rough rule of thumb is that the filter must be cleaned after accumulating 0.1 lbm suspended solids per sq ft of filter area per ft of headloss (Cleasby, 1990). Actual filters may capture between one-third and three times this amount before requiring cleaning.

Backwash rates depend on the media and degree of fluidization required. Full fluidization results in a bed expansion of 15 to 30%. Backwashing is continued until the wash water is visibly clear, generally about 10 min.

The economical number of filters is often estimated using the Morrill–Wallace (1934) formula:

$$n = 2.7 \sqrt{Q_{des}} \quad (9.229)$$

where n = the number of filter boxes (dimensionless)
 Q_{des} = the plant design flow in mgd

Filter Box Design

The usual requirement is that there be at least two filters, each of which must be capable of meeting the plant design flow (Water Supply Committee, 1987). If more than two filters are built, they must be capable of meeting the plant design flow with one filter out of service. The dimensions of rapid sand filters are more or less standardized and may be summarized as follows (Babbitt, Doland, and Cleasby, 1967; Joint Task Force, 1990; Culp/Wesner/Culp, Inc., 1986; Kawamura, 1991).

Vertical Cross Section

The vertical cross section of a typical rapid sand filter box is generally at least 8 to 10 ft deep (preferably deeper to avoid air binding) above the floor and consists of the following layers:

- At least 12 and more likely 16 to 18 in. of gravel and torpedo sand
- 24 to 30 in. of filter media, either fine or coarse sand or sand and crushed anthracite coal
- At least 6 ft of water, sufficient to avoid negative or zero gauge pressures anywhere in the filter and consequent air binding
- At least 6 in. of freeboard, and preferably more, to accommodate surges during backwashing

The backwash troughs are placed sufficiently high that the top of the expanded sand layer is at least 18 in. below the trough inlets.

Plan Dimensions

The plan area of the sand beds of gravity filters generally does not exceed 1000 ft², and larger sand beds are constructed as two subunits with separate backwashing.

Filters are normally arranged side by side in two parallel rows with a pipe gallery running between the rows. The pipe gallery should be open to daylight to facilitate maintenance.

Wash Water Effluent Troughs

The design of wash water effluent troughs is discussed earlier in Section 9.5, "Sedimentation." The troughs are submerged during filtration.

Air Scour

A major problem with air scour systems is disruption of the gravel layer and gravel/sand mixing. The gravel layer is eliminated in the nozzle/strainer and porous plate false bottom systems, and special gravel designs are used in the perforated block with gravel systems.

In some European designs (Degrémont, 1965), wash water over flow troughs are dispensed with, and the wash water is discharged over an end wall. The sand bed is not fluidized, and air scour and backwash water are applied simultaneously. An additional, simultaneous cross-filter surface flow of clarified water is used to promote movement of the dirty wash water to the wash water effluent channel.

Floor Design

Filter floors serve three essential purposes: (1) they support the filter media, (2) they collect the filtrate, and (3) they distribute the backwash water. In some designs, they also distribute the air scour. The usual designs are as follows (Cleasby, 1990; Joint Task Force, 1990; Kawamura, 1991):

- *Pipe laterals with gravel* consist of a manifold with perforated laterals placed on the filter box floor in at least 18 in. of gravel. The coarsest gravel must be deeper than the perforated laterals (at least 6 in. total depth), and there must be at least 10 to 16 in. of finer gravel and torpedo sand above the coarsest gravel. Precast concrete inverted "V" laterals are also available. The lateral orifices are drilled into the pipe bottoms or "V" lateral sides and are normally about 1/4 to 3/4 in. in diameter and 3 to 12 in. apart.
- The usual rules-of-thumb regarding sizing are (1) a ratio of orifice area to filter plan area of 0.0015 to 0.005, (2) a ratio of lateral cross-sectional area to total orifice area served of 2 to 4, and (3) a ratio of manifold cross-sectional area to lateral cross-sectional area served of 1.5 to 3.
- These systems generally exhibit relatively high headlosses and inferior backwash distribution and are discouraged. Poor backwash distribution can lead to gravel/sand mixing. This is aggravated by air scour, and air scour should not be applied through the laterals.
- *Blocks with gravel* consist of ceramic or polyethylene blocks overlain by at least 12 in. gravel. The blocks are grouted onto the filter box floor and to each other. The blocks are usually about 10 in. high by 11 in. wide by 2 ft long. The tops are perforated with 5/32 to 5/16 in. orifices typically numbering about 45 per sq ft. The filtrate and backwash water flow along channels inside the

block that run parallel to the lengths. Special end blocks discharge vertically into collection channels built into the filter box floor.

- Special gravel designs at least 12 to 15 in. deep are required if air scour is applied through the blocks. Porous plates and nozzle/strainer systems are preferred for air scour.
- *False bottoms with gravel* consist of precast or cast-in-place plates that have inverted pyramidal 3/4 in. orifices at 1 ft internals horizontally that are filled with porcelain spheres and gravel. The plates are installed on 2 ft high walls that sit on the filter box floor, forming a crawl space. The gravel layer above the false bottom is at least 12 in. deep. The flow is through the crawl space between the filter box floor and the false bottom.
- *False bottom without gravel* consists of precast plates or cast-in-place monolithic slabs set on short walls resting on the filter box floor. The walls are at least 2 ft high to provide a crawl space for maintenance and inspection. Cast-in-place slabs are preferred, because they eliminate air venting through joints. The plates are perforated, and the perforations contain patented nozzle/strainers that distribute the flow and exclude the filter sand. These systems are commonly used with air scour, which is applied through the nozzle/strainers.
- The nozzle/strainer openings are generally small, typically on the order of 0.25 mm, and are subject to clogging from construction debris, rust, and fines in the filter media and/or gravel. The largest available opening size should be used, and the effective size of the filter media should be twice the opening size. Some manufacturers recommend a 6 in. layer of pea stone be placed over the nozzles to avoid sand and debris clogging of the nozzle openings.
- Plastic nozzle/strainers are easily broken during installation and placement of media. Nozzle-strainer materials must be carefully matched to avoid differential thermal expansion and contraction.
- *Porous plates* consist of sintered aluminum oxide plates mounted on low walls or rectangular ceramic saddles set on the filter box floor. These systems are sometimes used when air scour is employed.
- The plates are fragile and easily broken during installation and placement of media. They are subject to the same clogging problems as nozzle/strainers. They are not recommended for hard, alkaline water, lime-soda softening installations, iron/manganese waters, or iron/manganese removal installations.

Good backwash distribution requires that headloss of the orifices or pores exceed all other minor losses in the backwash system.

Hydraulics

Filter hydraulics are concerned with the clean filter headloss, which is needed to select rate-of-flow controllers, and the backwashing headloss.

Clean Filter Headloss

For a uniform sand, the initial headloss is given by the Ergun (1952) equation:

$$\frac{\Delta p}{\gamma} = h_L = f_m \left(\frac{H}{d_{eq}} \right) \left(\frac{1-\epsilon}{\epsilon^3} \right) \left(\frac{U_f^2}{g} \right) \quad (9.230)$$

- where
- A_p = the cross-sectional area of a sand grain (m² or ft²)
 - d_{eq} = the equivalent diameter of a nonspherical particle (m or ft)
= 6 (V_p/A_p)
 - g = the acceleration due to gravity (9.80665 m/s² or 32.174 ft/sec²)
 - f_m = the MacDonal–El-Sayed–Mow–Dullien friction factor (dimensionless)
 - H = the thickness of the media layer (m or ft)
 - h_L = the headloss (m or ft)

Δp = the pressure drop due to friction (Pa or lbf/ft²)
 U_f = the filtration rate (m/s or ft/sec)
 V_p = the volume of a sand grain (m³ or ft³)
 ϵ = the bed porosity (dimensionless)
 γ = the specific weight of the water (N/m³ or lbf/ft³)

The friction factor f_m is given by the MacDonald–El-Sayed–Mow–Dullien (1979) equation:

$$f_m \geq 180 \frac{1-\epsilon}{Re} + 1.8, \text{ for smooth media;} \quad (9.231)$$

$$f_m \leq 180 \frac{1-\epsilon}{Re} + 4.0, \text{ for rough media;} \quad (9.232)$$

$$Re = \frac{\rho U_f d_{eq}}{\mu} \quad (9.233)$$

where μ = the dynamic viscosity of water (N·s/m² or lbf·sec/ft²)
 ρ = the water density (kg/m³ or lbm/ft³)

For filters containing several media sizes, the Fair and Geyer (1954) procedure is employed. It is assumed that the different sizes separate after backwashing and that the bed is stratified. The headloss is calculated for each media size by assuming that the depth for that size is,

$$H_i = f_i H \quad (9.234)$$

where f_i = the fraction by weight of media size class i (dimensionless)
 H = the depth of the settled filter media (m or ft)
 H_i = the depth of filter media size class i (m or ft)

The Fair–Geyer method yields a lower bound to the headloss. Filters do not fully stratify unless there is a substantial difference in terminal settling velocities of the media sizes. In a partially stratified filter, the bed porosity will be reduced because of intermixing of large and fine grains, and the headloss will be larger than that predicted by the Fair–Geyer method. An upper bound can be found by assuming that the entire bed is filled with grains equal in size to the effective size.

Backwashing

The headloss required to fluidize a bed is simply the net weight of the submerged media:

$$\frac{\Delta p}{\gamma} = h_L = H(\rho_s - \rho)(1 - \epsilon) \quad (9.235)$$

where ρ_p = the particle density (kg/m³ or lbm/ft³).

During backwashing, the headloss increases according to Eq. (9.230) until the headloss specified by Eq. (9.235) is reached; thereafter, the backwashing headloss is constant regardless of flow rate (Cleasby and Fan, 1981).

The only effect of changing the flow rate in a fluidized bed is to change the bed porosity. The expanded bed porosity can be estimated by the Richardson–Zaki (1954) equation:

$$\epsilon_e = \left(\frac{U_b}{v_s} \right)^{Re^{0.03}/4.35}, \text{ for } 0.2 < Re < 1 \quad (9.236)$$

$$\varepsilon_e = \left(\frac{U_b}{v_s} \right)^{Re^{0.1}/4.45}, \text{ for } 1 < Re < 500 \quad (9.237)$$

where U_b = the backwashing rate (m/s or ft/sec)
 v_s = the free (unhindered) settling velocity of a media particle (m/s or ft/sec)
 ε_e = the expanded bed porosity (dimensionless)

The Reynolds number is that of the media grains in free, unhindered settling:

$$Re = \frac{\rho v_s d_{eq}}{\mu} \quad (9.238)$$

The free settling velocity can be estimated by Stokes' (1856) equation,

$$C_D = \frac{24}{Re}, \text{ for } Re < 0.1 \quad (9.137)$$

$$v_s = \frac{g(\rho_p - \rho)d_{eq}^2}{18\mu} \quad (9.138)$$

or by Shepherd's equation (Anderson, 1941),

$$C_D = \frac{18.5}{Re^{0.60}}; \text{ for } 1.9 < Re < 500 \quad (9.144)$$

$$v_s = 0.153d_{eq}^{1.143} \left[\frac{g(\rho_p - \rho)}{\rho^{0.40}\mu^{0.60}} \right]^{0.714} \quad (9.145)$$

Generally, the particle size greater than 60% by weight of the grains, d_{60} , is used. The Reynolds number for common filter material is generally close to 1, and because of the weak dependence of bed expansion on Reynold's number (raised to the one-tenth power), it is often set arbitrarily to 1.

The depth of the expanded bed may be calculated from

$$H_e = H \frac{1 - \varepsilon}{1 - \varepsilon_e} \quad (9.239)$$

where H_e = the expanded bed depth (m or ft).

The maximum backwash velocity that does not fluidize the bed, U_{mf} can be estimated by setting the expanded bed porosity in Eqs. (9.236) or (9.237) equal to the settled bed porosity. Alternatively, one can use the Wen–Yu (1966) correlation:

$$Ga = \frac{\rho(\rho_p - \rho)gd_{eq}^3}{\mu} \quad (9.240)$$

$$U_{mf} = \frac{\mu(33.7^2 + 0.0408Ga)^{0.5}}{\rho d_{eq}} - \frac{33.7\mu}{\rho d_{eq}} \quad (9.241)$$

where Ga = the Gallileo number (dimensionless)
 U_{mf} = the minimum bed fluidization backwash rate (m/s or ft/sec).

In dual media filters, the expansion of each layer must be calculated, separated, and totalled. Each layer will experience the same backwash flow rate, but the minimum flow rates required for fluidization will differ.

The optimum expansion for cleaning without air scour is about 70%, which corresponds to maximum hydraulic shear (Cleasby, Amirtharajah, and Baumann, 1975).

Fluidization alone is not an effective cleaning mechanism, and fluidization plus air scour is preferred. Air scour is applied alone followed by bed fluidization or applied simultaneously with a backwash flow rate that does not fluidize the bed. The latter method is the most effective cleaning procedure.

For typical fine sands with an effective size of about 0.5 mm, air scour and backwash are applied separately. Generally, air is applied at a rate of about 1 to 2 scfm/ft² for 2 to 5 min followed by a water rate of 5 to 8 gpm/ft² (nonfluidized) to 15 to 20 gpm/ft² (fully fluidized) (Cleasby, 1990). Backwash rates greater than about 15 gpm/ft² may dislodge the gravel layer.

Simultaneous air scour and backwash may be applied to dual media filters and to coarse grain filters with effective sizes of about 1 mm or larger. Airflow rates are about 2 to 4 scfm/ft², and water flow rates are about 6 gpm/ft² (Cleasby, 1990).

Amirtharajah (1984) developed a theoretical equation for optimizing airflow and backwash rates:

$$0.45Q_a^2 + 100 \left(\frac{U_b}{U_{mf}} \right) = 41.9 \quad (9.242)$$

where Q_a = the airflow rate (scfm/ft²)
 U_b = the backwash rate (m/s or ft/sec)
 U_{mf} = the minimum fluidization velocity based on the d_{60} grain diameter (m/s or ft/sec)

Equation (9.242) may overestimate the water flow rates (Cleasby, 1990).

Water Treatment

U.S. EPA Surface Water Treatment Rule

Enteric viruses and the cysts of important pathogenic protozoans like *Giardia lamblia* and *Cryptosporidium parvum* are highly resistant to the usual disinfection processes. The removal of these organisms from drinking water depends almost entirely upon coagulation, sedimentation, and filtration. Where possible, source protection is helpful in virus control.

The U.S. Environmental Protection Agency (U.S. EPA, 1989; Malcolm Pirnie, Inc., and HDR Engineering, Inc., 1990) issued treatment regulations and guidelines for public water supplies that use surface water sources and groundwater sources that are directly influenced by surface waters. Such systems are required to employ filtration and must achieve 99.9% (so-called “three log”) removal or inactivation of *G. lamblia* and 99.99% (so-called “four log”) removal or inactivation of enteric viruses. Future treatment regulations will require 99% (“two log”) removal of *Cryptosporidium parvum* (U.S. EPA, 1998). The current performance requirements for filtration are that the filtered water turbidity never exceed 5 TU and that individual filter systems meet the following turbidity limits at least 95% of the time:

- Conventional rapid sand filters preceded by coagulation, flocculation, and sedimentation — 0.5 TU
- Direct filtration — 0.5 TU
- Cartridge filters and approved package plants — 0.5 TU
- Slow sand filters — 1.0 TU
- Diatomaceous earth filters — 1.0 TU

Public supplies can avoid the installation of filters if they meet the following basic conditions (Pontius, 1990):

- The system must have an effective watershed control program.
- Prior to disinfection, the fecal and total coliform levels must be less than 20/100 mL and 100/100 mL, respectively, in at least 90% of the samples.
- Prior to disinfection, the turbidity level must not exceed 5 TU in samples taken every 4 hr.
- The system must practice disinfection and achieve 99.9 and 99.99% removal or inactivation of *G. lamblia* cysts and enteric viruses, respectively, daily.
- The system must submit to third-party inspection of its disinfection and watershed control practices.
- The system cannot have been the source of a water-borne disease outbreak, unless it has been modified to prevent another such occurrence.
- The system must be in compliance with the total coliform rule requirements.
- The system must be in compliance with the total trihalomethane regulations.

The *Guidance Manual* (Malcolm Pirnie, Inc., and HDR Engineering, Inc., 1990) lists other requirements and options.

Media

The generally acceptable filtering materials for water filtration are silica sand, crushed anthracite coal, and granular activated carbon (Water Supply Committee, 1987; Standards Committee on Filtering Material, 1989):

- Silica sand particles shall have a specific gravity of at least 2.50, shall contain less than 5% by weight acid-soluble material and shall be free (less than 2% by weight of material smaller than 0.074 mm) of dust, clay, micaceous material, and organic matter.
- Crushed anthracite coal particles shall have a specific gravity of at least 1.4, a Mohr hardness of at least 2.7, and shall contain less than 5% by weight of acid-soluble material and be free of shale, clay, and debris.

In addition, filters normally contain a supporting layer of gravel and torpedo sand that retains the filtering media. In general, the supporting gravel and torpedo sand should consist of hard, durable, well-rounded particles with less than 25% by weight having a fractured face, less than 2% by weight being elongated or flat pieces, less than 1% by weight smaller than 0.074 mm, and less than 0.5% by weight consisting of coal, lignin, and organic impurities. The acid solubility should be less than 5% by weight for particles smaller than 2.36 mm, 17.5% by weight for particles between 2.36 and 25.4 mm, and less than 25% for particles equal to or larger than 25.4 mm. The specific gravity of the particles should be at least 2.5.

The grain size distribution is summarized in terms of an “effective size” and a “uniformity coefficient:”

- The effective size (e.s.) is the sieve opening that passes 10% by weight of the sample.
- The uniformity coefficient (U.C.) is the ratio of the sieve opening that passes 60% by weight of the sample and then the opening that passes 10% by weight of the same sample.

Typical media selections for various purposes are given in [Table 9.5](#).

Single Media Filters

The typical filter cross section for a single-media filter (meaning either sand, coal, or GAC used alone) is given in [Table 9.6](#). The various media are placed coarsest to finest from bottom to top, and the lowest layer rests directly on the perforated filter floor. Various manufacturers recommend different size distributions for their underdrain systems; two typical recommendations are given in [Table 9.7](#). Kawamura (1991) recommends a minimum gravel depth of 16 in. in order to avoid disruption during backwashing.

TABLE 9.5 Media Specification for Various Applications (Uniformity Coefficient 1.6 to 1.7 for Medium Sand and 1.5 for Coarse Sand or Coal)

Process	Media	Effective Size (mm)	Depth (ft)
Coagulation, settling, filtration; filtration rate = 4 gpm/ft ²	Medium sand	0.45–0.55	2.0–2.5
Coagulation, settling, filtration; filtration rate > 4 gpm/ft ² with polymer addition	Coarse sand	0.8–2.0	2.6–7.0
Coagulation, settling, filtration; filtration rate > 4 gpm/ft ²	Coarse sand	0.9–1.1	1.0–1.5
	Anthracite	0.9–1.4	1.5–2.0
Direct filtration of surface water	Coarse sand	1.5	1.0–1.5
	Anthracite	1.5	1.5–2.0
Iron and manganese removal	Coarse sand	<0.8	2.5–3.0
Iron and manganese removal	Coarse sand	0.9–1.1	1.0–1.5
	Anthracite	0.9–1.4	1.5–2.0
Coarse single media with simultaneous air scour and backwash for coagulation, settling, and filtration	Coarse sand	0.9–1.0	3.0–4.0
Coarse single media with simultaneous air scour and backwash for direct filtration	Coarse sand	1.4–1.6	3.5–7.0
Coarse single media with simultaneous air scour and backwash for iron and manganese removal	Coarse sand	1.0–2.0	5.0–10.0

Sources: Cleasby, J.L. 1990. "Chapter 8 — Filtration," p. 455 in *Water Quality and Treatment: A Handbook of Community Water Supplies*, 4th ed., F.W. Pontius, tech. ed., McGraw-Hill, Inc., New York.
Kawamura, S. 1991. *Integrated Design of Water Treatment Facilities*, John Wiley & Sons, Inc., New York.

TABLE 9.6 Typical Single Media, Rapid Sand Filter Cross Section and Media Specifications

Material	Effective Size (mm)	Uniformity Coefficient (dimensionless)	Depth (in.)
Silica sand	0.45–0.55	≤1.65	24–30
Anthracite Coal:			
Surface water turbidity removal	0.45–0.55	≤1.65	24–30
Groundwater Fe/Mn removal	≤0.8		24–30
Granular activated carbon	0.45–0.55	≤1.65	24–30
Torpedo sand	0.8–2.0	≤1.7	3
Gravel	$\frac{3}{16}$ – $\frac{3}{32}$ in.	—	2–3
	$\frac{1}{2}$ – $\frac{3}{16}$ in.	—	2–3
	$\frac{3}{4}$ – $\frac{1}{2}$ in.	—	3–5
	$1\frac{3}{4}$ – $\frac{3}{4}$ in.	—	3–5
	$2\frac{1}{2}$ – $1\frac{3}{4}$ in.	—	5–8

Source: Water Supply Committee. 1987. *Recommended Standards for Water Works*, 1987 ed., Health Research, Inc., Albany, NY.

Dual Media Filters

The principle problem with single-media filters is that the collected solids are concentrated in the upper few inches of the bed. This leads to relatively short filter runs. If the solids can be spread over a larger portion of the bed, the filter runs can be prolonged. One way of doing this is by using dual media filters. Dual media filters consist of an anthracite coal layer on top of a sand layer. The coal grains are larger than the sand grains, and suspended solids penetrate more deeply into the bed before being captured.

The general sizing principle is minimized media intermixing following backwashing. The critical size ratio for media with different densities is that which produces equal settling velocities (Conley and Hsiung, 1969):

$$\frac{d_1}{d_2} = \left(\frac{\rho_2 - \rho_m}{\rho_1 - \rho_m} \right)^{0.625} \quad (9.243)$$

TABLE 9.7 Gravel Specifications for Specific Filter Floors

Gravel Size Range (U.S. Standard Sieve Sizes, mm)	Layer Thickness (in.)		
	General ^a	Dual-Parallel Lateral Block ^{a,b}	Leopold Wheeler ^b
1.70–3.35	3	3	—
3.35–6.3	3	3	—
4.75–9.5	—	—	3
6.3–12.5	3	3	—
9.5–16.0	—	—	3
12.5–19.0	3	3	—
16.0–25	—	—	3
25.0–31.5	—	—	To cover drains
19.0–37.5	4–6	—	—

^a Kawamura, S. 1991. *Integrated Design of Water Treatment Facilities*, John Wiley & Sons, Inc., New York.

^b Williams, R.B. and Culp, G.L., eds. 1986. *Handbook of Public Water Systems*, Van Nostrand Reinhold, New York.

where d_1, d_2 = the equivalent grain diameters of the two media (m or ft)

ρ_1, ρ_2 = the densities of the two media grains (kg/m³ or lb/ft³)

ρ_m = the density of a fluidized bed (kg/m³ or lbm/ft³)

The fluid density is that of the fluidized bed, which is a mixture of water and solids:

$$\rho_m = \epsilon\rho + \frac{1}{2}(\rho_1 + \rho_2)(1 - \epsilon) \quad (9.244)$$

Kawamura (1991) uses the density of water, ρ , instead of ρ_m and an exponent of 0.665 instead of 0.625.

The media are generally proportioned so that the ratio of the weight fractions is equal to the ratio of the grain sizes:

$$\frac{d_1}{d_2} = \frac{f_1}{f_2} \quad (9.245)$$

where f_1, f_2 = the weight fractions of the two media (dimensionless).

Some intermixing of the media at the interface is desirable. Cleasby and Sejkora (1975) recommend the following size distributions of coal and sand:

- Sand — an effective size 0.46 mm and a uniformity coefficient of 1.29
- Coal — an effective size of 0.92 mm and an uniformity coefficient of 1.60
- Ratio of the diameter larger than 90% of the coal to the diameter larger than 10% of the sand was 4.05

An interfacial size ratio of coal to sand of at least 3 is recommended (Joint Task Force, 1990).

The coal layer is usually about 18 in. deep, and the sand layer is about 8 in. deep. A typical specification for the media is given in [Table 9.8](#) (Culp and Culp, 1974).

Operating Modes

Several different filter operating modes are recognized (AWWA Filtration Committee, 1984):

- Variable-control, constant-rate — In this scheme, plant flow is divided equally among the filters in service, and each filter operates at the same filtration rate and at a constant water level in the filter box. Each filter has an effluent rate-of-flow controller that compensates for the changing headloss in the bed.

TABLE 9.8 Size Specifications for Dual Media Coal/Sand Filters

U.S. Sieve Size (mm)	Percentage by Weight Passing	
	Coal	Sand
4.75	99–100	—
3.35	95–100	—
1.40	60–100	—
1.18	30–100	—
1.0	0–50	—
0.850	0–5	96–100
0.60	—	70–90
0.425	—	0–10
0.297	—	0–5

Source: Culp, G.L. and Culp, R.L. 1974. *New Concepts in Water Purification*, Van Nostrand Reinhold Co., New York.

- This is a highly automated scheme that requires only minimal operator surveillance. It requires the most instrumentation and flow control equipment, because each filter must be individually monitored and controlled.
- Flow control from filter water level — In this scheme, the plant flow is divided equally among the filters in service by a flow-splitter. Each filter operates at a constant water level that is maintained by a butterfly valve on the filtered water line. The water levels differ among boxes in accordance with the differences in media headloss due to solids captured.
- This is an automated scheme that requires little operator attention. Individual filters do not require flow measurement devices, so less hardware is needed than in the variable-control, constant-rate scheme.
- Inlet flow splitting (constant rate, rising head) — In this scheme, the plant flow is divided equally among the filters in service by a flow-splitter that discharges above the highest water level in each filter. Each filter operates at a constant filtration rate, but the rates differ from one filter to the next. Instead of a rate-of-flow controller, the constant filtration rate is maintained by allowing the water level in each filter box to rise as solids accumulate in the media. When a filter reaches its predetermined maximum water level, it is removed from service and backwashed. Automatic overflows between boxes are needed to prevent spillage. The filter discharges at an elevation above the media level, so that negative pressures in the media are impossible.
- The monitoring instrumentation and flow control devices are minimal, but the operator must attend to filter cleanings.
- Variable declining rate — In these schemes, all filters operate at the same water level (maintained by a common inlet channel) and discharge at the same level (which is maintained above the media to avoid negative pressure). The available head is the same for each filter, and the filtration rate varies from one filter to the next in accordance with the relative headloss in the media. When the inlet water level reaches some predetermined elevation, the dirtiest filter is taken out of service and cleaned. The flow rate on each filter declines step-wise as clean filters are brought on line that take up a larger share of the flow.
- This scheme produces a better filtrate, because the filtration rate automatically falls as the bed becomes clogged, which reduces shearing stresses on the deposit. It also makes better use of available head, because most of the water is always going through relatively clean sand. The control system is simplified and consists mainly of a flow rate limiter on each filter to prevent excessive filtration rates in the clean beds. The operator must monitor the water level in the filters and plant flow rate.

- Direct filtration — Direct filtration eliminates flocculation and settling but not chemical addition and rapid mixing. The preferred raw water for direct filtration has the following composition (Direct Filtration Subcommittee, 1980; Cleasby, 1990):
 - Color less than 40 Hazen (platinum-cobalt) units
 - Turbidity less than 5 formazin turbidity units (FTU)
 - Algae (diatoms) less than 2000 asu/mL (1 asu = 400 μm^2 projected cell area)
 - Iron less than 0.3 mg/L
 - Manganese less than 0.05 mg/L
- The coagulant dosage should be adjusted to form small, barely visible, pinpoint flocs, because large flocs shorten filter runs by increasing headlosses and promoting early breakthrough (Cleasby, 1990). The optimum dosage is determined by filter behavior and is the smallest that achieves the required effluent turbidity.
- Dual media filters are required to provide adequate solids storage capacity.
- Design filtration rates range from 4 to 5 gpm/ft², but provision for operation at 1 to 8 gpm/ft² should be made (Joint Task Force, 1990).

Wastewater Treatment

Granular media filters are used in wastewater treatment plants as tertiary processes following secondary clarification of biological treatment effluents. A wide variety of designs are available, many of them proprietary. The major problems in wastewater filters are the relatively high solids concentrations in the influent flow and the so-called “stickiness” of the suspended solids. These problems require that special consideration be given to designs that produce long filter runs and to effective filter cleaning systems.

Wastewater filters are almost always operated with the addition of coagulants. Provision should be made to add coagulants to the secondary clarifier influent, the filter influent, or both. Rapid mixing is required; it may be achieved via tanks and turbines or static inline mixers.

Filters may be classified as follows (Metcalf & Eddy, Inc., 1991):

- Stratified or unstratified media — Backwashing alone tends to stratify monomedia bed with the fines on top. Simultaneous air scour and backwash produces a mixed, unstratified bed. Deep bed filters almost always require air scour and are usually unstratified.
- Mono, dual or multimedia — Filter media may be a single layer of one material like sand or crushed anthracite, two separate layers of different materials like sand and coal, or multilayer filters (usually five) of sand, coal, and garnet or ilmenite.
- Continuous or discontinuous operation — Several proprietary cleaning systems are available that permit continuous operation of the filter: downflow moving bed, upflow moving bed, traveling bridge, and pulsed bed.
 - In downflow moving beds, the water and the filter media move downward. The sand is removed below the discharge point of the water, subjected to air scouring, and returned to the top of the filter.
 - In upflow beds, the water flows upward through the media, and the media moves downward. The media is withdrawn continuously from the bottom of the filter, washed, and returned to the top of the bed.
 - In traveling bridge filters, the media is placed in separate cells in a tank, and the backwashing system is mounted on a bridge that moves from one cell to the next for cleaning. At any moment, only one of the cells is being cleaned, and the others are in service.
 - Pulsed bed filters are really semicontinuous filters. Air is diffused just above the media surface to keep solids in suspension, and periodically, air is pulsed through the bed that resuspends the surface layer of the media, releasing collected solids. Solids migrate into the bed, and eventually, the filtering process must be shut down for backwashing.
- Conventional filters, which are taken out of service for periodic cleaning, are classified as discontinuous.

TABLE 9.9 Media for Wastewater Effluent Filtration (Uniformity Coefficient: 1.5 for Sand and 1.6 for Other Materials)

Filter Type and Typical Filtration Rate	Media	Effective Size (mm)	Media Depth (in.)
Monomedia, shallow bed, 3 gpm/ft ²	Sand	0.35–0.60	10–12
Monomedia, shallow bed, 3 gpm/ft ²	Anthracite	0.8–1.5	12–20
Monomedia, conventional, 3 gpm/ft ²	Sand	0.4–0.8	20–30
Monomedia, conventional, 4 gpm/ft ²	Anthracite	0.8–2.0	24–36
Monomedia, deep bed, 5 gpm/ft ²	Sand	2.0–3.0	36–72
Monomedia, deep bed, 5 gpm/ft ²	Anthracite	2.0–4.0	36–84
Dual media, 5 gpm/ft ²	Sand	0.4–0.8	6–12
	Anthracite	0.8–2.0	12–30
Trimedia, trilayer 5 gpm/ft ²	Anthracite (top)	1.0–2.0	8–20
	Sand (middle)	0.4–0.8	8–16
	Garnet/ilmenite (bottom)	0.2–0.6	2–6

Sources: Joint Task Force of the Water Environment Federation and the American Society of Civil Engineers. 1991. *Design of Municipal Wastewater Treatment Plants: Volume II — Chapters 13–20*, WEF Manual of Practice No. 8, ASCE Manual and Report on Engineering Practice No. 76, Water Environment Federation, Alexandria, VA; American Society of Civil Engineers, New York.

Metcalf & Eddy, Inc. 1991. *Waste Engineering: Treatment, Disposal, and Reuse*, 3rd ed., rev. by G. Tchobanoglous and F.L. Burton, McGraw-Hill, Inc., New York.

The most common designs for new facilities specify discontinuous service, dual media filters with coagulation, and flow equalization to smooth the hydraulic and solids loading. Older plants with space restrictions are often retrofitted with continuous service filters that can operate under heavy and variable loads.

Performance and Media

The liquid applied to the filter should contain less than 10 mg/L TSS (Metcalf & Eddy, 1991; Joint Task Force, 1991). Under this condition, dual media filters with chemical coagulation can produce effluents containing turbidities of 0.1 to 0.4 JTU. If the coagulant is aluminum or ferric iron salts, orthophosphate will also be removed, and effluent orthophosphate concentrations of about 0.1 mg/L as PO₄ can be expected. As the influent suspended solids concentration increases, filter efficiency falls. At an influent load of 50 mg/L TSS, filtration with coagulation can be expected to produce effluents of about 5 mg/L TSS.

Commonly used media are described in [Table 9.9](#).

Backwashing

The general recommendation is that the backwashing rate expand the bed by 10% so that the media grains have ample opportunity to rub against one another (Joint Task Force, 1991). Preliminary or concurrent air scour should be provided. The usual air scour rate is 3 to 5 scfm/ft². If two or more media are employed, a Baylis-type rotary water wash should be installed at the expected media interface heights of the expanded bed. The rotary water washes are operated at pressures of 40 to 50 psig and water rates of 0.5 to 1.0 gpm/ft² for single-arm distributors and 1.5 to 2.0 gpm/ft² for double-arm distributors. Distributor nozzles should be equipped with strainers to prevent clogging.

References

- Amirtharajah, A. 1984. "Fundamentals and Theory of Air Scour," *Journal of the Environmental Engineering Division, Proceedings of the American Society of Civil Engineers*, 110(3): 573.
- Anderson, E. 1941. "Separation of Dusts and Mists," p. 1850 in *Chemical Engineers Handbook*, 2nd ed., 9th imp., J.H. Perry, ed., McGraw-Hill Book Co., Inc., New York.
- AWWA Filtration Committee. 1984. "Committee Report: Comparison of Alternative Systems for Controlling Flow Through Filters," *Journal of the American Water Works Association*, 76(1): 91.

- Babbitt, H.E., Doland, J.J., and Cleasby, J.L. 1967. *Water Supply Engineering*, 6th ed., McGraw-Hill Book Co., Inc., New York.
- Cleasby, J.L. 1990. "Chapter 8 — Filtration," p. 455 in *Water Quality and Treatment: A Handbook of Community Water Supplies*, 4th ed., F.W. Pontius, tech. ed., McGraw-Hill, Inc., New York.
- Cleasby, J.L., Amirtharajah, A., and Baumann, E.R. 1975. "Backwash of Granular Filters," p. 255 in *The Scientific Basis of Filtration*, K.J. Ives, ed., Noordhoff, Leyden.
- Cleasby, J.L. and Baumann, E.R. 1962. "Selection of Sand Filtration Rates," *Journal of the American Water Works Association*, 54(5): 579.
- Cleasby, J. L. and Fan, K.S. 1981. "Predicting Fluidization and Expansion of Filter Media," *Journal of the Environmental Engineering Division, Proceedings of the American Society of Civil Engineers*, 107(3): 455.
- Cleasby, J.L. and Sejkora, G.D. 1975. "Effect of Media Intermixing on Dual Media Filtration," *Journal of the Environmental Engineering Division, Proceedings of the American Society of Civil Engineers*, 101(EE4): 503.
- Committee of the Sanitary Engineering Division on Filtering Materials for Water and Sewage Works. 1936. "Filter Sand for Water Purification Plants," *Proceedings of the American Society of Civil Engineers*, 62(10): 1543.
- Conley, W.R. and Hsiung, K.-Y. 1969. "Design and Application of Multimedia Filters," *Journal of the American Water Works Association*, 61(2): 97.
- Culp, G.L. and Culp, R.L. 1974. *New Concepts in Water Purification*, Van Nostrand Reinhold Co., New York.
- Culp/Wesner/Culp, Inc. 1986. *Handbook of Public Water Supplies*, R.B. Williams and G.L. Culp, eds., Van Nostrand Reinhold Co., Inc., New York.
- Degrémont, S.A. 1965. *Water Treatment Handbook*, 3rd English ed., trans. D.F. Long, Stephen Austin & Sons, Ltd., Hertford, UK.
- Direct Filtration Subcommittee of the AWWA Filtration Committee. 1980. "The Status of Direct Filtration," *Journal of the American Water Works Association*, 72(7): 405.
- Ergun, S. 1952. "Fluid Flow Through Packed Columns," *Chemical Engineering Progress*, 48(2): 89.
- Fair, G.M. and Geyer, J.C., 1954. *Water Supply and Waste-Water Disposal*, John Wiley & Sons, Inc., New York.
- Fuller, G.W. 1898. *The Purification of the Ohio River Water at Louisville, Kentucky*, D. Van Nostrand Co., New York.
- Gregory, J. 1975. "Interfacial Phenomena," p. 53 in *The Scientific Basis of Filtration*, K.J. Ives, ed., Noordhoff International Publishing, Leyden.
- Hazen, A. 1896. *The Filtration of Public Water-Supplies*, John Wiley & Sons, New York.
- Hazen, A., 1904. "On Sedimentation," *Transactions of the American Society of Civil Engineers*, 53: 63 (1904).
- Herzig, J.R., Leclerc, D.M., and Le Goff, P. 1970. "Flow of Suspension Through Porous Media, Application to Deep Bed Filtration," *Industrial and Engineering Chemistry*, 62(5): 8.
- Ives, K.J. 1975. "Capture Mechanisms in Filtration," p. 183 in *The Scientific Basis of Filtration*, K.J. Ives, ed., Noordhoff International Publishing, Leyden.
- Ives, K.J. and Sholji, I. 1965. "Research on Variables Affecting Filtration," *Journal of the Sanitary Engineering Division, Proceedings of the American Society of Civil Engineers*, 91(SA4): 1.
- Iwasaki, T. 1937. "Some Notes on Filtration," *Journal of the American Water Works Association*, 29(10): 1591.
- James M. Montgomery, Consulting Engineers, Inc. 1985. *Water Treatment Principles and Design*, John Wiley & Sons, New York.
- Joint Task Force of the American Society of Civil Engineers and the American Water Works Association. 1990. *Water Treatment Plant Design*, 2nd ed., McGraw-Hill Publishing Co., Inc., New York.
- Joint Task Force of the Water Environment Federation and the American Society of Civil Engineers. 1991. *Design of Municipal Wastewater Treatment Plants: Volume II — Chapters 13–20*, WEF Manual of Practice No. 8, ASCE Manual and Report on Engineering Practice No. 76, Water Environment Federation, Alexandria, VA; American Society of Civil Engineers, New York.
- Kawamura, S. 1991. *Integrated Design of Water Treatment Facilities*, John Wiley & Sons, Inc., New York.

- MacDonald, I.F., El-Sayed, M.S., Mow, K., and Dullien, F.A.L. 1979. "Flow Through Porous Media — The Ergun Equation Revisited," *Industrial & Engineering Chemistry Fundamentals*, 18(3): 199.
- Malcolm Pirnie, Inc. and HDR Engineering, Inc. 1990. *Guidance Manual for Compliance with the Surface Water Treatment Requirements for Public Water Systems*. American Water Works Association, Denver, CO.
- Metcalf & Eddy, Inc. 1991. *Waste Engineering: Treatment, Disposal, and Reuse*, 3rd ed., rev. by G. Tchobanoglous and F.L. Burton, McGraw-Hill, Inc., New York.
- Morrill, A.B. and Wallace, W.M. 1934. "The Design and Care of Rapid Sand Filters," *Journal of the American Water Works Association*, 26(4): 446.
- Pontius, F.W. 1990. "Complying with the New Drinking Water Quality Regulations," *Journal of the American Water Works Association*, 82(2): 32.
- Richardson, J. F. and Zaki, W.N. 1954. "Sedimentation and Fluidization," *Transactions of the Institute of Chemical Engineers: Part I*, 32: 35.
- Standards Committee on Filtering Material. 1989. *AWWA Standard for Filtering Material*, AWWA B100–89, American Water Works Association, Denver, CO.
- Stokes, G.G. 1856. "On the Effect of the Internal Friction of Fluids on the Motion of Pendulums," *Transactions of the Cambridge Philosophical Society*, 9(II): 8.
- Tien, C. 1989. *Granular Filtration of Aerosols and Hydrosols*, Butterworth Publishers, Boston.
- U.S. EPA. 1989. "Filtration and Disinfection: Turbidity, *Giardia lamblia*, viruses Legionella and Heterotrophic Bacteria: Final Rule," *Federal Register*, 54(124): 27486.
- U.S. EPA. 1998. "Interim Enhanced Surface Water Treatment Rule," *Federal Register*, 63(241): 69478.
- Water Supply Committee of the Great Lakes-Upper Mississippi River Board of State Public Health and Environmental Managers. 1987. *Recommended Standards for Water Works, 1987 Edition*, Health Research, Inc., Albany, NY.
- Wen, C.Y. and Yu, Y.H. 1966. "Mechanics of Fluidization," *Chemical Engineering Progress*, Symposium Series 62, American Institute of Chemical Engineers, New York.

9.7 Activated Carbon

Preparation and Regeneration

Pure carbon occurs as crystals of diamond or graphite or as fullerene spheres. The atoms in diamond are arranged as tetrahedra, and the atoms in graphite are arranged as sheets of hexagons. Activated carbon grains consist of random arrays of microcrystalline graphite. Such grains can be made from many different organic substances, but various grades of coal are most commonly used, because the product is hard, dense, and easy to handle.

The raw material is first carbonized at about 500°C in a nonoxidizing atmosphere. This produces a char that contains some residual organic matter and many small graphite crystals. The char is then subjected to a slow oxidation in air at about 500°C or steam or carbon dioxide at 800 to 950°C. The preferred activation atmospheres are steam and carbon dioxide, because the oxidation reactions are endothermic and more easily controlled. The slow oxidation removes residual organic matter and small graphite crystals and produces a network of microscopic pores. The higher temperature promotes the formation of larger graphite crystals, which reduces the randomness of their arrangement.

It is almost always economical to recover and regenerate spent carbon, unless the quantities are very small. This is true even of powdered carbon, if it can be easily separated from the process stream. The economic break point for on-site regeneration depends on carbon usage and varies somewhere between 500 and 2000 lb/day (Snoeyink, 1990). Larger amounts should be shipped to commercial regeneration plants.

Spent carbon can be regenerated as it was made by heating in rotary kiln, fluidized bed, multiple hearth, or infrared furnaces (von Dreusche, 1981; McGinnis, 1981). In multiple hearth furnaces, the required heat is supplied by the hot combustion gases of a fuel. The fuel is oxidized at only small excess

air to minimize the amount of oxygen fed to the furnace. In infrared furnaces, heating is supplied by electrical heating elements. This method of heating provides somewhat better control of oxygen concentration in the furnace, but some oxygen enters with the carbon through the feedlock.

The usual regeneration stages in any furnace are as follows (McGinnis, 1981; Snoeyink, 1990):

- Drying stage — usually operated at about 200 to 700°C, depending on furnace type
- Pyrolysis stage — usually operated at about 500 to 800°C
- Coke oxidation stage — usually operated at about 700°C for water treatment carbon and at about 900°C for wastewater treatment carbons (Culp and Clark, 1983)

The pyrolysis stage vaporizes and cokes the adsorbed organics. The vaporized material diffuses into the hot gases in the furnace and either reacts with them or is discharged as part of the furnace stack gas. The coked material is oxidized by water vapor or by carbon dioxide, and the oxidation products exit in the furnace stack gases:



For water treatment carbons, the pyrolysis and activation stages are operated at temperatures below those required to graphitize the adsorbate char. Consequently, the newly formed char is more reactive than the original, largely graphitized activated carbon, and it is selectively removed by the oxidation process. Wastewater treatment carbons are oxidized at temperatures that graphitize as well as oxidize the adsorbate char. Significant amounts of the original carbon are also oxidized at this temperature.

Regeneration losses are generally on the order of 5 to 10% by weight. This is due mostly to spillage and other handling and transport losses, not to furnace oxidation. There is usually a reduction in grain size, which affects the hydraulics of fixed bed adsorbers and the adsorption rates. However, the adsorptive capacity of the original carbon is little changed (McGinnis, 1981).

Characteristics

The properties of commercially available activated carbons are given in [Table 9.10](#). For water treatment, the American Water Works Association requires that (AWWA Standards Committee on Activated Carbon, 1990a, 1990b):

- “No soluble organic or inorganic substances in quantities capable of producing deleterious or injurious effects upon the health of those consuming the water of that would otherwise render the water ... unfit for public use.”
- “The carbon shall not impart to the water any contaminant that exceeds the limits as defined by the U.S. Environmental Protection Agency.”
- The moisture content shall not exceed 8% by weight when packed or shipped.
- The apparent density shall not be less than 0.36 g/cm³.
- The average particle size shall be at least 70% of its original size after subjection to either the stirred abrasion test or the Ro-Tap abrasion test. (These are described in the standard.)
- The adsorptive capacity as determined by the iodine number shall not be less than 500.

Uses

Taste and Odor

The traditional use of activated carbon is for taste and odor control. The usage is generally seasonal, and PAC slurry reactors (actually flocculation tanks) have often been the preferred mode of application.

TABLE 9.10 Properties of Commercially Available Activated Carbons

Property	Granular Activated Carbon	Powdered Activated Carbon
Effective size (mm)	0.6–0.9	<0.01 (65–90% < 0.044)
Uniformity coefficient (dimensionless)	<1.9	Not applicable
Real density of carbon excluding pores (g/cm ³)	2.0–2.1	Same
Dry density of grains (g/cm ³)	0.9–1.4	Same
Wet density of grains (g/cm ³)	1.5–1.6	Same
Dry, bulk density of packed bed (g/cm ³) (apparent density)	0.4–0.5	Same
Pore volume of grains (cm ³ /g)	0.6–0.95	Same
Specific surface area of grains (m ² /g)	600–1100	Same
Iodine number (mg I ₂ /g °C at 0.02 N I ₂ at 20–25°C)	600–1100	Same

Sources: Culp/Wesner/Culp, Inc. 1986. *Handbook of Public Water Supply Systems*, R.B. Williams and G.L. Culp, eds., Van Nostrand Reinhold Co., Inc., New York.

Joint Task Force. 1990. *Water Treatment Plant Design*, 2nd ed., McGraw-Hill, Inc., New York.

Joint Task Force of the Water Environment Federation and the American Society of Civil Engineers. 1991. *Design of Municipal Wastewater Treatment Plants: Volume II — Chapters 13–20*, WEF Manual of Practice No. 8, ASCE Manual and Report on Engineering Practice No. 76, Water Environment Federation, Alexandria, VA; American Society of Civil Engineers, New York.

Snoeyink, V.L. 1990. "Adsorption of Organic Compounds," p. 781 in *Water Quality and Treatment: A Handbook of Community Water Supplies*, 4th ed., American Water Works Association, F.W. Pontius, ed., McGraw-Hill, Inc., New York.

The principal sources of tastes and odors are (Thimann, 1963):

- Manufacturing — generally due to oils, phenols and cresols, ammonia and amines (especially diamines), sulfides and mercaptans, and volatile fatty acids (especially propionic, butyric and isobutyric, valeric and isovaleric, and caproic acids);
- Putrefaction of proteinaceous and fatty material — generally diamines (skatol, indole, γ -amino butyric acid, cadaverine, putrescine, tryptamine, and tyramine), sulfides and mercaptans, and volatile fatty acids
- Microbial and metazoan blooms — especially cyanobacterial blooms

The odors associated with algal and other blooms have been classified as shown in [Table 9.11](#).

Odors are normally measured by the threshold odor number (TON). This is defined as the sample with the smallest diluted volume that retains an odor. The samples are diluted with distilled water, and the TON is calculated as follows (Joint Editorial Board, 1992),

$$\text{TON} = \frac{V_{of} + V_s}{V_s} \quad (9.248)$$

where TON = the threshold odor number (dimensionless)

V_{of} = the volume of odor-free water used in the threshold odor test (mL)

V_s = the volume of original sample used in the threshold odor test (mL)

Conventional water treatment processes such as coagulation and settling do not substantially reduce the TON. In fact, coagulation with lime or soda ash frequently increases it (Anonymous, 1942). Coagulant chemicals sometimes change the character of the odor. Rapid sand filtration partially reduces the TON in some cases.

Disinfection By-Product (DBP) Precursors

The naturally occurring humic substances in surface and groundwaters react with chlorine to form chloroform (CHCl₃), which is a known carcinogen (Joint Task Force, 1990), and other disinfection

TABLE 9.11 Taste- and Odor-Producing Organisms

Organism	Odor when Numbers are Moderate	Odor when Numbers are Abundant
Cyanobacteria		
<i>Anabaena circinalis</i>	Grassy	Pigpen
<i>Anabaena flos-aquae</i>	Moldy, grassy, nasturtium	Pigpen
<i>Anabaenopsis</i>	—	Grassy
<i>Anacystis</i>	Grassy	Septic
<i>Aphanizomenon</i>	Moldy, grassy	Septic
<i>Clathrocystis</i>	Sweet, grassy	—
<i>Cylindrospermum</i>	Grassy	Septic
<i>Coelosphaerium</i>	Sweet, grassy	—
<i>Cylindrospermum</i>	Grassy	—
<i>Gloeotrichia</i>	—	Grassy
<i>Gomphosphaeria</i>	Grassy	Grassy
<i>Nostoc</i>	Musty	Septic
<i>Oscillatoria</i>	Grassy	Musty, spicy
<i>Rivularia</i>	Grassy	Musty
Green algae		
<i>Actinastrum</i>	—	Grassy, musty
<i>Chara</i>	Skunk, garlic	Garlic, spoiled
<i>Chlorella</i>	—	Musty
<i>Cladophora</i>	—	Septic
<i>Closterium</i>	—	Grassy
<i>Cosmarium</i>	—	Grassy
<i>Dictyosphaerium</i>	Grassy, nasturtium	Fishy
<i>Gleocystis</i>	—	Septic
<i>Hydrodictyon</i>	—	Septic
<i>Nitella</i>	Grassy	Grassy, septic
<i>Pandorina</i>	—	Fishy
<i>Pediastrum</i>	—	Grassy
<i>Scenedesmus</i>	—	Grassy
<i>Spirogyra</i>	—	Grassy, vegetable
<i>Staurastrum</i>	—	Grassy
Diatoms		
<i>Asterionella</i>	Geranium, spicy	Fishy
<i>Cyclotella</i>	Geranium	Fishy
<i>Diatoma</i>	—	Aromatic
<i>Fragilaria</i>	Geranium, aromatic	Musty
<i>Melosira</i>	Geranium	Musty
<i>Meridion</i>	—	Spicy
<i>Pleurosigma</i>	—	Fishy
<i>Synedra</i>	Earthy, grassy	Musty
<i>Stephanodiscus</i>	Aromatic geranium	Fishy
<i>Tabellaria</i>	Aromatic geranium	Fishy
Flagellated algae and protozoa		
<i>Bursaria</i>	Irish moss, salt marsh	Fishy
<i>Ceratium</i>	Fishy	Septic, vile stench
<i>Chlamydomonas</i>	Musty, grassy	Fishy, septic
<i>Chryso-sphaerella</i>	—	Fishy
<i>Cryptomonas</i>	Violet	Violet
<i>Codonella</i>	Fishy	—
<i>Dinobryon</i>	Violet	Fishy
<i>Eudorina</i>	—	Fishy
<i>Euglena</i>	—	Fishy

TABLE 9.11 (continued) Taste- and Odor-Producing Organisms

Organism	Odor when Numbers are Moderate	Odor when Numbers are Abundant
<i>Glenodinium</i>	—	Fishy
<i>Gonium</i>	—	Fishy
<i>Mallomonas</i>	Violet	Fishy
<i>Pandorina</i>	—	Fishy
<i>Peridinium</i>	Cucumber	Fishy
<i>Synura</i>	Cucumber, muskmelon	Fishy
<i>Uroglenopsis</i>	—	Fishy, cod liver oil, oily
Rotifera		
<i>Anuraea</i>	Fishy	—
Crustacea		
<i>Cyclops</i>	Fishy	—
<i>Daphnia</i>	Fishy	—

Sources: Palmer, C.M. 1967. *Algae in Water Supplies: An Illustrated Manual on the Identification, Significance, and Control of Algae in Water Supplies*, Public Health Service Publication No. 657 (reprint, 1967). U.S. Department of Health, Education, and Welfare, Public Health Service, Division of Water Supply and Pollution Control, Washington, DC.

Rohlich, G.A. and Sarles, W.B. 1949. "Chemical Composition of Algae and Its Relationship to Taste and Odor," *Taste and Odor Journal*, 18(10): 1.

Turre, G.J. 1942. "Pollution from Natural Sources, Particularly Algae," p. 17 in *Taste and Odor Control in Water Purification*, West Virginia Pulp and Paper Company, Industrial Chemical Sales Division, New York.

by-products. This problem presents itself continuously, so GAC-packed columns are the preferred mode of application. GAC will remove trihalomethanes (THMs), haloacetic acids (HAAs), and their precursor humic substances. The removal efficiency of the precursors is somewhat greater than that of the THMs. THM removal is best on fresh carbon, and removals are impaired by competitive adsorption on older carbons. The useful life of GAC replacement media in rapid sand filter boxes is about 2 months (Ohio River Valley Sanitation Commission, 1980).

Organic Poisons and Priority Pollutants

Water supply intakes on large rivers are subject to transport and processing spills of most industrial organic chemicals. Large spills are often detected early and tracked, so that utilities can shut down operations while they pass. However, many smaller spills go undetected, and medically significant concentrations of organic poisons can enter public water supplies. This problem is similar to the THM problem, and it requires continuous water treatment by GAC in packed columns. GAC filter adsorbers do not remove priority pollutants reliably, and desorption of small chlorinated organic molecules sometimes occurs (Ohio River Valley Water Sanitation Commission, 1980; Graese, Snoeyink, and Lee, 1987). GAC filter adsorbers also exhibit lower carbon capacities and earlier breakthrough due to pore clogging by water treatment chemicals and flocs.

Wastewater SOC

Stringent NPDES effluent permits may require GAC-packed columns to remove soluble organic carbon (SOC), like residual soluble BOD₅, priority pollutants, or THM precursors (Joint Task Force, 1991). The suspended solids content of biologically treated effluents usually must be removed by chemical coagulation, sedimentation, and filtration prior to carbon treatment. The Lake Tahoe results indicate that empty bed contacting times of 15 to 30 min can produce an effluent BOD₅, COD, and TOC of less than 1, 12, and 3 mg/L, respectively, if clear, biologically treated water is fed to the columns (Culp and Culp, 1971).

Equilibria

A nonpolar adsorbent like activated carbon will adsorb nonpolar solutes from polar solvents like water (Adamson, 1982). Furthermore, Traube's rule (Freundlich, 1922) is: The adsorption of a homologous series of organic substances from aqueous solution increases as the chain length increases.

Adsorption is an equilibrium process in which organic molecules dissolved in water displace water molecules from the surface of the activated carbon. The equilibrium depends on the water-phase activities of the organic molecules (a_o), the water-phase activity of the water (a_w), the mole fraction of the organic molecule in the adsorbed layer (x_o), and the mole fraction of water in the adsorbed layer (x_w), and it is characterized by a free energy of adsorption (Adamson, 1982):

$$K = \frac{a_w x_o}{a_o x_w} = e^{-\Delta G^\circ/RT} \quad (9.249)$$

where a_o = water-phase activity of organic molecules (mol/L)
 a_w = water-phase activity of water (mol/L)
 ΔG° = the standard free energy of a reaction (J/mol or ft-lbf/lb mol)
 K = the equilibrium constant (units vary)
 R = the gas constant (8.314 510 J/K·mol or 1,545 ft·lbf/°R·lb mol)
 T = the absolute temperature (K or °R)
 x_o = the mole fraction of organic matter in the adsorbed layer (dimensionless)
 x_w = the mole fraction of water in the adsorbed layer (dimensionless)

Langmuir

The Langmuir isotherm follows directly from the equilibrium constant if the following conditions are met:

- All adsorption sites on the carbon have equal free energies of adsorption.
- The solution is dilute so that concentrations are nearly equal to activities.
- The mole fraction of water is eliminated using the fact that the sum of the mole fractions ($x_o + x_w$) must be unity.
- The number of adsorption sites per unit mass of carbon can be estimated so that the mole fraction of adsorbed organic matter can be expressed as mass of organic matter per unit mass of carbon.

$$q_e = \frac{q_{\max} C_e}{K_C + C_e} \quad (9.250)$$

where C_e = the equilibrium concentration of organic matter in water (kg/m³ or lb/ft³)
 K_C = the affinity constant for the Langmuir isotherm (kg/m³ or lb/ft³)
 q_e = the mass of adsorbed organic matter per unit mass of activated carbon at equilibrium (kg/kg or lbm/lbm)
 q_{\max} = the maximum capacity of activated carbon to adsorb organic matter (kg/kg or lbm/lbm)

Freundlich

It is generally not true that the free energy of adsorption is equal for all sites, so the Langmuir isotherm fails to fit many data sets. However, good fits are usually obtained with the Freundlich isotherm. This can be derived from the Langmuir isotherm if it is assumed that the distribution of adsorption energies is a decaying exponential (Halsey and Taylor, 1947):

$$q_e = kC_e^{1/n} \quad (9.251)$$

where k = a positive empirical coefficient (units vary)
 n = a positive empirical exponent (dimensionless).

The representation of the exponent on the concentration as a fraction is traditional and has no special meaning.

Three-Parameter Isotherm

Occasionally, it is convenient to use a purely empirical three-parameter adsorption isotherm formula (Crittenden and Weber, 1978):

$$q_e = \frac{q_{\max} C_e}{K_C + C_e^\beta} \quad (9.252)$$

where β = an empirical exponent (dimensionless).

Freundlich Parameter Values

Freundlich parameter values for a number of important organic contaminants are given in [Table 9.12](#).

Kinetics

During operation, a packed column first becomes saturated at its inlet end, and the carbon grains are in equilibrium with the influent solute concentration, C_o . Downstream of the saturated zone is the mass transfer zone, in which the carbon is adsorbing solute from the pore water. In this zone, the pore water solute concentration varies from its influent value to some low nonzero value. The mass transfer zone moves through the bed at a constant velocity toward the outlet end, and as it does, the effluent concentration begins to rise. The so-called “breakthrough” curve is a plot of the effluent concentration vs. service time, and it is a mirror image of the concentration profile in the mass transfer zone. The breakthrough concentration, C_b , is set by the required product water quality, and when it is reached, the carbon must be taken out of service and replaced or regenerated.

Empirical Column Tests

In pilot studies, several small columns are connected in series, and sampling taps are installed in each column’s outlet line (Wagner and Julia, 1981; Hutchins, 1981). The test solution is pumped through the columns at some controlled rate, and a plot of effluent concentration vs. service time is prepared for each column. The columns will become saturated in sequence from first to last. The sampling taps represent distances along the intended field column’s depth, and the use of several columns in series permits determination of the rate at which the mass transfer zone moves through the bed. The service time, t_b , required to reach the specified breakthrough concentration, C_b , is determined for each column, and it is plotted against the cumulative hydraulic retention time (Hutchins, 1981):

$$t_b = a_1 \tau_h + a_o \quad (9.253)$$

where a_o = an empirical constant (sec)
 a_1 = an empirical coefficient (dimensionless)
 C_b = the specified breakthrough concentration (kg/m³ or lb/ft³)
 t_b = the service time to breakthrough (sec)
 τ_h = the hydraulic retention of the carbon columns (sec)

Column hydraulic retention times are usually reported as Empty Bed Contacting Times (EBCT), which is simply the hydraulic retention time calculated, assuming the bed is empty. The ratio of the true HRT to the EBCT is equal to the bed porosity:

$$\epsilon = \frac{\text{HRT}}{\text{EBCT}} = \frac{\epsilon V/Q}{V/Q} \quad (9.254)$$

TABLE 9.12 Approximate Values of Freundlich Adsorption Isotherm Parameters for Various Organic Substances Sorbed onto Filtrasorb 300™ Activated Carbon from Distilled Water at 22°C

Contaminant	k (mg/g)(L/mg) ^{1/n}	1/n
Acenaphthene, pH 5.3	190	0.36
Acenaphthylene, pH 5.3	115	0.37
Acetophenone, pH 3.0 to 9.0	74	0.44
2-Acetylaminofluorene, pH 7.1	318	0.12
Acridine orange, pH 3.0 to 7.0	180	0.29
Acridine orange, pH 9.0	210	0.38
Acridine yellow, pH 3.0	210	0.14
Acridine yellow, pH 7 to 9	230	0.12
Acrolein, pH 5.2	1.2	0.65
Acrylonitrile, pH 5.8	1.4	0.51
Adenine, pH 3.0	38	0.38
Adenine, pH 7 to 9	71	0.38
Adipic acid, pH 3.0	20	0.47
Aldrin, pH 5.3	651	0.92
4-Aminobiphenyl, pH 7.2	200	0.26
Anethole, pH 3 to 9	300	0.42
<i>o</i> -Anisidine, pH 3.0	20	0.41
<i>o</i> -Anisidine, pH 7 to 9	50	0.34
Anthracene, pH 5.3	376	0.70
Benzene, pH 5.3	1	1.6
Benzidine dihydrochloride, pH 3.0	110	0.35
Benzidine dihydrochloride, pH 7 to 9	220	0.37
Benzoic acid, pH 3.0	51	0.42
Benzoic acid, pH 7.0	0.76	1.8
Benzoic acid, pH 9.0	0.000 8	4.3
3,4-Benzofluoranthene [benzo(b)fluoranthene], pH 7.0	57	0.37
Benzo(k)fluoranthene, pH 7.1	181	0.57
Benzo(ghi)perylene, pH 7.0	10.7	0.37
Benzo(a)pyrene, pH 7.1	33.6	0.44
Benzothiazole, pH 3 to 9	120	0.27
α -BHC [hexachloro-cyclohexane], pH 5.4	303	0.43
β -BHC [hexachloro-cyclohexane], pH 5.4	220	0.49
γ -BHC [hexachloro-cyclohexane, Lindane], pH 5.3	256	0.49
Bromoform, pH 5.3	19.6	0.98
4-Bromophenyl phenyl ether, pH 5.3	144	0.68
5-Bromouracil, pH 3 to 7	44	0.47
5-Bromouracil, pH 9.0	21	0.56
Butylbenzyl phthalate, pH 5.3	1520	1.26
<i>n</i> -Butyl phthalate, pH 3.0	220	0.45
Carbon tetrachloride, pH 5.3	11.1	0.83
Chlorobenzene, pH 7.4	91	0.99
Chlordane, pH 5.3	245	0.38
Chloroethane, pH 5.3	0.59	0.95
<i>bis</i> (2-Chloroethoxy)methane, pH 5.8	11	0.65
<i>bis</i> (2-Chloroethyl)ether, pH 5.3	0.086	1.84
2-Chloroethyl vinyl ether, pH 5.4	3.9	0.80
Chloroform, pH 5.3	2.6	0.73
<i>bis</i> (2-Chloroisopropyl)ether, pH 5.4	24	0.57
<i>p</i> -Chloro- <i>m</i> -cresol, pH 3	122	0.29
<i>p</i> -Chloro- <i>m</i> -cresol, pH 5.5	124	0.16
<i>p</i> -Chloro- <i>m</i> -cresol, pH 9	99	0.42
2-Chloronaphthalene, pH 5.5	280	0.46
1-Chloro-2-nitrobenzene, pH 3 to 9	130	0.46
2-Chlorophenol, pH 3 to 9	51	0.41

TABLE 9.12 (continued) Approximate Values of Freundlich Adsorption Isotherm Parameters for Various Organic Substances Sorbed onto Filtrasorb 300™ Activated Carbon from Distilled Water at 22°C

Contaminant	k (mg/g)(L/mg) ^{1/n}	1/n
4-Chlorophenyl phenyl ether, pH 5.3	111	0.26
5-Chlorouracil, pH 3 to 7	25	0.58
5-Chlorouracil, pH 9	7.3	0.90
Cyclohexanone, pH 7.3	6.2	0.75
Cytosine, pH 3	0.63×10^{-12}	13.67
Cytosine, pH 7 to 9	1.1	1.6
DDE, pH 5.3	232	0.37
DDT, pH 5.3	322	0.50
Dibenzo(a,h)anthracene, pH 7.1	69.3	0.75
Dibromochloromethane, pH 5.3	4.8	0.34
1,2-Dibromo-3-chloropropane, pH 5.3	53	0.47
1,2-Dichlorobenzene, pH 5.5	129	0.43
1,3-Dichlorobenzene, pH 5.1	118	0.45
1,4-Dichlorobenzene, pH 5.1	121	0.46
3,3-Dichlorobenzidine, pH 7.2 to 9.1	300	0.20
Dichlorobromomethane, pH 5.3	7.9	0.61
1,1-Dichloroethane, pH 5.3	1.79	0.53
1,2-Dichloroethane, pH 5.3	3.57	0.83
1,2- <i>trans</i> -Dichloroethene, pH 6.7	3.05	0.51
1,1-Dichloroethene, pH 5.3	4.91	0.54
2,4-Dichlorophenol, pH 3	147	0.35
2,4-Dichlorophenol, pH 5.3	157	0.15
2,4-Dichlorophenol, pH 9	141	0.29
1,2-Dichloropropane, pH 5.3	5.86	0.60
1,2-Dichloropropene, pH 5.3	8.21	0.46
Dieldrin, pH 5.3	606	0.51
Diethyl phthalate, pH 5.4	110	0.27
4-Dimethylaminobenzene, pH 7.0	249	0.24
<i>n</i> -Dimethylnitrosamine, pH 7.5	68×10^{-6}	6.6
2,4-Dimethylphenol, pH 3.0	78	0.44
2,4-Dimethylphenol, pH 5.8	70	0.44
2,4-Dimethylphenol, pH 9.0	108	0.33
Dimethylphenylcarbinol, pH 3.0	110	0.60
Dimethylphenylcarbinol, pH 7 to 9	210	0.34
Dimethyl phthalate, pH 3 to 9	97	0.41
4,6-Dinitro- <i>o</i> -cresol, pH 3.0	237	0.32
4,6-Dinitro- <i>o</i> -cresol, pH 5.2	169	0.35
4,6-Dinitro- <i>o</i> -cresol, pH 9.0	42.74	0.90
2,4-Dinitrophenol, pH 3.0	160	0.37
2,4-Dinitrophenol, pH 7.0	33	0.61
2,4-Dinitrophenol, pH 9.0	41	0.25
2,4-Dinitrotoluene, pH 5.4	146	0.31
2,6-Dinitrotoluene, pH 5.4	145	0.32
Diphenylamine, pH 3 to 9	120	0.31
1,1-Diphenylhydrazine, pH 7.5	135	0.16
1,2-Diphenylhydrazine, pH 5.3	16,000	2
α -Endosulfan, pH 5.3	194	0.50
β -Endosulfan, pH 5.3	615	0.83
Endosulfan sulfate, pH 5.3	686	0.81
Endrin, pH 5.3	666	0.80
Ethylbenzene, pH 7.4	53	0.79
EDTA [ethylenediaminetetraacetic acid], pH 3 to 9	0.86	1.5
<i>bis</i> (2-Ethylhexyl) phthalate, pH 5.3	11,300	1.5

TABLE 9.12 (continued) Approximate Values of Freundlich Adsorption Isotherm Parameters for Various Organic Substances Sorbed onto Filtrasorb 300™ Activated Carbon from Distilled Water at 22°C

Contaminant	k (mg/g)(L/mg) ^{1/n}	1/n
Fluoranthene, pH 5.3	664	0.61
Fluorene, pH 5.3	330	0.28
2,4-Dinitrophenol, pH 3 to 7	5.5	1
2,4-Dinitrophenol, pH 9.0	1.3	1.4
Guanine, pH 3.0	75	0.48
Guanine, pH 7 to 9	120	0.40
Heptachlor, pH 5.3	1220	0.95
Heptachlor epoxide, pH 5.3	1038	0.70
Hexachlorobenzene, pH 5.3	450	0.60
Hexachlorobutadiene, pH 5.3	258	0.45
Hexachlorocyclopentadiene, pH 5.3	370	0.17
Hexachloroethane, pH 5.3	96.5	0.38
Hydroquinone, pH 3.0	90	0.25
Isophorone, pH 5.5	32	0.39
Methylene chloride, pH 5.8	1.30	1.16
4,4'-Methylene-bis(2-chloroaniline), pH 7.5	190	0.64
Naphthalene, pH 5.6	132	0.42
α -Naphthol, pH 3 to 9	180	0.32
β -Naphthol, pH 3 to 9	200	0.26
α -Naphthylamine, pH 3.0	140	0.25
α -Naphthylamine, pH 7 to 9	160	0.34
β -Naphthylamine, pH 7.5	150	0.30
ρ -Nitroaniline, pH 3 to 9	140	0.27
Nitrobenzene, pH 7.5	68	0.43
4-Nitrobiphenyl, pH 7.0	370	0.27
2-Nitrophenol, pH 3.0	101	0.26
2-Nitrophenol, pH 5.5	99	0.34
2-Nitrophenol, pH 9.0	85	0.39
4-Nitrophenol, pH 3.0	80.2	0.17
4-Nitrophenol, pH 5.4	76.2	0.25
4-Nitrophenol, pH 9.0	71.2	0.28
<i>N</i> -Nitrosodiphenylamine, pH 3 to 9	220	0.37
<i>N</i> -Nitrosodi- <i>n</i> -propylamine, pH 3 to 9	24.4	0.26
<i>p</i> -Nonylphenol, pH 3.0	53	1.04
<i>p</i> -Nonylphenol, pH 7.0	250	0.37
<i>p</i> -Nonylphenol, pH 9.0	150	0.27
PCB 1221, pH 5.3	242	0.70
PCB 1232, pH 5.3	630	0.73
Pentachlorophenol, pH 3.0	260	0.39
Pentachlorophenol, pH 7.0	150	0.42
Pentachlorophenol, pH 9.0	100	0.41
Phenanthrene, pH 5.3	215	0.44
Phenol, pH 3 to 9	21	0.54
Phenylmercuric acetate, pH 3 to 7	270	0.44
Phenylmercuric acetate, pH 9.0	130	0.54
Styrene, pH 3 to 9	120	0.56
1,1,2,2-Tetrachloroethane, pH 5.3	10.6	0.37
Tetrachloroethene, pH 5.3	50.8	0.56
1,2,3,4-Tetrahydronaphthalene, pH 7.4	74	0.81
Thymine, pH 3 to 9	27	0.51
Toluene, pH 5.6	26.1	0.44
1,2,4-Trichlorobenzene, pH 5.3	157	0.31
1,1,1-Trichloroethane, pH 5.3	2.48	0.34

TABLE 9.12 (continued) Approximate Values of Freundlich Adsorption Isotherm Parameters for Various Organic Substances Sorbed onto Filtrasorb 300™ Activated Carbon from Distilled Water at 22°C

Contaminant	k (mg/g)(L/mg) ^{1/n}	1/n
1,1,2-Trichloroethane, pH 5.3	5.81	0.60
Trichloroethene, pH 5.3	28.0	0.62
Trichlorofluoromethane, pH 5.3	5.6	0.24
2,4,6-Trichlorophenol, pH 3.0	219.0	0.29
2,4,6-Trichlorophenol, pH 6.0	155.1	0.40
2,4,6-Trichlorophenol, pH 9.0	130.1	0.39
Uracil, pH 3 to 9	11	0.63
<i>p</i> -Xylene, pH 7.3	85	0.19

Note: Filtrasorb 300™ is a trademark of Calgon Corporation, Inc.,

Source: Dobbs, R.A. and Cohen, J.M. 1980. *Carbon Adsorption Isotherms for Toxic Organics*, EPA-600/8-80-023, U.S. Environmental Protection Agency, Office of Research and Development, Municipal Environmental Research Laboratory, Cincinnati, OH.

The abscissal intercept, $-a_0/a_1$, is the smallest possible EBCT that produces the required effluent quality. The ordinal intercept, a_0 , represents that portion of the bed that is not exhausted when breakthrough occurs. It represents the length of the mass transfer zone. If the service time to column saturation, t_{sat} , is determined, the length of the MTZ is,

$$H_{mtz} = \frac{(t_{sat} - t_b)H}{t_{sat}} = \frac{a_0 H}{t_b} \quad (9.255)$$

where H = the bed length (m or ft)
 H_{mtz} = the length of the mass transfer zone (m or ft)
 t_{sat} = the service time to bed saturation (sec)

It is desirable to minimize the MTZ so as to maximize the efficiency of carbon usage. The length of the MTZ can be reduced by reducing the flow rate, but this increases the required column size.

The carbon usage rate for conventional GAC columns can be estimated as follows:

$$R_C = \frac{\rho_C(1-\epsilon)V}{t_b} \quad (9.256)$$

where R_C = the carbon usage rate (kg/s or lb/sec)
 V = the empty bed volume (m³ or ft³)
 ϵ = the bed porosity when filled with carbon (dimensionless)
 ρ_C = the bulk density of the dry carbon (kg/m³ or lb/ft³)

In this case, a portion of the carbon removed from the adsorber (equal to the volume of the MTZ) is not saturated with adsorbate and does not require regeneration. Pulsed column operation overcomes this deficiency, and the “base carbon usage rate” for a pulsed column is calculated as follows:

$$R_{bcu} = \frac{\rho_C(1-\epsilon)Q}{a_1} \quad (9.257)$$

where Q = the water flow rate (m³/s or ft³/sec)
 R_{bcu} = the base carbon usage rate (kg/s or lb/sec).

The Logistic Model

A purely empirical procedure has been developed by Oulman (1980). His model is based on the observation that the breakthrough curve is sigmoidal and can be approximated by the logistic equation:

$$\frac{C}{C_o} = \frac{1}{1 + e^{-(a+bt)}} \quad (9.258)$$

where a = an empirical constant (dimensionless)
 b = an empirical coefficient (per sec)
 C = the effluent contaminant concentration at time t (kg/m³ or lb/ft³)
 C_o = the influent contaminant concentration (kg/m³ or lb/ft³)
 t = the service time (sec)

This is actually a rearrangement of the Bohart–Adams equation, and the parameters in the exponential can be related to column properties and hydraulic loading as follows:

$$a = -\frac{k_a q_b H}{v_i \epsilon} \quad (9.259)$$

$$b = k_a C_o \quad (9.260)$$

where H = the bed depth (m or ft)
 k_a = the Bohart–Adams adsorption rate coefficient (per s)
 q_b = the adsorption capacity of a carbon bed at bed saturation (kg substance/kg C or lb substance/lb C)
 v_i = the interstitial water velocity in a packed bed (m/s or ft/sec)

The logistic equation can be linearized by rearrangement, and the coefficients a and b are the intercept and slope of plot:

$$\ln\left(\frac{C/C_o}{1 - C/C_o}\right) = a + bt \quad (9.261)$$

The only unknowns are the adsorption rate coefficient, k_a , and the bed capacity, q_b , and these may be calculated from the slope and intercept of the plot.

Clark, Symons, and Ireland (1986) derived a modified logistic formula by assuming that mass transfer to the carbon was controlled by transport through the water film, and that the solute concentration at the grain surface was in equilibrium with the quantity of adsorbed material. Freundlich's isotherm was used to describe the equilibrium. The effluent concentration vs. service time plot is,

$$C = \left(\frac{C_o^{n-1}}{1 + A e^{-rt}}\right)^{\frac{1}{n-1}} \quad (9.262)$$

$$A = \left(\frac{C_o^{n-1}}{C_b^{n-1}} - 1\right) e^{rt_b} \quad (9.263)$$

$$r = \frac{(n-1)k_t v_{az}}{v_i \epsilon} \quad (9.264)$$

where k_ℓ = the liquid film mass transfer coefficient (m/s or ft/sec)
 n = an empirical exponent in the Freundlich adsorption isotherm (dimensionless)
 r = an empirical coefficient (per sec)
 v_{az} = the velocity of the adsorption zone through an activated carbon bed (m/s or ft/sec)

Equation (9.262) can be linearized as follows for curve fitting:

$$\ln \left[\left(\frac{C_0}{C} \right)^{n-1} - 1 \right] = \ln A - rt \quad (9.265)$$

The logistic equation assumes that the breakthrough curve is symmetrical. When this is not the case, the modified logistic equation may give a better fit. The derivation of the modified logistic model shows that the coefficients A and r will vary with the liquid velocity in the bed, and they do (Clark, 1987). However, because the model ignores the effect of surface diffusion with the carbon grain pores, which is probably the rate-limiting process, Eqs. (9.263) and (9.264) cannot be used to calculate A and r and they should be determined empirically.

Packed Column Theory

A commonly used model is homogeneous surface diffusion model (HSDM) developed by Crittenden and Weber. This model was developed for the adsorption of single components.

It is assumed that the rate of adsorption is controlled by the rate of diffusion of adsorbed molecules along the walls of the pores inside the carbon grains. The water phase is assumed to be dilute everywhere, so that bulk flow in the pores and concentration effects on diffusivities can be ignored. The pore surface area is supposed to be uniformly distributed throughout the carbon particles, and the mass balance for adsorbate adsorbed to the carbon surface is written in spherical coordinates as follows:

$$\frac{\partial q}{\partial t} = D_s \left(\frac{\partial^2 q}{\partial r^2} + \frac{2}{r} \cdot \frac{\partial q}{\partial r} \right) \quad (9.266)$$

where D_s = the surface diffusivity (m²/s or ft²/sec)
 q = the mass of adsorbate per unit mass of carbon (kg adsorbate/kg C or lb adsorbate/lb C)
 r = the radial distance from the center of the carbon grain (m or ft)
 t = elapsed time (sec)

The water phase at any level in the bed is assumed to be of uniform composition (except for the boundary layer) and without channeling. Mass transfer from the interstitial water to the carbon grains is represented as transport across a surface film. The mass balance for the adsorbate dissolved in the water flowing through the bed is as follows (James M. Montgomery, Consulting Engineers, Inc., 1985),

$$\underbrace{\frac{\partial C}{\partial t}}_{\text{accumulation in water}} = \underbrace{D_p \frac{\partial^2 C}{\partial z^2}}_{\text{dispersive flux}} - \underbrace{v_i \frac{\partial C}{\partial z}}_{\text{advective flux}} - \underbrace{\frac{3k_\ell(1-\epsilon)}{a_p \phi \epsilon} (C - C_s)}_{\text{transfer to carbon}} \quad (9.267)$$

where a_p = the radius of an activated carbon grain (m or ft)
 C = the bulk water phase adsorbate concentration (kg/m³ or lb/ft³)
 C_s = the adsorbate concentration at the water-carbon interface (kg/m³ or lb/ft³)
 D_p = the water phase dispersion coefficient (m²/s or ft²/sec)
 k_ℓ = the liquid film mass transfer coefficient (m/s or ft/sec)
 v_i = the interstitial water velocity in a packed bed (m/s or ft/sec)
 z = the distance from the inlet of a granular activated carbon bed (m or ft)

ε = the filter bed porosity (dimensionless)

ϕ = the sphericity, the ratio of the surface area of an equivalent volume sphere to the surface area (not counting internal pores) of the carbon grain (dimensionless)

At the interface between the carbon grain and the interstitial water, there is an equilibrium between the adsorbed material and the dissolved material, which can be represented by some suitable isotherm such as the Freundlich:

$$q_s = kC_s^{1/n} \quad (9.251)$$

The interfacial area per unit bed volume is $3(1 - \varepsilon)/a_p\phi$.

Equations (9.266) and (9.271) are connected by the requirement that solute disappearing from the water appears as adsorbate in the carbon. The transfer of solute to the carbon can be represented on an areal flux basis,

$$D_s \rho_p \left. \frac{\partial q}{\partial r} \right|_{r=a_p} = k_\ell (C - C_s) \quad (9.268)$$

where ρ_p = the particle density (kg/m^3 or lbm/ft^3), or a bed volume basis,

$$\frac{3k_\ell(1-\varepsilon)(C-C_s)}{a_p\phi} = \rho_p(1-\varepsilon) \frac{\partial}{\partial t} \left(4\pi \int_0^{a_p} q r^2 dr \right) \quad (9.269)$$

The value of $q(r,z,t)$ is given by Eq. (9.269) with the condition that $q(a_p,z,t)$ be q_s .

The relevant boundary conditions are as follows:

$$C(z,t) = C_o + \frac{D_p}{v_i} \cdot \frac{\partial C}{\partial z} \quad \text{at} \quad z = 0 \quad (9.270)$$

$$\frac{\partial C}{\partial z} = 0 \quad \text{at} \quad z = H \quad (9.271)$$

$$\frac{\partial q}{\partial r} = 0 \quad \text{at} \quad r = 0 \quad (9.272)$$

$$q(r,t) = 0 \quad \text{at} \quad t = 0 \quad (9.273)$$

$$C(z,t) = 0 \quad \text{at} \quad t = 0 \quad (9.274)$$

Numerical procedures for solving these equations are presented by Weber and Crittenden (1975) and by Roy, Wang, and Adrian (1993).

A number of parameters must be evaluated before the model can be used:

- Freundlich isotherms constants
- Liquid film mass transfer coefficient
- Liquid film diffusivity
- Surface diffusivity

These parameters can be estimated using various published correlations, which are listed below, or by analyzing batch or continuous flow adsorption tests.

The Freundlich isotherm parameters must be determined experimentally for the substance of interest and the intended carbon. Typical values for a variety of substances are given in [Table 9.12](#).

The mass transfer coefficient can be estimated using any one of several correlations:

Williamson, Bazaire, and Geankoplis (1963):

$$\frac{k_\ell}{\epsilon v_i} \cdot \text{Sc}^{0.58} = 2.40 \cdot \text{Re}^{-0.66}; \quad 0.08 \leq \text{Re} \leq 125 \quad (9.275)$$

where D_ℓ = the molecular diffusivity of the adsorbate in the bulk water (m²/s or ft²/sec)

d_p = the diameter of a carbon grain (m or ft)

Re = the particle Reynolds number (dimensionless)

$$= \rho v_i d_p / \mu$$

Sc = the Schmidt number (dimensionless)

$$= \mu / \rho D_\ell$$

μ = the dynamic viscosity of water (N·s/m² or lbf·sec/ft²)

ρ = the water density (kg/m³ or lbf/ft³)

Wakao and Funazkri (1978):

$$\frac{k_\ell d_p}{D_\ell} = 2 + 1.1 \cdot \text{Re}^{0.6} \text{Sc}^{1/3}; \quad 3 \leq \text{Re} \leq 10^4 \quad (9.276)$$

where Re = the modified particle Reynolds number (dimensionless), = $\rho \epsilon v_i d_p / \mu$.

The liquid phase solute diffusivities can be estimated in several ways:

Stokes-Einstein (Einstein, 1956):

$$D_\ell = \frac{kT}{6\pi a_p \mu} \quad (9.277)$$

where k = Boltzmann's constant (1.380 658 × 10⁻²³ J/K or approximately 0.5658 × 10⁻²³ ft·lbf/°R)

T = the absolute temperature (K or °R).

Polson (1950):

$$D_\ell = 2.74 \times 10^{-5} \cdot M_r^{-1/3} \quad (9.278)$$

where D_ℓ = the diffusivity in cm²/s

M_r = the relative molecular weight (dimensionless).

Wilke-Chang (Wilke and Chang, 1955; Hayduk and Laudie, 1974):

$$\frac{D_{\ell i} \mu}{T} = 7.4 \times 10^{-8} \times \frac{\sqrt{2.6 M_{r\ell}}}{v_{mbp}^{0.6}} \quad (9.279)$$

where $D_{\ell i}$ = the diffusivity of species i in water in cm²/s

$M_{r\ell}$ = the molecular weight of water in g

$$= 18 \text{ g}$$

v_{mbp} = the molar volume of the liquid phase of species i at its boiling point in cm³/g-mole

μ = the viscosity of water in centipoise (cp)

Note that 1 cp = 0.001 N·s/m² (exactly).

TABLE 9.13 Components of the Molar Volume of Liquids

Structural Component	Molar Volumes ^a (cm ³ /g-mol)	Molar Volumes ^b (cm ³ /g-mol)
Bromine, add	27.0	—
Carbon, add	14.8	16.5
Chlorine, end (R-Cl), add	21.6	19.5
Chlorine, inner (R-Cl-R), add	24.6	19.5
Fluorine, add	8.7	—
Hydrogen, add	3.7	1.98
Iodine, add	37.0	—
Nitrogen, double bonded, add	15.6	5.69
Nitrogen, triple bonded, add	16.2	5.69
Nitrogen, primary amines (RNH ₂), add	10.5	5.69
Nitrogen, secondary amines (R ₂ NH), add	12.0	5.69
Nitrogen, tertiary amines (R ₃ N), add	10.8	5.69
Oxygen, if not combined as follows, add	7.4	5.48
Oxygen, in methyl esters, add	9.1	5.48
Oxygen, in methyl ethers, add	9.9	5.48
Oxygen, in other esters or ethers, add	11.0	5.48
Oxygen, in acids, add	12.0	5.48
Oxygen, combined with N, P, or S, add	8.3	5.48
Phosphorus, add	27.0	—
Sulfur, add	25.6	17.0
3-Member rings, deduct	6.0	—
4-Member rings, deduct	8.5	—
5-Member rings, deduct	11.5	—
6-Member rings (benzene, cyclohexane), deduct	15.0	20.2
Anthracene ring, deduct	47.5	20.2
Naphthalene ring, deduct	30.0	20.2

^a Le Bas, 1915. *The Molecular Volumes of Liquid Chemical Compounds*, Longmans, London. [Quoted in Perry, R.H. and Chilton, C.H. 1973. *Chemical Engineer's Handbook*, 5th ed., McGraw-Hill, Inc., New York.]

^b Bennet, C.O. and Myers, J.E. 1974. *Momentum, Heat, and Mass Transfer*, 2nd ed., McGraw-Hill, Inc., New York.

Perry and Chilton (1973) recommend the Le Bas volumes in place of v_{mbp} if values for the latter cannot be found. Table 9.13 gives the Le Bas volumes for common structural components of organic substances.

Surface diffusivities of volatile organic substances and polycyclic aromatic substances can be estimated by the Suzuki–Kawazoe (1975) correlation:

$$D_s = 1.1 \times 10^{-4} \cdot e^{-5.32T_b/T} \quad (9.280)$$

where D_s = the surface diffusivity in cm²/s

T = the adsorption temperature in K

T_b = the boiling point of the organic substance in K

It is expected that the coefficient in front of the exponential will depend only on the carbon used and not on the adsorbate. The correlation was developed using Takeda HGR 513™, which is derived from coconut shell and has a mean grain size of 3.41 mm and a specific surface area of 1225 m²/g.

A simplified approach has been developed by Hand, Crittenden and Thacker (1984) that eliminates the need for computer simulations. They fitted an empirical formula to the results of many computer solutions. The equations and boundary conditions are first nondimensionalized by introducing the following dimensionless variables and groups:

$$\bar{C} = \frac{C}{C_o} \quad (9.281)$$

$$\bar{C}_s = \frac{C_s}{C_o} \quad (9.282)$$

$$\bar{q} = \frac{q}{q_o} \quad (9.283)$$

$$\bar{r} = \frac{r}{a_p} \quad (9.284)$$

$$\bar{z} = \frac{z}{H} \quad (9.285)$$

$$\mathbf{Bi} = \frac{k_l a_p (1 - \varepsilon)}{D_s D_g \varepsilon \phi} \quad (9.286)$$

$$D_g = \frac{q_o \rho_p (1 - \varepsilon)}{C_o \varepsilon} \quad (9.287)$$

$$E_d = \frac{D_s D_g \tau_h}{a_p^2} \quad (9.288)$$

$$\mathbf{St} = \frac{k_l \tau_h (1 - \varepsilon)}{a_p \varepsilon \phi} \quad (9.289)$$

$$T = \frac{t}{\tau_h (1 + D_g)} \quad (9.290)$$

- where **Bi** = the Biot number (dimensionless)
 C_o = the adsorbate's influent concentration (kg/m³ or lb/ft³)
 D_g = the solute distribution parameter (dimensionless)
 E_d = the diffusivity modulus, the ratio of the Stanton to Biot numbers (dimensionless)
 H = the depth of the carbon bed (m or ft)
 q_o = the mass of adsorbate per unit mass of activated carbon at equilibrium with the influent concentration C_o (kg adsorbate/kg C or lb adsorbate/lb C)
St = the modified Stanton number (dimensionless)
 T = the throughput, the ratio of the adsorbate fed to the amount of adsorbate that may be adsorbed at equilibrium (dimensionless)

The resulting transport equations and boundary conditions are as follows (Hand, Crittenden, and Thacker, 1984):

$$\frac{1}{1 + D_g} \cdot \frac{\partial \bar{C}}{\partial T} = - \frac{\partial \bar{C}}{\partial \bar{z}} - 3 \cdot \mathbf{St} \cdot (\bar{C} - \bar{C}_s) \quad (9.291)$$

$$\frac{\partial \bar{q}}{\partial T} = \left(1 + \frac{1}{1 + D_g}\right) \cdot \frac{E_d}{\bar{r}^2} \cdot \frac{\partial}{\partial \bar{r}} \left(\bar{r}^2 \frac{\partial \bar{q}}{\partial \bar{r}} \right) \quad (9.292)$$

$$\left. \frac{\partial \bar{q}}{\partial \bar{r}} \right|_{\bar{r}=1} = \mathbf{Bi} \cdot (\bar{C} - \bar{C}_s) \quad (9.293)$$

$$\left. \frac{\partial \bar{q}}{\partial \bar{r}} \right|_{\bar{r}=0} = 0 \quad (9.294)$$

$$\bar{C}(\bar{z} = 0, T \geq 0) = 1 \quad (9.295)$$

$$\bar{C} \left[T(1 + D_g) < \bar{z} \leq 1, T < \frac{1}{1 + D_g} \right] = 0 \quad (9.296)$$

$$\bar{q}(0 \leq \bar{r} \leq 1, 0 \leq \bar{z} \leq 1, T = 0) = 0 \quad (9.297)$$

The nondimensional Freundlich isotherm is

$$\bar{q}_s = \bar{C}_s^{1/n} \quad (9.298)$$

If the solute distribution parameter, D_g , is greater than about 50, the Biot number, \mathbf{Bi} , is greater than about 0.5, and the Freundlich exponent, $1/n$, is less than 1, the numerical solution is controlled by \mathbf{Bi} , $1/n$, and the Stanton number, \mathbf{St} . Hand, Crittenden, and Thacker (1984) summarized the results of numerous computer simulations as parameters in the following empirical formula:

$$T = A_o + A_1 \left(\frac{C}{C_o} \right)^{A_2} + \frac{A_3}{1.10 - \left(\frac{C}{C_o} \right)^{A_4}} \quad (9.299)$$

Equation (9.299) gives the processing time in terms of the throughput parameter, T , required to achieve a specified effluent concentration, C . The breakthrough ratio, C/C_o , must lie between about 0.02 to 0.99. Values for the parameters are given in [Table 9.14](#). There are several apparent discontinuities in the parameter values, which make interpolation hazardous. However, a three-dimensional plot of the coefficients reveals a smoother pattern, and it should be used as the basis of interpolation.

Equation (9.299) is valid only if the bed contacting time is deep enough to develop a mass transfer zone. Minimum bed contacting times depend on the minimum Stanton number, which can be estimated from empirical correlation:

$$\mathbf{St}_{\min} = B_o + B_1 \cdot \mathbf{Bi} \quad (9.300)$$

Values of the correlation parameters are given in [Table 9.15](#). The minimum bed contacting time is given by:

$$\tau_{\min} = \frac{\mathbf{St}_{\min} a_p \varepsilon \phi}{k_\ell (1 - \varepsilon)} \quad (9.301)$$

TABLE 9.14 Parameter Values for the Hand–Crittenden–Thacker Breakthrough Formula

$1/n$	Bi	Equation (9.299) Parameters				
		A_0	A_1	A_2	A_3	A_4
0.05	0.5	-5.447	6.599	0.02657	0.01938	20.45
0.05	2.0	-5.468	6.592	0.004989	0.004988	0.5023
0.05	4.0	-5.531	6.585	0.02358	0.009019	0.2731
0.05	6.0	-5.607	6.582	0.02209	0.01313	0.2145
0.05	8.0	-5.606	6.505	0.02087	0.01708	0.1895
0.05	10.0	-5.664	6.457	0.01816	0.01994	0.1493
0.05	14.0	-0.6628	1.411	0.06071	0.02023	0.1439
0.05	25.0	-0.6628	1.351	0.03107	0.02035	0.1300
0.05	≥100.0	0.6659	0.7113	2.987	0.01678	0.3610
0.10	0.5	-1.920	3.055	0.005549	0.02428	15.31
0.10	2.0	-2.279	3.394	0.04684	0.004751	0.3847
0.10	4.0	-2.337	3.378	0.04399	0.00865	0.2434
0.10	6.0	-2.407	3.374	0.04132	0.01255	0.1966
0.10	8.0	-2.478	3.371	0.03899	0.01628	0.1764
0.10	10.0	-2.566	3.371	0.03500	0.01939	0.1508
0.10	16.0	-2.567	3.306	0.02097	0.01948	0.1368
0.10	30.0	-2.569	3.242	0.009595	0.01961	0.1218
0.10	≥100.0	-2.568	3.191	0.001555	0.01968	0.1101
0.20	0.5	-1.441	2.569	0.06092	0.002333	0.3711
0.20	2.0	-1.474	2.558	0.05848	0.005026	0.2413
0.20	4.0	-1.507	2.519	0.05552	0.008797	0.1875
0.20	6.0	-1.035	1.983	0.06928	0.01230	0.1679
0.20	8.0	-0.1692	1.078	0.01449	0.01550	0.1681
0.20	10.0	-1.403	2.188	0.05219	0.01842	0.1336
0.20	13.0	-1.369	2.119	0.03949	0.01845	0.1276
0.20	25.0	-1.514	2.209	0.01794	0.01851	0.1152
0.20	≥100.0	0.6803	0.649	2.570	0.01495	0.3698
0.30	0.5	-1.7587	2.847	0.04953	0.003022	0.1568
0.30	2.0	-1.6579	2.689	0.04841	0.005612	0.1409
0.30	4.0	-0.5657	1.538	0.08445	0.008808	0.1391
0.30	6.0	-0.1971	1.119	0.1179	0.01153	0.1359
0.30	8.0	-0.1971	1.069	0.1198	0.1392	0.1327
0.30	10.0	-0.1734	1.000	0.1203	0.01594	0.1340
0.30	15.0	-0.1734	0.9194	0.07177	0.01416	0.08627
0.30	35.0	0.6665	0.4846	1.719	0.01344	0.2595
0.30	≥100.0	0.6962	0.5170	2.055	0.01296	0.3032
0.40	0.5	-0.5343	1.604	0.09406	0.004141	0.1378
0.40	2.0	-0.1663	1.191	0.1223	0.006261	0.1348
0.40	4.0	-0.1663	1.132	0.1155	0.008634	0.1268
0.40	6.0	-0.1663	1.090	0.1123	0.01046	0.1243
0.40	9.0	0.4919	0.4918	0.4874	0.01137	0.1477
0.40	12.0	0.5641	0.4192	0.6398	0.01154	0.1490
0.40	15.0	0.6407	0.4325	1.048	0.01162	0.2127
0.40	25.0	0.6724	0.3970	1.153	0.01128	0.2169
0.40	≥100.0	0.7414	0.4481	1.930	0.01020	0.3064
0.50	0.5	-0.04080	1.100	0.1590	0.005467	0.1391
0.50	4.0	-0.04080	0.9828	0.1116	0.008072	0.1114
0.50	10.0	0.09460	0.7549	0.09207	0.009877	0.09076
0.50	14.0	0.02300	0.8021	0.05754	0.009662	0.08453
0.50	25.0	0.02300	0.7937	0.03932	0.009326	0.08275
0.50	≥100.0	0.5292	0.2918	0.08243	0.008317	0.07546
0.60	0.5	0.3525	0.6921	0.2631	0.005482	0.1218
0.60	2.0	0.5220	0.5042	0.3273	0.005612	0.1287
0.60	6.0	0.6763	0.3346	0.4823	0.005898	0.1389
0.60	14.0	0.7695	0.2595	0.7741	0.005600	0.1655

TABLE 9.14 (continued) Parameter Values for the Hand–Crittenden–Thacker Breakthrough Formula

1/n	Bi	Equation (9.299) Parameters				
		A ₀	A ₁	A ₂	A ₃	A ₄
0.60	50.0	0.8491	0.2158	1.343	0.004725	0.2238
0.60	≥100.0	0.8312	0.2273	1.175	0.004961	0.2121
0.70	0.5	0.575	0.4491	0.2785	0.004122	0.1217
0.70	4.0	0.7153	0.3072	0.4421	0.004371	0.1384
0.70	12.0	0.7879	0.2435	0.6616	0.004403	0.1626
0.70	25.0	0.8295	0.2041	0.7845	0.004050	0.1790
0.70	≥100.0	0.8470	0.1907	0.9317	0.003849	0.1832
0.80	0.5	0.7089	0.3141	0.3575	0.003276	0.1193
0.80	4.0	0.7846	0.2397	0.4844	0.003206	0.1350
0.80	14.0	0.8394	0.1890	0.6481	0.003006	0.1577
0.80	100.0	0.8827	0.1462	0.808	0.002537	0.1745
0.90	0.5	0.8654	0.1576	0.4450	0.001650	0.1408
0.90	4.0	0.8548	0.1714	0.4950	0.001910	0.1423
0.90	16.0	0.8662	0.1640	0.5739	0.001987	0.1576
0.90	100.0	0.8932	0.1330	0.6241	0.001740	0.1642

Source: Hand, D.W., Crittenden, J.C., and Thacker, W.E. 1984. "Simplified Models for Design of Fixed-Bed Adsorption Systems," *Journal of Environmental Engineering*, 110(2): 440. With permission.

TABLE 9.15 Parameter Values for Estimating Minimum Stanton Number for Establishment of Mass Transfer Zone

Freundlich Exponent 1/n	0.5 ≤ Bi ≤ 10		Bi ≥ 10	
	B ₀	B ₁	B ₀	B ₁
	0.05	1.990	0.02105	0.0
0.10	2.189	0.02105	0.0	0.24
0.20	2.379	0.04211	0.0	0.28
0.30	2.547	0.1053	0.0	0.36
0.40	2.684	0.2316	0.0	0.50
0.50	2.737	0.5263	0.0	0.80
0.60	3.421	1.158	0.0	1.50
0.70	7.105	1.789	0.0	2.50
0.80	13.16	3.684	0.0	5.00
0.90	56.84	6.316	0.0	12.0

Source: Hand, D.W., Crittenden, J.C., and Thacker, W.E. 1984. "Simplified Models for Design of Fixed-Bed Adsorption Systems," *Journal of Environmental Engineering*, 110(2): 440. With permission.

The minimum processing time before regeneration or replacement is required is calculated from the throughput:

$$t_{\min} = \tau_{\min} (1 + D_g) T \tag{9.302}$$

If longer processing times are desired, the hydraulic retention time must be increased proportionately.

Rapid Small-Scale Column Test

The rapid small-scale column test (RSSCT) can be used to predict the performance of pilot- or full-scale GAC columns (Crittenden, Berrigan, and Hand, 1986; Crittenden et al., 1987, 1991; Summers et al., 1995). In this approach, a representative sample of activated carbon is crushed (typically to U.S. No. 60 × 80 mesh), washed and dried, and then placed in a small diameter (~1 cm) column for testing. Feed solution is then passed through the column, and the effluent is monitored as a function of time. By using small diameter columns, the RSSCT is performed in a fraction of the time as required for pilot-scale testing. However, the short duration of the RSSCT prevents simulation of biodegradation within the GAC column and does not allow for evaluation of long-term changes in water quality.

The RSSCT is based on the dispersed flow, pore surface diffusion model, which takes into account advection, dispersion, diffusion, liquid-phase mass transfer resistance, local adsorption equilibrium, surface diffusion, pore diffusion, and competition between solutes. Based on this model, a number of dimensionless parameters are developed that remain constant from the small-scale to the pilot- or full-scale. If diffusivity is independent of the size of activated carbon, the EBCT of a large-scale GAC adsorber is related to the EBCT of a small-scale column by:

$$\frac{\text{EBCT}_{lc}}{\text{EBCT}_{sc}} = \left[\frac{a_{p,lc}}{a_{p,sc}} \right]^2 \quad (9.303)$$

where *lc* and *sc* denote variables corresponding to the large column and the small column, respectively. The hydraulic loading of the full-scale adsorber is related to the hydraulic loading of the small-scale column as follows:

$$\frac{v_{lc}}{v_{sc}} = \frac{a_{p,sc}}{a_{p,lc}} \quad (9.304)$$

Alternative scaling relations can be developed if the diffusivity is proportional to the size of the activated carbon (Crittenden et al., 1987).

Batch and Ideal Plug Flow Reactors

The Biot number is the ratio of the mass flux through the liquid film surrounding a carbon grain to the mass flux due to surface diffusion within the grain. For Biot numbers greater than about 100, mass transfer is controlled by surface diffusion, whereas liquid film diffusion controls at small Biot numbers (Traegner and Suidan, 1989).

For large Biot numbers, the HSDM has an exact power series solution in closed, batch systems (Crank, 1956):

$$\frac{q(t)}{q_e} = 1 - \frac{6}{\pi^2} \cdot \sum_{i=1}^{\infty} \frac{1}{i^2} \cdot \exp\left(-\frac{i^2 \pi^2 D_s t}{a_p^2}\right) \quad (9.305)$$

where q_e = the mass of adsorbate per unit mass of activated carbon at equilibrium (kg adsorbate/kg C or lb adsorbate/lb C).

Note that the solution depends only on the grain size and the surface diffusivity. Particle size does not affect the equilibrium position or the surface diffusivity, but small particles adsorb solute more quickly (Najm et al., 1990). Consequently, batch tests are more quickly performed if powdered carbon is used.

Numerical solutions to the HSDM model for large Biot numbers have been summarized in the form of power series by Hand, Crittenden, and Thacker (1983).

If both liquid film transport and surface diffusion are important, only a numerical solution is possible. Traegner and Suidan (1989) have shown how the Levenberg–Marquardt nonlinear optimization procedure can be used to adjust D_s and k_l so that model predictions match experimental data.

PAC Slurry Reactors

The batch adsorption solution may also be applied to turbulent, completely mixed reactors. Taking into account the residence time distribution for a continuous flow stirred tank, one obtains (Nakhla, Suidan, and Traegner-Duhr, 1989; Najm et al., 1990; Adham et al., 1993),

$$C = C_o - X_{PAC} \cdot kC^{1/n} \cdot \left[1 - \frac{6}{\pi^2} \cdot \sum_{i=1}^{\infty} \frac{1}{i^2 \left(1 + \frac{i^2 \pi^2 D_s \tau_h}{a_p^2} \right)} \right] \quad (9.306)$$

Multicomponent Adsorption

In many applications of activated carbon, multiple solutes compete for sites on the adsorbent surface. Ideal adsorbed solution theory (IAST) can be used to predict solution- and solid-phase equilibrium concentrations for systems containing multiple solutes (Radke and Prausnitz, 1972; Crittenden et al., 1985; Najm et al., 1991; Qi et al., 1994).

The basic premise underlying the IAST is that the spreading pressure of the pure component system is equal to the spreading pressure of the mixture. Subsequently, single-solute adsorption information can be used to predict adsorption behavior in multisolute systems. Using the Freundlich isotherm to relate the solution-phase and solid-phase concentrations of pure components, it can be shown that:

$$C_{e,i} = \frac{q_{e,i}}{\sum_{j=1}^N q_{e,j}} \left(\frac{\sum_{j=1}^N n_j q_{e,j}}{n_i k_i} \right)^{n_i} \quad (9.307)$$

where $C_{e,i}$ = the equilibrium concentration of solute i in water
 $q_{e,i}$ = the mass of adsorbed solute i per unit mass of activated carbon at equilibrium
 $q_{e,j}$ = the mass of adsorbed solute j per unit mass of activated carbon at equilibrium
 n_i = the single-solute Freundlich empirical exponent for component i
 k_i = the single-solute Freundlich empirical coefficient for component i
 n_j = the single-solute Freundlich empirical exponent for component j
 N = the number of independent adsorbing solutes in the system

The equilibrium concentration of solute i can be replaced with the initial concentration of solute i by noting the following relationship valid for a batch adsorption experiment:

$$q_{e,i} = \frac{C_{o,i} - C_{e,i}}{C_c} \quad (9.308)$$

where $C_{o,i}$ = the initial concentration of solute i in water
 C_c = the concentration of activated carbon used.

Combining the above equations gives:

$$C_{o,i} - C_c q_{e,i} - \frac{q_{e,i}}{\sum_{j=1}^N q_{e,j}} \left(\frac{\sum_{j=1}^N n_j q_{e,j}}{n_i k_i} \right)^{n_i} = 0 \quad (9.309)$$

which for a two-component system reduces to the following two equations:

$$C_{o,1} - C_c q_{e,1} - \left(\frac{q_{e,1}}{q_{e,1} + q_{e,2}} \right) \left(\frac{n_1 q_{e,1} + n_2 q_{e,2}}{n_1 k_1} \right)^{n_1} = 0 \quad (9.310)$$

$$C_{o,2} - C_c q_{e,2} - \left(\frac{q_{e,2}}{q_{e,1} + q_{e,2}} \right) \left(\frac{n_1 q_{e,1} + n_2 q_{e,2}}{n_2 k_2} \right)^{n_2} = 0 \quad (9.311)$$

For systems of more than two components, additional equations may be developed and the set of equations solved numerically, for example, using the Newton–Raphson technique.

Application

Powdered Activated Carbon

Powdered activated carbon is usually applied by adding it to the water or wastewater to be treated and mixing the carbon and water in a slurry reactor for the requisite contacting time. The carbon is subsequently removed from the liquid by settling or filtration. Unless the treated water is nearly free of other suspended solids, the spent carbon cannot be regenerated and is wasted. Carbon wasting is practicable only for intermittent, short duration treatment.

If the treated water is clear, settling, filtration, or both will recover a product suitable for regeneration. Furthermore, it is possible to operate a countercurrent flow of carbon and water so as to minimize carbon requirement. In such a system, several slurry reactors are constructed and operated in series. Each reactor is equipped with a filter or settler, and the solids captured are pumped to the next upstream reactor (Hutchins, 1981).

The required contacting times must be empirically determined; the homogeneous surface diffusion model (HSDM) described above is widely used as a design aid. The adsorption rate is inversely proportional to the square of the carbon grain size, so the required contacting time for equal removal efficiencies is proportional to the square of the grain diameter (Najm et al., 1990):

$$\tau_h \propto a_p^2 \quad (9.312)$$

The adsorptive capacity and surface diffusivity are independent of grain size (Randtke and Snoeyink, 1983; Najm et al., 1990).

Most reported carbon adsorption studies have employed pure solutions of single substances. Studies in complex natural waters indicate that the background organic matter may reduce the sorptive capacity for the test substance by about 50% (Najm et al., 1990).

Granular Activated Carbon

Granular activated carbon systems are usually preferred when continuous carbon treatment is required, because carbon recovery for regeneration is easier. Plant surveys indicated several design deficiencies that require special attention (Culp and Clark, 1983; Graese, Snoeyink, and Lee, 1987; Akell, 1981):

- Wet carbon forms electrolytic cells and is corrosive.
- Wet carbon is abrasive to steel.
- Dry, fresh carbon in large piles adsorbs oxygen and can spontaneously ignite; the ignition temperature depends strongly on how the carbon was manufactured and is about 300°C for steam-activated carbons.
- Idle carbon beds loaded with ketones, aldehydes, and some organic acids are subject to “temperature excursions” and occasional bed fires.

- Carbon dust is explosive if it contains more than 8% by weight organic matter; most steam-activated carbons are well below this limit.
- Adsorbents are generally devoid of oxygen and cannot be entered without respirators and/or ventilation.
- Wastewater adsorbates may undergo anaerobic decomposition, producing explosive gases like methane and poisonous gases like hydrogen sulfide; control of column-dissolved oxygen levels is necessary.
- GAC and slurry transfer and feed equipment is often undersized.
- Backwash lines must be vented.
- Backwash nozzles subject to breakage or clogging must be avoided. (See Chapter 9, Section 9.6, “Filtration.”)
- Regeneration furnace feeds must be uniform to avoid temperature fluctuations and inconsistent reactivation.
- Control systems and drive motors must be protected from the weather and from furnace emissions and radiant heat.

Granular activated carbon systems come in three general types:

- *Packed columns* are large steel or reinforced concrete tanks, generally pressurized to maximize throughput rates (Culp and Clark, 1983; Culp/Wesner/Culp, Inc., 1986; Snoeyink, 1990; Joint Task Force, 1990). Prefabricated tanks must be less than 12 ft in diameter for transport. Larger tanks are constructed on site.
- In water treatment plants, the columns are installed after the rapid sand filters and operated downflow. Filtration rates between 3 and 7 gpm/ft² and depths of 2.5 to 15 ft are employed. The governing variable is contact time. This should be determined by pilot studies and model studies as described above. The most important restriction is that the contacting time be long enough to establish a mass transfer zone. Contacting times longer than this are needed to provide adequate service life, and the actual value chosen depends on the economics of the particular application. An empty bed contacting time (EBCT) of 10 to 20 min is common; 5 min suffices for taste and odor control. However, some applications may require an EBCT of a few hours.
- *Pulsed columns* are designed to permit intermittent replacement of carbon in operating columns (Hutchins, 1981; Snoeyink, 1990). Liquid flow is upward, and carbon is withdrawn from the column bottom at specified intervals. Fresh carbon is added at the top of the column. The columns have no freeboard, so the carbon cannot move during operation or cleaning, unless it is being withdrawn. This prevents vertical mixing of the bed.
- The carbon discharged from pulsed beds is always saturated with adsorbate at the raw water solute concentration. This is the most efficient way to use carbon. Carbon usage rates are calculated as “base rate,” discussed above (Hutchins, 1981).
- *Rapid sand filters* are used, but it has become common to remove the sand from rapid sand filters and replace it with activated carbon (Culp and Clark, 1983; Graese, Snoeyink, and Lee, 1987; Joint Task Force, 1990). Unless the filter box is extended, the contacting time will be short (usually less than 9 min) and may not be sufficient to establish a mass transfer zone. Such installations are normally restricted to taste and odor control. Taste and odor control systems may be in service for 1 to 5 years before the carbon must be replaced.
- Because the carbon also acts as a particle filter, several operational problems must be considered:
 - Backwashing rates sufficient to remove accumulated solids and prevent mudball formation may lead to carbon loss; careful carbon sizing and backwash control are needed.
 - Carbon grain pores may be fouled by deposition of calcium carbonate, magnesium hydroxide, and ferric and manganic oxides, all of which reduce adsorptive capacity.

References

- Adamson, A.W. 1982. *Physical Chemistry of Surfaces*, 4th ed. John Wiley & Sons, Inc., New York.
- Adham, S.S., Snoeyink, V.L., Clark, M.M., and Anselme, C. 1993. "Predicting and Verifying TOC Removal by PAC in Pilot-Scale UF Systems," *Journal of the American Water Works Association*, 85(12): 59.
- Akell, R.B. 1981. "Safety Aspects of Activated Carbon Technology," p. 223 in *Activated Carbon for Wastewater Treatment*, J.R. Perrich, ed., CRC Press, Inc., Boca Raton, FL.
- Anonymous. 1942. "Effect of Water Treatment Processes on Tastes and Odors," p. 35 in *Taste and Odor Control in Water Purification*. West Virginia Pulp and Paper Company, Industrial Chemical Sales Division, New York.
- AWWA Standards Committee on Activated Carbon. 1990a. *AWWA Standard for Granular Activated Carbon*, B604–90. American Water Works Association, Denver, CO.
- AWWA Standards Committee on Activated Carbon. 1990b. *AWWA Standard for Powdered Activated Carbon*, B600–90. American Water Works Association, Denver, CO.
- Bennet, C.O. and Myers, J.E. 1974 *Momentum, Heat, and Mass Transfer*, 2nd ed. McGraw-Hill Book Co., Inc., New York.
- Clark, R.M., Symons, J.M., and Ireland, J.C. 1986. "Evaluating Field Scale GAC Systems for Drinking Water," *Journal of Environmental Engineering*, 112(4): 744.
- Clark, R.M. 1987. "Modeling TOC Removal by GAC: The General Logistic Equation," *Journal of the American Water Works Association*, 79(1): 33.
- Crank, J. 1956. *The Mathematics of Diffusion*, Oxford University Press, London.
- Crittenden, J.C. and Weber, W.J., Jr. 1978a. "Predictive Model for Design of Fixed-Bed Adsorbers: Parameter Estimation and Model Development," *Journal of the Environmental Engineering Division, Proceedings of the American Society of Civil Engineers*, 104(EE2): 185.
- Crittenden, J.C. and Weber, W.J., Jr. 1978b. "Predictive Model for Design of Fixed-Bed Adsorbers: Single Component Model Verification," *Journal of the Environmental Engineering Division, Proceedings of the American Society of Civil Engineers*, 104(EE3): 433.
- Crittenden, J.C. and Weber, W.J., Jr. 1978c. "A Model for Design of Multicomponent Systems," *Journal of the Environmental Engineering Division, Proceedings of the American Society of Civil Engineers*, 104(EE6): 1175.
- Crittenden, J.C., Luft, P., Hand, D.W., Oravitz, J.L., Loper, S.W., and Ari, M. 1985. "Prediction of Multicomponent Adsorption Equilibria Using Ideal Adsorbed Solution Theory," *Environmental Science and Technology*, 19(11): 1037.
- Crittenden, J.C., Berrigan, J.K., and Hand, D.W. 1986. "Design of Rapid Small-Scale Adsorption Tests for Constant Diffusivity," *Journal of the Water Pollution Control Federation*, 58(4): 312.
- Crittenden, J.C., Berrigan, J.K., Hand, D.W., and Lykins, B. 1987. "Design of Rapid Fixed-Bed Adsorption Tests for Nonconstant Diffusivities," *Journal of Environmental Engineering*, 113(2): 243.
- Crittenden, J.C., Reddy, P.S., Arora, H., Trynoski, J., Hand, D.W., Perram, D.L., and Summers, R.S. 1991. "Predicting GAC Performance with Rapid Small-Scale Column Tests," *Journal of the American Water Works Association*, 83(1): 77.
- Culp, R.L. and Clark, R.M. 1983. "Granular Activated Carbon Installations," *Journal of the American Water Works Association*, 75(8): 398.
- Culp, R.L. and Culp, G.L. 1971. *Advanced Wastewater Treatment*. Van Nostrand Reinhold Company, Inc., New York.
- Culp/Wesner/Culp, Inc., 1986. *Handbook of Public Water Supply Systems*, R.B. Williams and G.L. Culp, eds., Van Nostrand Reinhold Co., Inc., New York.
- Dobbs, R.A. and Cohen, J. M. 1980. *Carbon Adsorption Isotherms for Toxic Organics*, EPA-600/8–80–023, U.S. Environmental Protection Agency, Office of Research and Development, Municipal Environmental Research Laboratory, Cincinnati, OH.
- Einstein, A. 1956. *Investigations on the Theory of the Brownian Movement*, R. Fürth, ed., A.D. Cowper, trans. Dover Publications, Inc., New York.

- Freundlich, H. 1922. *Colloid & Capillary Chemistry*. Trans. H.S. Hatfield. E.P. Dutton and Co., New York.
- Graese, S.L., Snoeyink, V.L., and Lee, R.G. 1987. *GAC Filter-Adsorbers*. American Water Works Association, Research Foundation, Denver, CO.
- Halsey, G. and Taylor, H.S. 1947. "The adsorption of Hydrogen on Tungsten," *The Journal of Chemical Physics*, 15(9): 624.
- Hand, D.W., Crittenden, J.C., and Thacker, W.E. 1983. "User-Oriented Batch Reactor Solutions to the Homogeneous Surface Diffusion Model," *Journal of Environmental Engineering*, 109(1): 82.
- Hand, D.W., Crittenden, J.C., and Thacker, W.E. 1984. "Simplified Models for Design of Fixed-Bed Adsorption Systems," *Journal of Environmental Engineering*, 110(2): 440.
- Hayduk, W. and Laudie, H. 1974. "Prediction of Diffusion Coefficients for Nonelectrolytes in Dilute Aqueous Solutions," *Journal of the American Institute of Chemical Engineers*, 20(3): 611.
- Hutchins, R.A. 1981. "Development of Design Parameters," p. 61 in *Activated Carbon for Wastewater Treatment*, J.R. Perrich, ed., CRC Press, Inc., Boca Raton, FL.
- James M. Montgomery, Consulting Engineers, Inc. 1985. *Water Treatment: Principles and Design*, John Wiley & Sons, Inc., New York.
- Joint Editorial Board. 1992. *Standard Methods for the Examination of Water and Wastewater*, 18th ed. American Public Health Association, Washington, DC.
- Joint Task Force American Society of Civil Engineers and American Water Works Association. 1990. *Water Treatment Plant Design*, 2nd ed. McGraw-Hill Publishing Co., Inc., New York.
- Joint Task Force of the Water Environment Federation and the American Society of Civil Engineers. 1991. *Design of Municipal Wastewater Treatment Plants: Volume II — Chapters 13–20*, WEF Manual of Practice No. 8, ASCE Manual and Report on Engineering Practice No. 76. Water Environment Federation, Alexandria, VA; American Society of Civil Engineers, New York.
- Le Bas. 1915. *The Molecular Volumes of Liquid Chemical Compounds*. Longmans, London.
- Liu, K.-T. and Weber, W.J., Jr. 1981. "Characterization of Mass Transfer Parameters for Adsorber Modeling and Design," *Journal of the Water Pollution Control Federation*, 53(10): 1541.
- McGinnis, F.K. 1981. "Infrared Furnaces for Reactivation," p. 155 in *Activated Carbon for Wastewater Treatment*, J.R. Perrich, ed., CRC Press, Inc., Boca Raton, FL.
- Najm, I.N., Snoeyink, V.L., and Richard, Y. 1991. "Effect of Initial Concentration of a SOC in Natural Water on its Adsorption by Activated Carbon," *Journal of the American Water Works Association*, 83(8): 57.
- Najm, I.N., Snoeyink, V.L., Suidan, M.T., Lee, C.H., and Richard, Y. 1990. "Effect of Particle Size on Background Natural Organics on the Adsorption Efficiency of PAC," *Journal of the American Water Works Association*, 82(1): 65.
- Nakhla, G.F., Suidan, M.T., and Traegner-Duhr, U.K. 1989. "Steady State Model for the Expanded Bed Anaerobic GAC Reactor Operating with GAC Replacement and Treating Inhibitory Wastewaters," *Proceedings of the Industrial Waste Symposium, 62nd Annual Conference of the Water Pollution Control Federation, San Francisco*. Water Pollution Control Federation, Alexandria, VA.
- Ohio River Valley Water Sanitation Commission. 1980. *Water Treatment Process Modifications for Trihalomethane Control and Organic Substances in the Ohio River*, EPA-600/2-80-028. U.S. Environmental Protection Agency, Office of Research and Development, Municipal Environmental Research Laboratory, Cincinnati, OH.
- Oulman, C.S. 1980. "The Logistic Curve as a Model for Carbon Bed Design," *Journal of the American Water Works Association*, 72(1): 50.
- Palmer, C.M. 1967. *Algae in Water Supplies: An Illustrated Manual on the Identification, Significance, and Control of Algae in Water Supplies*, Public Health Service Publication No. 657 (reprint, 1967). U.S. Department of Health, Education, and Welfare, Public Health Service, Division of Water Supply and Pollution Control, Washington, DC.
- Perry, R.H. and Chilton, C.H. 1973. *Chemical Engineer's Handbook*, 5th ed. McGraw-Hill Book Co., Inc., New York.

- Polson, A. 1950. "Some Aspects of Diffusion in Solution and a Definition of a Colloidal Particle," *Journal of Physical Colloid Chemistry*, 54: 649.
- Qi, S., Adham, S.S., Snoeyink, V.L., and Lykins, B.W. 1994. "Prediction and Verification of Atrazine Adsorption by PAC," *Journal of Environmental Engineering*, 120(1): 202.
- Radke, C.J. and Prausnitz, J.M. 1972. "Thermodynamics of Multisolute Adsorption from Dilute Liquid Solutions," *AIChE Journal*, 18(4): 761.
- Randtke, S.J. and Snoeyink, V.L. 1983. "Evaluating GAC Adsorptive Capacity," *Journal of the American Water Works Association*, 75(8): 406.
- Rohlich, G.A. and Sarles, W.B. 1949. "Chemical Composition of Algae and Its Relationship to Taste and Odor," *Taste and Odor Journal*, 18(10): 1.
- Roy, D., Wang, G.-T., and Adrian, D.D. 1993. "Simplified Calculation Procedure for Carbon Adsorption Model," *Water Environment Research*, 65(6): 781.
- Snoeyink, V.L. 1990. "Adsorption of Organic Compounds," p. 781 in *Water Quality and Treatment: A Handbook of Community Water Supplies*, 4th ed. American Water Works Association, F.W. Pontius, ed., McGraw-Hill, Inc., New York.
- Summers, R.S., Hooper, S.M., Solarik, G., Owen, D.M., and Hong, S. 1995. "Bench-Scale Evaluation of GAC for NOM Control," *Journal of the American Water Works Association*, 87(8): 69.
- Suzuki, M. and Kawazoe, K. 1975. "Effective Surface Diffusion Coefficients of Volatile Organics on Activated Carbon During Adsorption from Aqueous Solution," *Journal of Chemical Engineering of Japan*, 8(5): 379.
- Thimann, K.V. 1963. *The Life of Bacteria: Their Growth, Metabolism, and Relationships*, 2nd ed. The Macmillan Company, New York.
- Traegner, U.K. and Suidan, M.T. 1989. "Parameter Evaluation for Carbon Adsorption," *Journal of Environmental Engineering*, 115(1): 109.
- Turre, G.J. 1942. "Pollution from Natural Sources, Particularly Algae," p. 17 in *Taste and Odor Control in Water Purification*, West Virginia Pulp and Paper Company, Industrial Chemical Sales Division, New York.
- von Dreuseche, C. 1981. "Regeneration systems," p. 137 in *Activated Carbon for Wastewater Treatment*, J.R. Perrich, ed., CRC Press, Boca Raton, FL.
- Wagner, N.J. and Julia, R.J. 1981. "Activated Carbon Adsorption," p. 41 in *Activated Carbon for Wastewater Treatment*, J. R. Perrich, ed., CRC Press, Boca Raton, FL.
- Wakao, N. and Funazkri, T. 1978. "Effect of Fluid Dispersion Coefficients in Dilute Solutions," *Chemical Engineering Science*, 33: 1375.
- Weber, W.J., Jr., and Crittenden, J.C. 1975. "MADAM I: A numeric method for design of adsorption systems," *Journal of the Water Pollution Control Federation*, 47(5): 924.
- Wilke, C.R. and Chang, P. 1955. "Correlation of Diffusion Coefficients in Dilute Solutions," *American Institute of Chemical Engineering Journal*, 1: 264.
- Williamson, J.E., Bazaire, K.E., and Geankoplis, C.J. 1963. "Liquid-Phase Mass Transfer at Low Reynolds Numbers," *Industrial and Engineering Chemistry Fundamentals*, 2(2): 126.

9.8 Aeration and Gas Exchange

Equilibria and Kinetics of Unreactive Gases

Equilibria

According to Henry's Law, at equilibrium, the concentration of a dissolved gas in a liquid is proportional to the partial pressure of the gas in the gas phase (Brezonik, 1994):

$$C = K_H p \quad (9.313)$$

where C = the concentration of dissolved gas in the liquid (kg/m^3 or lb/ft^3)
 K_H = the Henry's Law constant ($\text{kg}/\text{m}^3 \cdot \text{Pa}$ or $\text{lb} \cdot \text{ft}/\text{lbf}$)
 p = the partial pressure of the dissolved gas in the gas phase (Pa or lb/ft^2)

Equation (9.313) can be written in a variety of ways. The pressure on the right-hand side can be replaced by a concentration, in which case the Henry's Law constant takes on the units of a volume ratio, e.g., $\text{m}^3 \text{ gas}/\text{m}^3 \text{ liquid}$. This is frequently (and incorrectly) called the dimensionless Henry's Law constant. Also, it is often convenient to work in moles or pound-moles instead of kilograms or pounds. Other variants are discussed later in the section entitled "Air Stripping of Volatile Organic Substances."

Equation (9.313) is often written with the constant on the left-hand side:

$$p = HC \quad (9.314)$$

where H = the (reciprocal) Henry's Law constant ($\text{Pa} \cdot \text{m}^3/\text{kg}$ or $\text{lb}/\text{lb} \cdot \text{ft}$).

Equation (9.313) will be used in order that the symbol H may be used without confusion for depth in various mass transfer formulae.

Mass Transfer Kinetics

The simplest model of mass transfer between two phases is the Lewis–Whitman two-film theory (Brezonik, 1994). It is assumed that a "stagnant" film exists on each side of the phase interface. Each film exists only statistically. Its fluid properties may differ from the bulk fluid only on average and not at each instant. Its thickness depends on the details of the flow regime in the bulk fluid. Mass transport through each film is supposed to occur by molecular diffusion, and Fick's Law applies. If the films are in steady state (which does not mean that the bulk fluids are, although they may be), the total mass flux through each film will be the same, and the fluxes will be proportional to the pressure or concentration differences across the films:

$$\underbrace{\vec{F}}_{\text{total flux}} = \underbrace{k_g \left(\frac{p - p_i}{RT} \right)}_{\text{flux through gas film}} = \underbrace{k_\ell (C_i - C)}_{\text{flux through liquid film}} \quad (9.315)$$

where C = the gas concentration in the bulk liquid (mol/m^3 or $\text{lb mol}/\text{ft}^3$)
 C_i = the gas concentration in the liquid at the gas/liquid interface (mol/m^3 or $\text{lb mol}/\text{ft}^3$)
 F = the total flux through the two films ($\text{mol}/\text{m}^2 \cdot \text{s}$ or $\text{lb mol}/\text{ft}^2 \cdot \text{sec}$)
 k_g = the gas film mass transfer coefficient (m/s or ft/sec)
 k_ℓ = the liquid film mass transfer coefficient (m/s or ft/sec)
 p = the partial pressure of the dissolving gas in the bulk gas phase (Pa or lb/ft^2)
 p_i = the partial pressure of the dissolving gas at the gas/liquid interface (Pa or lb/ft^2)
 R = the gas constant ($8.314 \text{ J}/\text{mol} \cdot \text{K}$ or $1,545.356 \text{ ft} \cdot \text{lb}/\text{lb mol} \cdot \text{°R}$)
 T = the absolute temperature (K or °R)

Henry's law connects the interfacial partial pressure and the interfacial dissolved gas concentration, and it also allows the bulk gas-phase partial pressure to be expressed as the equivalent gas solubility:

$$C_i = K_H p_i \quad (9.316)$$

$$C_s = K_H p \quad (9.317)$$

where C_s = the dissolved gas concentration equivalent to the gas's partial pressure in the gas phase, its equilibrium concentration (kg/m^3 or lb/ft^3).

The overall concentration difference, $C_s - C$, may be partitioned as follows:

$$C_s - C = (C_s - C_i) + (C_i - C) \quad (9.318)$$

$$C_s - C = K_H(p - p_i) + (C_i - C) \quad (9.319)$$

The pressures and concentrations may be eliminated via the flux relationships in Eq. (9.315), and the overall liquid film mass transfer coefficient may be defined as follows:

$$\frac{1}{K_\ell} = \frac{RTK_H}{k_g} + \frac{1}{k_\ell} \quad (9.320)$$

where K_ℓ = the overall liquid film mass transfer coefficient (m/s or ft/sec); = $F/C_s - C$.

A similar analysis, which starts by writing the overall pressure difference analogously to Eq. (9.318), yields,

$$\frac{RT}{K_g} = \frac{RT}{k_g} + \frac{1}{k_\ell K_H} \quad (9.321)$$

where K_g = the overall gas film mass transfer coefficient (m/s or ft/sec)

$$= F/p - p_{eq}$$

p_{eq} = the gas partial pressure equivalent to the bulk liquid-phase concentration (Pa or lbf/ft²)

$$= K_H C$$

If the Henry's law constant and the flux are defined in terms of molar concentration in the gas and liquid phases, the product RT does not appear in Eqs. (9.341), (9.347) or (9.348).

Note that the two overall transfer coefficients are connected by the Henry's Law constant:

$$K_H = \frac{K_g}{K_\ell} = \frac{RT(C_s - C)}{p - p_{eq}} \quad (9.322)$$

It is a matter of convenience as to which overall mass transfer coefficient is employed. If K_H is small, then K_ℓ is approximately equal to k_ℓ . Similarly, if K_H is large, then K_g is nearly equal to k_g . Furthermore, a large Henry's Law constant means that K_g is larger than K_ℓ , the mass transfer rate is limited by diffusion through the water film, and the concentration gradient across the water film is large. Conversely, a small Henry's Law constant means that mass transfer is controlled by diffusion through the gas film, and the pressure gradient across the gas film is large.

The underlying film mass transfer coefficients are supposed to depend upon the molecular diffusivities of the substances. Depending on whether the fluid regime is laminar, transitional, or turbulent (which affects the film structure), the dependency is to the first power of the diffusivity or to its square root. The diffusivity depends on the reciprocal square root of the relative molecular weight. Consequently, if the mass transfer coefficient for one substance is known, the coefficient for another can be estimated (Brezonik, 1994):

$$\frac{k_{r1}}{k_{r2}} = \left(\frac{D_{r1}}{D_{r2}} \right)^n = \left(\frac{M_{r2}}{M_{r1}} \right)^{n/2} \quad (9.323)$$

$$\frac{k_{g1}}{k_{g2}} = \left(\frac{D_{g1}}{D_{g2}} \right)^n = \left(\frac{M_{r2}}{M_{r1}} \right)^{n/2} \quad (9.324)$$

where D_{ij} = the diffusivity of the j -th substance in the i -th phase (m²/s or ft²/sec)
 M_{rj} = the relative molecular weight of the j -th substance (g/mol or lb/lb-mol).

The exponent n in Eq. (9.324) varies from 0.5 under turbulent conditions to 1 under laminar and must be determined experimentally (Brezonik, 1994).

The diffusivities can be estimated by using Eqs. (9.277), (9.278), or (9.279), presented above.

K_g and K_l are areal mass transfer coefficients, because the flux must be multiplied by the interfacial area to get the total rate of mass transfer. In many systems, the interfacial area cannot be determined, but the gas or liquid volumes can. It is then easier to use an overall volumetric mass transfer coefficient. The areal and volumetric coefficients are related by,

$$K_l a = \frac{K_g A}{V} \quad (9.325)$$

where A = the (possibly unknown) interfacial area (m² or ft²)
 $K_l a$ = the overall volumetric mass transfer coefficient (per sec).

Oxygen Transfer

Oxygen is an unreactive, high Henry's Law constant gas, with gas transfer kinetics that are liquid film limited.

Oxygen Solubility

The solubility of oxygen depends on the temperature of the water, the humidity of the air, and the mean submergence of the gas bubbles as they rise from the diffusers to the tank surface. Henry's Law for oxygen solubility is as follows:

$$C_s = K_H p_{O_2} \quad (9.326)$$

where C_s = the solubility of oxygen in water (kg/m³ or lb/ft³)
 K_H = the Henry's Law equilibrium constant (kg/m³·Pa or lb/ft³·lbf)
 p_{O_2} = the partial pressure of oxygen in the gas phase (Pa or lbf/ft²)

Because dry air is 20.946% by volume oxygen (Weast, Astle, and Beyer, 1983), Henry's Law can also be written as,

$$C_s = 0.20946 K_H p_{da} \quad (9.327)$$

where p_{da} = the pressure of dry air (Pa or lbf/ft²).

Air usually contains some water vapor, and Henry's Law for humid air is,

$$C_s = 0.20946 K_H (p_{ha} - p_v) \quad (9.328)$$

where p_v = the pressure of the water vapor (Pa or lbf/ft²).

By convention, tabulated values of oxygen solubility are given for standardized conditions of 1 atmosphere (101.325 kPa or 2116.22 lbf/ft²) total humid air pressure and 100% relative humidity in the gas phase:

$$C'_s = 0.20946 K_H (p_{sa} - p_{vsat}) \quad (9.329)$$

where C'_s = oxygen's solubility in pure water under standard conditions or 20°C and 1 atm total pressure of water-saturated air (kg/m³ or lb/ft³) and p_{vsat} = the vapor pressure of water at 20°C (Pa or lbf/ft²).

TABLE 9.16 Solubilities of Oxygen in Pure Water in Contact with Water Saturated Air at 1 atm Total Pressure

Temp. (°C)	Oxygen Solubility (mg/L) for Salinity (g/kg) of					
	0.0	0.5	1.0	1.5	2.0	2.5
0	14.62	14.57	14.52	14.47	14.42	14.37
5	12.77	12.73	12.69	12.64	12.60	12.56
10	11.29	11.25	11.22	11.18	11.14	11.11
15	10.08	10.05	10.02	9.99	9.96	9.93
20	9.09	9.07	9.04	9.01	8.99	8.96
25	8.26	8.24	8.22	8.19	8.17	8.15
30	7.56	7.54	7.52	7.50	7.48	7.46
35	6.95	6.93	6.91	6.89	6.88	6.86
40	6.41	6.40	6.38	6.36	6.35	6.33
45	5.93	5.92	5.90	5.89	5.87	5.86
50	5.49	5.48	5.47	5.45	5.44	5.43

Computed from formula of Joint Editorial Board, 1992. *Standard Methods for the Examination of Water and Wastewater*, 18th ed. American Public Health Association, Washington, DC.

Because the vapor pressure of water depends only on temperature, one can also write,

$$P_{sa} - P_{vsat} = c \cdot P_{sa} \quad (9.330)$$

$$C'_s = 0.20946 \cdot c \cdot K_H P_{sa} \quad (9.331)$$

The value of c varies from about 0.993 to 0.905 as the temperature increases from 0 to 45°C.

Standard values of the oxygen solubility are given in [Table 9.16](#). These concentrations may be calculated from (Joint Editorial Board, 1992):

$$\ln C'_s = -139.444 \ln T + \frac{157.570 \times 10^3}{T} - \frac{66.423 \times 10^6}{T^2} + \frac{12.438 \times 10^9}{T^3} - \frac{862.1949 \times 10^9}{T^4} - S(\text{‰}) \left[0.017674 - \frac{10.754}{T} + \frac{2140.7}{T^2} \right] \quad (9.332)$$

where $S(0/00)$ = the salinity (g “dissolved solids”/kg water)

T = the absolute temperature in K.

The salinity is discussed below.

Salinity and Chlorinity

The solubilities of dissolved gases are reduced by the presence of dissolved salts, which is called the “salting out” effect (Glasstone, 1947).

The original definition of “salinity” was “mass of salt per unit mass of seawater.” This proved to be a difficult chemical determination, because simple drying leads to loss of hydrogen chloride and carbon dioxide, and the residue readily absorbs moisture from the atmosphere (Riley and Chester, 1971). The definition due to Knudsen is that the salinity is the grams of dissolved inorganic matter in 1 kg of water after the carbonate has been replaced by oxide, and bromide and iodide have been replaced by chloride. This would be approximately equivalent to the ash left in a volatile solids test of fresh water.

It is simpler to measure the total halides by a silver titration. The “chlorinity” is defined to be the grams of silver needed to precipitate all the halides in 328.5233 g of water. With this definition, the empirical relationship between salinity and chlorinity is as follows (Riley and Chester, 1971):

$$S(\text{‰}) = 0.03 + 1.805Cl(\text{‰}) \quad (9.333)$$

Nowadays, salinity is determined via conductance measurements. The currently accepted formula is below (Lewis, 1980; Perkin and Lewis, 1980):

$$S(\text{‰}) = \sum_{j=0}^5 [a_j + b_j f(T)] R_T^{j/2} \quad (9.334)$$

$$R_T = \frac{R}{R_p r_T} \quad (9.335)$$

$$R_p = 1 + \frac{A_1 p + A_2 p^2 + A_3 p^3}{1 + B_1 T + B_2 T^2 + B_3 R + B_4 R T} \quad (9.336)$$

$$r_T = c_0 + c_1 T + c_2 T^2 + c_3 T^3 + c_4 T^4 \quad (9.337)$$

where $A_1, A_2, A_3 = 2.070 \times 10^{-5}, -6.370 \times 10^{-10}, 3.989 \times 10^{-15}$
 $a_0, a_1, a_2, a_3, a_4, a_5 = 0.0080, -0.1692, 25.3851, 14.0941, -7.0261, 2.7081$
 $B_1, B_2, B_3, B_4 = 3.426 \times 10^{-2}, 4.464 \times 10^{-4}, 4.215 \times 10^{-1}, 3.107 \times 10^{-3}$
 $b_0, b_1, b_2, b_3, b_4, b_5 = 0.0005, -0.0056, -0.0066, -0.0375, 0.0636, 0.0144$
 $c_0, c_1, c_2, c_3, c_4 = 0.6766097, 0.0200564, 1.104259 \times 10^{-4}, 6.6698 \times 10^{-7}, 1.0031 \times 10^{-9}$
 $f(T) = T - 15/1 + 0.0162(T - 15)$

p = the gage pressure of the *in situ* sample in decibars

R = the ratio of the measured *in situ* conductivity of the sample to the conductivity of a solution containing 32.4356 g KCl in 1 kg solution at 15°C and 1 atm total pressure

R_p = a pressure correction factor (dimensionless)

r_T = a temperature correction factor (dimensionless)

T = the *in situ* sample temperature in °C

Equation (9.334) is valid for salinities ranging from 2 to 39 g/kg, temperatures from -2 to 35°C, and pressures from 0 to about 2000 decibars. The pressure correction factor can be ignored in most treatment plant designs.

For the lower salinities normally encountered in water and wastewater treatment (0 to 1 g/kg), the following formula may be used (Hill and Dauphinee, 1986):

$$S(\text{‰}) = \sum_{j=0}^5 [a_j + b_j f(T)] R_T^{j/2} - \frac{0.0080}{1 + 600R_T + 1.6 \times 10^5 R_T^2} - \frac{0.0005 f(T)}{1 + 10R_T + 1000R_T^{3/2}} \quad (9.338)$$

Effect of Pressure

An air bubble just released from a diffuser is subjected to a total pressure equal to the local barometric pressure plus the hydrostatic head due to the submergence, $p_b + \gamma h$. Air bubbles in contact with water quickly reach the water temperature and become saturated with water vapor, so the dry air pressure in the bubble is $p_b + \gamma h - p_{vsat}$. The partial pressure of oxygen near the diffuser would be $0.20946(p_b + \gamma h - p_{vsat})$.

The hydrostatic head falls as the bubble rises. Moreover, the volume percentage of oxygen in the bubble declines as oxygen is absorbed by the surrounding water. Consequently, one needs to average hydrostatic pressure and bubble oxygen pressure to get an average aeration tank solubility. The result would be as follows:

$$C_s = 0.20946 \bar{f} K_H (p_b + \frac{1}{2} \gamma h - p_{vsat}) \quad (9.339)$$

TABLE 9.17 Densities of Pure Water at Selected Temperature

Temperature (°C)	Mass Density (kg/m ³)	Weight Density (N/m ³)	Temperature (°C)	Mass Density (kg/m ³)	Weight Density (N/m ³)
0	999.84	9805.1	25	997.04	9777.6
5	999.96	9806.2	30	995.65	9764.0
10	999.70	9803.7	35	994.03	9748.1
15	999.09	9797.7	40	992.02	9728.4
20	998.20	9789.0	45	990.21	9710.6

Recalculated from Dean, J.A. 1992. *Lange's Handbook of Chemistry*, 14th ed. McGraw-Hill, Inc., New York.

TABLE 9.18 Vapor Pressures of Pure Water in Contact with Air at Selected Temperatures

Temperature (°C)	Vapor Pressure (kPa)	Vapor Pressure (lbf/in. ²)	Temperature (°C)	Vapor Pressure (kPa)	Vapor Pressure (lb/in. ²)
0	0.615	0.0892	25	3.192	0.4629
5	0.879	0.1275	30	4.275	0.6201
10	1.237	0.1794	35	5.666	0.8218
15	1.717	0.2490	40	7.432	1.0780
20	2.356	0.3417	45	9.623	1.3956

Recalculated from Dean, J.A. 1992. *Lange's Handbook of Chemistry*, 14th ed. McGraw-Hill, Inc., New York.

where \bar{f} = the depth-averaged ratio of the oxygen partial pressure at any depth to the initial oxygen partial pressure (dimensionless)
 h = the depth of submergence of the diffuser (m or ft)
 ν = the weigh density of water (N/m³ or lbf/ft³)

The oxygen transfer efficiency is typically around 10%, so \bar{f} is typically around 0.95.

The mean oxygen solubility in an aeration tank, corrected for all these effects, is related to the standard oxygen solubility by,

$$\bar{C}_s = C'_s \cdot \frac{\bar{f}}{c} \cdot \frac{p_b + \frac{1}{2}\gamma h - p_{vsat}}{p_{sa}} \quad (9.340)$$

where \bar{C}_s = the depth-averaged oxygen solubility (kg/m³ or lb/ft³).

The ratio \bar{f}/c ranges from about 0.96 to 1.05 as the temperature increases from 0 to 45°C, but under summer conditions in the temperate zone, which usually control the design, the ratio is about 0.99.

Density and vapor pressure data for water are given in [Tables 9.17](#) and [9.18](#), respectively. Air properties versus elevation above or below sea level are given in [Table 9.19](#).

Gas Diffusers

There are two broad classes of air diffusion devices, based on bubble size — coarse bubble and fine bubble. Coarse bubble diffusers produce air bubbles that are 6 to 10 mm in diameter, and new fine bubble diffusers produce bubbles that are 2 to 5 mm in diameter.

The standard oxygen transfer efficiencies of several kinds of diffusers are given in [Table 9.20](#). It should be noted that the fine bubble systems are generally two to three times as efficient as coarse bubble systems. The cost of the increased efficiency is additional maintenance; the benefit is reduced energy usage. Nowadays, fine bubble systems are cost-effective.

Coarse Bubble Diffusion

The most common coarse bubble diffusers consist of perforated pipes and valved orifices. Such devices have low transfer efficiencies, but they resist clogging. Coarse bubble diffusers are generally installed along the bottom of one or both walls to develop spiral flow.

TABLE 9.19 Properties of the Standard Atmosphere vs. Altitude

Altitude Above Mean Sea Level (m)	Pressure (kPa)	Density (kg/m ³)	Absolute Viscosity (N·s/m ²)	Temperature (K)
-1000	113.93	1.3470	1.8206×10^{-5}	294.65
-500	107.47	1.2849	1.8050×10^{-5}	291.40
0	101.325	1.2250	1.7894×10^{-5}	288.15
500	95.461	1.1673	1.7737×10^{-5}	284.90
1000	89.876	1.1117	1.7579×10^{-5}	281.65
1500	84.559	1.0581	1.7420×10^{-5}	278.40
2000	79.501	1.0066	1.7260×10^{-5}	275.15
2500	74.691	0.9570	1.7099×10^{-5}	271.91
3000	70.121	0.9092	1.6938×10^{-5}	268.66

Source: Weast, R.C., Astle, M.J., and Beyer, W.H. 1983. *CRC Handbook of Chemistry and Physics*, 64th ed, CRC Press, Boca Raton, FL.

TABLE 9.20 Comparative Efficiencies of Diffusers in Clean Water at 15-ft Submergence

Diffuser System	Airflow Rate (scfm/diffuser)	Standard Oxygen Transfer Efficiency (%)
Ceramic plate grids	2.0–5.0 (scfm/ft ²)	26–33
Ceramic disc grids	0.4–3.4	25–40
Ceramic dome grids	0.5–2.5	27–39
Porous plastic disc grids	0.6–3.5	24–35
Perforated membrane grids	0.5–20.5	16–38
Rigid porous tube grids	2.4–4.0	28–32
Rigid porous tube in dual spiral roll	3–11	17–28
Rigid porous tube in single spiral roll	2–12	13–25
Nonrigid porous tube grid	1–7	26–36
Nonrigid porous tube in single spiral roll	2–7	19–37
Perforated membrane grid	1–4	22–29
Perforated membrane mid-width	2–6	16–19
Perforated membrane mid-width	2–12	21–31
Perforated membrane in single spiral roll	2–6	15–19
Coarse bubble in dual spiral roll	3.3–9.9	12–13
Coarse bubble mid-width	4.2–45	10–13
Coarse bubble in single spiral roll	10–35	9–12

Source: ASCE Committee on Oxygen Transfer. 1989. *Design Manual: Fine Pore Aeration Systems*, EPA/625/1–89/023, U.S. Environmental Protection Agency, Office of Research and Development, Center for Environmental Research Information, Risk Reduction Engineering Laboratory, Cincinnati, OH.

The “oxygen transfer rate” (OTR) for a completely mixed reactor is,

$$R = \alpha \cdot K_{\ell} a \cdot (\beta \cdot C_s - C) \cdot V \quad (9.341)$$

- where
- C = the oxygen concentration in the aeration tank (kg/m³ or lb/ft³)
 - C_s = the oxygen solubility in the aeration tank under the given temperature and diffusers submergence (kg/m³ or lb/ft³)
 - $K_{\ell} a$ = the volumetric mass transfer coefficient (per sec)
 - R = the oxygen transfer rate (kg/s or lb/sec)
 - V = the aeration tank volume (m³ or ft³)

TABLE 9.21 Observed and Standard Oxygen Transfer Efficiencies at Selected Wastewater Treatment Plants

Location	System	Observed Transfer Efficiency (%)	Average Alpha Value	Range of Alpha Values	Expected Efficiency under Standard Conditions (%)
Madison, WI	Ceramic grid, step feed	17.8	0.64	0.42–0.98	25–37
Whittier Narrows, CA	Ceramic grid, plug flow	11.2	0.45	0.35–0.60	25–37
Seymour, WI	Ceramic grid, plug flow	16.5	0.66	0.49–0.75	25–37
Lakewood, OH	Ceramic grid, plug flow	14.5	0.51	0.44–0.57	25–37
Lakewood, OH	Ceramic grid, plug flow	8.9	0.31	0.26–0.37	25–37
Madison, WI	Ceramic and plastic tubes, step feed	11.0	0.62	0.46–0.85	13–32
Madison, WI	Wide-band, fixed orifice nonporous diffusers, step feed	10.0	1.07	0.83–1.19	9–13
Orlando, FL	Wide-band, fixed orifice, nonporous diffusers, complete mix	7.6	0.75	0.67–0.83	9–13
Nassau Co., NY	Flexible membrane tubes, plug flow	7.6	0.36	0.27–0.42	15–29
Whittier Narrows, CA	Jet aerators, plug flow	9.4	0.58	0.48–0.72	15–24
Brandon, WI	Jet aerators, complete mix	10.9	0.45	0.40–0.50	15–24
Brandon, WI	Jet aerators, complete mix	7.5	0.47	0.46–0.48	15–24

Source: Joint Task Force of the Water Pollution Control Federation and the American Society of Civil Engineers. 1988. *Aeration: A Wastewater Treatment Process*, WPCF Manual of Practice No. FD-13, ASCE Manuals and Reports on Engineering Practice No. 68. Water Pollution Control Federation, Alexandria, VA; American Society of Civil Engineers, New York.

α = the ratio of the mass transfer coefficient under conditions in the aeration tank to the mass transfer coefficient under standard conditions (dimensionless)

β = the ratio of the oxygen solubility for the salinity in the aeration tank to the oxygen solubility in pure water (dimensionless)

The alpha and beta values depend on water composition, and alpha also depends on the aeration equipment. They should be determined by field testing.

Beta is generally near 1, unless the salinity of the water is high. The effect is accounted for by Eq. (9.315) and Table 9.16. And, if oxygen solubilities are calculated from Eq. (9.315), beta should be set to unity.

Some aeration field data are given in Table 9.21 (Joint Task Force, 1988). For diffused air and oxygen systems, the alpha value for raw and settled municipal wastewater is about 0.2 to 0.3; it rises to about 0.5 to 0.6 for conventional, unnitrified effluents and to about 0.8 to 0.9 for highly treated, nitrified effluents. Alpha values for fine bubble diffusers are smaller than those for coarse bubble systems. For surface aeration systems, the alpha value for raw and settled municipal wastewater is about 0.6; it may rise to 1.2 for clean water.

The volumetric mass transfer coefficient is temperature dependent (Stenstrom and Gilbert, 1981):

$$\frac{K_L a(T_1)}{K_L a(T_0)} = 1.024^{T_1 - T_0} \tag{9.342}$$

where T_0 = the reference temperature in °C
 T_1 = the aeration tank temperature in °C.

The usual reference temperature is 20°C.

The so-called “standard oxygen transfer rate” (SOTR) of equipment is usually reported under standard conditions of clean water, zero dissolved oxygen, 20°C, 1 standard atmosphere (101.325 kPa or 2116.22 lbf/ft²) of ambient air pressure, and a specified depth of submergence. The SOTR is calculated as,

$$R_{std} = K_L a \cdot C_s \cdot V \tag{9.343}$$

where R_{std} = the standard oxygen transfer rate (kg/s or lb/sec).

The conversion of SOTRs to OTRS is as follows:

$$\frac{R}{R_{std}} = \frac{\alpha \cdot 1.024^{T-20} \cdot [\beta \cdot C_s(T) - C]}{C_s(20^\circ\text{C})} \quad (9.344)$$

The oxygen transfer efficiency (OTE) is the ratio of the oxygen absorbed to the oxygen supplied in the airflow through the diffuser:

$$E_{O_2} = \frac{R}{0.20946 Q_a \rho_a M_{r,O_2}} \quad (9.345)$$

where E_{O_2} = the oxygen transfer efficiency (dimensionless)

M_{r,O_2} = the relative molecular weight of oxygen (31.998, either g/mol or lb/lb-mol)

Q_a = the airflow rate under standard conditions of 1 atm pressure and 0°C (m³/s or ft³/sec)

ρ_a = the molar oxygen density (mol/m³ or lb-mol/ft³)

The standard oxygen transfer efficiency (SOTE) is the efficiency for clean water at 20°C and 1 atm pressure at a specified submergence.

The molar density of oxygen can be calculated from the ideal gas law:

$$\rho_a = \frac{n}{V} = \frac{P}{RT} \quad (9.346)$$

Fine Bubble Diffusers

There are three types of fine bubble diffusers (ASCE Committee on Oxygen Transfer, 1989):

- Sintered ceramic plates made from alumina, aluminum silicate, and silica
- Rigid porous plastic plates and tubes, usually made from high-density polyethylene (HDPE) and styrene-acrylonitrile
- Nonrigid porous plates and tubes made from rubber and HDPE
- Perforated plastic membrane, both discs and tube sheaths, usually made from polyvinyl chloride (PVC) with added plasticizer

Presently, only the first and last types are in widespread use. The diffusers are installed as plate holders and air manifolds set on the aeration tank floor or as disc, dome, or tube diffusers attached to air manifolds that cover the tank floor and are set somewhat above it.

Fine bubble diffusers gradually lose oxygen transfer efficiency. This is usually modeled as (ASCE Committee on Oxygen Transfer, 1989),

$$R = \alpha \cdot F \cdot K_L a \cdot (\beta \cdot C_s - C) \cdot V \quad (9.347)$$

where F = the fouling factor (dimensionless).

The fouling factor decreases with time of service. This occurs because the diffuser pores accumulate airborne particulates and precipitates from the water (Type I) or because biofilm grows on the diffuser surface (Type II). For design purposes, the rate of fouling may be taken as constant so that the fouling factor may be modeled as,

$$F = 1.0 - k_f t \quad (9.348)$$

where k_f = the fouling rate (per sec), and t = the service time (sec).

Typical values for k_f range from 0.03 to 0.07 per month.

TABLE 9.22 Effect of Airflow Rate on Diffuser Oxygen Transfer Efficiency

Diffuser System	m
Ceramic dome grid	0.150
Ceramic disc grid	0.133
Ceramic disc grid	0.126
Rigid porous disc grid	0.097
Rigid porous tube in double spiral roll	0.240
Nonrigid tube in spiral roll	0.276
Perforate membrane disc grid	0.195
Perforated membrane disc grid (9 in.)	0.11
EPDM perforated membrane tube grid	0.150

Source: ASCE Committee on Oxygen Transfer, 1989. *Design Manual: Fine Pore Aeration Systems*, EPA/625/1-89/023. U.S. Environmental Protection Agency, Office of Research and Development, Center for Environmental Research Information, Risk Reduction Engineering Laboratory, Cincinnati, OH.

The standard oxygen transfer efficiencies of fine bubble diffusers depend somewhat on airflow rate (ASCE Committee on Oxygen Transfer, 1989):

$$\frac{E_{stdO_2,2}}{E_{stdO_2,1}} = \left(\frac{Q_{ad1}}{Q_{ad2}} \right)^m \quad (9.349)$$

Values of m for various diffusers are given in [Table 9.22](#).

Air Piping

The volumetric airflow rate for the piping temperature and pressure can be estimated from the ideal gas law:

$$\frac{p_2 Q_{a2}}{T_2} = \frac{p_{sa} Q_{Ra}}{T_{sc}} \quad (9.350)$$

- where
- p_2 = the blower outlet pressure (Pa or lbf/ft²)
 - p_{sa} = the pressure of the standard atmosphere (101.325 kPa or 2,116.22 lbf/ft²)
 - Q_a = the airflow rate (m³/s or ft³/sec)
 - Q_{Ra} = the required process airflow rate at standard conditions of 1 atm pressure and 0°C (m³/s or ft³/sec)
 - T_2 = the blower outlet temperature (K or °R)
 - T_{sc} = the temperature for standard conditions for gases (273.15 K or 491.67°R)

The piping inlet temperature may be estimated from the adiabatic polytropic process (Perry and Chilton, 1973),

$$T_2 = T_1 \left(\frac{p_2}{p_1} \right)^{(n-1)/n} \quad (9.351)$$

- where
- n = the exponent for the polytropic process (dimensionless)
 - = 1.40, for air
 - p_1 = the blower intake pressure (N/m² or lbf/ft²);

p_2 = the blower outlet pressure (N/m² or lbf/ft²)
 T_1 = the blower intake temperature (K or °R)
 T_2 = the blower outlet temperature (K or °R)

The blower power requirement is (Perry and Chilton, 1973),

$$P = \left(\frac{n}{n-1} \right) \rho_a Q_a R T_1 \left[\left(\frac{p_2}{p_1} \right)^{(n-1)/n} - 1 \right] \quad (9.352)$$

where P = the blower power (W or ft-lbf/sec)
 Q_a = the airflow rate (m³/s or ft³/sec)
 R = the gas constant 8314.510 J/mol·K or 1545.356 ft·lbf/lb-mol·°R)
 ρ_a = the mass density of the air (mol/m³ or lb-mol/ft³)

The blower power is the power in the compressed air, and the power required by the blower motor will be larger in inverse proportion to the blower efficiency.

For small temperature and pressure changes (less than 10%), air may be treated as an incompressible fluid (Metcalf & Eddy, Inc., 1991). The principle difference from water distribution is that the blower exit gas is hot (about 140°F to 180°F), and allowances must be made for piping expansion and contraction.

The headloss may be calculated using the Darcy–Weisbach equation and friction factors from the Moody diagram. The air density may be calculated from the ideal gas law. The viscosity of air is given by the Chapman–Enskog formula (Blevins, 1984):

$$\mu_a = 26.69 \times 10^{-7} \frac{M_{ra}^{1/2} T^{1/2}}{\sigma^2 \Omega_v} \quad (9.353)$$

$$\Omega_v = 1.147 \left(\frac{T}{T_e} \right)^{-0.145} + \left(\frac{T}{T_e} + 0.5 \right)^{-2.0} \quad (9.354)$$

where M_{ra} = the relative molecular weight for air (28.966 g/mol, for air)
 T = the air temperature in K
 T_e = the effective temperature of the force potential in K (78.6 K, for air)
 μ_a = the dynamic viscosity of air in N·s/m²
 σ = the collision diameter in Å (3.711 Å, for air)

Surface Aerators

The common surface aerators are the Kessener brush and its derivatives (brushes or discs mounted on a horizontal shaft and normally found in oxidation ditches), low-speed radial flow turbines and high-speed axial flow turbines (usually equipped with draft tubes and found in aerated lagoons).

Surface aerators are rated in terms of mass of oxygen transferred per unit time per unit power, e.g., kg/kW·s or lb/hp·hr. The design equation is shown below (Joint Task Force, 1988):

$$\frac{R/P}{R_{std}/P} = \frac{\alpha \cdot 1.024^{T-20} \cdot [\beta \cdot C_s(T) - C]}{C_s(20^\circ C)} \quad (9.355)$$

Both alpha and beta values are often reported to be about 1 in municipal wastewater. The usual theta value, 1.024, applies. Standard aeration rates for low-speed radial flow systems range from about 2 to 5 lb O₂/hp·hr; for high-speed axial flow aerators, from 2 to 3.6 lb O₂/hp·hr; and for brushes, from 1.5 to 3.6 lb O₂/hp·hr (Metcalf & Eddy, 1991).

TABLE 9.23 Acid Ionization Constants for Selected Gases (pK_a Values)

Acid	Temperature (°C)									
	0	5	10	15	20	25	30	35	40	50
NH ₄ ⁺	10.081	9.904	9.731	9.564	9.400	9.425	9.093	8.947	8.805	8.539
H ₂ CO ₃ [*]	6.577	6.517	6.465	6.429	6.382	6.352	6.327	6.309	6.296	6.285
HCO ₃ ⁻	10.627	10.558	10.499	10.431	10.377	10.329	10.290	10.250	10.220	10.172
HCl	—	—	—	—	—	-6.2	—	—	—	—
HCN	—	—	9.63	9.49	9.36	9.21	9.11	8.99	8.88	—
HOCl	7.82	7.75	7.69	7.63	7.58	7.54	7.50	7.46	—	7.05
H ₂ S	—	7.33	7.24	7.13	7.05	6.97	6.90	6.82	6.79	6.69
HS ⁻	—	13.5	—	13.2	—	12.90	12.75	12.6	—	—
H ₂ SO ₃	1.63	—	1.74	—	—	1.89	—	1.98	—	2.12
HSO ₃ ⁻	—	—	—	—	6.91	7.20	—	—	—	—
					(at 18°C)					
pK _w	14.938	14.727	14.528	14.340	14.163	13.995	13.836	13.685	13.542	13.275

Sources: Mostly from Dean, J.A., ed. 1992. *Lange's Handbook of Chemistry*, 14th ed. McGraw-Hill, Inc., New York. Supplemented by Weast, R.C., Astle, M.J., and Beyer, W.H. 1983. *CRC Handbook of Chemistry and Physics*, 64th ed. CRC Press, Inc., Boca Raton, FL; Blaedel, W. J. and Meloche, V.W. 1963. *Elementary Quantitative Analysis*, 2nd ed. Harper & Row, Pub., New York.

Absorption of Reactive Gases

Some gases react with water or with other solutes in it. If the reactions are fast (like most acid/base reactions), the reaction increases the amount of gas that is adsorbed and its adsorption rate.

Equilibria

Henry's Law applies only to the dissolved gas molecule and not to any of its reaction products.

Ammonia

Ammonia chemistry is outlined in Chapter 8. Ammonia reacts with water to form the ammonium ion, NH₄⁺:



The molar fraction of the total ammonia concentration that is unprotonated ammonia is,

$$f = \frac{[\text{NH}_3]}{[\text{NH}_3] + [\text{NH}_4^+]} = \frac{1}{1 + \frac{[\text{H}^+]}{K_a}} = \frac{1}{1 + \frac{K_b}{[\text{OH}^-]}} \quad (9.357)$$

where K_a = the acid ionization constant (mol/L)
 K_b = the base ionization constant (mol/L).

Values of the acid ionization constant for various temperatures are given in [Table 9.23](#).

Carbon Dioxide

Atmospheric carbon dioxide goes into solution, forming aqueous carbon dioxide, and this reacts with water to form carbonic acid (Stumm and Morgan, 1970):



The reaction in Eq. (9.358) goes virtually to completion, and dissolved carbon dioxide and carbonic acid are not distinguished by the usual analytical methods. Therefore, it is customary to define a “composite carbonic acid” concentration:

$$[H_2CO_3^*] = [H_2CO_3] + [CO_{2(aq)}] \quad (9.360)$$

At equilibrium, the ratio of $CO_{2(aq)}$ to H_2CO_3 is constant, depending only on temperature, so this convention merely introduces a constant factor into the equilibrium constants. The composite carbonic acid ionizes to produce bicarbonate, and bicarbonate ionizes to make carbonate:



The system is completed by the ionization of water:



The equilibrium constants for this system may be written as:

$$K_{HCO_2}^* = \frac{[H_2CO_3^*]}{p_{CO_2}} \quad (9.364)$$

$$K_1 = \frac{[H^+][HCO_3^-]}{[H_2CO_3^*]} \quad (9.365)$$

$$K_2 = \frac{[H^+][CO_3^{2-}]}{[HCO_3^-]} \quad (9.366)$$

$$K_w = [H^+][OH^-] \quad (9.367)$$

where $[X]$ = the activity of species X (moles/L), usually approximated as the molar concentration in dilute solutions

p_{CO_2} = the partial pressure of carbon dioxide in the atmosphere (atm).

Numerical values for these constants at several temperatures are given in [Table 9.23](#).

The molar concentrations of the various species can be written in terms of the proton concentration and the equilibrium constants by using Eq. (9.364) through (9.367) to eliminate variables:

$$f_o = \frac{[H_2CO_3^*]}{[H_2CO_3^*] + [HCO_3^-] + [CO_3^{2-}]} = \frac{1}{1 + \frac{K_1}{[H^+]} + \frac{K_1 K_2}{[H^+]^2}} \quad (9.368)$$

$$f_1 = \frac{[HCO_3^-]}{[H_2CO_3^*] + [HCO_3^-] + [CO_3^{2-}]} = \frac{1}{1 + \frac{[H^+]}{K_1} + \frac{K_2}{[H^+]}} \quad (9.369)$$

TABLE 9.24 Distribution of Alkaline Species for the Carbonate System

Ratio of Phenolphthalein to Total Alkalinity P/T	Bicarbonate (meq/L)	Carbonate (meq/L)	Hydroxide (meq/L)
0	T	0	0
$<1/2$	$T - 2P$	$2P$	0
$1/2$	0	$2P$ or T	0
$>1/2$	0	$2(T - P)$	$2P - T$
1	0	0	T

Source: Hardenbergh, W.A. and Rodie, E.B. 1963. *Water Supply and Waste Disposal*. International Textbook Co., Scranton, PA.

$$f_2 = \frac{[\text{CO}_3^{2-}]}{[\text{H}_2\text{CO}_3^*] + [\text{HCO}_3^-] + [\text{CO}_3^{2-}]} = \frac{1}{1 + \frac{[\text{H}^+]}{K_2} + \frac{[\text{H}^+]^2}{K_1 K_2}} \quad (9.370)$$

where f_0 = the molar fraction of the carbonate species in the form of the composite acidity (dimensionless)
 f_1 = the molar fraction of the carbonate species in the form of bicarbonate (dimensionless)
 f_2 = the molar fraction of the carbonate species in the form of carbonate (dimensionless)

The rather wide separation in the values of K_1 and K_2 and the fact that significant quantities of bicarbonate and hydroxide do not occur together make possible a simple procedure for determining the distribution of hydroxide, carbonate, and bicarbonate. The alkalinity titrated to pH 8.3 is called the “phenolphthalein alkalinity” (because phenolphthalein is used to detect the endpoint), and the total quantity of acid needed to reduce the pH from the original sample value past pH 8.3 down to pH 4.5 is traditionally called the “methyl orange alkalinity,” or total alkalinity (which is better, because bromcresol green is the preferred indicator). The ratio of these two values determines the distribution of carbonate forms, as indicated in [Table 9.24](#).

Chlorine

Chlorine gas readily dissolves in water according to Henry’s Law (Stover et al., 1986):

$$[\text{Cl}_2(\text{aq})] = K_H p_{\text{Cl}_2} \quad (9.371)$$

$$K_H = 4.805 \times 10^{-6} e^{2818.48/T} \quad (9.372)$$

where $[\text{Cl}_2(\text{aq})]$ = the concentration of molecular chlorine in mol/L
 K_H = Henry’s Law constant in mol/L·atm
 p_{Cl_2} = the partial pressure of molecular chlorine in the gas phase in atm
 T = the absolute temperature in K

Dissolved chlorine reacts strongly with water to form hypochlorous acid (White, 1986):



$$K_o = \frac{[\text{H}^+][\text{Cl}^-][\text{HOCl}]}{[\text{Cl}_2(\text{aq})]} \quad (9.374)$$

$$pK_o = -0.579 + \frac{1190.7}{T} \quad (9.375)$$

where T = the absolute temperature in K.

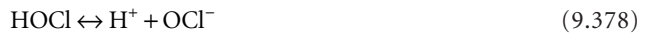
In pure water, the total concentration can be written as follows (Stover et al., 1986):

$$[\text{Cl}_2(\text{aq})] + [\text{HOCl}] = K_H P_{\text{Cl}_2} + (K_o K_H P_{\text{Cl}_2})^{1/3} \quad (9.376)$$

In buffered water with significant background chloride concentrations, the total solubility is as shown:

$$[\text{Cl}_2(\text{aq})] + [\text{HOCl}] = K_H P_{\text{Cl}_2} \left[1 + \frac{K_o}{[\text{H}^+][\text{Cl}^-]} + \frac{K_o K_a}{[\text{H}^+]^2[\text{Cl}^-]} \right] \quad (9.377)$$

The hypochlorous acid ionizes to form hypochlorite ion:



$$K_a = \frac{[\text{H}^+][\text{OCl}^-]}{[\text{HOCl}]} \quad (9.379)$$

$$pK_a = -10.069 + 0.025T - \frac{3000}{T} \quad (9.380)$$

where T = kelvin.

The molar fraction of hypochlorous acid depends strongly on pH and can be estimated from,

$$f = \frac{[\text{HOCl}]}{[\text{HOCl}] + [\text{OCl}^-]} = \frac{1}{1 + \frac{K_a}{[\text{H}^+]}} \quad (9.381)$$

Below pH 7, a mixture of hypochlorous acid and hypochlorite is found in nearly all un-ionized acid, but at about pH 9, hypochlorous acid comprises nearly all of the ion.

Values of the acid ionization constants are given in [Table 9.23](#).

Chlorine Dioxide

The solubility of chlorine dioxide follows Henry's Law (Haas, 1990):

$$C_{\text{ClO}_2} = K_H P_{\text{ClO}_2} \quad (9.382)$$

$$\ln K_H = 58.84621 + \frac{47.9133}{T} - 11.0593 \ln T \quad (9.383)$$

where C_{ClO_2} = the mole fraction of chlorine dioxide in water (dimensionless)

K_H = the Henry's Law constant per atm

P_{ClO_2} = the partial pressure of chlorine dioxide in the gas phase in atm

T = the absolute temperature in K

Above pH 9, chlorine dioxide disproportionates according to,



An equilibrium constant is not yet available.

Hydrogen Chloride

The solubility of hydrogen chloride in pure water ranges from 823 g/L at 0°C to 633 g/L at 40°C (Dean, 1992).

Hydrogen chloride is a strong acid with an acid ionization constant of about 1.3×10^6 (Dean, 1992) and is nearly completely ionized in water:



Hydrogen Cyanide

The solubility of hydrogen cyanide is virtually unlimited. The cyanide ion forms complexes with many metals, which further enhances the solubility.

Hydrogen cyanide is a weak acid:



$$K_a = \frac{[\text{H}^+][\text{CN}^-]}{[\text{HCN}]} \quad (9.387)$$

Values of the acid ionization constant for several temperatures are given in [Table 9.23](#).

Hydrogen Sulfide

The solubility of hydrogen sulfide in pure water ranges from about 7.1 g/L at 0°C to about 1.9 g/L at 50°C (Dean, 1992).

Hydrogen sulfide is a weak acid, and it dissociates twice as the pH is raised:



$$K_1 = \frac{[\text{H}^+][\text{HS}^-]}{[\text{H}_2\text{S}]} \quad (9.389)$$



$$K_2 = \frac{[\text{H}^+][\text{S}^{2-}]}{[\text{HS}^-]} \quad (9.391)$$

The sulfide ion forms highly insoluble precipitates with many metals, which greatly enhances its solubility. Values of the acid ionization constant are given in [Table 9.23](#).

Ozone

The solubility of ozone follows Henry's Law (Joint Task Force, 1990):

$$C_{\text{O}_3} = K_H P_{\text{O}_3} \quad (9.392)$$

$$K_H = \frac{1.29 \times 10^6}{T} - 3720.5 \quad (9.393)$$

where C_{O_3} = the ozone concentration in mg/L

K_H = the Henry's Law constant in mg/L·%

P_{O_3} = the partial pressure of ozone in the gas phase in % of one atm

T = the temperature in K

The units of pressure are somewhat peculiar. For example, if the exit gas from the generator is at 1 atm total pressure and 20°C, and if it contains 0.05% ozone, the solubility of ozone is 0.34 mg/L.

Ozone decomposes spontaneously, even in the absence of reductants.

Sulfur Dioxide

Sulfur dioxide is used as a reductant to remove excess chlorine following disinfection.

The solubility of sulfur dioxide in pure water ranges from 798 g/L at 0°C to about 188 g/L at 45°C (Dean, 1992).



$$C_{\text{SO}_2} = K_H p_{\text{SO}_2} \quad (9.395)$$

The Henry's Law constant is approximately 247, 75, and 22.9 g/L·atm at 4, 16, and 27°C, respectively (Stover et al., 1986).

Sulfur dioxide reacts with water to form sulfurous acid, which ionizes step-wise to form bisulfite and sulfite ions (Stover et al., 1986):



$$K_o = \frac{[\text{H}_2\text{SO}_3]}{[\text{SO}_2(\text{aq})]} \quad (9.397)$$



$$K_1 = \frac{[\text{H}^+][\text{HSO}_3^-]}{[\text{H}_2\text{SO}_3]} \quad (9.399)$$



$$K_2 = \frac{[\text{H}^+][\text{SO}_3^{2-}]}{[\text{HSO}_3^-]} \quad (9.401)$$

Acid ionization constants are given in [Table 9.23](#).

Kinetics

The effect of fast reactions is to increase the concentration gradient in the interfacial layers and, consequently, the rate of gas absorption. This is expressed mathematically and experimentally by an increase in the liquid film mass transfer coefficient, k_l (Sherwood, Pigford, and Wilke, 1975). The increase depends on the details of the reaction, including the other reactants, and must be determined empirically.

Air Stripping of Volatile Organic Substances

Nowadays, an important treatment process is the removal of volatile organic substances — many of which are toxic and/or carcinogenic — from water by air stripping in packed towers or by air diffusion or surface aeration in tanks.

Packed Towers

The common packing materials are 1 to 2 in Berl saddles, Pall rings, Rasching rings, plastic rods, spheres, and plastic Tellerettes. The air and water flow rates are countercurrent, with the water generally trickling down over the packing and the air being forced upwards through the bed by blowers.

If the contaminant concentration in water is dilute so that Henry's law governs its solubility, the required height of packing is given by the following (Sherwood, Pigford, and Wilke, 1975):

$$H = \left(\frac{Q_\ell/A}{K_\ell a} \right) \cdot \left(\frac{K_{HC} Q_a}{Q_\ell} \right) \cdot \ln \left[\frac{\left(C_{\ell,i} - \frac{C_{a,i}}{K_{HC}} \right) \left(\frac{K_{HC} Q_a}{Q_\ell} - 1 \right) + 1}{\left(C_{\ell,e} - \frac{C_{a,i}}{K_{HC}} \right) \left(\frac{K_{HC} Q_a}{Q_\ell} \right)} \right] \quad (9.402)$$

where A = the cross-sectional area of the packed tower (m^2 or ft^2)
 $C_{a,i}$ = the concentration of contaminant in the influent air (kg/m^3 or lb/ft^3)
 $C_{\ell,e}$ = the concentration of contaminant in the effluent water (kg/m^3 or lb/ft^3)
 $C_{\ell,i}$ = the concentration of contaminant in the influent water (kg/m^3 or lb/ft^3)
 H = the height of the packing (m or ft)
 K_{HC} = the so-called "dimensionless" Henry's law constant (m^3 water/ m^3 air or ft^3 water/ ft^3 air)
 $= C_a/C_\ell$
 K_ℓ = the overall areal liquid phase mass transfer coefficient for clean water (m/s or ft/sec)
 Q_a = the airflow rate (m^3/s or ft^3/sec)
 Q_ℓ = the water flow rate (m^3/s or ft^3/sec)

In environmental engineering practice, the influent air has no contaminant in it, so $C_{a,i}$ in Eq. (9.402) is zero. Henry's Law constants are given in a variety of units, and one must be careful to use the appropriate numerical value.

The principal problem in using Eq. (9.402) is evaluation of the overall mass transfer coefficient. This has been the subject of numerous studies, and the Onda correlations are currently preferred (Roberts et al., 1985; Lamarche and Droste, 1989; Staudinger, Knocke, and Randall, 1990):

$$\frac{A_w}{A_v} = 1 - \exp \left\{ -1.45 \cdot \left(\frac{\sigma_c}{\sigma_\ell} \right)^{0.45} \left(\frac{\rho_\ell Q_\ell/A}{A_v \mu_\ell} \right)^{0.1} \left[\frac{\rho_\ell^2 g}{A_v (\rho_\ell Q_\ell/A)^2} \right]^{0.05} \left[\frac{(\rho_\ell Q_\ell/A)^2}{\rho_\ell \sigma_\ell A_v} \right]^{0.2} \right\} \quad (9.403)$$

$$\frac{k_a}{A_v D_a} = 5.23 \cdot \left(\frac{\rho_a Q_a/A}{A_v \mu_a} \right)^{0.7} \left(\frac{\mu_a}{\rho_a D_a} \right)^{1/3} \quad (9.404)$$

$$k_\ell \left(\frac{\rho_\ell}{\mu_\ell g} \right)^{1/3} = 0.0051 \left(\frac{\rho_\ell Q_\ell}{A_w \mu_\ell} \right)^{2/3} \left(\frac{\mu_\ell}{\rho_\ell D_\ell} \right)^{0.5} (A_v d_p)^{0.4} \quad (9.405)$$

where A = the plan area of the packed tower (m^2 or ft^2)
 A_v = the specific surface area of the packing (m^2/m^3 or ft^2/ft^3)
 A_w = the wetted specific surface area of the packing (m^2/m^3 or ft^2/ft^3)
 D_a = the diffusivity of the contaminant vapor in air (m^2/s or ft^2/sec)
 D_ℓ = the diffusivity of the contaminant in water (m^2/s or ft^2/sec)
 d_p = the nominal packing size (m or ft)
 g = the acceleration due to gravity (9.80665 m/s² or 32.174 ft/sec²)
 k_a = the air film mass transfer coefficient (m/s or ft/sec)
 k_ℓ = the water film mass transfer coefficient (m/s or ft/sec)
 Q_a = the airflow rate (m^3/s or ft^3/sec)
 Q_ℓ = the water flow rate (m^3/s or ft^3/sec)
 μ_a = the dynamic viscosity of air ($N/m^2 \cdot s$ or $lbf/ft^2 \cdot sec$)

μ_ℓ = the dynamic viscosity of water (N/m²·s or lbf/ft²·sec)
 ρ_a = the mass density of air (kg/m³ or lb/ft³)
 ρ_ℓ = the mass density of water (kg/m³ or lb/ft³)
 σ_c = the critical surface tension of the packing (N/m or lbf/ft)
 σ_ℓ = the surface tension of water (N/m or lbf/ft)

Staudinger et al. (1990) estimated that the Onda correlations yield a $\pm 30\%$ error in the mass transfer rate, $K_\ell a$. LaMarche and Droste (1989) also found that the Onda predictions were uniformly too high, but their error was smaller. For design purposes, use 70% of the predicted $K_\ell a$.

Properties of Packings

Physical properties of common packing materials are given in [Table 9.25](#).

The critical surface tension is that which produces a contact angle of zero between the solid surface and the liquid film surface that is in contact with air (Adamson, 1982). [Table 9.26](#) lists some critical surface tensions.

Henry's Law Constants

Henry's Law can be written in several different ways, and each way assigns different units to the constant (Munz and Roberts, 1987):

$$p_i = K_{HXp} \cdot X_{\ell i} \quad (9.406)$$

$$p_i = K_{HCp} \cdot C_{\ell i} \quad (9.407)$$

$$C_{ai} = K_{HC} \cdot C_{\ell i} \quad (9.408)$$

The different constants are connected by the following:

$$K_{HC} = K_{HXp} \cdot \frac{v_\ell M_{r\ell}}{RT} \quad (9.409)$$

$$K_{HCp} = K_{HXp} \cdot v_\ell \quad (9.410)$$

where

- C_{ai} = the concentration of contaminant in the air (kg/m³ or lbm/ft³)
- $C_{\ell i}$ = the concentration of contaminant in the water (kg/m³ or lbm/ft³)
- K_{HC} = the so-called "dimensionless" Henry's law constant (m³ water/m³ air or ft³ water/ft³ air) = C_a/C_ℓ
- K_{HCp} = the Henry's Law constant (Pa·m³/kg or lbf·ft/lb)
- K_{HXp} = the Henry's Law constant (Pa in lbf/ft²)
- $M_{r\ell}$ = the molecular weight of water (18 g/mol or 18 lb/lb-mol)
- p_i = the partial pressure of species i in air (Pa or lbf/ft²)
- R = the gas constant (8.314 J/mol·K or 1545 ft·lbf/lb-mol·°R)
- T = the absolute temperature (K or °R)
- v_ℓ = the specific volume of water (m³/kg or ft³/lb)
- $X_{\ell i}$ = the mole fraction of species i in water (dimensionless)

Henry's Law constants for several important volatile organic compounds are listed in [Table 9.27](#). The temperature dependency is represented by an empirical fit to the van't Hoff relationship. This is done separately for each form of the constant, e.g.,

$$\log K_{HXp} = a - \frac{b}{T} \quad (9.411)$$

TABLE 9.25 Physical Properties of Packings

Packing	Nominal Size (in.)	Bulk Density (lb/ft ³)	Specific Surface Area (ft ² /ft ³)	Porosity (%)
Berl saddles, ceramic	2	39	32	72
	1½	40	46	71
	1	45	76	68
	¾	49	87	66
	½	54	142	62
	¼	56	274	60
Intalox saddles, ceramic	3	37	28	80
	2	42	36	79
	1½	42	59	80
	1	44	78	77
	¾	44	102	77
	½	45	190	78
Pall rings, ceramic	¼	54	300	75
	3	40	20	74
Pall rings, polypropylene	2	38	29	74
	¾	4.25	26	92
Pall rings, steel	2	4.5	31	92
	1½	4.75	39	91
	1	5.5	63	90
	5/8	7.25	104	87
	2	24	31	96
Raschig rings, carbon	1½	26	39	95
	1	30	63	94
	5/8	37	104	93
	3	23	19	78
	2	27	28	74
	1½	34	38	67
Raschig rings, ceramic	1	27	57	74
	¾	34	75	67
	½	27	114	74
	¼	46	212	55
	4	36	14	80
	3	37	19	75
	2	41	28	74
	1	46	36	68
	1	43	37	73
	1	42	58	74
Raschig rings, steel	¾	50	74	72
	½	55	112	64
	¼	60	217	62
	3	25	20	95
	2	37	29	92
	1	49	39	90
	1	71	56	86
	¾ (1/16 in wall)	94	75	80
	¾ (1/32 in wall)	52	81	89
5/8	62	103	87	
Tellerites, LDPE	½ (1/16 in wall)	132	111	73
	½ (1/32 in wall)	75	122	85
Tellerites, LDPE	1	10	76	83

Source: Perry, R.H. and Chilton, C.H., ed. 1973. *Chemical Engineer's Handbook*, 5th ed. McGraw-Hill, Inc., New York.

TABLE 9.26 Critical Surface Tensions
for Typical Materials

Material	Critical Surface Tension (dyne/cm)
Carbon	56
Ceramic	61
Glass	73
Parafin	20
Polyethylene	33
Polyvinyl chloride	40
Steel	75

Source: Onda, Takeuchi, and Koyama.1967.
Kagaku Kogaku, 31: 126.

$$\log K_{HC} = a' - \frac{b'}{T} \quad (9.412)$$

$$\log K_{HCP} = a'' - \frac{b''}{T} \quad (9.413)$$

where $a, a', a'' =$ empirical constants (dimensionless)
 $b, b', b'' =$ empirical constants (K or °R).

Diffused Air and Surface Aeration

Volatile organic contaminants can be removed by diffused and surface aeration. The laws governing oxygen transfer also apply. The gas and liquid film mass transfer coefficient s depends on molecular diffusivities, which in turn, depend on molecular weights. Therefore, if one knows k_ℓ and k_g for one substance in a particular mass transfer system, one can, in principal, calculate for any other substance. One needs to distinguish between surface aerators and diffused air, because the air bubbles accumulate contaminant as they rise through the liquid.

Surface Aerators

In the case of surface aerators, there is no contaminant concentration in the ambient air, so the solubility of the contaminant is zero. For a completely mixed reactor, the steady state mass balance is as follows (Roberts, Munz, and Dändliker, 1984):

$$Q_\ell(C_{\ell,i} - C_{\ell,e}) = K_\ell a_j \cdot C_{\ell,e} V \quad (9.414)$$

where $C_{\ell,e}$ = the concentration of contaminant in the effluent water (kg/m³ or lb/ft³)
 $C_{\ell,i}$ = the concentration of contaminant in the influent water (kg/m³ or lb/ft³)
 $K_\ell a_j$ = the overall volumetric liquid-phase mass transfer coefficient for species j (per sec)
 Q_ℓ = the water flow rate (m³/s or ft³/sec)
 V = the tank volume (m³ or ft³)

In the more general case of mixed-cells-in-series and in ideal plug flow, one gets the following:

$$\frac{C_{\ell,e}}{C_{\ell,i}} = \left[\frac{1}{1 + K_\ell a_j (V_1/Q_\ell)} \right]^n \quad (9.415)$$

TABLE 9.27 Henry's Law Constants for Volatile Organic Substances

Substance	K_{HC} at 20°C (m ³ water/m ³ air)	K_{Hxp} at 20°C (atm)	a, a'	b, b' (K)	Reference
Benzene			8.68	1852	3
	0.306	—	—	—	7
Bromoform	—	35	—	—	3
	0.017	—	4.729	1905	6
Carbon, tetrachloride	—	1290	10.06	2038	3
	0.98	—	5.853	1718	6
	0.936	—	—	—	7
Chlorobenzene	0.131	—	—	—	7
Chloroform	0.13	170	9.10	2013	3
	0.15	—	1.936	809.1	4
	0.12	—	4.990	1729	6
Chloromethane	—	480	6.93	1248	3
<i>p</i> -Dichlorobenzene	0.078	—	—	—	7
1,1-Dichloroethane			8.87	1902	3
	0.22	—	2.080	803.8	4
1,2-Dichloroethane	—	61	—	—	3
	0.046	—	5.156	1904	4
<i>cis</i> -1,2-Dichloro-ethylene	0.181	—	—	—	7
<i>trans</i> -1,2-Dichloro-ethylene	0.375	—	—	—	7
Dichlorodifluoro-methane	—	—	8.18	1470	3
	11	—	5.811	1399	6
1,2-Dichloromethane	—	—	7.92	1822	3
Dieldrin	—	0.0094	—	—	3
Diethyl ether	0.039	—	5.953	2158	4
Hexachloroethane	0.12	—	6.982	2320	6
Methylene chloride	0.077	—	—	—	7
Naphthalene	0.015	—	—	—	7
Pentachlorophenol	—	0.12	—	—	3
Phenol	11×10^{-6}	—	—	—	1
Tetrachloroethylene	—	1100	10.38	2159	3
	0.12	—	5.920	1802	6
	0.535	—	—	—	7
Toluene	—	340 (25°C)	—	—	3
	0.15	—	11.18	3518	4
	0.244	—	—	—	7
Toxaphene	—	3500	—	—	3
1,1,1-Trichloroethane	—	430	9.39	1993	3
	0.55	—	5.327	1636	6
	0.645	—	—	—	7
Trichloroethylene	—	550	8.59	1716	3
	0.37	—	2.189	767.8	4
	0.32	—	6.026	1909	6
	0.43	—	—	—	7
1,2,4-Trimethyl-benzene	—	353	—	—	3
	0.195	—	—	—	7
<i>o</i> -xylene	0.175	—	—	—	7
Vinyl chloride	—	3.55×10^5	—	—	3

Note: Reference 3 used Eq. (9.411) and calculated K_{Hxp} , References 4 and 6 used Eq. (9.412) and calculated K_{HC} .

Note: References are as follows:

1. Berger, B.B. 1983. *Control of Organic Substances in Water and Wastewater*, EPA-600/8-83-011. U.S. Environmental Protection Agency, Office of Research and Development, Washington, DC.
2. Gosset, J.M. 1987. "Measurement of Henry's Law Constants for C₁ and C₂ Chlorinated Hydrocarbons," *Environmental Science and Technology*, 21: 202.
3. Kavanaugh, M.C. and Trussell, R.R. 1980. "Design of Aeration Towers to Strip Volatile Organic Contaminants for Drinking Water," *Journal of the American Water Works Association*, 71(12): 684.

4. LaMarche, P. and Droste, R.L. 1989. "Air-Stripping Mass Transfer Correlation for Volatile Organics," *Journal of the American Water Works Association*, 81(1): 78.
5. McKinnon, R.J. and Dyksen, J.E. 1984. "Removing Organics from Groundwater Through Aeration Plus GAC," *Journal of the American Water Works Association*, 76(5): 42.
6. Munz, C. and Roberts, P.V. 1987. "Air-Water Phase Equilibria of Volatile Organic Solutes," *Journal of the American Water Works Association*, 79(5): 62.
7. Yuteri, C., Ryan, D.F., Callow, J.J., and Gurol, M.D. 1987. "The Effect of Chemical Composition of Water on Henry's Law Constant," *Journal of the Water Pollution Control Federation*, 51(10): 950.

$$\frac{C_{\ell,e}}{C_{\ell,i}} = \exp\left(-\frac{K_{\ell}a_j V}{Q_{\ell}}\right) \quad (9.416)$$

where n = the number of mixed-cells-in-series (dimensionless).

For relatively insoluble substances like oxygen and many volatile organics, the gas film resistance is small and may be neglected (Kavanaugh and Trussel, 1980). In that case, K_{ℓ} is nearly equal to k_{ℓ} . The organic vapor mass transfer coefficient for a particular system may be estimated from the coefficient for oxygen, if it is known, via Eq. (9.324).

Air Diffusion

Assuming a completely mixed reactor, the ratio of the liquid effluent to liquid influent concentrations of the volatile organic substance removal is given by Roberts, Munz, and Dändliker, 1984):

$$\frac{C_{\ell,e}}{C_{\ell,i}} = \frac{1}{1 + \frac{Q_a K_{HCj}}{Q_{\ell}} \left[1 - \exp\left(-\frac{K_{\ell}a_j V}{K_{HCj} Q_a}\right) \right]} \quad (9.417)$$

The concentration of the contaminant in the off-gas is,

$$C_{a,e} = K_{HCj} \cdot C_{\ell,e} \left[1 - \exp\left(-\frac{K_{\ell}a_j V}{K_{HCj} Q_a}\right) \right] \quad (9.418)$$

where $C_{a,e}$ = the concentration of contaminant in the effluent air (kg/m³ or lb/ft³)
 K_{HCj} = the "dimensionless" Henry's Law constant for species j (m³ water/m³ air or ft³ water/ft³ air)
 $K_{\ell}a_j$ = the overall volumetric liquid-phase mass transfer coefficient for species j (per sec)
 Q_a = the airflow rate (m³/s or ft³/sec)

References

- Adamson, A.W. 1982. *Physical Chemistry of Surfaces*, 4th ed. John Wiley & Sons, Inc., New York.
- ASCE Committee on Oxygen Transfer. 1989. *Design Manual: Fine Pore Aeration Systems*, EPA/625/1-89/023, U.S. Environmental Protection Agency, Office of Research and Development, Center for Environmental Research Information, Risk Reduction Engineering Laboratory, Cincinnati, OH.
- Bennet, C.O. and Myers, J.E. 1974. *Momentum, Heat, and Mass Transfer*, 2nd ed. McGraw-Hill, Inc., New York.
- Berger, B.B. 1983. *Control of Organic Substances in Water and Wastewater*, EPA-600/8-83-011. U.S. Environmental Protection Agency, Office of Research and Development, Washington, DC.
- Blevins, R.D. 1984. *Applied Fluid Dynamics Handbook*. Van Nostrand Reinhold Co., New York.
- Brezonik, P.L. 1994. *Chemical Kinetics and Process Dynamics in Aquatic Systems*. Lewis Publishers, CRC Press, Boca Raton, FL.

- Dean, J.A., ed. 1992. *Lange's Handbook of Chemistry*, 14th ed. McGraw-Hill, Inc., New York.
- Glasstone, S. 1947. *Thermodynamics for Chemists*, Van Nostrand, Princeton, NJ.
- Gosset, J.M. 1987. "Measurement of Henry's Law Constants for C₁ and C₂ Chlorinated Hydrocarbons," *Environmental Science and Technology*, 21: 202.
- Haas, C.N. 1990. "Disinfection," p. 877 in *Water Quality and Treatment: A Handbook of Community Water Supplies*, 4th ed., F.W. Pontius, ed. McGraw-Hill, Inc., New York.
- Hardenbergh, W.A. and Rodie, E.B. 1963. *Water Supply and Waste Disposal*. International Textbook Co., Scranton, PA.
- Hill, K.D. and Dauphinee, T.M. 1986. "The Extension of the 'Practical Salinity Scale 1978' to Low Salinities," *IEEE Journal of Oceanic Engineering*, OE-11(1): 109.
- Joint Editorial Board. 1992. *Standard Methods for the Examination of Water and Wastewater*, 18th ed. American Public Health Association, Washington, DC.
- Joint Task Force of the American Society of Civil Engineers and American Water Works Association. 1990. *Water Treatment Plant Design*, 2nd ed. McGraw-Hill, Inc., New York.
- Joint Task Force of the Water Pollution Control Federation and the American Society of Civil Engineers. 1988. *Aeration: A Wastewater Treatment Process*, WPCF Manual of Practice No. FD-13, ASCE Manuals and Reports on Engineering Practice No. 68. Water Pollution Control Federation, Alexandria, VA; American Society of Civil Engineers, New York.
- Kavanaugh, M.C. and Trussel, R.R. 1980. "Design of Aeration Towers to Strip Volatile Contaminants from Drinking Water," *Journal of the American Water Works Association*, 72(12): 684.
- Lamarche, P. and Droste, R.L. 1989. "Air-Stripping Mass Transfer Correlation for Volatile Organics," *Journal of the American Water Works Association*, 81(1): 78.
- Lewis, E.L. 1980. "The 'Practical Salinity Scale 1978' and Its Antecedents," *IEEE Journal of Oceanic Engineering*, OE-5(1): 3.
- Metcalf & Eddy, Inc. 1991. *Wastewater Engineering: Treatment, Disposal, and Reuse*, 3rd ed., revised by G. Tchobanoglous and F.L. Burton. McGraw-Hill, Inc., New York.
- McKinnon, R.J. and Dyksen, J.E. 1984. "Removing Organics from Groundwater Through Aeration Plus GAC," *Journal of the American Water Works Association*, 76(5): 42.
- Morris, J.C. 1966. "The Acid Ionization Constant of HOCl from 5 to 35°C," *Journal of Physical Chemistry*, 70: 3798.
- Munz, C. and Roberts, P.V. 1987. "Air-Water Phase Equilibria of Volatile Organic Solutes," *Journal of the American Water Works Association*, 79(5): 62.
- Perkin, R.G. and Lewis, E.L. 1980. "The 'Practical Salinity Scale 1978': Fitting the Data," *IEEE Journal of Oceanic Engineering*, OE-5(1): 9.
- Perry, R.H. and Chilton, C.H., eds. 1973. *Chemical Engineer's Handbook*, 5th ed. McGraw-Hill, Inc., New York.
- Riley, J. P. and Chester, R. 1971. *Introduction to Marine Chemistry*. Academic Press, New York.
- Roberts, P.V., Munz, C., and Dändliker, P. 1984. "Modeling Volatile Organic Solute Removal by Surface and Bubble Aeration," *Journal of the Water Pollution Control Federation*, 56(2): 157.
- Roberts, P.V., Hopkins, G.D., Munz, C., and Riojas, A.H. 1985. "Evaluating Two-Resistance Models for Air Stripping of Volatile Organic Contaminants in a Countercurrent, Packed Column," *Environmental Science and Technology*, 19(2): 164.
- Sherwood, T.K., Pigford, R.L., and Wilke, C.R. 1975. *Mass Transfer*, McGraw-Hill, Inc., New York.
- Staudinger, J., Knocke, W.R., and Randall, C.W. 1990. "Evaluating the Onda Mass Transfer Correlation for the Design of Packed-Column Air Stripping," *Journal of the American Water Works Association*, 82(1): 73.
- Stenstrom, M.K. and Gilbert, R.G. 1981. "Effects of Alpha, Beta and Theta Factor Upon the Design, Specification and Operation of Aeration Systems," *Water Research*, 15(6): 643.
- Stover, E.L., Haas, C.N., Rakness, K.L., and Scheible, O.K. 1986. *Design Manual: Municipal Wastewater Disinfection*, EPA/625/1-86-021. U.S. Environmental Protection Agency, Office of Research and Development, Water Engineering Research Laboratory, Center for Environmental Research Information, Cincinnati, OH.

- Stumm, W. and Morgan, J.J. 1970. *Aquatic Chemistry*. Wiley-Interscience, John Wiley & Sons, Inc., New York.
- Weast, R.C., Astle, M.J., and Beyer, W.H. 1983. *CRC Handbook of Chemistry and Physics*, 64th ed. CRC Press, Boca Raton, FL.
- White, G. 1986. *Handbook of Chlorination*, 2nd ed. Van Nostrand, Princeton, NJ.
- Yuteri, C., Ryan, D.F., Callow, J. J., and Gurol, M.D. 1987. "The Effect of Chemical Composition of Water on Henry's Law Constant," *Journal of the Water Pollution Control Federation*, 51(10): 950.